Role of *Hoxa2* and its Putative Downstream Target *Htra1* in Osteogenic Differentiation of the Palatal Mesenchyme

A Thesis Submitted to the College of Graduate and Postdoctoral Studies in Partial Fulfilment of the Requirements for the Degree of Doctor of Philosophy in the College of

Pharmacy and Nutrition

University of Saskatchewan

Saskatoon

By

Paul Pown Raj Iyyanar

Permission to Use Postgraduate Thesis

In presenting this thesis in partial fulfillment of the requirements for a Doctor of Philosophy degree from the University of Saskatchewan, I consent that the Libraries of this University may make it freely available for inspection. I further acknowledge that permission for copying this thesis, in whole or in part, for scholarly purposes may be granted by my supervisor Dr. Jane Alcorn. However, any copying, publication, or use of this thesis for financial gain will not be allowed without my written permission. In addition, recognition shall be given to the University of Saskatchewan, as well as myself for any scholarly use that may be made of any data in my thesis.

Requests for permission to copy or make use of information in this thesis in whole or in part should be addressed to:

Dean of the College of Pharmacy and Nutrition

University of Saskatchewan

104 Clinic Place

Saskatoon, Saskatchewan

S7N 2Z4, Canada.

OR

Dean of the College of Graduate and Postdoctoral Studies

University of Saskatchewan

116 – 110 Science Place

Saskatoon, Saskatchewan

S7N 5C9, Canada.

Abstract

Cleft palate is one of the most common structural birth defects in humans. *Hoxa2* is the most anteriorly expressed gene of the homeobox family that define the anterior-posterior axis during embryonic development. *Hoxa2* is expressed in the palatal shelves and plays an intrinsic role regulating cell proliferation. *Hoxa2*$^{-/-}$ mice develop cleft palate, albeit many of the cellular and molecular mechanisms remain to be explored. In this thesis, I have tested the hypothesis that *Hoxa2* inhibits osteogenic differentiation of the palatal mesenchyme. I present here evidence that loss of *Hoxa2* results in increased canonical BMP signaling dependent osteogenic program spatially and temporally in the developing *Hoxa2*$^{-/-}$ palatal shelves *in vivo* and in *Hoxa2*$^{-/-}$ palatal mesenchymal cells *in vitro*.

In the second part of this thesis, I investigated the role of a serine protease *Htra1*, a putative downstream target of *Hoxa2* in osteogenic differentiation of the palatal mesenchyme. The results indicate that *Htra1* is a positive regulator of osteogenic differentiation and is upregulated in the *Hoxa2*$^{-/-}$ palatal shelves. In addition, I identified that *Runx2*, a master regulator of osteogenic differentiation, binds to the proximal 5' flanking region region of *Htra1* to induce its expression.

Collectively, the data reveals that aberrant osteogenic signaling in the *Hoxa2*$^{-/-}$ palatal shelves due to increased osteoprogenitor commitment and proliferation may lead to cleft palate in these mice. In addition, I show for the first time that *Htra1* is a novel direct downstream target of *Runx2* during osteogenic differentiation. In summary, this thesis contributes to a better understanding of the cellular and molecular mechanisms governing osteogenic differentiation in the palatal mesenchyme during normal palate development and in cleft palate pathogenesis.

Acknowledgements

I would like to sincerely thank my mentor Dr. Adil J. Nazarali for his everlasting support and encouragement throughout the past six years. His constant motivation and confidence in me pushed me to excel in my program. I render my sincere thanks and gratitude to Dr. Jane Alcorn, who kindly stepped in to fill the role of my supervisor after the sudden demise of Dr. Nazarali. I am grateful for her time and help with my thesis preparation and revisions, without expecting anything from my side and I have no words to thank her for the support and help during the most difficult time in the program.

My earnest thanks to Dr. Bill Kulyk, who served as a graduate advisory member in the committee for the past five years. His valuable insights and directions have been instrumental for my graduate program research to head in the right direction. I will never forget that he turned up on crutches to be part of my qualifying exam and I am indebted for his help in many ways including several letters of support he has written for me. I honestly appreciate the valuable suggestions and advice of Dr. B. Frank Eames. His expertise on skeletogenesis, his involvement and help with my manuscripts was instrumental in getting my manuscripts to publication quality. He kindly made me part of his lab meetings after Dr. Nazarali's demise and he has kept an eye on me to ensure my completion of the program. I was fortunate to have studied a graduate course in developmental biology under the supervision of Dr. Pat Krone, which helped me learn diverse tools and systems in developmental biology. Dr. Krone's encouragement, ideas along with his friendly nature to go out of his way to help me has been a strong factor in my program and I thank him for his help, support, and letters of support from him. I thank Dr. David Blackburn for serving as the chair of the advisory committee, who has been flexible and helpful in his approach.

I thank Dr. Marc Ekker, University of Ottawa for agreeing to serve as the external examiner for my defense.

I render my special gratitude to Dr. Phyllis Paterson, who has gone out of her ways to help me morally, financially and academically during my program. I recall the countless number of volunteering meetings she had to help sort out stuff for the members of Nazarali group after his demise, which is an invaluable amount of time and effort. I also acknowledge her in allowing me to use her light microscope for imaging during this thesis work. I also would like to thank Dr. Troy Harkness, Department of Anatomy and Cell Biology, U of S, for his help with my coursework in cell and molecular biology. His motivation gave me the inspiration for writing grants and critical readings of papers and concepts.

I am grateful to have had some wonderful people around me as colleagues in the lab – Merlin Thangaraj, Larhonda Sobchishin, Kendra Furber, Dennis Okello, Glai Tan, Ran bi and Jotham Gan. I also thank the members of Dr. Alcorn and Dr. Eames labs, many of them are my friends with whom I share my high and low points of the graduate student life.

My special thanks to Ms. Larhonda Sobchishin, from whom I learned a great deal in terms of techniques, skills and her help made it easier for me to push further with my research. My sincere thanks to Dr. Kendra Furber who along with Dr. Eames read my *Hoxa2* manuscript and gave valuable comments to make it a quality one for publication.

I sincerely thank the College of Pharmacy and Nutrition to have supported me fully to get through some difficult situation in the past one year. I also acknowledge the support from the staff of the College, in particular, Dr. Erin Smith-Windsor (Graduate program administrator), Ms. Claire Sutton and Ms. Jean Oakley.

I would like to sincerely acknowledge College of Pharmacy and Nutrition, College of Graduate and Postdoctoral Studies and Apotex, for my scholarships during different times of the program. I also sincerely look back with gratitude all these years the scholarship from Dr. Nazarali's NSERC grant to match my scholarship to par level when needed.

I thank the research grant support for my graduate program research from the American Cleft Palate-Craniofacial Association, who had faith in me to award a Subtelny Orthodontic Clinical Research Grant as a junior investigator. My sincere thanks to my supervisors Drs. Nazarali and Alcorn to have let me use the grant money for my research with complete freedom.

I sincerely thank Mr. Erling Madsen, Manager and his staff in the Health Science Supply Center for their help at various time points. I also thank the Ms. Michelle Moroz and the LASU staff especially Ms. Carmen Whitehead for help with maintaining animals for the research.

I look back with sincere gratitude to have received the never-ending support of my teachers from higher secondary school days, my botany teacher Mr. Ezhilarasu Velayudham, my undergraduate program mentor Mr. Winfred Thomas, M.Sc. supervisor Dr. Sangeetha Jerald and many others who have supported me to reach this far in academics. My sincere appreciation and thanks to my family, close friends, and well-wishers, who have been the pillars of support not just during these last six years but forever.

Dedicated to

My family, especially my lovely wife Merlin P. Thangaraj and my loving mother Prabhavathy Kadarkarai, who instilled all their faith and backed me completely. I would not have made it without them.

The manuscripts from this thesis work are dedicated to the memory of my beloved mentor, Dr. Adil J. Nazarali, whose values and principles about research and life beyond are an inspiration.

Publications

Manuscripts

Iyyanar, P. P. R*., and Nazarali, A. J. (2017). Hoxa2 Inhibits Bone Morphogenetic Protein Signaling during Osteogenic Differentiation of the Palatal Mesenchyme. *Front. Physiol.* 8, 929. *Corresponding author

Okello, D. O†., Iyyanar, P. P. R†., Kulyk, W. M., Smith, T. M., Lozanoff, S., Ji, S., et al. (2017). Six2 Plays an Intrinsic Role in Regulating Proliferation of Mesenchymal Cells in the Developing Palate. *Front. Physiol.* 8, 955. †co-first author.

Iyyanar, P. P. R*., Thangaraj M. P., Eames B. F., and Nazarali, A. J. *Htra1* is a novel direct downstream target of *Runx2* during osteogenic differentiation. Manuscript to be submitted to Osteoarthritis and Cartilage. *Corresponding author

Reviews

Smith, T. M., Lozanoff, S., Iyyanar, P. P., and Nazarali, A. J. (2013). Molecular signaling along the anterior-posterior axis of early palate development. *Front. Physiol.* 3, 488.

Table of Contents

List of Figures

List of Tables

List of Abbreviations

A-P axis	Anterior-Posterior axis
ANOVA	Analysis of variance
Alk	Activin receptor-like kinase
AlpI	Alkaline phosphatase I
ARS	Alizarin red S
ATRA	All-trans retinoic acid
Barx1	Barx Homeobox 1
Bglap	Bone carboxy-glutamic acid containing protein
Bmp	Bone morphogenetic protein
Bmpr	Bone morphogenetic protein receptor
Cbfa1*	Core-binding factor alpha 1
CCD	Cleidocranial dysplasia
cDNA	Complementary DNA
ChIP	Chromatin immunoprecipitation
Col10a1	Collagen type X, alpha 1
Col2a1	Collagen type II, alpha 1
d	Day
Dlx5	Distal-Less Homeo Box-5
DMEM	Dulbecco's modified Eagle's medium
DMSO	Dimethyl sulfoxide
E	Embryonic day
EGFR	Epidermal growth factor receptor
ERK	Extracellular signal-regulated kinases
FBS	Fetal bovine serum
FGF	Fibroblast growth factor
FGFR	Fibroblast growth factor receptor
GDF5	Growth differentiation factor 5
GFP	Green fluorescent protein
Gli1	Glioma-associated oncogene homolog 1

Hand2	Heart and neural crest derivatives expressed 2
HH	Hamburger Hamilton stage
Hoxa2	Homeobox-a2
Htra1	High temperature requirement factor A1
Htra3	High temperature requirement factor A3
IU	Infection units
IVD	Intervertebral disc
JNK	c-Jun N-terminal kinase
kDa	kiloDalton
MAPK	Mitogen-activated protein kinase
MEE	Medial edge epithelia
MEK	MAPK/ERK kinase
Meox2	Mesenchyme homeo box 2
MEPM	Mouse embryonic palatal mesenchymal cells
miR	micro-RNA
Mmp	Matrix metalloproteinase
Mn1	Meningioma 1
Msx1	Msh (*Drosophila*) homeo box homolog 1
Mxp	Maxillary prominence
Ocn*	Osteocalcin
OSE	Osteoblast-specific elements
Osx*	Osterix
PCR	Polymerase chain reaction
PDZ	Post synaptic density protein (PSD95) Drosophila disc large tumor suppressor (Dlg1) and Zonula occludens-1 protein (zo-1)
qPCR	Quantitative real time PCR
Runx2	Runt-related transcription factor 2
SAPA	Streptavidin agarose pull-down assay
Satb2	Special AT-Rich Sequence-Binding Protein
SDS	Sodium dodecylsulphate
Shh	Sonic hedgehog

Shox2	Short stature homeobox 2
siRNA	Small interfering RNA
Sox	Sry-related HMG box genes
Spp1	Secreted phosphoprotein 1
Sp7	Sp7 transcription factor
Tbx22	T-Box 22
Tgfβ	Transforming growth factor-beta
Tgfbr1	Transforming growth factor-beta receptor-I
Tgfbr2	Transforming growth factor-beta receptor-II
Tgfbr3	Transforming growth factor-beta receptor-III
18s rRNA	18s ribosomal RNA

Note:

When word is italicized it is referring to the gene. When the word is written in uppercase letters, it is referring to the protein (eg. *Hoxa2*: gene; HOXA2: protein)

1. GENERAL INTRODUCTION

The palate forms the upper roof of the mouth separating the oral and nasal structures. Cleft palate is one of the most common congenital birth defects in humans with an incidence of 1 in 700 to 1 in 1000 live births (Dixon et al., 2011). Children born with this error often have issues with suckling, feeding and speech. These children often require multiple surgeries, therefore affecting the physiological and psychological part of their early life. Thus, understanding the mechanisms of proper palate formation and the cleft palate pathogenesis is of critical importance in future prevention or therapy for cleft palate.

Studies using mouse model, which has a high similarity to human palate development, helped to identify several key stages and cellular processes during palate formation (Yu et al., 2017). In humans, secondary palate development occurs from six weeks to nine weeks, while in mice, it begins at embryonic day (E) 11.5 and the palatal fusion is complete by E15.5 (Ferguson, 1988). By E15.5, the developing palatal bones ossify. During palate development, the vertical palatal shelves grow downward along both sides of the tongue, elevate above the tongue and then contact with each other resulting in subsequent formation and disintegration of the midline epithelial seam. Cleft palate can occur due to failure in any of the aforementioned events during palatogenesis. While the structural changes during palate development are well defined, there is a scarcity of knowledge on the molecular mechanisms governing the patterning of the palate.

Hox genes play vital roles in defining the anterior-posterior axis during development. *Hoxa2* is the most anteriorly expressed *Hox* gene with its anterior limit at the rhombomeres r1/r2 boundary (Krumlauf, 1993). However, *Hoxa2* is not expressed in cranial neural crest cells that emigrate from rhombomeres r1/r2 boundary to populate the first pharyngeal arch (Prince and Lumsden, 1994), which makes first pharyngeal arch devoid of *Hox* gene expression (Köntges and

Lumsden, 1996). Mutation in the *Hoxa2* gene is associated with cleft palate in humans (Alasti et al., 2008) and animal models (Gendron-Maguire et al., 1993; Rijli et al., 1993). Previously, cleft palate in the *Hoxa2*$^{-/-}$ mice was attributed to the tongue musculature in these mice, as *Hoxa2* is not expressed in the cranial neural crest cells of first pharyngeal arch, which give rise to the palate (Barrow and Capecchi 1999). However, our group previously demonstrated that *Hoxa2* is expressed in palatal shelves (Nazarali et al., 2000) and plays a direct role in secondary palate development by regulating cell proliferation (Smith et al., 2009; Okello et al., 2017). Hence, *Hoxa2* expression in the migrating cranial neural crest cells from rhombomere 1 and rhombomere 2 does not appear to be a pre-requisite for its role in palatogenesis, and tongue musculature is unlikely to be the causative for the cleft palate phenotype in the *Hoxa2*$^{-/-}$ mice (Smith et al., 2009).

The maxillary region comprises of pairs of premaxilla, maxilla and palatine bones, which are all derived from the cranial neural crest cells through intramembranous ossification (Iwata et al, 2010). *Hoxa2* is a known inhibitor of osteoblast differentiation in the second pharyngeal arch (Kanzler et al., 1998), in calvaria (Dobreva et al., 2006), in long bones (Deprez et al., 2012) and in ST2 stromal cells (Hu et al., 2011). However, the mechanism involved in regulation of palate development by *Hoxa2* is largely unknown. In this study, I used a combination of *in vivo* and *in vitro* approaches to study the role of *Hoxa2* in osteoblast differentiation of the palatal mesenchyme. My results suggest that *Hoxa2* plays a crucial role in regulating the spatial and temporal expression of osteoblast markers via inhibiting bone morphogenetic protein (BMP) signaling in the developing palatal shelves.

High Temperature Requirement Factor A- HTRA1 and HTRA3 belong to the conserved family of serine proteases that mediate proliferation, apoptosis and epithelial-mesenchymal transition in cancer as tumor suppressor genes (Chien et al., 2004; Wang et al., 2012; Xia et al.,

2013). A previous finding from our group showed that HOXA2 acts as a transcriptional repressor of *Htra* family members by binding to the intronic region to inhibit the expression during spinal cord development (Yan, 2008). Here, I examined the expression pattern of *Htra1* and *Htra3* during palatogenesis. *Htra1* is expressed in osteoblasts (Tocharus et al., 2004) and its role in osteoblast differentiation remains elusive. Hence, I investigated the role of *Htra1* in osteoblast differentiation of mesenchymal cells from the palate. My results support the role of *Htra1* as an inducer of osteoblast differentiation and the data reveal that *Htra1* is a putative direct downstream target of *Runx2* during osteoblast differentiation.

1.1 Hypothesis

Hoxa2 inhibits BMP-dependent osteogenic differentiation of the palatal mesenchyme spatially and temporally and its putative downstream target *Htra1* is a positive regulator of osteogenic differentiation in the palatal mesenchyme induced by *Runx2*.

1.2 Objectives

1) To determine the role of *Hoxa2* in osteoblast differentiation of the palatal mesenchyme *in vivo* and *in vitro*.

2) To examine the spatiotemporal expression of *Htra3* during mouse palate development and to determine whether *Htra3* plays a role in the degradation of midline epithelial seam for palatal fusion using lentiviral aided small interfering-RNA (siRNA).

3) To determine the role of *Htra1* in osteogenic differentiation of mouse embryonic palatal mesenchymal cells (MEPM) cells.

1.3 Overview of chapters

Chapter 3 is focussed on the role of *Hoxa2* as an inhibitor of osteogenic differentiation in the palatal mesenchyme during development. In this chapter, I have used immunohistochemistry (IHC), quantitative real-time PCR (qPCR), Western blot to study osteogenic differentiation of the palatal mesenchyme before and after palatal fusion in the wild-type and *Hoxa2* null embryos. In addition, mouse embryonic palatal mesenchymal (MEPM) cells from wild-type and *Hoxa2*$^{-/-}$ mice were differentiated to osteoblasts to determine the role of *Hoxa2* in osteogenic differentiation of the palatal mesenchyme. The data indicate that loss of *Hoxa2* leads to accelerated osteogenic differentiation due to enhanced BMP signaling-dependent osteogenic program. This finding was published in *Frontiers in Physiology* in 2017. I designed the study, performed experiments, analyzed the data, and wrote the manuscript. Dr. Adil J. Nazarali was the senior author who conceived, coordinated the study and after his passing away, I corresponded the manuscript for publication.

Chapter 4 explores the temporal expression pattern of two Htra serine proteases *Htra1* and *Htra3*, which are previously identified targets of *Hoxa2*. Furthermore, *Htra1* and *Htra3* are known to inhibit TGFβ signaling in other systems. Given the importance of TGFβ signaling in cell proliferation, osteogenic differentiation, and fusion during palatogenesis, the expression patterns of *Htra1* and *Htra3* during palatogenesis are explored in this chapter using qPCR and Western blot. The data indicate that the expressions of *Htra1* and *Htra3* increase during palatogenesis. IHC staining shows that *Htra3* is mainly expressed in the palatal epithelia and in the midline epithelial seam, which may be indicative that *Htra3* might play a significant role in palatal fusion. The expression of *Htra3* in the osteogenic centers of the palatal mesenchyme may be indicative of the role of *Htra3* in osteogenic differentiation. These data have not yet been submitted for publication.

I designed and performed the experiments in this chapter and analyzed the data. Dr. Adil J. Nazarali was the senior author conceived and coordinated the study.

Chapter 5 deals with the functional role of *Htra1* during osteogenic differentiation of the palatal mesenchyme. IHC staining indicates that *Htra1* is mainly expressed in the osteogenic domains of the craniofacial bones during development. The gain of function of *Htra1* in MEPM cells results in increased matrix deposition and mineralization *in vitro*. Based on the similarity in the expression profile of *Htra1* and *Runx2,* I investigated the molecular interaction between *Htra1* and *Runx2* during osteogenic differentiation of the palatal mesenchyme. The data reveal that *Htra1* is a direct transcriptional target of *Runx2*. RUNX2 binds to the proximal promoter region of *Htra1* to induce its expression during osteogenic differentiation. The data from this chapter are written and are about to be submitted to the journal *Osteoarthritis and Cartilage*. I designed, performed experiments, analyzed the data and wrote the manuscript. Adil J. Nazarali was the senior author who conceived and coordinated the study. Merlin P. Thangaraj assisted in performing the luciferase assay and osteogenic arrays, while I performed the experiments. B. Frank Eames was involved in the conception of the study and critical analysis of the data and in manuscript revisions.

Appendix at the end of the thesis has published papers from this thesis and related work.

2. REVIEW OF LITERATURE

Cleft palate is one of the most common congenital birth defects in humans with both environmental and genetic factors playing a crucial role in the pathogenesis (Dixon et al., 2011). Palate development requires precise regulation of gene expression changes, morphogenetic movements and alterations in cell physiology (Murray and Schutte, 2004). In mice, secondary palate arises from the maxillary prominences (Mxp) at E11.5. The palatal shelves grow vertically downward on either side of the tongue until E14, during which the palatal shelves elevate to reorient above the tongue (Figure 2.1) (Ferguson, 1987). At E14.5, the palatal shelves contact each other forming MES. The MES subsequently undergoes rapid degeneration by apoptosis and epithelial-mesenchymal transition leading to mesenchymal confluence at E15.5 (Ferguson 1987) (Figure 2,1). By E15.5, the anterior palatal mesenchyme begins to ossify leading to the formation of the palatal process of maxilla (Nelson et al., 2011), while the palatal process of the palatine bone ossifies early at E13.5 (Wu et al., 2008). Cleft palate may result from failure in any of the critical events such as vertical growth, elevation and reorientation above the tongue, contact of the palatal shelves to form MES, degradation of the MES and consolidation of the mesenchymal confluence. In addition, abnormal osteogenic differentiation prior to the elevation of palatal shelves has been associated with the manifestation of cleft palate (Fu et al., 2017; Jia et al., 2017a, b).

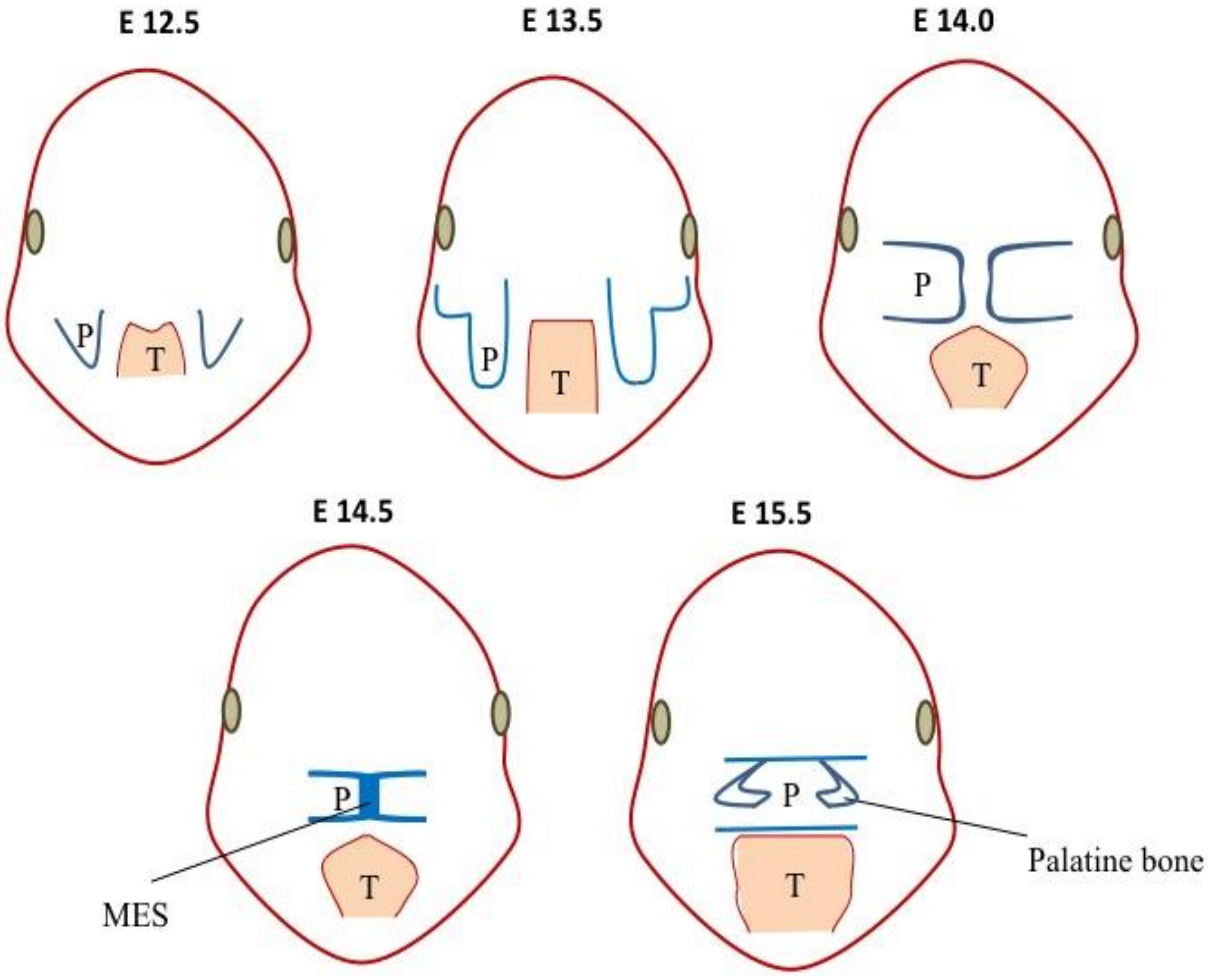

Figure 2.1 Schematics showing the stages of palate development in mice. At E12.5, the palatal shelves which arose from the Mxp lie on either side of the tongue. At E13.5, the palatal shelves grow vertically downward and at E14.0 the palatal shelves elevate above the tongue. At E14.5, the palatal shelves grow horizontally and contact each other to form MES. At E15.5, the MES is degraded to result in mesenchymal confluence, which ensures that the palatal fusion is complete. At this stage the developing palatine bone starts to ossify as well. T, tongue; P, palatal shelf, MES, midline epithelial seam.

The developing secondary palate is composed of mesenchymal cells mainly derived from cranial neural crest cells (Ito et al., 2003) covered by multilayered epithelia from the facial ectoderm (Noden, 1983). Palatal epithelia are heterogeneous, with epithelia on the oral side made up of stratified, keratinizing, squamous cells, while the nasal side is of pseudo-stratified, ciliated, columnar cells (Ferguson, 1987; Han et al., 2009). Initially, the cranial neural crest cells derived mesenchyme was regarded as a homogenous cell population. However, several findings highlight the demarcations amongst the mesenchymal cells on the oro-nasal axis. Nasal side mesenchyme of the palate is marked by the expression of *distal-Less homeobox 5* (*Dlx5*), *fibroblast growth factor 7* (*Fgf7*) and canonical Bmp signaling mediated by pSMAD 1/5/8, whereas the oral side mesenchyme is occupied by the expressions of *glioma-associated oncogene homolog 1* (*Gli1*) and *Fgf10* (Han et al., 2009). In addition, *sonic hedgehog* (*Shh*) is expressed on the oral side of the palatal epithelia (Han et al., 2009). These signaling molecules demarcate the nasal and oral sides of the palate that would form the prospective palatal bones and soft tissues respectively.

In mammals, the palate tissue can be distinguished into anterior bony hard palate and posterior soft palate. Hard palate is required for speech and swallowing, while the soft palate is necessary for occlusion (Bush and Jiang, 2012; Smith et al., 2013). Regional heterogeneity at the molecular and cellular level along the A-P axis and oral-nasal (dorsal ventral) axis is a hallmark of murine secondary palate development (Hilliard et al., 2005; Bush and Jiang, 2012; Smith et al., 2013). Several networks and signaling pathways have been found to be anterior (*Msx1, Bmp4, Shh, Bmp2, Fgf10, Fgf7* and *Shox2*) (Figure 2.2) or posterior specific (*Meox2, Mn1, Tbx22* and *Barx1*) (Figure 2.3) in the developing palatal shelves (Hilliard et al., 2005; Bush and Jiang, 2012; Smith et al., 2013).

2.1 Anterior palate specific gene expressions

The anterior palate was initially considered as a signaling center involving multiple networks and signaling pathways coordinating proper palate development (Figure 2.2) (Smith et al., 2013). Failure in cell proliferation leading to defect in growth or elevation of the palatal shelves in the anterior palate would result in a complete cleft palate rather than an anterior palatal cleft (Smith et al., 2013). For example, deletion of an anterior palate specific gene *Msx1*, results in overt cleft palate along the A-P axis in *Msx1*$^{-/-}$ mice (Zhang et al., 2002). Consistent with the structure and function of the anterior palate to form the palatal bones, BMP signaling, and related transcription factor networks play vital roles in the anterior palatal morphogenesis.

2.1.1 Msx1 network

Msh (Drosophila) homeo box homolog 1 (Msx1) was the first gene reported as expressed specifically in the anterior palate. Despite the exclusive expression on the anterior palate (Zhang et al., 2002), *Msx1*$^{-/-}$ mice develop overt cleft palate along A-P axis (Satokata and Maas, 1994; Zhang et al., 2002). *Msx1* is required for the expression of *Bmp4, Shh* and *Bmp2* in the anterior palate to regulate cell proliferation (Figure 2.2). Interestingly, mice expressing a *Bmp4* transgene could rescue the cleft palate phenotype of *Msx1*$^{-/-}$ mutants. Also, *Bmp4* in turn induces the expression of *Msx1* in the anterior palate but not in the posterior palate (Zhang et al., 2002). Since then numerous findings have explored the role of this network in the anterior palate cell proliferation.

2.1.2 Shh

Shh is expressed in oral side epithelium of the palatal shelves, which is involved in rugae patterning (Rice et al., 2006). Rugae are the epithelial ridges present on the oral side of the palate,

which were initially considered as the signaling centre coordinating several signaling molecules to regulate cell proliferation during secondary palate development (Welsh and O'Brien, 2009). Transgenic mice with deletion of *Shh* in the epithelia (*K14-Cre; Shh$^{fl/fl}$*) develop cleft palate with an incidence of 70-85% (Rice et al., 2004; Lan and Jiang, 2009). SHH in the palatal epithelia signals through Smoothened (SMO), a transmembrane protein in the mesenchyme, to induce *Fgf10* expression to positively regulate cell proliferation (Lan and Jiang, 2009). *Shh* regulates the downstream expression of *Bmp2* in the palatal mesenchyme for cell proliferation (Figure 2.2) (Rice et al., 2004). SHH signaling regulates Forkhead Box (Fox) family of transcription factors *Foxf1*, *Foxf2* and *Osr2* in the palatal mesenchyme and deletion of *Smo* gene in the palatal mesenchyme (*Osr2-IresCre; Smo$^{fl/fl}$*) results in downregulation of *Foxf1*, *Foxf2* and *Osr2* (Lan et al., 2004). *Foxf1* is mainly expressed in the mesenchyme along the middle region of the palatal shelves, whereas *Foxf2* is expressed in the mesenchyme throughout the anterior-posterior axis during palatogenesis (Xu et al., 2016). Deletion of *Foxf1* (*Wnt1-Cre*; *Foxf1$^{fl/fl}$*) or *Foxf2* in the cranial neural crest cells (*Wnt1-Cre; Foxf2 $^{fl/fl}$*) results in cleft palate manifestation due to reduced cell proliferation (Xu et al., 2016). In the *Foxf2* mutants (*Wnt1-Cre; Foxf2 $^{fl/fl}$*), the expression of *Shh* and *Shox2* are downregulated in the very anterior and posterior regions of the palate, in contrast *Fgf18* mRNA was upregulated in the corresponding regions. In the *Foxf1*; *Foxf2* double mutants (*Wnt1-Cre; Foxf1 $^{fl/fl}$ Foxf2 $^{fl/fl}$*), there was a significant upregulation of *Fgf18* along the anterior-posterior axis of the palate with concomitant downregulation of *Shh* with complete lack of rugae formation (Xu et al., 2016). These new lines of evidence suggest that *Foxf1* and *Foxf2* are redundant in repressing *Fgf18* to regulate *Shh* expression and cell proliferation downstream of *Shh*. Indeed, some elegant experiments using FGF18 soaked beads on palatal explant cultures completely abolished the expression of *Shh* and rugae formation in the palate (Xu et al., 2016).

Wnt1-Cre; Foxf2 $^{fl/fl}$ palatal shelves exhibit reduced TGFβ signaling characterized by pSMAD 2/3 with the downregulation of TGFβR3. In addition, in the *Wnt1-Cre; Foxf2* $^{fl/fl}$ palatal shelves there is enhanced activation of non-canonical phospho-p38 signaling, indicating a strong interplay between different signaling pathways downstream of SHH in regulating cell proliferation (Nik et al., 2016).

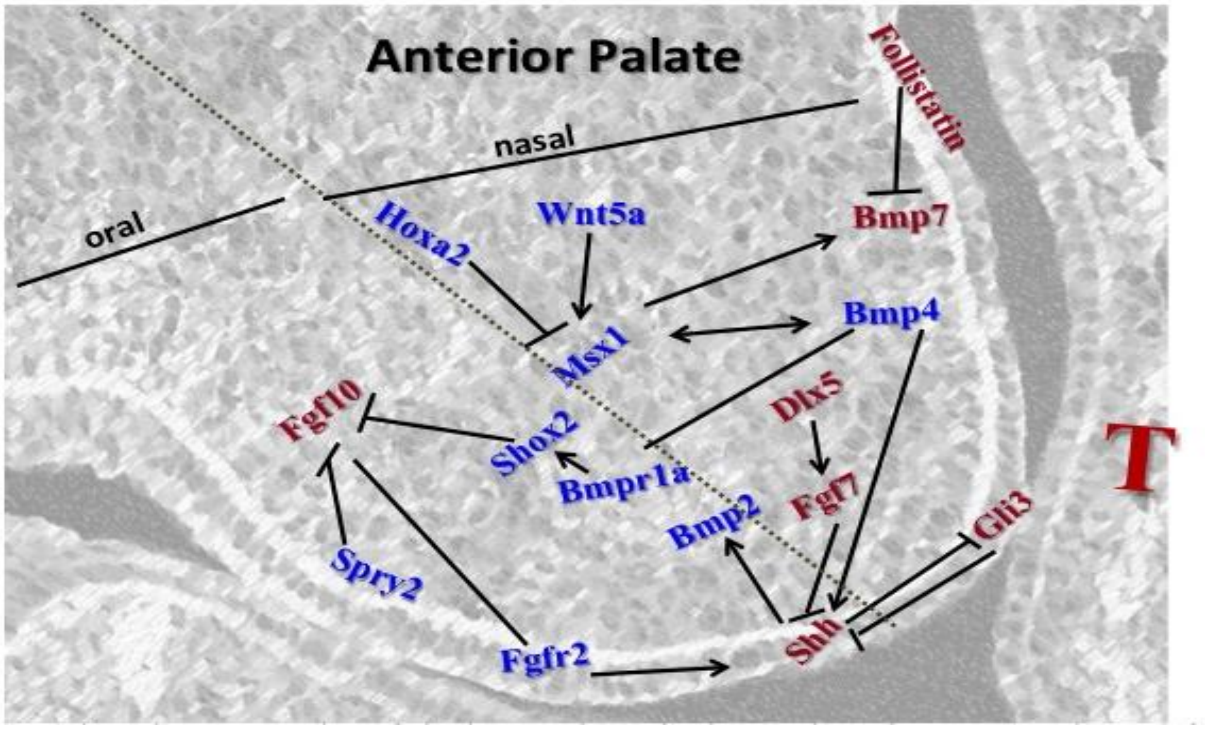

Figure 2.2 Schematic representation of the key regulators in the developing anterior palatal shelves. *Msx1* and *Bmp4* function in an autoregulatory loop mechanism in the mesenchyme. *Bmp4* induces *Shh* expression in the epithelium which signals backs to mesenchyme to positively regulate *Bmp2* to enhance cell proliferation in the mesenchyme (Zhang et al., 2002). *Hoxa2* inhibits *Msx1* expression in early palatal development. *Spry2* regulates Fgfs and their receptors for proper balance of proliferation and prevention of premature apoptosis in the epithelium. *Fgf10* induces *Shh* where as *Fgf7* acts as an antagonist. Genes represented in red are restricted to either oral or nasal side of the palate, whereas those represented in blue are expressed across the shelf. T, Tongue. I drew this figure as part of a review on molecular signaling along the anterior-posterior axis during palate development that was published (Smith et al., 2013).

2.1.3 Dlx5

Distal-less homeobox-5 (*Dlx5*) is expressed in the nasal side (medial) mesenchyme in the middle region of the palate in the preosteoblast region at E13.5 (Han et al., 2009). In addition to other craniofacial defects, *Dlx5*$^{-/-}$ mutants develop cleft of the secondary palate with an incidence of 88% (Levi et al., 2006). In these mice, the horizontal laminae of the palatal bones are missing (Acampora et al., 1999). Interestingly, deletion of *Dlx5* rescues the cleft palate phenotype of *Msx1*$^{-/-}$ mice (*Dlx5*$^{-/-}$ *Msx1*$^{-/-}$) (Levi et al., 2006). Although *Msx1* and *Dlx5* are expressed in anterior palatal mesenchyme, their interaction in the network might be indirect, as *Msx1* is not altered in the *Dlx5*$^{-/-}$ mutants and vice-versa (Han et al., 2009). In the wild-type mice, *Fgf7* expressed in the osteogenic front on the nasal side of the palate could inhibit *Shh* expression and narrow its domain to the oral side epithelia to control cell proliferation (Figure 2.2). Hence the decrease in cell proliferation due to the diminished *Shh* expression in the *Msx1*$^{-/-}$ mutant is rescued by downregulated *Fgf7* expression in the *Dlx5*$^{-/-}$ *Msx1*$^{-/-}$ double mutants (Han et al., 2009). Moreover, increased *Bmp7* in the palatal epithelia along the A-P axis as well as decreased BMP antagonist Follistatin in the posterior palatal epithelia in the double mutants (*Dlx5*$^{-/-}$ *Msx1*$^{-/-}$) may also account for the rescue of cell proliferation and cleft palate in the *Dlx5*$^{-/-}$ *Msx1*$^{-/-}$ double mutants (Levi et al., 2006).

2.1.4 BMP signaling

BMP signaling plays a critical role in cell proliferation and osteogenic differentiation during palatogenesis (Baek et al., 2011). In *Nestin-Cre; Bmpr1a*$^{fl/fl}$ mutants, in which the bone morphogenetic protein receptor *Bmpr1a* expression is removed from the facial primordia, develop cleft lip and cleft palate due to decreased cell proliferation in the Mxp mesenchyme at E11.5 (Liu

et al., 2005). Surprisingly, in the palatal shelves of these mice, *Msx1* expression was not altered. However, there was expansion in the expression domain of posterior specific *Barx homeobox 1* (*Barx1)* towards the anterior side of the palate (Liu et al., 2005). In addition, *Nestin-Cre; Bmp4*$^{fl/fl}$ mice exhibit isolated unilateral cleft lip (2/9) without any cleft palate, which highlights the redundancy of the BMP ligands in lip fusion and palate development (Liu et al., 2005). *Bmpr1a* is expressed prominently in the anterior palate both in mesenchyme and epithelia, whereas its expression is mainly concentrated in the epithelia on the posterior side. Similarly, *Bmp1b* is expressed only in the anterior palatal epithelia and mesenchyme (Li et al., 2011). Deletion of *Bmpr1a* in the cranial neural crest cells (*Wnt1-Cre; Bmpr1a*$^{fl/fl}$) results in a cleft between the primary palate and anterior secondary palate. Constitutive activation of *Bmpr1*b in the *Bmpr1a* mutants failed to rescue the cleft palate phenotype (Li et al., 2011), although the tooth development defect was partially rescued. *Wnt1-Cre; Bmpr1a*$^{fl/fl}$ mice exhibit reduced expression of pSMAD 1/5/8, *Msx1*, *Bmp4*, *Pax9* and *Short stature homeobox 2* (*Shox2)* leading to decreased cell proliferation in the palatal shelves (Li et al., 2011). Furthermore, the role of *Bmpr1a* specifically in palate development was studied using *Osr2-Cre; Bmpr1a*$^{fl/fl}$ mice in which the expression of *Bmpr1a* was deleted only in the palatal mesenchyme (Baek et al., 2011), as *Osr2* is exclusively expressed in the oral side of the palatal mesenchyme and in the developing molar tooth buds (Lan et al., 2004). Similar to *Wnt1-Cre; Bmpr1a*$^{fl/fl}$ mice, these mice exhibit cleft between the primary palate and the anterior secondary palate (Baek et al., 2011) due to decreased cell proliferation in the anterior, mid and primary palate. Although *Msx1* and *Fgf10* were downregulated, *Bmp4* and *Bmp2* were surprisingly upregulated in these mutants, underlining the complex signaling involved in this pathway. In addition, these mice exhibit submucous cleft palate with a failure in the initiation of osteogenesis in the palatal process of the maxilla and decrease in the size of the palatal

process of the palatine bone (Baek et al., 2011). Surprisingly, constitutive activation of *Bmpr1a* (with Gln203 to Asp) in the cranial neural crest cells (*Wnt1-Cre; pMes-caBmpr1a*) results in ectopic cartilage formation in the posterior side leading to cleft palate (Li et al., 2013). Although BMP signaling has been known to induce cell proliferation during palatogenesis, constitutive *Bmpr1a* mutants exhibit reduced cell proliferation in the anterior palate. *Msx1*, *Shox2* and pSMAD 1/5/8 are all ectopically induced in the posterior palate in the area of cartilage formation. In addition, pSMAD1/5/8 expression is shifted from nasal side mesenchyme of the palatal shelves to the oral side. Non-canonical Bmp signaling via phospho-p38 Mitogen-activated protein kinase (MAPK) and phosphorylated c-Jun N-terminal kinase are also activated in the ectopic cartilage formation area in the posterior palatal shelves (Li et al., 2013). Constitutive activation of *Bmpr1a* in the epithelia of the palatal shelves (*K14-Cre; pMes-caBmpr1a*) leads to cleft palate due to fusion of the palatal shelves to the mandible (He, et al., 2010). This phenotype is consistent with that of *Noggin* mutants in the epithelia (*K14-Cre; Nog*$^{fl/fl}$) in which the palatal shelves fuse with the mandible resulting in cleft palate. *Noggin* mutant mice exhibit increased cell proliferation in anterior palatal epithelia, posterior palatal epithelia and decreased proliferation in anterior palatal mesenchyme. Ectopic *Bmp2* could at least partially account for the ectopic expression of pSMAD1/5/8 in the oral epithelia of these *Noggin* mutant palates. TGFβ3 induced cell death was found in the oral side of the palatal shelves instead of the MES leading to fusion of the palatal shelves to the mandible. Similar to the *Noggin* mutant phenotype, epithelial specific deletion of *heart and neural crest derivatives expressed 2* (*Hand2)* (*Pitx2-Cre; Hand2*$^{fl/fl}$) leads to cleft palate due to fusion of the palatal shelves to the mandible at the posterior side (Xiong et al., 2009). There is decreased cell proliferation in the anterior palate of these mice consistent with the decrease in expression of *Bmp2* and *Shh,* but not *Msx1* and *Fgf10*, showing that *Hand2* could be a downstream

target of *Msx1*. Intriguingly, Noggin inhibits the expression of *Hand2* in the palatal shelves (Xiong et al., 2009).

2.1.5 Shox2

Shox2 is another transcription factor expressed specifically in the anterior palate. Deletion of *Shox2* in the cranial neural crest cells (*Wnt-Cre; Shox2*$^{fl/fl}$) results in cleft between the primary palate and the anterior secondary palate, with increased apoptosis and decreased cell proliferation in the palatal mesenchyme (Yu et al., 2005). Consistent with this, there is an increase in expression of *Fgf10* and *Fibroblast growth factor receptor 2c* (*Fgfr2c)* covering the entire anterior palatal mesenchyme. Also, loss of *Noggin* in the epithelia (Yu et al., 2005; He et al., 2010) or *Bmpr1a* in the cranial neural crest cells result in the reduction of *Shox2* expression in the anterior palatal mesenchyme (Li et al., 2011). However, exposure of the palatal mesenchyme to BMP4, BMP2 or SHH-soaked beads *in vitro* is not sufficient to induce *Shox2* expression. These suggest that BMP signaling is not capable of inducing *Shox2* expression on its own but is necessary for *Shox2* expression.

2.1.6 FGF signaling

FGF10 is expressed in the oral side mesenchyme of the palate and signals through its receptor FGFR2B in the oral side epithelia to induce the expression of *Shh* (Figure 2) (Rice et al., 2004; Alappat et al., 2005). Similar to the *Noggin* and *Hand2* mutants, *Fgf10* mutant palatal shelves in the posterior side fuse with the mandible due to the mislocalization of *Tgfβ3* expression to the oral side epithelia instead of the MEE. Deletion of *Fgfr2* (*K14Cre-Fgfr2*$^{fl/fl}$) in the epithelia in mice results in cleft palate due to reduced cell proliferation in the palatal epithelia. Consistent with this, there is a lack of organized rugae formation due to failure in the expression of *Shh*

(Hosokawa et al., 2009). Also, FGFR1B, another FGF receptor is expressed in the mesenchyme of the anterior and posterior palate during development. *Fgfr1b* regulates cell proliferation by inhibiting *Wnt11* during the growing stages of palate development. In turn, *Wnt11* induces apoptosis during fusion of the palatal shelves by inhibiting *Fgfr1b* (Lee et al., 2008).

Fgf antagonist *Sprouty2* (*Spry2*) is strongly expressed on the nasal and oral sides of anterior palatal mesenchyme and epithelia, with negligible expression in the posterior palate (Welsh et al., 2007). Mice homozygous for an Mb-scale deletion (pie bald deletion) that removes the *Spry2* locus exhibit cleft palate with an incidence of 83% and cleft lip with an incidence of 27% (Welsh et al., 2007). In these mice, there is an increase in cell proliferation accompanied with an expansion in the expression domain of anterior specific *Msx1* and *Ets variant 5* into the posterior palate, whereas posterior specific *Barx1* is expanded into the anterior palate. Also, *T-box 22* (*Tbx22)* domain in the posterior palate is reduced. These mice also have disorganized rugae formation due to decreased *Shh* expression. The antagonism on *Fgf9* relieved by the loss of *Spry2* may account for the expanded and ectopic domain of *Msx1* (Welsh et al., 2007). These findings highlight the necessary control of FGF gradients to maintain the A-P axis during palatogenesis (Figure 2.4). Interestingly, *Fgf9* is expressed in the nasal side of the palate (Iwata et al., 2012) and $Fgf9^{-/-}$ mice develop cleft palate with an incidence of 40% (Colvin et al., 2002). Recently, FGF9 has been shown to induce *Pitx2* expression, which in turn activates *Cyclin D1* (*Ccnd1*) and *Cyclin D3* (*Ccnd3*) expression to promote cell proliferation in the palatal shelves of *Wnt1-Cre; Tgfbr2*$^{fl/fl}$ mice.

2.2 Posterior palate specific gene expression

In contrast to signaling in anterior palate, very little information is available on posterior palate specific gene expression. Transcription factors such as MEOX2, TBX22 and BARX1 are expressed in the posterior palate (Figure 2.3).

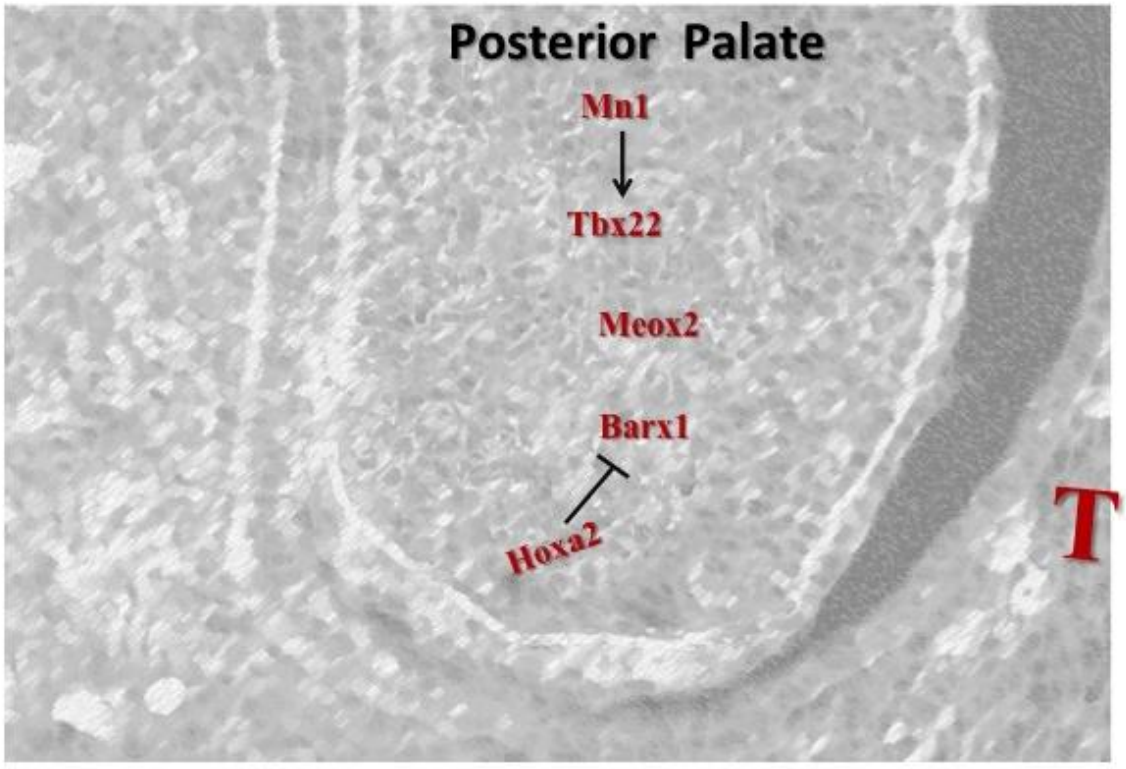

Figure 2.3 Schematic representation of the key regulators in the posterior palate. *Barx1* and *Tbx22* induce cell proliferation in the posterior palate. *Hoxa2* also controls the expression of *Barx1* in the early stage of palatogenesis. *Meningioma 1* (*Mn1)* positively regulates *Tbx22*. *Mesenchyme homeo box 2* (*Meox2*) plays a role in fusion of the posterior palate. T, Tongue. This figure is published in Smith et al., 2013.

2.2.1 Meox2

Mesenchyme homeo box 2 (*Meox2*) is expressed in the extreme posterior regions of the palate. *Meox2*$^{-/-}$ mice exhibit a low penetrance of cleft palate (35%) (Jin and Ding, 2006). In these mice, palatal shelves grow, elevate and fuse but the fusion is weak that the palatal shelves separate from each other resulting in cleft of the posterior palate. TGFβ1 mediated *Meox2* induces *p21* to inhibit cell proliferation in mammary epithelial cells (Valcourt et al., 2007). Interestingly, *p21* is necessary for *Smad4* mediated phospho-p38 MAPK signaling for apoptosis and MES degeneration during palatal fusion (Xu et al., 2008). However, whether *Meox2* promotes *p21* expression in the palate remains to be tested to identify the network downstream of *Meox2* during palatal fusion in the posterior palate.

2.2.2 Tbx22

T-box transcription factor 22 (*Tbx22*) is expressed in the posterior part of the developing palatal shelves (Herr et al., 2003). *Tbx22*$^{-/-}$ mice develop submucous cleft palate with a small minority (2/30) exhibiting overt cleft palate (Pauws et al., 2009). Palatal shelves of the *Tbx22*$^{-/-}$ mutants have an aberrant rugae pattern in the posterior half of the hard palate and translucency in the posterior rugal regions. Beads soaked with BMP4 protein inhibit *Tbx22* expression in palatal explant cultures *in vitro* (Fuchs et al., 2010). Ectopic expression of *Msx1* in *Spry2* piebald mutants coincides with the restricted expression pattern of *Tbx22* (Welsh et al., 2007). However, in the *Msx1*$^{-/-}$ mutant palatal shelves, *Tbx22* expression is not altered. Hence BMP4 could be regulating *Tbx22* expression in the posterior palatal shelves through *Msx1* independent mechanism.

Transcription factor MN1 is expressed in the middle to the posterior regions of the palatal shelves (Liu et al., 2008). In *Mn1*$^{-/-}$ palatal shelves, expression of *Tbx22* is reduced in the posterior

regions. *Mn1*$^{-/-}$ mice exhibit cleft palate due to reduced cell proliferation in the middle and posterior regions of the palate with reduction in the expression of *Ccnd2* (Liu et al., 2008).

2.2.3 Barx1

Barx1 is expressed in the posterior regions of the palatal shelves. A-P axis characterized by the expression of anterior *Msx1* and posterior *Barx1* is set up in the pharyngeal arch (PA) where *Msx1* is expressed in the distal region and *Barx1* in the proximal region (Barlow et al., 1999). Relative gradients of BMP and FGF signaling maintain the A-P axis in the developing palatal shelves (Figure 2.4) (Welsh et al., 2007). Consistently, loss of *Bmpr1a* in the cranial neural crest cells leads to expansion in the region of *Barx1* expression. *Hoxa2* inhibits *Barx1* in the developing palatal shelves at E12.5, which may partially account for the elevated cell proliferation in the *Hoxa2* null palatal shelves (Smith et al., 2009).

2.3 TGFβ signaling pathway in cell proliferation

The TGFβ signaling pathway plays a critical role in regulating cell proliferation, apoptosis and differentiation during embryonic palate development (Chai et al., 2003). Canonical TGFβ signaling is mediated by the binding of ligands (TGFβ1 or TGFβ2 or TGFβ3) to the receptor TGFBR2, which initiates the heterodimeric binding of TGFBR1. This heterodimerization leads to the phosphorylation of TGFBR1, which in turn phosphorylates the receptor associated SMADs such as SMAD2 and/or SMAD3 depending on the context (Chai et al., 2003; Iwata et al., 2011). The phosphorylated receptor-associated SMADs then cooperate with SMAD4 to translocate into the nucleus to regulate the transcription of downstream target genes. Mutants of TGFβ ligands *TGFβ2*$^{-/-}$ (Sanford et al., 1997) and *TGFβ3*$^{-/-}$ (Kaartinen et al., 1995; Proetzel et al., 1995) develop cleft palate with the incidences of 23% and 100%, respectively.

The role of TGFβ signaling in the cranial neural crest cells derived palatal mesenchyme has been extensively studied using *Wnt1-Cre; Tgfbr2*$^{fl/fl}$ mice (Ito et al., 2003; Iwata et al., 2012a; Iwata et al., 2012b; Iwata et al., 2014). In addition to other craniofacial defects, *Wnt1-Cre; Tgfbr2*$^{fl/fl}$ mice develop overt cleft palate with complete penetrance. In these mice, there is decreased cell proliferation at E14.5 along with diminished expression of *Ccnd1* (Ito et al., 2003). Loss of *Tgfbr2* results in an increase in the mRNA expression of *Tgfβ2* and *Tgfbr3*. In the *Tgfbr2* mutants, upregulated TGFβ2 binds and signals through TGFBR3 to activate non-canonical TGFβ signaling via p38 MAPK signaling resulting in defective cell proliferation (Iwata et al., 2012a). Neutralizing antibodies against TGFβ2 or TGFBR3 rescue cell proliferation in the *Tgfbr2* mutant palatal explants. More importantly, the cleft palate phenotype of *Tgfbr2* mutants is rescued by the haploinsufficiency of *Tgfβ2* (82.5%) or *Tgfbr1* (91.7%) (Iwata et al., 2012a). In addition, activation of phospho-p38 MAPK signaling in the *Tgfbr2* mutant palatal shelves results in the decreased expression of *Fgf9* and *Pitx2* (Iwata et al., 2012b). Exogenous addition of FGF9 rescued cell proliferation in the *Tgfbr2* mutant palatal mesenchymal cells (MEPM) (Iwata et al., 2012b). In addition, MEPM cells of the *Tgfbr2* mutants in culture display spontaneous accumulation of lipid droplets due to failed lipolysis (Iwata et al., 2014). In the MEPM cells of the *Tgfbr2* mutants, exogenous addition of SHH failed to induce *Gli1* expression as well as proliferation. As expected, phospho-p38 MAPK signaling is responsible for the impaired SHH signaling in the *Tgfbr2* palatal shelves. Interestingly, telmisartan (a clinical angiotensin II receptor blocker) rescued the aberrant phospho-p38 MAPK signaling, lipid metabolic activity and cell proliferation in the *Tgfbr2* mutant palatal shelves. More importantly, oral administration of telmisartan (20mg/kg body weight per day) to the pregnant dams from E11.5 to E15.5 rescued cleft palate phenotype in the *Tgfbr2* mutants (44%) (Iwata et al., 2014).

2.4 TGFβ signaling during palatal fusion

Transforming growth factors and their receptors play a major role in embryonic palatal fusion. *Tgfβ3* null mutant mice exhibit complete penetrance of secondary cleft palate, as the palatal shelves elevate, make contact but fail to fuse (Proetzel et al., 1995; Kaartinen et al., 1995). While numerous recent findings have allowed for a better understanding of cleft palate pathogenesis in *Tgfβ3* null mice, gaps in our knowledge still remain. TGFβ3 in palatal epithelium induces p-SMAD2 but not p-SMAD3. Indeed, in *Tgfβ3* null mice, phosphorylation of SMAD2 fails to take place in the palatal epithelia, which renders the palatal epithelium more proliferative and devoid of apoptosis resulting in the persistence of MEE (Cui et al., 2003). TGFβ3 is required for the expression of matrix metalloproteinase *Mmp-13* in MEE during palatal fusion and loss of *Tgfβ3* leads to reduced expression of *Mmp13* in the MEE in *Tgfβ3* null mice (Blavier et al., 2001). Our group recently reported that knockdown of *Mmp-25* in palatal shelves impairs palatal fusion in *in vitro* organ culture system. Also, bio-neutralization of TGFβ3 using specific neutralizing antibody results in reduced expression of *Mmp-25* (Brown and Nazarali, 2010). In chick embryos, the beak physically separates the palatal shelves from contact with each other, resulting in a physiological cleft palate. It is pertinent to note that unlike the rodent palatal MEE, the chick MEE is devoid of TGFβ3. Addition of TGFβ3, but not TGFβ1 or TGFβ2 proteins, aids in palatal fusion resulting in mesenchymal confluence in the chick embryos in palatal organ cultures (Sun et al., 1998). Moreover, transgenic mice carrying a knock-in of *Tgfβ1* in the *Tgfβ3* locus could only partially rescue the cleft palate phenotype of *Tgfβ3* null mice due to the failure to rescue the reduced apoptosis and downregulated expression of *Mmp13* (Yang and Kaartinen, 2007). Loss of *Tgfβ3* in the mutant mice and absence of *Tgfβ3* in avian palatal shelves results in failure of induction of chondroitin sulfate proteoglycan (Gato et al., 2002) and absence of filopodia (Taya et al., 1999)

leading to failure of palatal fusion. Epidermal growth factor (EGF) signaling through epidermal growth factor receptor (EGFR) mediated by phosphorylated extracellular signal-regulated kinases (p-ERK) is vital for cell proliferation and survival in the palatal epithelium and TGFβ3 is presumed to inhibit p-ERK to render the epithelial cells pro-apototic (Yamamoto et al., 2003). However, this mechanism has not been characterized yet.

TGFβ ligands signal through their receptors, TGFBR1, TGFBR2 and TGFBR3. Among these receptors, TGFBR3 (Nakajima et al., 2007) is expressed in palatal epithelium before the elevation of the palatal shelves and in the MES at E14.5, whereas TGFBR1 (Dudas et al., 2004) and TGFBR2 are expressed in both palatal epithelium and mesenchyme and also in the ossification centers of the palatine bone (Cui et al., 1998; Cui and Shuler, 2000). TGFBR3 is important for the phosphorylation of SMAD2 (P-SMAD2) and for the disintegration of palatal epithelium during palatal fusion in organ culture system *in vitro* (Nakajima et al., 2007). It is important to note that only P-SMAD2, but not P-SMAD3, is expressed in the palatal epithelium during fusion (Cui et al., 2003) and inhibition of *Smad2* by siRNA in palatal organ culture is sufficient to inhibit palatal fusion preventing the MEE from degeneration (Shiomi et al., 2006). Moreover, Keratin 14 promoter driven overexpression of *Smad2* could partially rescue the cleft phenotype in *Tgfβ3*$^{-/-}$ mice (Cui et al., 2005). Activin receptor-like kinase-5 (Alk-5, synonymous to Tgfbr1) in the anterior MEE is necessary for p-SMAD2 expression and overexpression of constitutively active Alk-5 could rescue the palatal fusion in *Tgfβ3*$^{-/-}$ palatal shelves by 46% (Dudas et al., 2004).

Ablation of *Tgfbr2* in the palatal epithelial cells (*K14-Cre; Tgfbr2*$^{fl/fl}$ mice) results in soft palate cleft, submucous cleft and failure of the primary palate to fuse with the anterior secondary palate (Figure 2.4) (Xu et al., 2006). Loss of *Tgfbr2* in the palatal epithelium resulted in loss of

expression of interferon regulatory factor 6, *Mmp13*, p-SMAD2 and failure in the induction of apoptosis at the MES.

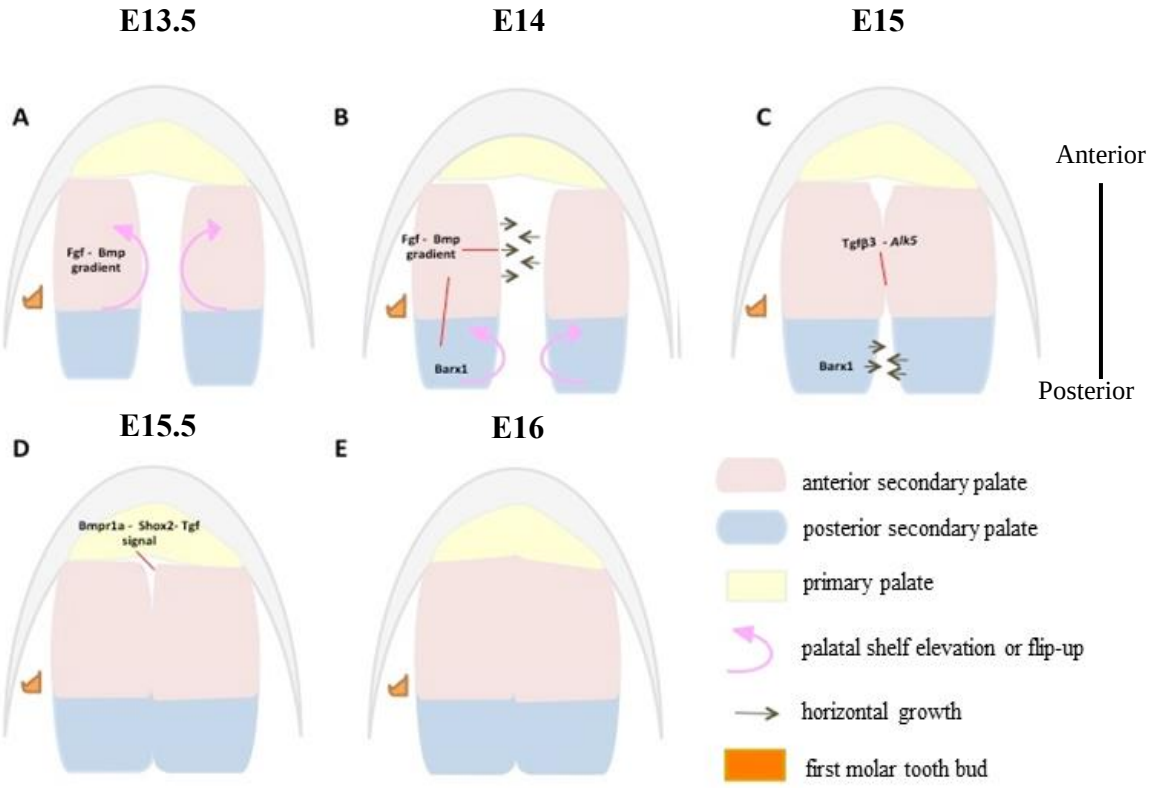

Figure 2.4 Overview of signaling mechanisms governing embryonic palate development. FGF-BMP gradients/thresholds maintain proper palatal growth and elevation through proliferation. (A-B) Anterior FGF10 and BMPs control proliferation via *Shh* expression. This directs anterior palate to elevate and grow horizontally at E13.5-E14. After E13.5 to E14, the anterior palatal shelves first elevate to orient themselves horizontally above the tongue when the posterior palatal shelves are still lying in vertical position (A). Anterior FGF-BMP gradients along with posterior FGF8 regulate proliferation and growth via *Barx1* in the posterior palate at E14-15. At E14, the posterior palatal shelves follow the anterior palatal shelves in orienting horizontally above the tongue, whereas the anterior palates begin to grow horizontally towards each other to make contact (B). At E15, TGFβ3 initiates fusion at the anterior palate through its receptor and the anterior palatal shelves have made contact and fused, whereas the posterior shelves grow horizontally (C). Then the fusion extends posteriorly through TGFβ-*Meox2* and by E15.5, both the anterior and posterior palates have fused (D). *Bmpr1a* mediated *Shox2* and TGFβ signaling through its receptors aid in the fusion between the primary and secondary palate at the future secondary choana, which marks the completion of palatal fusion at E16 (D, E). Palatal shelves are divided into anterior (pink) *Msx1* and posterior (aqua) *Barx1* expression domains (A-E) representing future hard and soft palate respectively.

2.5 Osteogenesis

In higher vertebrates, bones provide support and protection for various organs of the body. In addition to mechanical support, bones also aid in metabolic functions. Bone homeostasis is maintained as a balance between two processes namely, bone formation and bone resorption mediated by osteoblasts and osteoclasts, respectively (Zuo et al., 2012). Any impairment in the balance could result in deformed bones due to failure in the remodeling process.

Bone and cartilage form the vertebrate skeleton. Bones are formed by either endochondral ossification or by intramembranous ossification. During endochondral ossification, initially the chondrocytes proliferate, undergo hypertrophy and die, which are then replaced by osteoblasts to form bone. In chondrocyte differentiation, the mesenchymal cells become immature chondrocytes, which express Collagen type II, alpha 1 (*Col2a1)* and proteoglycan, which then form hypertrophic chondrocytes characterized by Collagen type X, alpha 1 (*Col10a1).* These mature chondrocytes further differentiate into terminal hypertrophic chondrocytes, which express Secreted phosphoprotein 1 (*Spp1)* and *Mmp13* (Komori et al., 2010).

Intramembranous ossification is the process of laying down osteoblasts directly from the mesenchymal progenitor cells upon condensation (Komori et al., 2010). During intramembranous bone formation, the multipotent mesenchymal cells condense to differentiate into osteoblasts (Dobreva et al 2006) characterized by the expression of runt-related transcription factor 2 (*Runx2)* or *core-binding factor alpha 1* (*Cbfa1*) and *Sp7* transcription factor (*Sp7*) or *Osterix* (*Osx*). These osteoblasts then lay matrix and differentiate further into mineralized osteocytes, which express *bone carboxy-glutamic acid containing protein* (*Bglap*) or *Osteocalcin* (*Ocn*) (Komori et al., 2010; Javed et al., 2010).

Endochondral ossification is mainly seen in the long bones, whereas intramembranous ossification dominates in the craniofacial bones (Javed et al., 2010), although there are craniofacial bones derived from endochondral ossification. A majority of the craniofacial bones arise from the cranial neural crest cells and the rest arise from the paraxial mesoderm (Figure 2.5). The palatal bones are formed via intramembranous ossification include the anterior palatal process of the maxilla and the posterior palatal process of the palatine bone (Baek et al., 2011). The palatal process of the maxilla ossifies after the palatal fusion, as two mesenchymal condensations on either side of the degraded MES (Baek et al., 2011). The palatal process of the palatine bone ossifies early during palate development prior to elevation of palatal shelves at E13.5 (Wu et al., 2008).

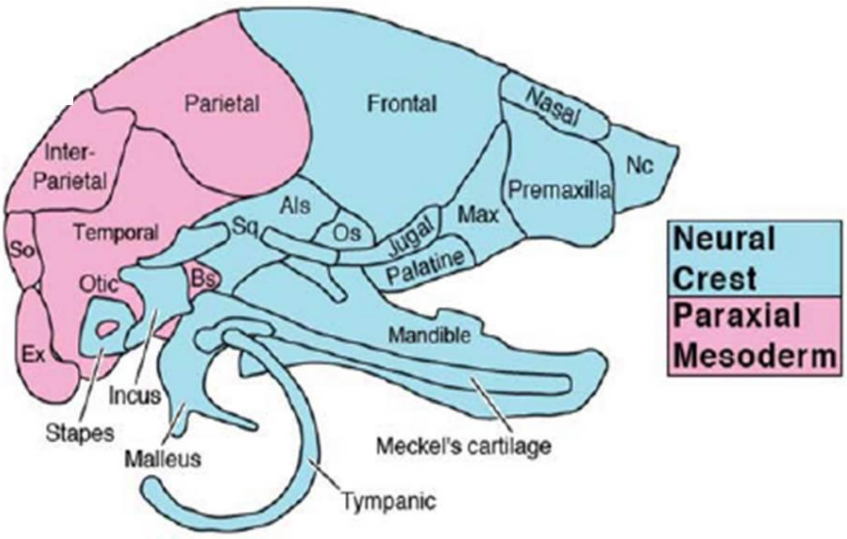

Figure 2.5 Craniofacial bones and their source of origin. Contribution of cranial neural crest cells and paraxial mesoderm to the development of craniofacial bones (Taken from Lee and Saint-Jeannet, 2011, with permission).

2.6 Runt-related transcription factor 2 (Runx2)

Runt related transcription factor 2 (Runx2), also previously known as core-binding factor alpha 1 (Cbfa1), has been extensively studied in osteoblast differentiation. The gene *Runx2* encodes for a full-length protein of about 57 kilo Dalton (kDa), with N-terminal runt homology DNA binding domain followed by nuclear localization signal and a C-terminal sub-nuclear targeting nuclear matrix targeting signal (Choi et al., 2001; Lou et al., 2009). *Runx2*$^{-/-}$ mice die immediately after birth due to breathing problems (Komori et al., 1997) and the majority of *Runx2*$^{-/-}$ mice develop cleft palate (Aberg et al., 2004). These mice exhibit complete lack of ossification due to inhibited osteoblast differentiation and defective hypertrophic chondrocytes. Although the progenitors express *alkaline phosphatase* (*Alpl*) weakly in these mice, the expression of late markers such as *Bglap* and *Spp1* are completely absent (Komori et al., 1997). Moreover, dosage of full length RUNX2 protein is critical, as 70% of full length protein leads to conditions like cleidocranial dysplasia (CCD) (Lou et al., 2009). The hypomorphic *Runx2* allele generated by insertion of neomycin cassette into the intron before exon 8 leads to reduced level (55-70%) of wild type mRNA and protein, leading to no skeletal abnormalities, except in the clavicle and calvaria featuring the defects of CCD in humans (Lou et al., 2009). Also, in the deletion mutant mice, where the C-terminal nuclear matrix targeting signal domain of RUNX2 is deleted, a similar phenotype to the *Runx2* null mice was observed. This C-terminal mutant of RUNX2 protein retained the DNA binding but exhibited decreased luciferase activity of *Spp1*, *Bglap* and *Tgfbr1* promoters. However, the intra-nuclear targeting is completely lost, which is essential for RUNX2 function in osteoblasts (Choi et al., 2001). It has been shown that BMP2 induces *Runx2* mediated by *Dlx5* in C2C12 cells (Lee et al., 2003). FGF2 induces *Runx2* mRNA expression in preosteoblastic MC3T3-E1 cell line, premyoblastic C2C12 cells and in rat osteosarcoma ROS 17

cells. FGF2 also induces *Runx2* expression and its binding activity to the *Bglap* (*Ocn*) promoter (Kim et al., 2003). FGF2 induced ERK-MAPK signaling is important for RUNX2 phosphorylation at Serine 301 residue, which leads to acetylation of RUNX2 protein and its stabilization (Park et al., 2010). Indeed, site directed mutagenesis of two serine residues to alanine (S301A, S319A) reduced RUNX2 ability to induce osteoblast specific gene expression (Ge et al., 2009). Moreover, BMP2 also induces p-ERK signaling in the osteoblasts resulting in increased acetylation and stability of RUNX2 via increasing p300 protein levels and its histone acetyl transferase activity (Jun et al., 2010).

2.7 Sp7 transcription factor (Sp7)/ Osterix (Osx)

Sp7 zinc finger transcription factor, also referred as *Osterix* (*Osx*), is another important regulator of osteoblast differentiation. The mouse *Sp7* gene codes a 428-amino acid polypeptide with a molecular mass of 46 kDa comprising of C-terminal C2H2 zinc finger domain and a N-terminal proline rich region (Zhang, 2010). *Sp7* null mice also lack both intramembranous and endochondral bone formation (Nakashima et al., 2002) and craniofacial bones are severely affected in the absence of *Sp7* (Nakashima et al., 2002; Baek et al., 2013). In these mice, in addition to the absence of *Spp1* and *Bglap*, ectopic expression of chondrogenic markers such as Sry-related HMG box genes, *Sox9*, *Sox5*, *Col2a1* and Indian hedgehog protein in the intramembranous bones is observed, characterizing a failure in the induction of pre-osteoblasts to osteoblasts (Nakashima et al., 2002). RUNX2 binds to the proximal promoter region of *Sp7* at a consensus binding sequence AGTGGTT (-713 to -707 bp), which is conserved between human, mouse and rat (Nishio et al., 2006). SP7 binds to the promoter of WNT antagonist *Dkk1* (Zhang et al., 2008) and *Sost* (Yang et al., 2010) to activate their transcription to inhibit WNT signaling. It also disrupts the transcriptional activity of β-CATENIN/TCF and its target gene *Ccnd1*, thereby inhibiting proliferation (Zhang et

al., 2008). Thus, *Sp7* controls feedback mechanism of WNT signaling in the osteoblasts (Zhang et al., 2008; Zhang 2010; Tang et al., 2011). *Mmp13* is another direct target of *Sp7* in the osteoblasts and is important for degradation of extracellular matrix proteins particularly collagens type II, I and X (Zhang C et al., 2012). Recently, *Sp7* acts upstream of special AT-Rich Sequence-Binding Protein (*Satb2*), another transcription factor known to bind to AT rich regions in the nuclear matrix attachment regions. SP7 binds to the proximal promoter region (-130 bp) of *Satb2* to induce its expression in the osteoblasts (Tang et al., 2011).

2.8 Special AT-Rich Sequence-Binding Protein (Satb2)

Satb2 null mice have a shortened mandible and malformation of several intramembranous bones such as premaxilla, maxilla, nasal bones, frontal bones and the temporal process of the squamous bone (Dobreva et al., 2006). SATB2 binds to upstream promoter region (-290 to -181 bp) of *Spp1* to activate its transcription (Dobreva et al., 2006). Furthermore, SATB2 augments the DNA binding activity of RUNX2 and activating transcription factor 4 to the Osteoblast-specific elements (OSE) in the *Bglap* promoter for enhancing the transactivation of *Bglap* (Dobreva et al., 2006). However, SATB2 does not directly bind to OSE elements of the *Bglap* promoter (Dobreva et al., 2006). SATB2 also binds to the 3′ enhancer region of *Hoxa2* gene that has characteristics of nuclear matrix attachment region and represses its expression in osteoblasts (Dobreva et al., 2006).

2.9 Osteogenic differentiation and cleft palate pathogenesis

Palatal bones comprise the palatal process of the maxilla in the anterior half of the palate and the palatal process of the palatine bone in the posterior half of the palate (Baek et al., 2011). The palatal process of the maxilla ossifies after the palatal fusion at E15.5, in the form of two mesenchymal condensations on either of the degraded MES (Baek et al., 2011). However, the

palatal process of the palatine bone ossifies independently at E13.5, prior to the elevation of the palatal shelves (Wu et al., 2008). Augmented expression of *Pax3* (*Pax3*$^{Cre/Cre}$, *R26*$^{Pax3/Pax3}$) leads to cleft palate with decreased osteogenesis due to downregulation of *Runx2* at E13.5 (Wu et al., 2008). It is intriguing to note that the mutants of several osteoblast markers including *Runx2*$^{-/-}$ (Aberg et al., 2004), *Dlx5*$^{-/-}$ (Han et al., 2009), *Satb2*$^{-/-}$ (Dobreva et al., 2006) develop cleft palate. However, there are only a handful of reports on the role of osteogenic differentiation leading to cleft palate (Wu et al., 2008; Fu et al., 2017; Jia et al., 2017a, b). RNA-seq data from *Osr2*$^{-/-}$ palatal shelves at E13.5 mainly revealed upregulation of genes involved in skeletogenesis and osteogenesis, including *Runx2*, *Dlx5*, *Sp7* and several Bmp ligands such as *Bmp3*, *Bmp5* and *Bmp7* (Fu et al., 2017). In addition to decreased cell proliferation (Lan et al., 2004), enhanced osteogenic differentiation could be causative for the cleft palate in the *Osr2*$^{-/-}$ mice (Fu et al., 2017). *Pax9* is required for maintaining the expression of *Osr2* in the palatal mesenchyme and *Pax9*$^{-/-}$ mice develop overt cleft palate due to reduced proliferation in the posterior palate. Restoration of *Osr2* in the *Pax9*$^{-/-}$ background using knock-in of *Osr2* (*Pax9*$^{Osr2KI/Osr2KI}$) rescues the palatal shelf elevation and cleft palate in 50% embryos, although the anterior secondary palate failed to fuse with the primary palate (Zhou et al., 2013). *Pax9*$^{-/-}$ palatal shelves exhibit decreased β-CATENIN mediated canonical WNT signaling in the posterior region of the palatal shelves at E13.5 and small molecule WNT agonist rescued palatal shelf elevation and cleft palate phenotype (Li et al., 2017) accompanied by restoration of defective cell proliferation and osteogenic differentiation (Jia et al., 2017a). These works highlight the importance of controlled cell proliferation and osteogenic differentiation for elevation of palatal shelves during development.

2.10 Hoxa2 in cranial neural crest cell migration and skeletal development

Cranial neural crest cells are a pluripotent migratory cell population specific to vertebrates which give rise to different cell lineages to give rise to bones, cartilage, nerves and connective tissue (Gammill and Bronner-Fraser, 2003; LeDouarin and Kalcheim, 1999; Morales et al., 2005; Steventon et al., 2005). During development of craniofacial skeleton, rostral (anterior) cranial neural crest cells largely give rise to the fronto-nasal skeleton and intramembranous bones of the skull, while the posterior cranial neural crest cells populate the pharyngeal arches to form the jaw, middle ear, hyoid and thyroid cartilages (Nodan, 1983). During early vertebrate development, the anterior region of the neural tube differentiates into forebrain (prosencephalon), midbrain (mesencephalon) and the hindbrain (rhombencephalon) (Lumsden and Keynes, 1989). Further during development, rhombencephalon segments into seven compartments called rhombomeres. In each rhombomere, an unique population of cells is maintained without exchange with other compartments. Cranial neural crest cells from posterior mesencephalon, rhombomere 1 and rhombomere 2, fill the first pharyngeal arch, whereas rhombomere 4 fills the second pharyngeal arch. Cranial neural crest cells from rhombomere 6 and rhombomere 7 mix to form the PA3 and PA4. Cranial neural crest cells from rhombomere 3 and rhombomere 5 undergo massive apoptosis, which makes minimal contribution to the arches (Graham et al., 1993; Minnoux and Rjili, 2010).

Hox genes are necessary for maintenance of the A-P axis and for the patterning of PAs (Santagati and Rijli, 2003). *Hoxa2* is the most anteriorly expressed *Hox* gene with its anterior limit at rhombomeres r1/r2 boundary (Krumlauf, 1993). However, *Hoxa2* is not expressed in cranial neural crest cells which emigrate from rhombomeres boundary r1/r2 to populate the first pharyngeal arch (Prince and Lumsden, 1994), which makes the first pharyngeal arch devoid of *Hox* gene expression (Köntges and Lumsden, 1996). In the *Hoxa2*$^{-/-}$ mice, mirror duplication of

the proximal first pharyngeal arch elements such as malleus, incus, tympanic ring, gonial, squamosal and ptergoid bones in place of the second pharyngeal arch elements takes place (Gendron-Maguire et al 1993; Rijli et al., 1993). Hence, *Hoxa2* is considered a selector gene of the second pharyngeal arch (Grammatopoulos et al., 2000; Pasqualetti et al., 2000; Hunter and Prince, 2002; Santagati et al., 2005).

Hoxa2 expression is excluded from the chondrogenic condensations in the second pharyngeal arch, which express *Sox9* and in the *Hoxa2*$^{-/-}$ mice, *Sox9* expression domain is shifted into the *Hoxa2* expression domain (Kanzler et al., 1998). Overexpression of *Hoxa2* in the *Col2a1* chondrogenic lineage leads to stunted growth in the long bones due to the inhibition of WNT/β-CATENIN signaling (Deprez et al., 2012). HOXA2 binds to the promoters of several WNT signaling genes and activates their expression in early development of the second pharyngeal arch at E10.5 (Donaldson et al., 2012). Also, *Runx2* is upregulated in the second pharyngeal arch of *Hoxa2* null mutants (Kanzler et al., 1998). Moreover, *Runx2* is downregulated in ST2 cells (stromal cell line) when overexpressed with *Hoxa2* expression plasmid and during osteoblast differentiation *Runx2* induces micro-RNA 3960 to inhibit translation of *Hoxa2* (Hu et al., 2011). Also, *Hoxa2*$^{-/-}$ embryos exhibit increased bone mineralization in the calvaria and the double mutants of *Hoxa2* and *Satb2* (*Satb2*$^{-/-}$ *Hoxa2*$^{-/-}$) were able to rescue the reduced mineralization defects in the frontal and interparietal bones of the *Satb2* mutants (Dobreva et al., 2006).

2.11 Hoxa2 in palate development

In addition to the complete penetrance of middle ear abnormalities (Rijli et al., 1993; Gendron-Maguire et al., 1993), *Hoxa2*$^{-/-}$ mice develop cleft palate with a penetrance of 81% (Barrow and Capecchi 1999). The cleft palate in the *Hoxa2*$^{-/-}$ mice was initially believed to be due

to the tongue musculature in these mice, as *Hoxa2* is not expressed in the cranial neural crest cells, which populate the first pharyngeal arch, that gives rise to the palate (Barrow and Capecchi 1999). However, we have found that *Hoxa2* is expressed in the palatal shelves (Nazarali et al., 2000) and plays a direct role in secondary palate development by regulating cell proliferation (Smith et al., 2009). Hence, expression in the migrating cranial neural crest cells from rhombomere 1 and rhombomere 2 does not appear to be a pre-requisite of the genes that are important in regulating palatogenesis. When *Hoxa2*$^{-/-}$ mouse embryonic heads devoid of their tongue were cultured in chemically defined media in rolling bottle cultures, the palatal shelves failed to fuse. Also, knocking down of *Hoxa2* expression with antisense retroviral infections in the wild type cultures resulted in decreased palatal fusion rate (Smith et al., 2009). Hence, tongue musculature may not be the main reason for the cleft palate phenotype in the *Hoxa2*$^{-/-}$ mice (Smith et al., 2009). In the palatal shelves of the *Hoxa2*$^{-/-}$ mice, there was increase in the expression of *Msx1*, *Bmp4*, *Ptx1* and *Barx1*. It is pertinent to note that *Msx1* along with *Bmp4* in the anterior palate and *Barx1* in the posterior palate are necessary for cell proliferation. However, the role of *Hoxa2* in the osteogenic differentiation of the embryonic palatal mesenchyme have not been investigated and whether abnormal osteogenic differentiation in the *Hoxa2*$^{-/-}$ palatal mesenchyme could be a reason for the cleft palate pathogenesis in the *Hoxa2*$^{-/-}$ mutants remains to be studied.

2.12 High temperature requirement factor A (Htra) family of proteins

Serine proteases HTRA family members are known to regulate TGFβ ligands (Oka et al., 2004). TGFβ family members play vital roles in palatal shelf growth (Cui et al., 2003) and fusion (Kaartinen et al., 1995). In addition, *Hoxa2* binds to intronic region of *Htra3* to repress its expression in the spinal cord during development (Yan., 2008). The role of Htra family members during palatogenesis has not been investigated yet.

Htra are a family of serine proteases which are conserved from bacteria to humans (Chien et al., 2009). In bacteria, HTRA proteins are involved in quality control and signal transduction in periplasmic space. HTRA proteins are vital in bacteria for survival at high temperature and hence their name High temperature requirement factor A. In vertebrates, there are four Htra family members, namely HTRA1 to HTRA4. Among them, HTRA2 has unique mitochondrial localization signal with the N-terminal region found to be present in the mitochondrial transmembrane domain and the protease domain is believed to protrude into the intermembrane space. *Htra2* is known to play role in apoptosis in caspase dependent and independent manners. *Htra2* null mice exhibit a Parkinsonian phenotype due to the loss of neurons in the striatum (Martins et al., 2004).

Htra-1, 3 and 4 have a mac-25 domain at the N-terminal end, which includes an insulin-like growth factor binding domain and a Kazal-type protease inhibitor domain. The mac-25 domain has homology with follistatin, which is a known inhibitor of activin. Mac-25 domain is followed by a serine protease domain that is indispensable for its activity and a PDZ [abbreviated from Post synaptic density protein (PSD95), *Drosophila* disc large tumor suppressor (Dlg1) and Zonula occludens-1 protein (zo-1)] domain for interaction with the target substrates (Figure 2.6).

HTRA1 was initially identified as the serine protease that was downregulated in SV40 transformed fibroblasts. It was believed to modulate the availability of insulin growth factors (IGFs) by cleaving the IGF binding proteins (Zumbrunn and Trueb, 1996). Since then *Htra1* has been extensively studied as a candidate gene in various forms of cancers, osteoarthritis, cerebral autosomal recessive arteriopathy with subcortical infarcts and leukoencephalopathy, Alzheimer's disease, age related macular degeneration, and during development.

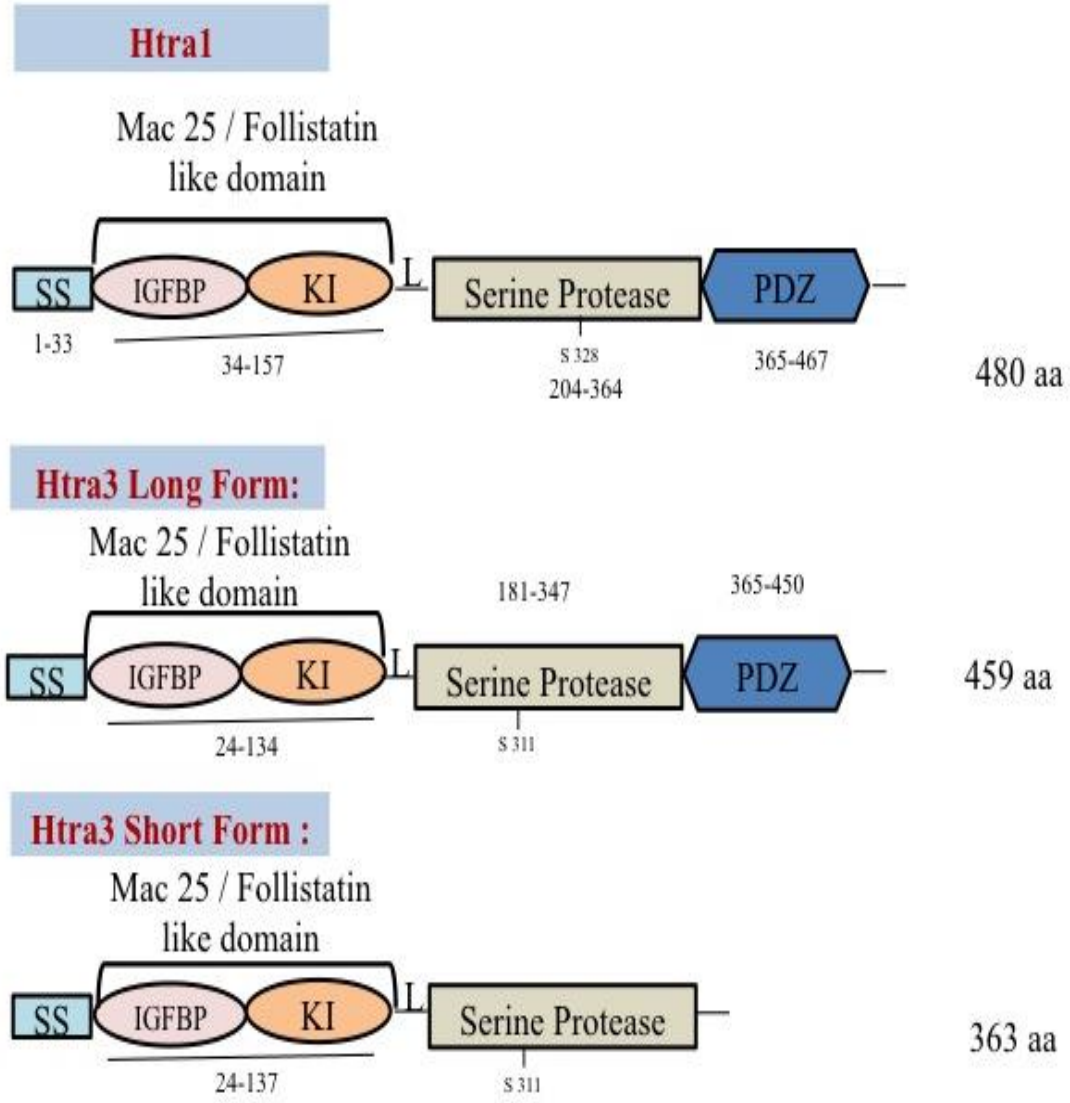

Figure 2.6 Schematic diagram of HTRA1 and HTRA3 protein domains. SS, signal sequence; IGFBP, Insulin Growth Factor Binding Protein; KI, Kazal protease inhibitor; PDZ, (abbreviated from Post synaptic density protein (PSD95), *Drosophila* disc large tumor suppressor (Dlg1) and Zonula occludens-1 protein (zo-1).

2.12.1 HTRA and TGFβ

HTRA1 binds to and inhibits TGFβ/BMP family members such as TGFβ1, TGFβ2, BMP4 and growth differentiation factor 5 (GDF5) *in vitro* (Oka et al., 2004). The affinity of HTRA1 for mature TGFβ proteins decreases as follows: BMP4>TGFβ2>TGFβ1>ACTIVIN>GDF5 (Oka et al., 2004). The serine protease domain along with the linker region (aa 155-202) that precedes it was essential and sufficient for the binding of HTRA1 to the TGFβ family members (Oka et al., 2004). It is interesting to note that HTRA1 was not bound to FGF2 and EGF. The authors also ruled out the possibility of HTRA1 inhibiting the intracellular signaling of BMPR, as *Htra1* failed to inhibit the signal that originated from constitutively active BMPRIB (Oka et al., 2004). Like HTRA1, HTRA3 has been shown to bind to and inhibit TGFβ/BMP family members such as TGFβ1, 2, GDF5 and BMP4 *in vitro* (Tocharus et al., 2004). In contrast, HTRA1 has been shown to co-localize and cleave the pro-domain of pro-TGFβ1 in the endoplasmic reticulum to block signaling of pSMAD2. However, HTRA1 failed to bind to mature TGFβ1 (Shiga et al., 2011). Similarly, several other findings did not identify a negative correlation in expression between TGFβ1 and HTRA1 (Wang et al., 2012). Recently, HTRA1 is demonstrated to positively regulate TGFβ1 mediated pSMAD2/3 signaling by binding, to process latent TGFβ binding protein 1 to mature TGFβ1 (Beaufort et al., 2014). Further evidence is needed to address the discrepancies and to validate the role of *Htra1* in TGFβ signaling.

2.12.2 HTRA1 and FGF signaling

In *Xenopus* embryos, *Htra1* was found to share similar expression domains with FGFs. FGF4 and FGF8-soaked beads induced *Htra1* expression and similarly microinjection of *Htra1* mRNA into the embryos induced FGF proteins and p-ERK signaling by cleavage of proteoglycans such as biglycan, syndecan-4 and glypican-4 (Hou et al., 2007). In contrast, knockdown of *Htra1*

in zebrafish induces FGF8 expression and p-ERK activation, whereas overexpression of *Htra1* inhibits FGF8 and p-ERK expression (Kim et al., 2012). The discrepancy with the earlier report was suggested to be due to the difference in the *Htra1* expression across the stages in the different model organisms. *Xenopus Htra1* is not detected from the maternal to the blastula periods but detected at low levels in the early gastrula, whereas at these stages *Htra1* is highly expressed in zebrafish leading to difference in FGF signaling regulation (Kim et al., 2012). Another report identified FGF8 as an inducible factor of *Htra1* in chick facial mesenchyme at Hamilton and Hamburger (HH) 19 stage (Ferrer-Vaquer et al., 2008). *Fgf8* is expressed at high levels in the ectoderm between the two olfactory placodes and in the forebrain and *Htra1* transcripts are detected in the underlying mesenchyme. Chick facial mesenchyme explants cultured without the overlying ectoderm show no *Htra1* expression; however, when mesenchyme is cultured together with FGF8-soaked heparin acrylic beads, strong *Htra1* expression is detected around the bead. In addition, *Htra1* transcripts were downregulated in explants cultured with FGFR1 inhibitor SU5402 (Ferrer-Vaquer et al., 2008). Although *Htra1* is induced by FGF8 in facial mesenchyme (HH19) and in forelimb bud (HH17), *Htra1* is not downregulated by SU5402 in younger embryo explants (HH11). The overall expression pattern of *Htra1* is found to be different from that of FGF signaling and it can be argued that *Htra1* is not a member of the FGF syn-expression group (Ferrer-Vaquer et al., 2008). Together these data suggest that FGF signaling regulates *Htra1* in a tissue and stage dependent manner. Recently, a Flp-In system (Invitrogen) was used to overexpress and silence *Htra1* in MCF10A mammary epithelial cells to study the role of *Htra1* in epithelial-mesenchymal transition and its downstream targets. Silencing of *Htra1* leads to increase in FGFR3, FGFR4 and Fibroblast growth factor binding protein 1 (FGFBP1) expression and overexpression of *Htra1* induces downregulation of the FGF family members (Wang et al., 2012). Hence the interaction

between *Htra1* and FGF signaling cannot be neglected and the two may have a reciprocal feedback signaling.

2.12.3 HTRA1 intracellular localization and cell signaling

Htra1 has been extensively studied in cancer development and progression, as a tumor suppressor gene (Chien et al., 2004; Narkiewicz et al., 2009; He, X., et al., 2010; Mullany et al., 2011; Wang et al., 2012; Xia et al., 2012). HTRA1 was initially believed to be a secreted protease but recently HTRA1 was also reported to be expressed in the cytoplasm (Chien et al., 2009) and in the nucleus (Clawson et al., 2008; He, X., et al., 2010; Wang et al., 2012). HTRA1 is associated with the microtubules in nocadazole dependent manner and co-precipitated with α-, β- and γ-tubulins. The PDZ domain is important for this association and bound HTRA1 inhibits cell motility (Chien et al., 2009). Moreover, a 29 kilodalton (kDa) isoform that lacks the PDZ domain is found localized in the nucleus (Wang et al., 2012), and retains its proteolytic activity (Clawson et al., 2008). However, a majority of the HTRA1 protein is localized in the cytoplasm with some in the nucleus and only a limited amount is secreted (Wang et al., 2012). HTRA1 binds to EGFR both in the cell membrane and in the nucleus and inhibits EGFR phosphorylation. The downregulation of EGFR by *Htra1* has been shown to be important for anoikis in suspension SKOV3 ovarian carcinoma cell line (He et al., 2010). HTRA1 binds to and degrades tuberous sclerosis protein 2 but not tuberous sclerosis protein 1 in cytoplasm both *in vivo* and *in vitro* to activate the downstream targets such as eukaryotic translation initiation factor 4E binding protein and S6 kinase (Campioni et al., 2010). HTRA1 also degrades X-linked inhibitor of apoptosis protein in presence of cisplatin drug to render SKOV3 cancer cells responsive to chemotherapy (He et al., 2012). HTRA1 protein when incubated with fibronectin protein produces fibronectin fragments, which is important for the transcriptional expression of *Mmp-1* and *Mmp-3* in human synovial

fibroblasts (Grau et al., 2006). Similar mechanisms are also noted in IVD cell cultures and the induction of *Mmp*s by *Htra1* was blocked by mitogen activated protein kinase kinase (MEK) inhibitor PD98059, showing that the mechanism is MEK dependent (Tiaden et al., 2012b).

2.12.4 Htra1 and osteoblast differentiation

Htra1 is expressed in bone matrix during development (Oka et al., 2004; Tsuchiya et al., 2005). However, its role in bone matrix mineralization is not clear as it has been shown to regulate matrix mineralization both positively (Tiaden et al., 2012a) as well as negatively (Hadfield et al., 2008). HTRA1 is found to colocalize with integrin-binding sialoprotein (IBSP) during bone regeneration (Tiaden et al., 2012a). *Htra1* is involved in the lineage commitment of mesenchymal stem cells to form osteoblasts, inhibiting adipogenic differentiation (Tiaden et al., 2016). *Htra1* induces the expression of MMPs during osteogenesis in a MAPK dependent manner (Tiaden et al., 2016). However, *Htra1* has also shown to be involved in RANKL-induced osteoclastogenesis in KusaO cells and to inhibit osteogenic differentiation via downregulation of BMP2 induced pSMAD 1/5/8, p-ERK and p38 MAPK signaling (Wu et al., 2014b). Therefore, the role of *Htra1* in osteogenic differentiation remains to be determined and the molecular targets upstream and downstream of *Htra1* are yet to be delineated.

2.12.5 Htra3

High temperature requirement factor A 3 (HTRA3) has similar structural domains to that of HTRA1(Figure 2.6) suggesting that both these serine proteases may have similar functions but with differential expression patterns (Zumbrunn and Trube, 1996; Nie et al., 2003). Indeed, HTRA3 also binds to TGFβ/BMP family members such as TGFβ1 and BMP4 to inhibit their downstream *Smad* luciferase reporters (Tocharus et al., 2004). In contrast to *Htra1*, *Htra3* produces two variants namely long and short forms due to alternative splicing (Figure 2.6) (Nie et al., 2003).

Although *Htra3* expression is limited in the cartilaginous condensations, it is upregulated when the ossifications are initiated (Tocharus et al., 2004). *Htra3* is essential during placental development and inhibition of *Htra3* in HTR-8 cells (derived from the first trimester placenta) results in an increase in invasion. While exogenous addition of TGFβ1 would be expected to result in a similar effect to the inhibition of *Htra3* in invasion; however, excess of TGFβ1 results in a decrease in placental cell invasion (Singh et al., 2010; Singh et al., 2011). Thus, this finding did not demonstrate the inhibitory effect of HTRA3 on TGFβ1 (Singh et al., 2010). *Htra3* is downregulated in lung cancer with smoking leading to methylation induced gene silencing of *Htra3* (Beleford et al., 2010a). Overexpression of *Htra3* promotes etopside- and cisplatin-induced apoptosis in lung cancer cells. Interestingly, mac-25 domain deletion variant of HTRA3 attenuated cell survival and caused greater induction of apoptosis than the full length HTRA3 (Beleford et al., 2010b). *Htra3* expression is significantly downregulated during osteogenic differentiation *in vitro* (Filliat et al., 2017). However, the role of *Htra3* in osteogenic differentiation is yet to elucidated.

Previous thesis work from our lab has identified *Htra3* as a downstream target of *Hoxa2* during spinal cord development. *HOXA2* binds to the fifth intron of *Htra3* gene and inhibits *Htra3* gene expression (Yan., 2008). It remains to be characterized whether *Htra3* or any of the Htra family members are direct downstream targets of *Hoxa2* in other regions during development, including the secondary palate.

Preamble to Chapter 3: *Hoxa2* inhibits osteogenic differentiation of the palatal mesenchyme via BMP signaling

Rationale

A previous work from our group showed that *Hoxa2* is expressed intrinsically in palatal shelves during development and it regulates cell proliferation in the palatal mesenchyme. Furthermore, during craniofacial development, *Hoxa2* inhibits osteogenesis in the second pharyngeal arch and in the calvaria. Given that *Hoxa2* is expressed in the palatal shelves during development, I hypothesized that *Hoxa2* regulates the timing of osteogenic differentiation. I also tested to see if there is any abnormal osteogenic differentiation in the *Hoxa2*$^{-/-}$ palatal shelves prior to elevation at E13.5, which could be causative for cleft palate pathogenesis. Also, I explored the underlying signaling pathway that could be responsible for the aberrant osteogenic differentiation in the palatal mesenchymal cells due to the loss of *Hoxa2*.

Publication

Iyyanar, P. P. R*., and Nazarali, A. J. (2017). *Hoxa2* Inhibits Bone Morphogenetic Protein Signaling during Osteogenic Differentiation of the Palatal Mesenchyme. Front. Physiol. 8, 929.

*Corresponding author

Contribution statement

Paul P. R. Iyyanar designed the study, performed experiments, analyzed data and wrote the manuscript. Adil J. Nazarali was the senior author who conceived, coordinated the study and after his passing away, Paul P. R. Iyyanar corresponded the manuscript for publication.

3. *HOXA2* INHIBITS OSTEOGENIC DIFFERENTIATION OF THE PALATAL MESENCHYME VIA BMP SIGNALING

3.1 Summary

Hoxa2 plays a direct role in secondary palate development and *Hoxa2* null (*Hoxa2*$^{-/-}$) mice exhibit cleft palate due to failure in the elevation of palatal shelves after E13.5. However, the molecular mechanism governing the cleft palate phenotype in *Hoxa2*$^{-/-}$ mice is largely unknown. In this study I report that *Hoxa2* inhibits spatial and temporal osteogenic differentiation in the developing palate by modulating the expression of osteoblast markers. Loss of *Hoxa2* increased the expression of osteoblast markers including *Runx2*, *Alpl* and *Sp7* in the palatal shelves at E13.5 and E15.5. Consistent with this, mouse embryonic palatal mesenchymal (MEPM) cells from *Hoxa2*$^{-/-}$ embryos exhibit increased ossified matrix deposition and mineralization *in vitro*. Moreover, loss of *Hoxa2* results in increased osteoprogenitor commitment and osteoprogenitor proliferation prior to the elevation of palatal shelves at E13.5. Consistent with the upregulation of osteoblast markers, *Hoxa2*$^{-/-}$ palate exhibited higher expression of canonical BMP signaling in *Hoxa2*$^{-/-}$ palatal shelves. Blocking BMP signaling using dorsomorphin restores the increase in cell proliferation and osteogenic differentiation in *Hoxa2*$^{-/-}$ primary palatal mesenchymal cells. Collectively, the data show for the first time that *Hoxa2* regulates palate development by inhibiting osteogenic differentiation of palatal mesenchyme via modulation of BMP signaling in the developing palate.

3.2 Introduction

Cleft palate is one of the most common congenital birth defects in humans with an incidence of 1 in 700 to 1 in 1000 live births and is influenced by genetic and environmental factors (Dixon et al., 2011). In mice, secondary palate development begins at E11.5 and the palatal fusion is complete by E15.5 (Ferguson, 1988). Impairment in any of the aforementioned events during palatogenesis results in cleft palate. The maxillary region comprises of six primordia namely pairs of premaxilla, maxilla and palatine bones, which are all derived from the cranial neural crest cells through intramembranous ossification (Iwata et al., 2010). The palatal bones comprise of the palatal process of the maxilla and the palatal process of the palatine bone constituting the anterior and posterior part of the hard palate, respectively (Baek et al., 2011). While the structural changes during palate development are well defined, there is a scarcity of knowledge on the molecular mechanisms governing the patterning of the palate.

Hoxa2 is the most anteriorly expressed *Hox* gene with its anterior limit at rhombomeres r1/r2 boundary (Krumlauf, 1993). Mutation in the *Hoxa2* gene in humans is associated with cleft palate (Alasti et al., 2008). In the *Hoxa2*$^{-/-}$ mice, cleft palate phenotype had been attributed to the physical obstruction of the tongue preventing elevation and fusion of the palatal shelves above the tongue (Barrow and Capecchi, 1997). Our group previously reported that *Hoxa2* is expressed in the palatal shelves after emerging from the maxillary prominence (Nazarali et al., 2000) and plays a direct role in secondary palate development by regulating cell proliferation (Smith et al., 2008). The palatal shelves from *Hoxa2*$^{-/-}$ mouse embryonic heads devoid of tongue grown in rolling bottle cultures failed to fuse. In addition, knock-down of *Hoxa2* with antisense retroviral infections in the wild type organ cultures resulted in reduced palatal fusion (Smith et al., 2008). Hence, tongue

musculature may not be the reason for the cleft palate phenotype in *Hoxa2*$^{-/-}$ mice (Smith et al., 2008).

Bone morphogenetic protein (BMP) signaling plays a critical role in palate development regulating cell proliferation (Zhang et al., 2002). *Bmp4* is upstream of *Bmp2* to induce proliferation in the palatal mesenchyme and is able to reverse the reduced cell proliferation and cleft palate phenotype in the *Msx1*$^{-/-}$ mice (Zhang et al., 2002). Defective cell proliferation observed in *Pax9*$^{-/-}$ embryos is consistent with the reduced *Bmp4* expression in the palatal mesenchyme at E13.5 (Zhou et al., 2013). Similarly, reduced expression of *Bmp2* is associated with reduced cell proliferation in the palatal shelves of *Hand2* hypomorphic mice (*Hand2*$^{LoxP/-}$) (Xiong et al., 2009). In addition, growing evidence highlight the importance of osteogenic differentiation in the elevation of palatal shelves and abnormal osteogenic differentiation could lead to cleft palate manifestations (Fu et al., 2017; Jia et al., 2017a, 2017b; Wu et al., 2008). BMP signaling is critical for osteogenic differentiation in the palatal mesenchyme (Baek et al., 2011; Hill et al., 2014; Wu et al., 2008), where it is required for the expression of osteoblast markers such as *Runx2*, *Sp7* and *Alpl* (Baek et al., 2011). During craniofacial development, *Hoxa2* restricts the bone mineralization in the calvaria (Dobreva et al., 2006). Moreover, *Hoxa2*$^{-/-}$ mice exhibit ectopic *Runx2*-positive osteogenic center in the second pharyngeal arch that results in duplication of tympanic ring (Kanzler et al., 1998). During palatogenesis, *Hoxa2* appears to be a key regulator, yet the molecular signaling pathways downstream of *Hoxa2* remain largely unknown.

In this study, I used a combination of *in vivo* and *in vitro* approaches to investigate the role of *Hoxa2* in osteoblast differentiation of the palatal mesenchyme. My findings reveal that *Hoxa2* plays a vital role in regulating the spatial and temporal expression of osteoblast markers during

palate development via modulating bone morphogenetic protein (BMP) signaling pathway in the developing palate.

3.3 Materials and Methods

3.3.1 Animals

Wild type and *Hoxa2*$^{-/-}$ embryos were obtained from timed pregnant *Hoxa2*$^{+/-}$ (heterozygous) mice. Genotype was confirmed using PCR as previously described (Gendron-Maguire et al., 1993). This research was approved by the University of Saskatchewan's Animal Research Ethics Board and adhered to the Canadian Council on Animal Care guidelines for humane animal use.

3.3.2 Primary MEPM cell culture and osteogenic induction

Primary MEPM cells were isolated by microdissection of palatal shelves from wild type or *Hoxa2*$^{-/-}$ mouse embryos at E13.5. The palatal shelves were treated with 0.25% trypsin-ethylenediaminetetraacetic acid (EDTA) for 15 min, passed through a 70 µm cell strainer and cultured as monolayer cells (Iwata et al., 2012) in Dulbecco's Modified Eagle's Medium (DMEM): Ham's F12 (DMEM/F12) (1:1) media containing 10% fetal bovine serum (FBS), 1% antibiotic-antimycotic solution (Sigma). Osteogenic differentiation was carried out as described previously (Kwong et al., 2008) with minor modifications. Briefly, MEPM cells were seeded on 0.1% PDL-coated plates at a cell density of 5×10^4 cells per well in 24 well plates and cultured until they reached confluence. Osteogenic differentiation was induced with osteogenic differentiation media (DMEM, 10% FBS, 2 mM L-glutamine and 1% antibiotic-antimycotic solution) supplemented with osteogenic inducing agents, including 50 µg/ml L-ascorbic acid 2-phosphate sesquimagnesium salt (Sigma), 10 mM β-glycerophosphate (Sigma) and 100 nM dexamethasone

(Sigma). Cells were differentiated for up to 21 days (d). In case of dorsormorphin treatment, MEPM cells were treated with 5 µM final concentrations of dorsomorphin or dimethyl sulfoxide (DMSO) and the cells were harvested for RNA isolation or fixed for alkaline phosphatase (ALPL) staining at d8.

3.3.3 ALPL staining

ALPL staining in the palatal shelves *in vivo* was carried out as previously described (Baek et al., 2011). Embryonic mouse heads were fixed overnight in freshly prepared 4% paraformaldehyde at 4°C. Frozen coronal sections (10 µm) were prepared on slides coated with 0.5% gelatin. The sections were air dried for at least 2 hours (h) and then rehydrated with TBS with 0.08% tween-20 twice for 10 min each. Subsequently, the sections were treated with ALPL buffer (100 mM NaCl, 100 mM Tris–HCl pH 9.5, 50 mM MgCl2, 0.1% Tween-20) for 20 min and stained with 4.5 µl/ml of 5-Bromo-4-chloro-3-indolyl phosphate (Roche) and 3.5 µl/ml of nitro blue tetrazolium (Roche) in alkaline phosphatase buffer for 10 min. The reaction was stopped with phosphate buffer saline (PBS) containing 20 mM (EDTA) buffer and counter stained with nuclear fast red stain. The stained sections were dehydrated in a series of PBS/ethanol, ethanol/xylene and finally mounted in DPX mounting media (Sigma). In primary MEPM cells, ALPL staining was carried out after fixing the cells with 4% paraformaldehyde for 15 min.

3.3.4 Alizarin red (ARS) staining and quantification

The ARS staining and quantification was carried out according to the method of Gregory *et al*., 2004, with minor modifications. Briefly, monolayer MEPM cells were fixed in 4% paraformaldehyde for 15 min and stained with 250 µl of 40 mM ARS (Sigma) solution (pH 4.1) at room temperature (RT) for 20 min with gentle shaking. Excess dye was aspirated and washed

with deionized water before imaging. ARS quantification was carried using an acid extraction method (Gregory *et al*., 2004). Standard plot of ARS concentration was constructed by serially diluting the 40 mM ARS in the buffer containing 10% (v/v) acetic acid and 10% (v/v) ammonium hydroxide. The absorbance values of the standard concentrations were used to interpolate the concentrations of the test samples.

3.3.5 Quantitative real-time polymerase chain reaction (qPCR)

Total RNA from the micro-dissected palatal shelves was isolated using RNA mini spin column (Bio-Rad) as per the manufacturer's protocol. First strand complementary DNA (cDNA) synthesis (reverse transcription) was performed in 20 µl reactions with 500 ng of total RNA using High-Capacity complementary DNA Reverse Transcription Kit (Invitrogen). qPCR was carried out by according to Thangaraj *et al.,* (2017) using SYBR green (Applied Biosystems) in 7300-real time PCR system (Applied Biosystems) with primers listed in Table 3.1.

3.3.6 Western Blotting

Western blot analyses were carried out as previously described (Brown and Nazarali, 2010). Briefly, palatal tissues were homogenized in radioimmunoprecipitation assay buffer (RIPA) buffer. Total protein content was quantified using the Bradford assay and proteins were separated in 10% sodium dodecyl sulfate (SDS)-polyacrylamide gel. Primary antibodies used were: RUNX2 (1:500; Abcam), SP7 (1:1500; Abcam), pSMAD 1/5/8 (1:500; Cell signaling), SMAD 1/5/8 (1:500; Santa Cruz Biotechnology) and β-ACTIN (1:2000; Developmental Studies Hybridoma). Densitometric analyses were carried out using AlphaView software.

3.3.7 Immunohistochemistry

Embryonic mouse heads were fixed overnight in freshly-prepared 4% paraformaldehyde and rehydrated in 30% sucrose at 4°C. Frozen coronal sections (10 μm) were rehydrated with PBS for 45 min, pre-permeabilized with 0.1% Triton-x-100 and blocked with 3% skim milk containing 0.1% Triton-x-100 in 1x PBS for 1 h at RT. Sections were then incubated overnight with RUNX2 (1:200; Abcam) or SP7 (1:800; Abcam) in 1X PBS with 0.1% triton-x-100 at 4° C. Double labeling was carried out by co-incubating: Ki67 (1:100) and RUNX2 (1:200; Abcam) overnight at 4°C. Sections were then washed three times five min each and treated with secondary antibodies conjugated with Alexa Fluor® 488 (1:200) or Alexa Fluor® 594 (1:400) in 1X PBS with 0.1% Triton-x-100 RT for 1.5 h. Cell counting analyses were carried out manually using ImageJ software platform (NIH).

3.3.8 Cell proliferation assay

Cell proliferation assay was carried out in MEPM cells using cell-counting kit-8 (Dojindo) as previously described (Iwata et al., 2010). CCK-8 reagent was added 1 h prior to reading and the absorbance measured at 450 nm was plotted to calculate the relative cell proliferation rate.

3.3.9 Statistical analyses

Statistical analyses were carried out by Prism5 software (Graphpad). Unpaired t-test was used in the case of two groups, one-way ANOVA or two-way ANOVA with Bonferroni multiple comparison test was used where applicable. Data were analyzed and represented as mean ± S.E.M relative to wild type. A p-value of <0.05 was considered significant.

Table 3.1 Primer sequences used for the relative quantification of the transcripts by qPCR using SYBR green assay.

Transcript	**Primer sequences**	**Length (bases)**	**Amplicon size (bp)**
Alkaline phosphatase (*Alpl*)	CCTTGACTGTGGTTACTGCT CCTGGTAGTTGTTGTGAGCG	20 20	216
Bone morphogenic protein 2 (*Bmp2*)	CAGTAGTTTCCAGCACCGAA CACTTCCACCACAAACCCAT	20 20	199
Bone morphogenic protein 4 (*Bmp4*)	AGGAAGGAGTAGATGTGAGAG AGGGACGGAGACCAGATAC	21 19	158
Bone carboxy-glutamic acid containing protein (*Bglap*)	GCAGGAGGGCAATAAGGTAG ATGCGTTTGTAGGCGGTC	20 18	159
CyclinD1 (*Ccnd1*)	ACCCTGACACCAATCTCCTC AAGCGGTCCAGGTAGTTCAT	20 20	214
Sp7 transcription factor (*Sp7*)	CACAAAGAAGCCATACGCTG CCAGGAAATGAGTGAGGGAAG	20 21	165
Runt-related transcription factor 2 (*Runx2*)	TGCCTCCGCTGTTATGAAAA CTGTCTGTGCCTTCTTGGTT	20 20	187
Beta- actin (*β-actin*)	ATTGTAACCAACTGGGACG TTGCCGATAGTGATGACCT	19 19	180

3.4 Results

3.4.1 *Hoxa2*$^{-/-}$ palate exhibits increased expression of osteogenic markers *in vivo*

To understand the cellular and molecular mechanisms underlying the role of *Hoxa2* in palate development, I first examined if the loss of *Hoxa2* leads to changes in the osteogenic differentiation of the palatal mesenchyme using alkaline phosphatase (ALPL; a marker of osteoblast differentiation) staining in E16.5 embryonic palate, a stage when both the prospective palatal processes of the maxilla and the palatine bone evidently ossify (Baek et al., 2010). Results indicate an expansion in the ALPL expression domain in the *Hoxa2*$^{-/-}$ palatal mesenchyme compared to wild type (Figure 3.1A-H). In wild type, at the anterior region of the hard palate, ALPL staining is restricted to the nasal half of the palate in the two condensations of the prospective palatal process of the maxilla on either side of the degraded midline epithelial seam (Figure 3.1A and E). In contrast, the domain of ALPL positive preosteoblast area in the *Hoxa2*$^{-/-}$ palate is increased and expanded towards the oral side covering the nasal-oral axis of the palate (Figure 3.1B and F). In the posterior half of the hard palate, ALPL staining is present in the ossifying centers of the palatal process of the palatine bone in the wild type palate (Figure 3.1C and G), whereas in the *Hoxa2*$^{-/-}$ palate, there is an expansion in the expression domain of ALPL positive preosteoblasts (Figure 3.1D and H).

Runx2 (Komori et al., 1997) and *SP7* (Osterix) (Nakashima et al., 2002) are well-known regulators of osteogenic differentiation and are critical for the patterning of the palatal bones (Baek et al., 2010). Hence, I next investigated if the spatial expression domains of these two osteoblast-specific transcription factors are altered in the *Hoxa2*$^{-/-}$ palate. Immunohistochemical analyses revealed that RUNX2 (Figure 3.1I) and SP7 (Figure 3.1M) are expressed in the condensations of the palatal process of the maxilla at the anterior hard palate in E16.5 wild type embryos, whereas in the *Hoxa2*$^{-/-}$ palate, RUNX2 (Figure 3.1J) and SP7 (Figure 3.1N) expression is increased leading to an expansion in the developing palatal process of the maxilla. In the posterior side along the developing palatal process of the palatine bone, the expression of RUNX2 (Figure 3.1L) is increased; whereas the expression of SP7 (Figure 3.1P), a downstream target of *Runx2* and a marker of mature osteoblasts, was not evidently increased in the *Hoxa2*$^{-/-}$ palate. This suggests

that cells at the oral sides of the *Hoxa2* null palate could be at an immature preosteoblast stage and may not have developed bone matrix yet. Nevertheless, loss of *Hoxa2* resulted in an increase in mRNA expression of osteoblast markers such as *Runx2, Alpl, Sp7* and *Bglap* or *Osteocalcin* (*Ocn*) in the *Hoxa2*$^{-/-}$ palate at E13.5 (Figure 3.2A-D) and E15.5 (Figure 3.2E-H). At E13.5, compared to the wild type, *Runx2*, *Alpl* and *Sp7* mRNA expression was increased to ~6.36, ~9.65 and ~2.62-fold, respectively, in *Hoxa2*$^{-/-}$ palate; in contrast, mRNA expression of *Bglap* was not significantly altered. At E15.5, loss of *Hoxa2* upregulated the mRNA expression of *Runx2* ~1.86-fold; *Alpl* ~2.29-fold; *Sp7* ~1.42-fold and *Bglap* ~3.27-fold. Consistent with this, protein expression of RUNX2 was upregulated ~1.4-fold at E13.5 and E15.5 (Figure 3.2I and J), whereas SP7, both long (Figure 3.2I and K) and short isoforms (Figure 3.2I and L) were upregulated ~1.4-fold at E15.5. These data indicate that *Hoxa2* could be a potential inhibitor of osteoblast differentiation in the palatal mesenchyme by spatially restricting the expression of osteoblast markers in the palate during development *in vivo*.

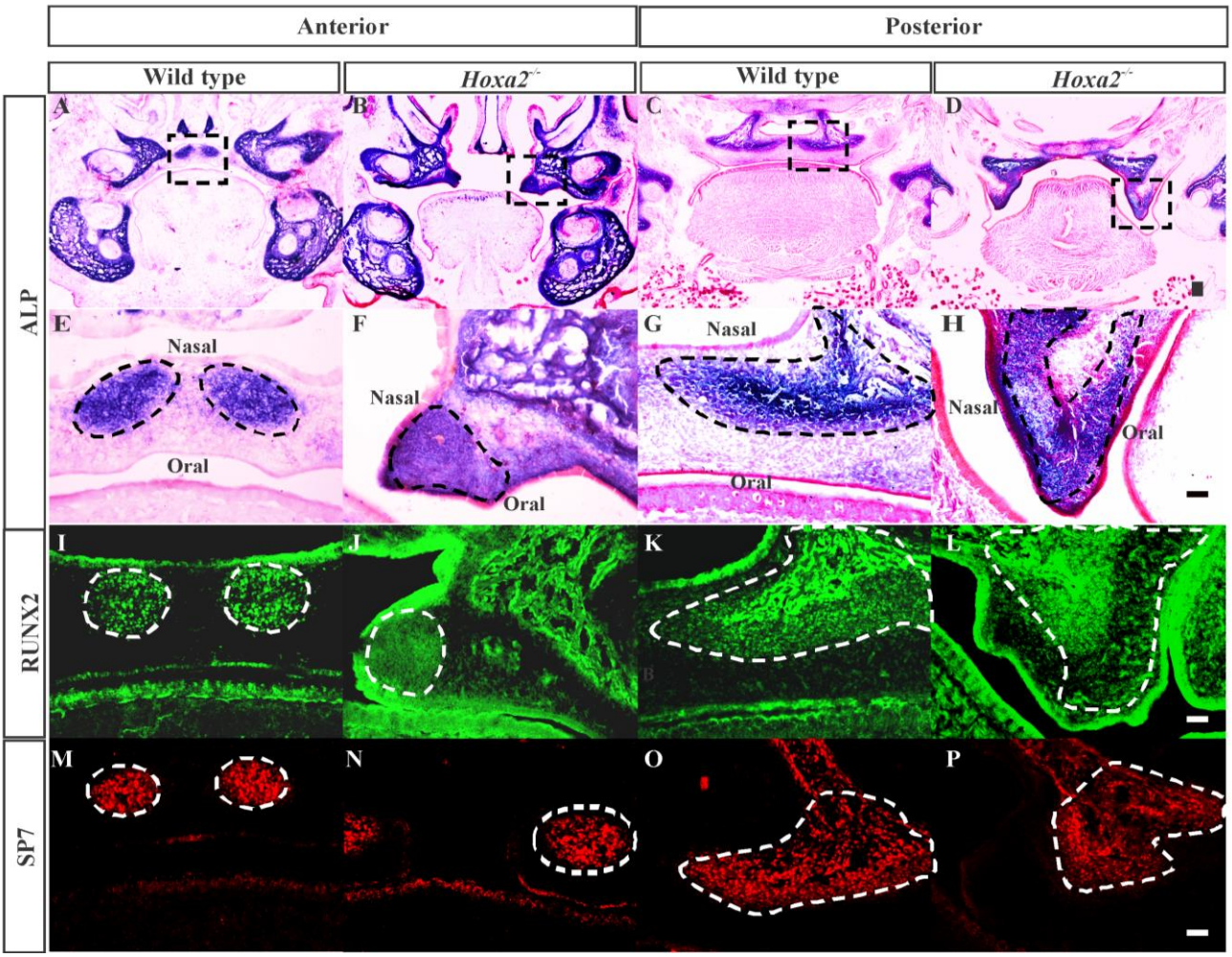

Figure 3.1 Loss of *Hoxa2* leads to increased osteogenic differentiation of the palatal mesenchyme at E16.5. Position matched coronal sections of wild type and *Hoxa2*$^{-/-}$ embryos at E16.5 were stained for ALPL (A-H), RUNX2 (I-L) and SP7 (M-P). Sections in the anterior region (A, B, E, F, I, J, M and N) were through the middle of the first molar tooth bud to detect osteogenic condensation of the palatal process of the maxilla. Sections in the posterior region (C, D, G, H, K, L, O and P) were through the osteogenic centers of the developing palatal process of the palatine bone. A-D, ALPL staining (blue) counterstained with nuclear fast red. Scale bar, 100 µm. Boxed regions in A-D are enlarged (E-H). Scale bar, 50 µm. E and F, in the anterior hard palate, ALPL staining in the two condensations of the palatal process of the maxilla is marked in black dotted lines in wild type (E) and is evidently increased in the *Hoxa2*$^{-/-}$ embryos (F). G and H, in the posterior hard palate, ALPL stained developing palatal process of the palatine bone (marked in black dotted lines) in the *Hoxa2*$^{-/-}$ embryos (H) is increased compared to the wild type (G). I-P, Immunohistochemical analyses of RUNX2 (green; I-L) and SP7 (red; M-P) in wild type and *Hoxa2*$^{-/-}$ palate at E16.5. RUNX2 is increased in both anterior (J) and posterior regions (L) of the *Hoxa2*$^{-/-}$ palate. SP7 was upregulated only in the anterior hard palate (N). Scale bar, 50 µm.

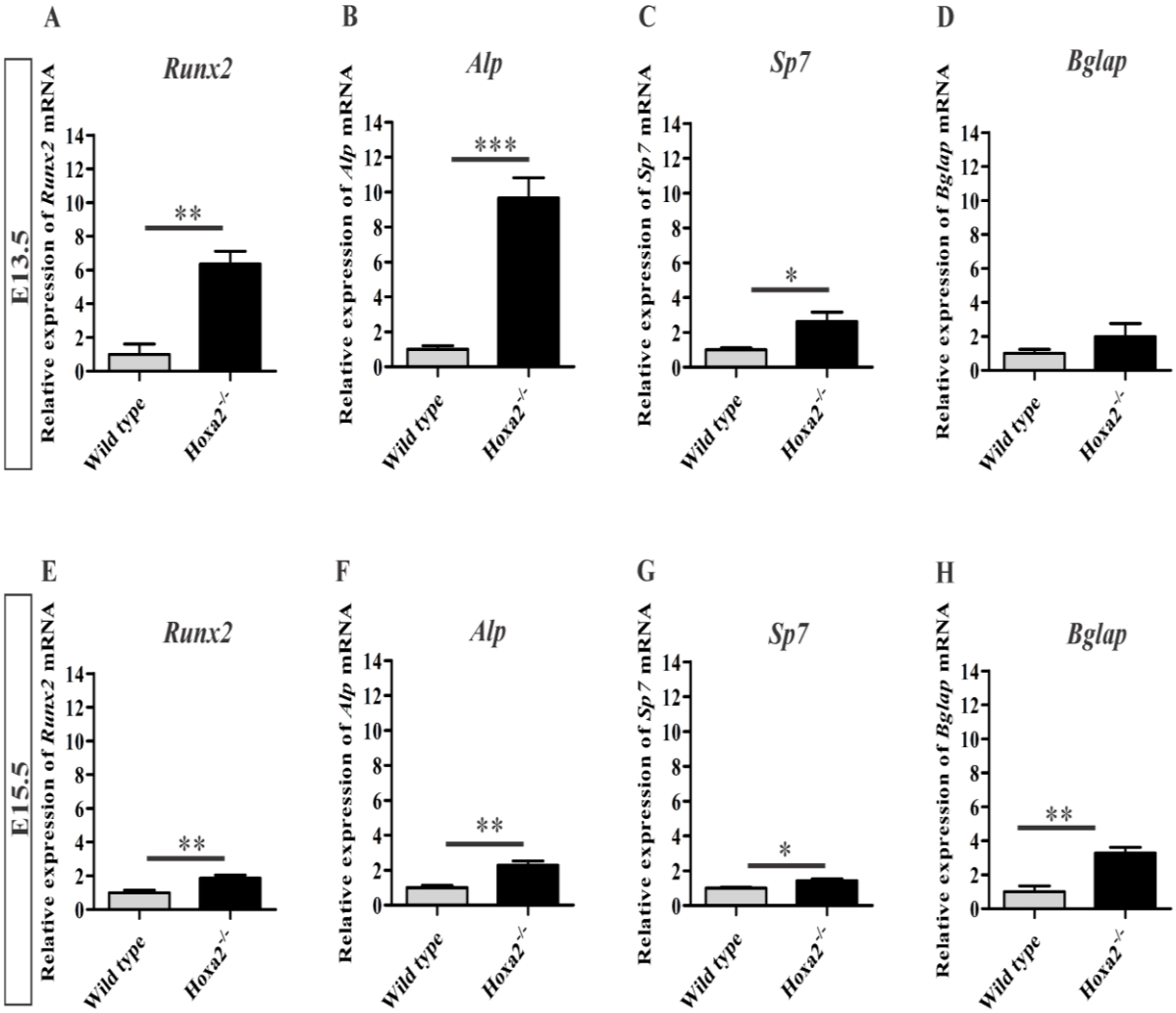
A
B
C
D
E13.5
Runx2
Alp
Sp7
Bglap
Relative expression of Runx2 mRNA
Relative expression of Alp mRNA
Relative expression of Sp7 mRNA
Relative expression of Bglap mRNA
**
***
*
Wild type
Hoxa2-/-
E
F
G
H
E15.5
Runx2
Alp
Sp7
Bglap
Relative expression of Runx2 mRNA
Relative expression of Alp mRNA
Relative expression of Sp7 mRNA
Relative expression of Bglap mRNA
**
**
*
**
Wild type
Hoxa2-/-

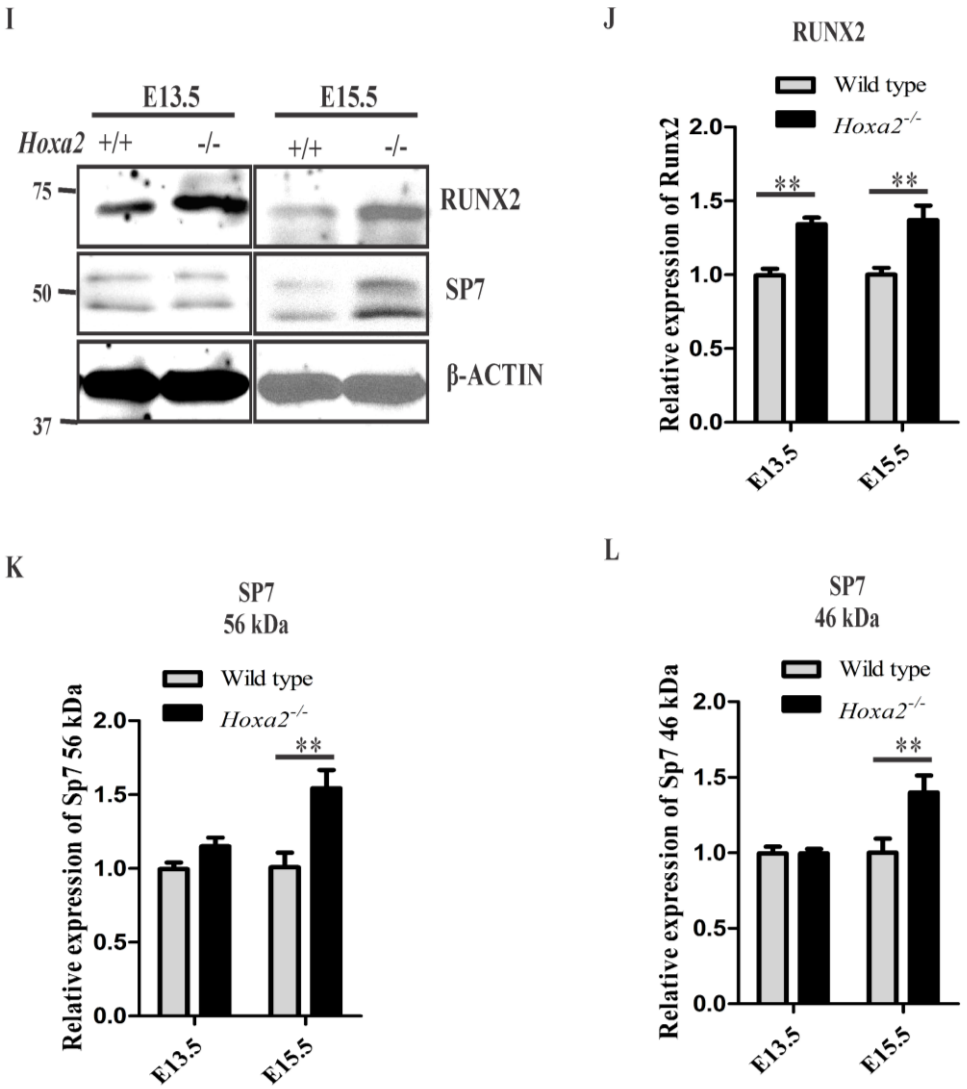

Figure 3.2 Loss of *Hoxa2* leads to increase in quantitative expression of osteogenic markers in the developing palate at E13.5 and E15.5. Quantitative real-time PCR (qPCR) analyses indicate that the gene expression of osteogenic markers such as *Runx2* (A and E), *Alpl* (B and F), *Sp7* (C and G) and *Bglap* (D and H) were upregulated in the developing *Hoxa2*$^{-/-}$ palate at E13.5 (A-D) and E15.5 (E-H). qPCR data (n=5 biological replicates) were normalized to *β-actin* (mean ± S.E.M; unpaired t-test, *, $p<0.05$; **, $p<0.01$; ***, $p<0.001$). Western blot analyses of RUNX2 (I and J) and SP7 (I, K and L) were carried out from the microdissected palatal shelves from wild type and *Hoxa2*$^{-/-}$ mice at E13.5 and E15.5. RUNX2 protein expression was upregulated in the *Hoxa2*$^{-/-}$ palate at E13.5 and E15.5 (I and J), whereas SP7 isoforms are upregulated at E15.5 (I, K and L). Densitometric analyses (n=4 biological replicates) were normalized to β-ACTIN and represented relative to wild type (mean ± S.E.M; unpaired t-test, **, $p<0.01$).

3.4.2 *Hoxa2* inhibits osteogenic differentiation of mouse embryonic palatal mesenchymal (MEPM) cells *in vitro*

Osteogenesis involves sequential stages of proliferation, osteogenic commitment followed by matrix deposition and mineralization (Gordon et al., 2010). To identify the temporal role of *Hoxa2* in osteogenic differentiation of the palatal mesenchyme, the primary mesenchyme cells from the wild type and *Hoxa2*$^{-/-}$ palatal shelves were subjected to osteogenic differentiation *in vitro* for up to d21. The differentiated cells were then stained for ALPL at d8 and ARS staining at d15 and d21. ALPL staining revealed an increase in osteoblast differentiation at d8 in *Hoxa2*$^{-/-}$ MEPM cells compared to the wild type cells (Figure 3.3A and B). In addition, ARS staining and quantification of ARS extracted matrix revealed that *Hoxa2*$^{-/-}$ MEPM cells exhibit increased matrix deposition ~2-fold at d15 (Figure 3.3C, D and G) and mineralization ~1.5-fold at d21 (Figure 3.3E, F and H) compared to the wild type MEPM cells. Next, I examined the gene expression of osteogenic markers in wild type and *Hoxa2*$^{-/-}$ MEPM cells during osteogenic differentiation *in vitro*. The mRNA expression of *Runx2* was increased ~1.9-fold in *Hoxa2*$^{-/-}$ MEPM compared to wild type during osteoblast commitment stage at d8 (Figure 3.3I). Expression of *Alpl* and *Sp7* mRNA in *Hoxa2*$^{-/-}$ MEPM cells were increased ~2.85-fold and ~3.37-fold, respectively, during matrix deposition and maturation stage at d15 (Figure 3.3J and K). Expression of *Bglap* mRNA was increased ~6.37-fold during matrix deposition at d15 and ~8.09-fold during matrix mineralization stage at d21 in *Hoxa2*$^{-/-}$ MEPM cells (Figure 3.3L). Thus, loss of *Hoxa2* results in upregulation of osteogenic marker expression in a stage-specific manner as early as d8 (osteogenic commitment stage) in MEPM cells. These data indicate that *Hoxa2* might play a role in early osteoblast differentiation by inhibiting the expression of osteoblast markers temporally.

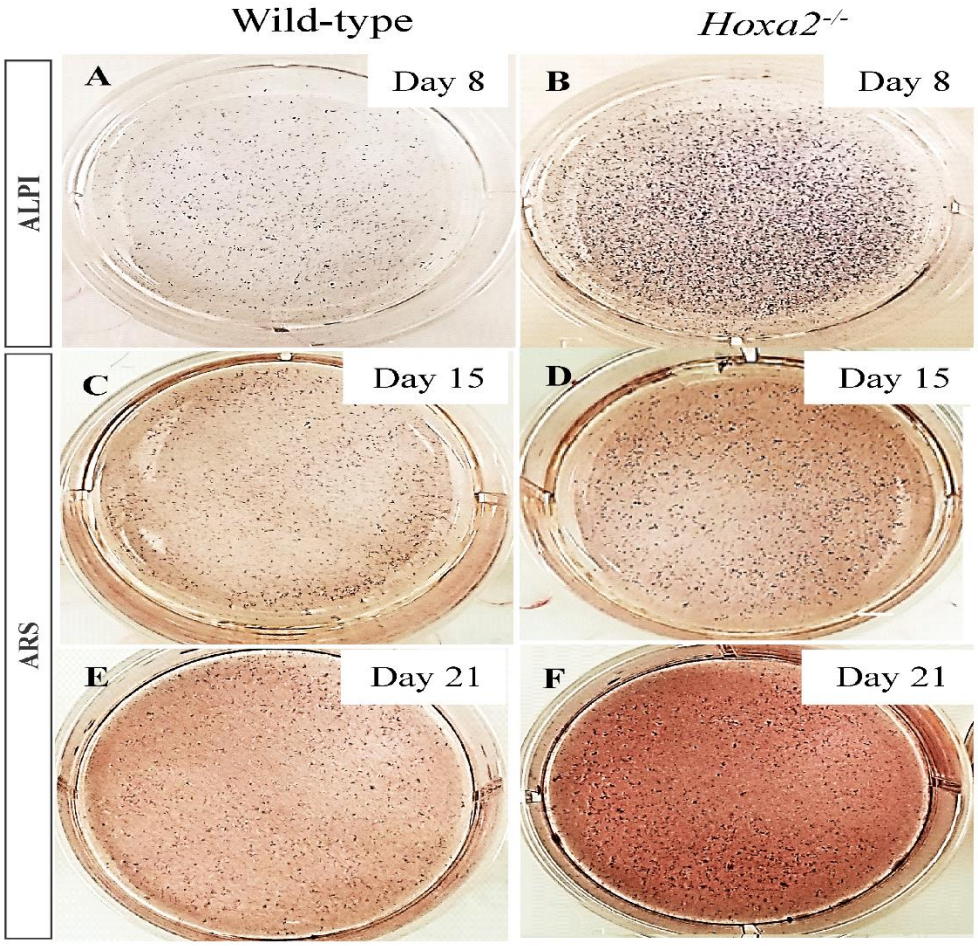
Wild-type
Hoxa2-/-
ALPI
ARS
A
Day 8
B
Day 8
C
Day 15
D
Day 15
E
Day 21
F
Day 21

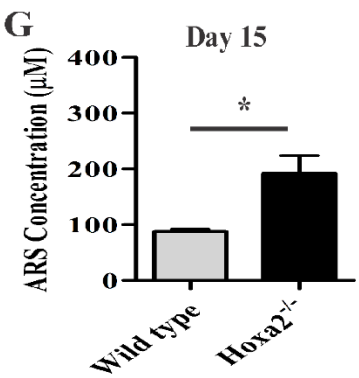
G
Day 15
ARS Concentration (µM)
400
300
200
100
0
*
Wild type
Hoxa2-/-

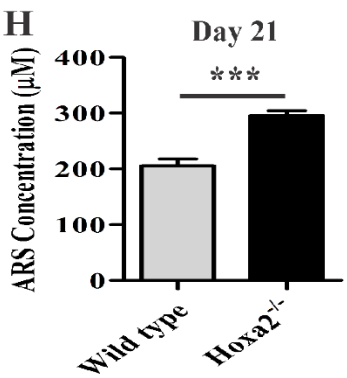
H
Day 21
ARS Concentration (µM)
400
300
200
100
0
***
Wild type
Hoxa2-/-

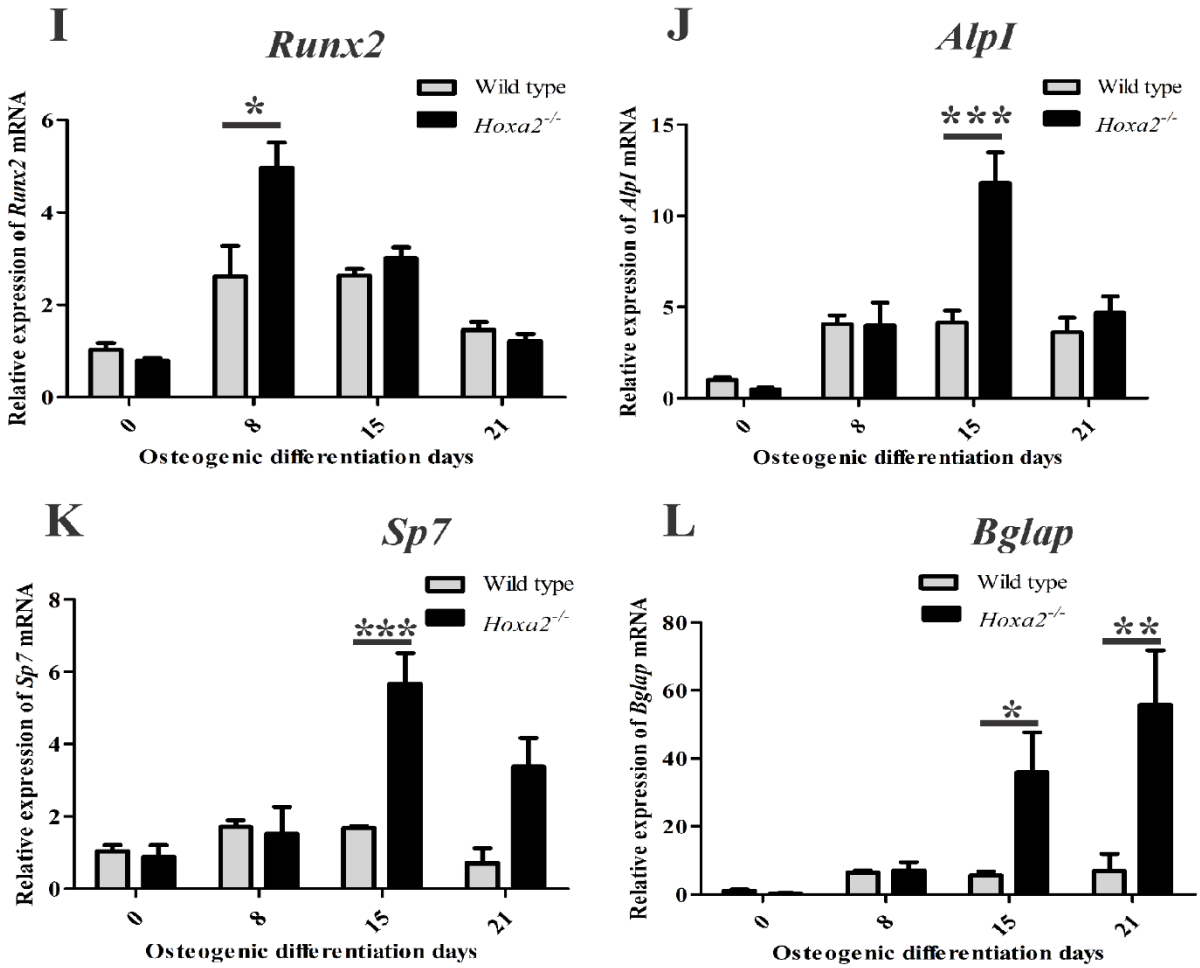

Figure 3.3 *Hoxa2* inhibits osteoblast differentiation of MEPM cells *in vitro*. Wild type and *Hoxa2*$^{-/-}$ MEPM cells were allowed to differentiate into osteoblasts for up to 21 days (d). The differentiated cells were stained for ALPL at d8 (A and B), ARS at d15 (C and D) and d21 (E and F). Scale bar, 200 µm. ARS stained osteocyte matrices from wild type and *Hoxa2*$^{-/-}$ MEPM cells were extracted and quantified at d15 (G) and d21 (H) (n=3 biological replicates; mean ± S.E.M; unpaired t-test, *, p<0.05; ***, p<0.001). *Hoxa2*$^{-/-}$ MEPM cells displayed increased matrix deposition and mineralization at d15 (G) and d21 (H), respectively. I-L, qPCR analyses revealed that gene expression of osteogenic markers such as *Runx2* (I), *Alpl* (J), *Sp7* (K) and *Bglap* (L) were upregulated in the *Hoxa2*$^{-/-}$ MEPM cells in a stage-specific manner during osteoblast differentiation. Data was normalized to *β-actin* (n=3 biological replicates; mean ± S.E.M; two-way ANOVA with Bonferroni post-hoc test, *, p<0.05; **, p<0.01; ***, p<0.001) and represented relative to wild type at d0.

3.4.3 Increased osteoprogenitor commitment and cell proliferation in the palatal mesenchyme during early palate development

Hoxa2$^{-/-}$ mice exhibit cleft palate due to failure in the palatal shelves to elevate and reorient horizontally above the tongue (Barrow and Capecchi, 1999). Abnormal osteogenic differentiation could affect palatal shelf elevation and result in cleft palate phenotype (Wu et al., 2008; Fu et al., 2017; Jia et

al., 2017a and b). *Hoxa2* expression peaks in the developing palate at E13.5 (Smith et al., 2009), a stage when the mesenchymal cells simultaneously proliferate and commit to form preosteoblasts of the prospective palatal process of the palatine bone. To gain further insight into the role of *Hoxa2* during palate development, the commitment of mesenchymal cells to osteoprogenitor cells and the mesenchymal cell proliferation rate in E13.5 wild type and *Hoxa2*$^{-/-}$ palatal shelves was examined. ALPL staining (Figure 3.4A and B) and RUNX2 immunohistochemistry (Figure 3.4C and D) was carried out to evaluate osteoprogenitor commitment in wild type and *Hoxa2*$^{-/-}$ palatal shelves. Our results indicate an increase in the expression domain of ALPL (Figure 3.4B) and RUNX2 (Figure 3.4D) in the *Hoxa2*$^{-/-}$ mutants similar to E16.5, whereas in the wild type, ALPL (Figure 3.4A) and RUNX2 (Figure 3.4C) expression were restricted to the bend region in the nasal side of the palate. In addition, the number of RUNX2^{+ve} osteoprogenitor cells in the nasal side of the palatal shelves were significantly higher in the *Hoxa2*$^{-/-}$ mutants (~64%) compared to wild type (~33%) (Figure 3.4J). Next, I assessed the rate of cell proliferation using Ki67 immunostaining in the wild type and *Hoxa2*$^{-/-}$ palatal mesenchyme. The percentage of Ki67^{+ve} cells was significantly increased in the *Hoxa2*$^{-/-}$ palatal mesenchyme (~50%) compared to wild type (~26%) (Figure 3.4E, F and K). In the nasal side of the palatal shelves, the percentage of Ki67^{+ve} cells was ~53%, which was higher in *Hoxa2*$^{-/-}$ mice compared to ~26% in the wild type (Figure 3.4K). Interestingly, in *Hoxa2*$^{-/-}$ palatal shelves, the nasal side mesenchyme displayed higher proliferation rates of ~53% compared to the oral side at ~23% (Figure 3.4K). In addition, the percentage of proliferating osteoprogenitor cells (RUNX2^{+ve}/Ki67^{+ve}) in the nasal side of the *Hoxa2* null palatal shelves was higher (~20%) compared to ~11% in wild type (Figure 3.4G, H and L). Furthermore, the mRNA expression of cyclin D1 (*Ccnd1*), a critical G1 phase cell cycle regulator was also upregulated in the *Hoxa2*$^{-/-}$ palatal shelves from E12.5 to E14.5 (Figure 3.4I), indicating the role of *Hoxa2* as an inhibitor of cell proliferation in the developing palatal shelves. These results indicate that *Hoxa2* plays a critical role by inhibiting osteoprogenitor commitment and mesenchymal cell proliferation during early palate development.

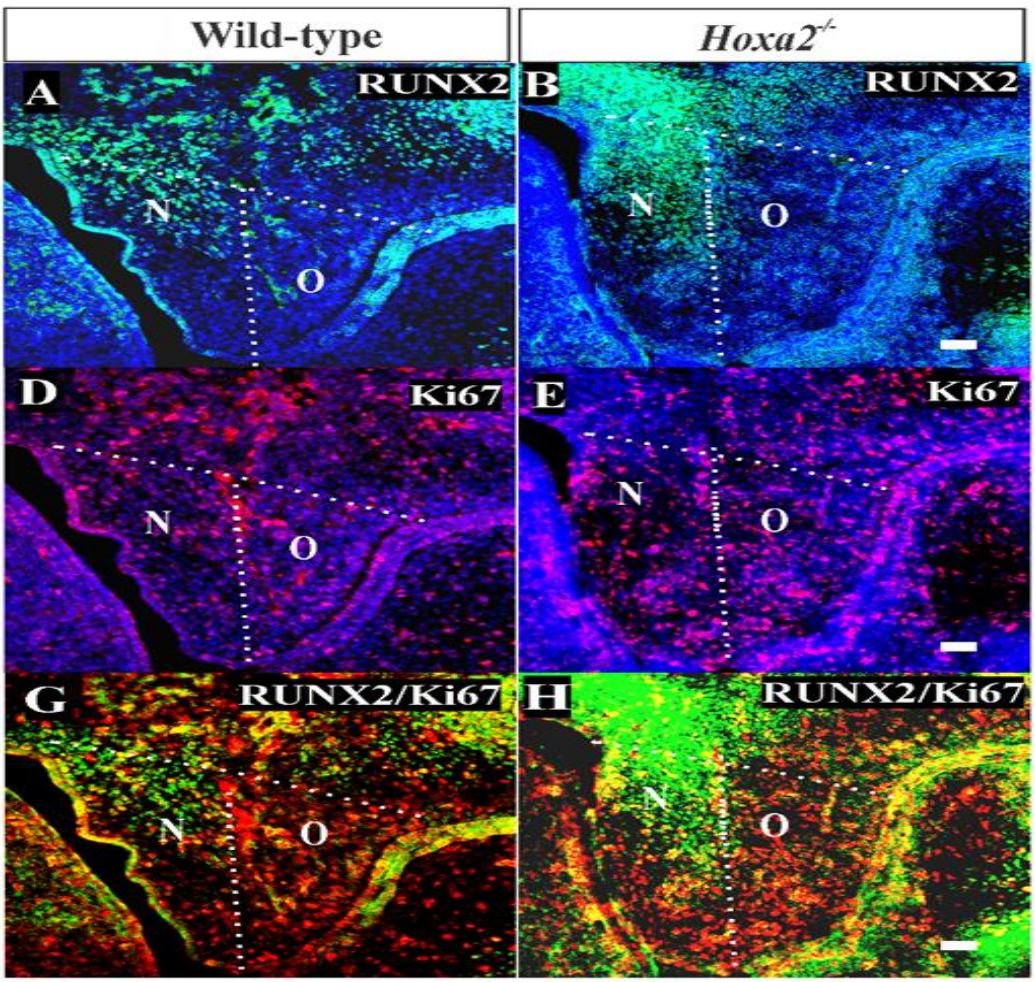
Wild-type
Hoxa2-/-
A
RUNX2
B
RUNX2
N
O
N
O
D
Ki67
E
Ki67
N
O
N
O
G
RUNX2/Ki67
H
RUNX2/Ki67
N
O
N
O

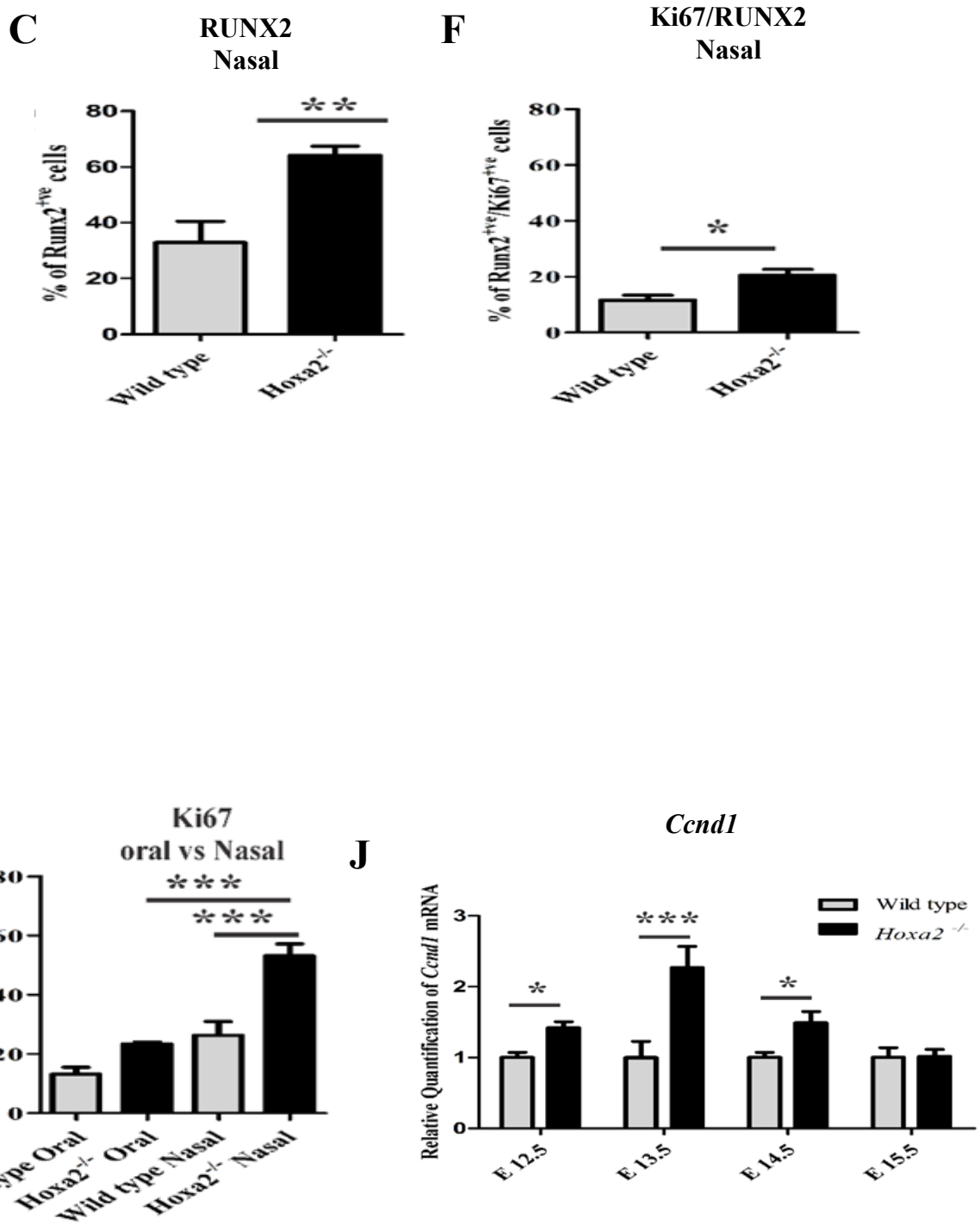

Figure 3.4 *Hoxa2*$^{-/-}$ palatal shelves exhibit increased osteoprogenitor cell commitment and mesenchyme cell proliferation at E13.5. Osteoprogenitor cells in the developing palatal shelves of wild type and *Hoxa2*$^{-/-}$ embryos were stained using ALPL (A and B) and RUNX2 (C and D). Proliferation rate was assessed using Ki67 (E and F) at E13.5. Scale bar, 50 µm; N, nasal; O, oral. Double-positive cells (RUNX2^{+ve}/Ki67^{+ve}) (G and H) amongst a total number of mesenchymal cells (DAPI^{+ve}) from wild type and *Hoxa2*$^{-/-}$ palatal shelves were counted in the nasal side (L). *Hoxa2*$^{-/-}$ embryos exhibit increased RUNX2^{+ve} (J), Ki67^{+ve} (K) and RUNX2^{+ve}/Ki67^{+ve} (L) in the nasal side of the palate (n=5 biological

replicates; mean ± S.E.M; unpaired t-test, *, $p<0.05$; **, $p<0.01$; ***, $p<0.001$). Expression of cell cycle regulator *Cyclin D1* (*Ccnd1*) mRNA was upregulated in the *Hoxa2*$^{-/-}$ palatal shelves (I) from E12.5 to E14.5. qPCR data was normalized to *β-actin* (n=6 biological replicates; mean ± S.E.M; unpaired t-test, *, $p<0.05$; ***, $p<0.001$) and represented relative to wild type at respective embryonic stages.

3.4.4 Increased canonical BMP signaling pathway in the *Hoxa2*$^{-/-}$ palatal shelves

The molecular mechanisms by which *Hoxa2* regulates cell proliferation and osteogenic differentiation remain elusive. Canonical BMP signaling is critical for proliferation (Zhang et al., 2002; Han et al., 2009; Baek et al., 2011) and osteogenic differentiation (Baek et al., 2011; Wu et al., 2008; Hill et al., 2014) in the developing palate. To investigate if canonical BMP signaling is altered in the developing *Hoxa2*$^{-/-}$ palate, the mRNA expression of bmp ligands that are critical for osteoblast differentiation namely, *Bmp2* and *Bmp4,* in the developing palatal shelves were examined. Indeed, the mRNA expression of *Bmp2* (Figure 3.5A) and *Bmp4* (Figure 3.5B) are upregulated by ~3.5-fold and ~4.3-fold, respectively, in the *Hoxa2* null palatal shelves at E13.5. In addition, immunoblotting analyses revealed that canonical BMP signaling mediated by phosphorylated SMAD 1/5/8 (pSMAD 1/5/8) was also upregulated to ~1.5-fold in the *Hoxa2*$^{-/-}$ palate at E15.5 (Figure 3.5C and D). These results indicate that canonical BMP signaling pathway is upregulated and could be responsible for the increased osteoblast differentiation in the *Hoxa2*$^{-/-}$ palate.

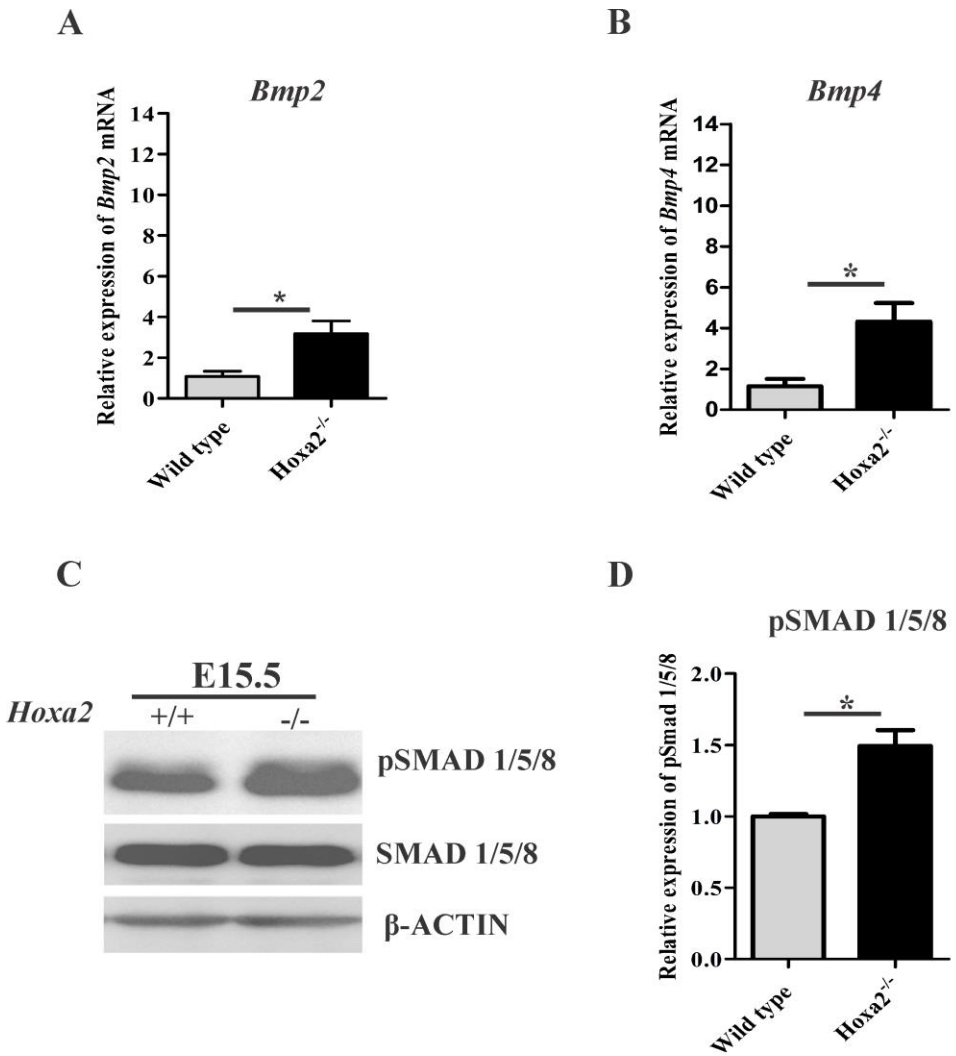

Figure 3.5 *Hoxa2* regulates canonical BMP signaling in the developing palate. Gene expression of Bmp ligands, *Bmp2* (A) and *Bmp4* (B), were upregulated in *Hoxa2*$^{-/-}$ palatal shelves at E13.5. qPCR data (n=4 biological replicates) were normalized to *β-actin* (mean ± S.E.M; unpaired t-test, *, $p<0.05$). Immunoblotting analyses (C and D) of pSMAD 1/5/8 protein from the developing palate of wild type and *Hoxa2*$^{-/-}$ embryos at E15.5. D, Densitometric analysis represents the relative expression of pSMAD 1/5/8 normalized to SMAD 1/5/8 and represented relative to wild type (n=4 biological replicates; mean ± S.E.M; unpaired t-test, *, $p<0.05$).

3.4.5 Blocking canonical BMP signaling rescues aberrant cell proliferation and osteogenic differentiation in *Hoxa2*$^{-/-}$ MEPM cells

To determine if upregulated canonical BMP signaling is functionally responsible for the increased mesenchymal cell proliferation and osteogenic differentiation observed in the *Hoxa2*$^{-/-}$ palate,

dorsomorphin was used to inhibit BMP signaling during osteogenic differentiation of MEPM cells *in vitro.* Upon dorsomorphin treatment, the mRNA expression of *Bmp2* (Figure 3.6A), *Bmp4* (Figure 3.6B) and *Runx2* (Figure 3.6C) upregulated in the *Hoxa2*$^{-/-}$ MEPM cells were restored to the wild type levels. Moreover, increased protein expression of RUNX2 and pSMAD 1/5/8 (Figure 3.6D) in the *Hoxa2*$^{-/-}$ MEPM cells were brought close to wild type levels after dorsomorphin treatment. Furthermore, the increased cell proliferation (Figure 3.6E) and osteogenic differentiation (Figure 3.6F) in the *Hoxa2*$^{-/-}$ MEPM cells were also reduced after dorsomorphin treatment. These results reveal that upregulated canonical BMP signaling is functionally responsible for the increased cell proliferation and osteogenic differentiation in the *Hoxa2*$^{-/-}$ palate.

Together, the data here reveal that *Hoxa2* inhibits cell proliferation and commitment of mesenchymal cells to osteoprogenitor cells in the developing palatal shelves. *Hoxa2* controls the spatial and temporal expression of osteoblast markers by inhibiting BMP signaling for proper patterning of the palatal bones.

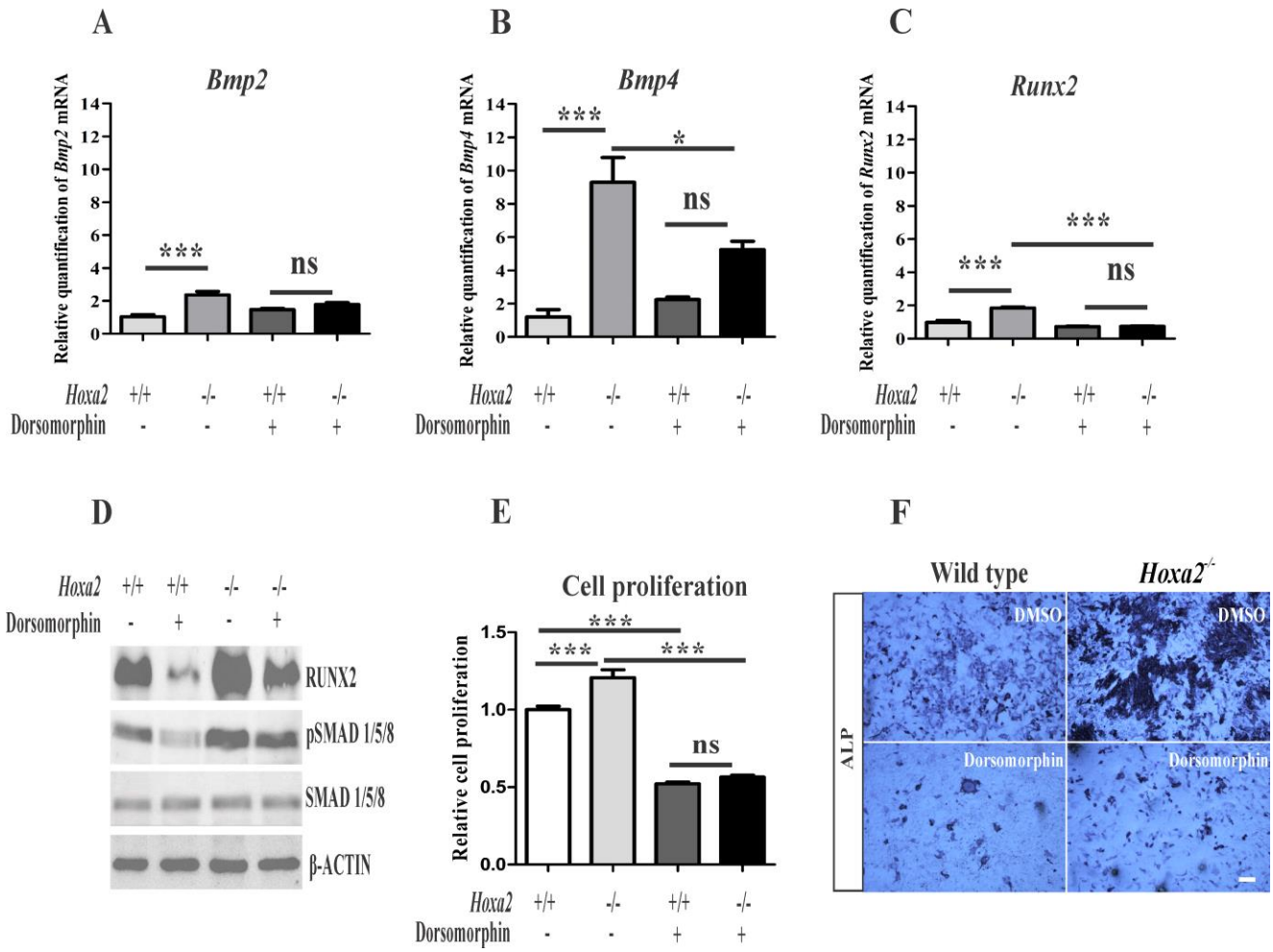

Figure 3.6 Blocking canonical BMP signaling with dorsomorphin rescues the aberrant cell proliferation and osteogenic differentiation in the *Hoxa2*$^{-/-}$ MEPM cells. Dorsomorphin treatment restored gene expression of *Bmp2* (A), *Bmp4* (B) and *Runx2* (C) in *Hoxa2*$^{-/-}$ MEPM cells during osteogenic differentiation *in vitro* at d8. Data represented relative to wild type MEPM cells treated with DMSO (n=4 biological replicates; mean ± S.E.M; one-way ANOVA followed by Bonferroni post-hoc test, *, $p<0.05$; ***, $p<0.001$; ns, not significant). D, Representative immunoblot showing restoration of RUNX2 and pSMAD 1/5/8 in *Hoxa2*$^{-/-}$ MEPM cells treated with dorsomorphin during osteogenic differentiation *in vitro* at d8 (n=3 biological replicates). E, Cell proliferation analysis in the wild type and *Hoxa2*$^{-/-}$ MEPM cells treated with DMSO or dorsomorphin during osteogenic differentiation at d3 (n=5 biological replicates; mean ± S.E.M; one-way ANOVA followed by Bonferroni post-hoc test, ***, $p<0.001$; ns, not significant). F, ALPL staining revealed that treatment with dorsomorphin nullified the aberrant osteogenic differentiation in *Hoxa2*$^{-/-}$ MEPM cells *in vitro* at d8. Scale bar, 200 µm.

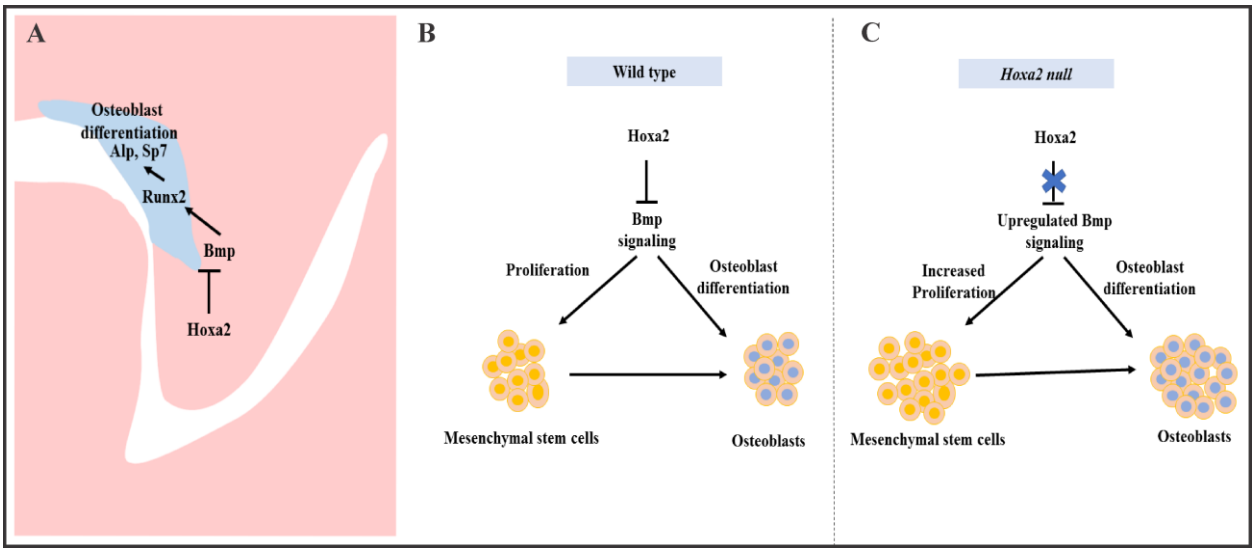

Figure 3.7 Schematic diagram depicting the role of *Hoxa2* in proliferation and osteogenic differentiation of the palatal mesenchyme. A, *Hoxa2* inhibits canonical BMP signaling in the developing palate, which in turn restricts the expression domain of osteogenic markers such as *Runx2*, *Alpl* and *Sp7*. B, in wild type, *Hoxa2* expression peaks during early palatogenesis to control cell proliferation and to maintain mesenchymal cells in an undifferentiated stage by regulating BMP signaling pathway. C, Loss of *Hoxa2* leads to upregulation of BMP signaling resulting in increased cell proliferation and osteogenic differentiation.

3.5 Discussion

Mice lacking *Hoxa2* exhibit cleft palate (Barrow and Capecchi, 1999; Gendron-Maguire et al., 1993; Rijli et al., 1993) and microtia (Minoux et al., 2013), which are consistent with *Hoxa2* mutations in

humans (Alasti et al., 2008). Our group has previously shown that *Hoxa2* is expressed in the palatal shelves during development (Nazarali et al., 2000) reaching a maximal expression at E13.5 and regulates cell proliferation in the developing palate (Smith et al., 2009). There are several lines of evidence that *Hoxa2* regulates palate development intrinsically (Smith et al., 2009), yet the mechanism is largely unknown. In this study, I have found that *Hoxa2* inhibits BMP signaling dependent osteogenic differentiation spatially and temporally to regulate palate formation. The present study deepens the current understanding of the role of *Hoxa2* in palate formation and the mechanisms underlying the cleft palate phenotype in *Hoxa2*$^{-/-}$ mice linking *Hoxa2*, BMP signaling and osteogenesis.

The findings here reveal that *Hoxa2* controls the temporal and spatial expression pattern of osteoblast markers in the developing palatal mesenchyme. Ossifying domains characterized by RUNX2 and ALPL were increased in the palatal process of the maxilla and in the palatal process of the palatine bone in *Hoxa2*$^{-/-}$ mice. In contrast, SP7 a marker of mature osteoblasts was expanded only in the palatal process of the maxilla and not in the palatal process of the palatine bone at E16.5. This suggests that cells towards the oral side of the palatal process of the palatine bone are at an immature osteoblast stage and may not have developed bone matrix by E16.5. Patterning of the palatal process of the palatine bone and of the maxilla are through independent skeletogenic processes (Baek et al., 2011). The palatal process of the palatine bone ossifies at E13.5, whereas the ossification of the palatal process of the maxilla begins only at E15.5. Consistent with this, qPCR and immunoblot analyses revealed a corresponding upregulation of osteogenic markers in the *Hoxa2*$^{-/-}$ palate at these two critical stages E13.5 and E15.5. In addition, primary *Hoxa2*$^{-/-}$ MEPM cells displayed an increase in osteogenic differentiation and a stage-specific increase in the expressions of the osteoblast-specific transcripts indicating that *Hoxa2* regulates temporal differentiation of mesenchyme cells to osteoblasts in the palate. Together, my results reveal that *Hoxa2* functions as an inhibitor of osteogenic differentiation in the palatal mesenchyme during development. The findings from this study are in agreement with previous studies showing the role of *Hoxa2* as an inhibitor of bone formation in other craniofacial regions (Kanzler et al., 1998; Dobreva et al., 2006).

Very little is known about the signaling network downstream of *Hoxa2* during palatogenesis. Here, I have demonstrated that *Hoxa2*$^{-/-}$ palatal shelves exhibit upregulated canonical BMP signaling mediated by pSMAD 1/5/8. In addition, the expression of BMP ligands such as *Bmp2* and *Bmp4* are upregulated in *Hoxa2*$^{-/-}$ palatal shelves *in vivo* and in *Hoxa2*$^{-/-}$ MEPM cells *in vitro*. BMP signaling plays a critical role in proliferation (Zhang et al., 2002; Baek et al., 2011) and osteogenic differentiation of the palatal mesenchyme (Baek et al., 2011; Han et al., 2009; Wu et al., 2008). Importantly, abnormal BMP signaling in the palatal mesenchyme leads to cleft palate manifestation (Zhang et al., 2002; He et al., 2008). Inactivation of *Bmpr1a* in the palatal mesenchyme (*Osr2-IresCre; Bmpr1a*$^{f/f}$) results in submucous cleft palate, absence in the patterning of the palatal process of the maxilla and defective palatal process of the palatine bone (Baek et al., 2011). ChIP-seq analysis revealed that *Bmp2*, *Bmp4* and *Bmpr1a* are possible targets of *Hoxa2* (Donaldson et al., 2012) and HOXA2 protein binds to the intronic region of *Bmp4* (Minoux et al., 2013) in the developing pharyngeal arch2. In this study, dorsomorphin was used to inhibit BMP signaling in the wild-type and *Hoxa2*$^{-/-}$ primary palatal mesenchymal cells during osteogenic differentiation. In this study, dorsomorphin treatment not only rescued the upregulated gene expression of osteogenic factors such as *Bmp2*, *Bmp4* and *Runx2,* but also the aberrant cell proliferation and osteogenic differentiation in the *Hoxa2*$^{-/-}$ MEPM cells. These experiments highlight the involvement of BMP signaling in the abnormal osteoprogenitor cell proliferation and osteogenic differentiation in the *Hoxa2*$^{-/-}$ palate, which could attribute to the cleft palate phenotype in these mutants.

To my knowledge, there is no report available on the characterization of osteoprogenitor cell proliferation and commitment in the palatal mesenchyme during development. In this study, we have unraveled the role of *Hoxa2* in maintaining the palatal mesenchymal cells in an undifferentiated stage by inhibiting osteoprogenitor proliferation and commitment preventing abnormal ossification in the developing palate. Palatal mesenchymal cells derived from cranial neural crest undergo osteogenic proliferation and commit to form osteoblasts (Iwata et al., 2010). Double immunolabeling analyses of RUNX2 and Ki67 at E13.5 revealed that among the total population of mesenchyme cells, there was a significantly higher number of (i) proliferating cells (Ki67-positive cells), (ii) osteoprogenitor cells

(RUNX2-positive cells) and (iii) proliferating osteoprogenitor cells (RUNX2-positive /Ki67-positive cells) in the nasal side of the *Hoxa2*$^{-/-}$ palatal shelves compared to the wild-type. In the palatal mesenchyme, increased or decreased cell proliferation could result in failure of the palatal shelves to elevate and reorient above the tongue leading to cleft palate (Bush and Jiang, 2012; Smith et al., 2013). Recent studies show evidence for abnormal osteogenic signaling prior to the elevation of palatal shelves in several well-studied cleft palate mutant mice models including *Pax9*$^{-/-}$ mice (Jia et al., 2017a and b) and *Osr2*$^{-/-}$ mice (Fu et al., 2017). Consistent with our findings here in the *Hoxa2*$^{-/-}$ mice, *Osr2*$^{-/-}$ exhibit increased osteogenic centers of the palatal process of the palatine bone prior to the elevation of the palatal shelves at E13.5 and in addition to defective cell proliferation, enhanced osteogenesis could contribute to cleft palate phenotype in *Osr2*$^{-/-}$ mice (Fu et al., 2017). In addition, RNA-Seq data from *Osr2*$^{-/-}$ palatal shelves revealed upregulation of several positive regulators of osteogenesis including *Runx2*, *Runx3, Sp7* and Bmp ligands-*Bmp3*, *Bmp5* and *Bmp7*. Furthermore, *Pax9*$^{-/-}$ mice exhibit reduced cell proliferation and osteogenesis in the developing palate (Jia et al., 2017a). Restoration of reduced cell proliferation and osteogenesis by Wnt agonists (Dkk inhibitors) rescued the cleft palate phenotype in *Pax9*$^{-/-}$ mice (Jia et al., 2017a). The increase in cell proliferation in the nasal side of the *Hoxa2*$^{-/-}$ palate indicates a strong role for *Hoxa2* in the spatial maintenance of mesenchymal cells in an undifferentiated state for temporal coordination of osteoblast differentiation (Figure 3.7). The findings here exemplify the regional heterogeneity in proliferation and osteogenic differentiation by *Hoxa2* along the oral-nasal axis in the palatal mesenchyme prior to the elevation of palatal shelves. The data argue that improper BMP signaling leading to the increased osteoprogenitor cell proliferation and commitment could be a reason for the cleft palate pathogenesis in the *Hoxa2*$^{-/-}$ mice. Further studies are needed to address if the cleft palate phenotype in the *Hoxa2*$^{-/-}$ mice could be rescued using other mutant mice with impaired osteogenesis.

The data demonstrate that *Hoxa2* inhibits osteoprogenitor cell proliferation and osteogenic commitment via modulating BMP signaling in the mouse embryonic palatal mesenchyme. *Hoxa2* regulates spatial and temporal programs of osteogenesis by maintaining mesenchymal cells in an undifferentiated stage until osteogenic clues arrive. In conclusion, the findings from this study provide

new insights into the signaling mechanism underlying the role of *Hoxa2* during embryonic palate development.

Preamble to Chapter 4: Expressions of *Htra1* and *Htra3* increase during mouse palatogenesis and *Htra3* expression in the palatal epithelium may be indicative of its role in palatal fusion

Rationale

In the previous chapter, I demonstrated the role of *Hoxa2* in osteogenic differentiation of the palatal mesenchyme. In pursuit of identifying targets of *Hoxa2* during palatogenesis, this chapter explores the temporal and spatial expression pattern of a serine protease *Htra3*, which was identified as a direct target of *Hoxa2* in spinal cord during development. HTRA family members, *Htra1* and *Htra3,* are known to influence TGFβ signaling. In this transitioning chapter, I examined the mRNA and protein expression profile of Htra1 and Htra3 in comparison with TGFβ1 and TGFβ3 across the palate development stages E12 to E15. This chapter provides a novel expression pattern of *Htra3* in the developing palate and gives directions on the speculative role of *Htra3* during palatogenesis.

Contribution statement

Paul P. R. Iyyanar designed the study, performed experiments, analyzed data in this chapter. Adil J. Nazarali conceived, coordinated the study. These data have not yet been submitted for any publication.

4.0 EXPRESSIONS OF *HTRA1* AND *HTRA3* INCREASE DURING MOUSE PALATOGENESIS AND *HTRA3* EXPRESSION IN THE PALATAL EPITHELIUM MAY BE INDICATIVE OF ITS ROLE IN PALATAL FUSION

4.1 Summary

HTRA are a conserved family of serine proteases involved in several cellular processes. Among HTRA proteases, HTRA1 and HTRA3 are reported to bind and inhibit transforming Growth Factor β (TGFβ) signaling. TGFβ signaling plays a vital role in palatal development and perturbing TGFβ signaling leads to cleft palate in mice. I examined the expression of *Htra3* in developing mouse secondary palate using quantitative PCR, western blot and immunohistochemistry. *Htra3* mRNA and protein increase from E12 to E15 and are highest at E15 during which the palatal shelves fuse. Immunohistochemistry showed that HTRA3 is exclusively expressed in the palatal epithelia at E13.5 and at the midline epithelial seam during fusion at E14.5. Interestingly, from E13.5 to E15.5, HTRA3 has similar overlapping expression patterns with TGFβ3. Hence, it is plausible that HTRA3 might mediate TGFβ signaling rather than inhibiting it. To answer this question, I used lentiviral siRNA to silence *Htra3* during palatal fusion in *ex-vivo* organ culture. Despite the efficiency of the siRNA to knockdown *Htra3* in primary palatal epithelial cells *in vitro*, I failed to demonstrate a significant knockdown of *Htra3* mRNA *ex-vivo*, which hindered the identification of a possible role of *Htra3* in palatal fusion. Here, I report the novel expression of HTRA3 in mouse embryonic secondary palate development. The expression of HTRA3 in the epithelium and in osteogenic domains may be indicative of its role in palatal fusion and osteogenic differentiation, respectively.

4.2 Introduction

Several gene networks and signaling pathways have been implicated in governing palate development (Smith et al., 2012). Secondary palate development begins at E11.5 in mice and is complete

by E15.5 (Ferguson 1988). During these stages, the vertical palatal shelves grow, elevate above the tongue, contact with each other resulting in subsequent formation and disintegration of midline epithelial seam. Cleft palate can occur due to failure in any of these events. Proliferation, apoptosis and epithelial-mesenchymal transition mediated by signaling molecules are important for proper palate growth and fusion (Bush and Jiang, 2012).

TGFβ signaling plays a critical role in palate development. TGFβ3 in the palatal epithelia and signaling through the serine threonine kinase receptors namely, TGFβRI and TGFβRIII, are indispensable for phosphorylation of SMAD-2 (Nakajima et al., 2007), activation of matrix metalloproteinases (MMP), *Mmp13* (Blavier et al., 2001) and *Mmp25* transcripts (Brown and Nazarali, 2010), expression of chondroitin sulfate proteoglycan (Gato et al., 2002) and subsequent degeneration of medial edge epithelia (MEE). TGFβ3 is also vital for the inhibition of palatal epithelial proliferation, induction of apoptosis (Cui et al., 2003) and epithelial-mesenchymal transition (Kaartinen et al., 1995).

High temperature requirement factor A, HTRA1 and HTRA3, belong to the conserved family of serine proteases that mediate proliferation, apoptosis and epithelial-mesenchymal transition in cancer as tumor suppressor genes (Chien et al., 2004; Wang et al., 2012; Xia et al., 2013). Both HTRA1 and HTRA3 bind to transforming growth factor beta/bone morphogentic protein (TGFβ/BMP) family members and inhibit signaling of Smad responsive luciferase reporters (Oka et al 2004; Tochorus et al., 2004). Moreover, expression and function of HTRA family of serine proteases has not been determined in the palate. Hence, I sought to delineate the expression patterns and functional role of *Htra3* in developing mouse secondary palate.

4.3 Materials and methods

4.3.1 RNA isolation and qPCR

Total RNA from the micro-dissected palatal shelves was isolated using RNA miniprep kits as per the manufacturer's protocol. First strand cDNA synthesis (Reverse transcription) was performed in 20 µl

reactions with 500 ng of total RNA using QuantiTect Reverse Transcription Kit (QIAGEN) with universal primers.

qPCR was carried out using the E12 to E15 palatal shelves cDNA and SYBR green assay with the 7300 Real Time PCR System (Applied Biosystems) using primers listed in Table 4.1. Relative quantitation values for the secondary palate were obtained in comparison to an E12 sample with values normalized to *beta actin* (*β-actin*). All data are presented as mean ± standard error of mean (SEM). Data was analyzed by one-way ANOVA followed by Bonferroni's multiple comparison test for comparison between the stages (GraphPad Prism) to determine statistically significant difference. A p value < 0.05 was considered significant.

Table 4.1 Primer sequences used for the relative quantification of the transcripts in palatal shelves by qPCR using SYBR green assay.

Transcript	**Primer sequences**	**Length (bases)**	**Amplicon size (bp)**
High temperature requirement factor A1 (Htra1)	AGTTCTTGACAGAGTCCCACGA TATGCCCCAGAGAGCACATCC	22 21	154
High temperature requirement factor A3 (Htra3 short form)	TCTCACCAGCACTGCACT TCTGCCTGCTCCTGTCATCTT	18 21	178
High temperature requirement	CAAGAGGTGGTTCCCAAT	18	181

factor A3 (Htra3 long form)	GGATGATGCTGAAGAGGAGA	20	
Glyceraldehyde 3-phosphate dehydrogenase (Gapdh)	ACCACAGTCCATGCCATCAC TCCACCACCCTGTTGCTGTA	20 20	452
Beta-actin (*β-actin*)	ATTGTAACCAACTGGGACG TTGCCGATAGTGATGACCT	19 19	180

4.3.2 Western blot analysis

Western blot analysis was carried out as previously described (Brown and Nazarali, 2010). Briefly, palatal tissues were homogenized in RIPA buffer (5 mM ethylenediaminetetraacetic acid, 10 mM Tris pH 8.0, 0.1% sodium deoxycholate, 0.01% sodium dodecyl sulfate (SDS), 1% Triton X-100, 150 mM sodium chloride, 1 μg/mL aprotinin, 1 μg/mL pepstatin). Homogenized samples were centrifuged at 11,000 rpm at 4°C for 15 minutes (min). Supernatant total protein content was quantified using Bradford assay (Bio-Rad; Mississauga, ON, Canada) and separated using SDS poly-acrylamide gel electrophoresis with a 10.0% separating gel. Proteins were transferred to a polyvinylidene fluoride membrane. After separation, the proteins were transferred to a polyvinylidene difluoride (PVDF) membrane, which was blocked overnight in 4% skim milk in PBS at 4°C. The membranes were then probed for protein expression with specific primary antibodies: HTRA1 (R&D systems, Minneapolis, MN; 1:3000), HTRA3 (goat polyclonal; Santa-Cruz Biotechnologies, CA; 1:1000) and β-ACTIN (mouse monoclonal; Developmental Studies Hybridoma, IA; 1:2000). This was followed by three consecutive washes of 10 min each in PBST (PBS with 0.08% Tween-20). Horseradish peroxidase (HRP) conjugated species specific secondary antibodies were probed and after four washes of 20 min with PBST, the membranes were then exposed to chemiluminescence reagent for 1-3 min and images were captured in CCD camera. Densitometric analyses were carried out using Alpha View Imaging software. One-way ANOVA followed by Bonferroni's multiple comparison tests for comparison between the stages (GraphPad Prism) to determine statistically significant difference and a p value < 0.05 was considered significant.

4.3.3 Immunohistochemistry

Immunohistochemical analysis was done as previously described (Brown and Nazarali, 2010) with minor modifications. Embryonic mouse heads were preserved in freshly-prepared 4% paraformaldehyde and dehydrated in 30% sucrose at 4°C. Frozen coronal sections (10 μm) were prepared on slides coated with 0.5% gelatin. The sections were air dried for at least 2 h and then rehydrated with PBS twice, each 10 min. Then the sections were blocked with 4% skim milk with 0.1% Triton-X-100 in PBS at RT for 1 h. Primary antibodies were incubated overnight at 4°C with the following dilutions: HTRA3 (Tochorus et al., 2004; 1:500), and TGFβ3 (chicken monoclonal; Developmental Studies Hybridoma, IA; 1:40). The sections were washed with PBS twice for 7 min each time, followed by probing with secondary antibodies labeled with Alexa Fluor® 488 or Alexa Fluor® 594 at RT for 1.5 h, followed by washes with PBS twice for 7 min each time. The sections were then exposed to 30 μl of Hoechst for 15 min followed by followed by washes with PBS twice for 7 min each time. Coverslips were mounted over the sections using ProLong® Gold antifade reagent (Invitrogen). The slides were then imaged using fluorescent microscope (Olympus America Inc., Center Valley, PA).

4.3.4 *In vitro* palatal organ culture

Palatal shelves were cultured based on a modified Trowell type organ culture method as described previously (Shiomi et al 2006; Nakajima et al 2007; Brown and Nazarali, 2010) with minor modifications. Briefly, timed-pregnant C57BL/6J mice were sacrificed at E13.5. Palatal shelves were dissected from the fetal murine head under sterile conditions and placed in pairs on 0.4 μm Millipore filters inserts with correct anterior–posterior orientation and with their medial edges in contact. The palatal shelves were cultured in BGJB medium for 60 h (Gibco) at 37°C with 5% CO_2.

4.3.5 Generation of lentiviral particles

Lentiviral particles expressing green fluorescent protein (GFP) were generated using iLenti-siRNA-GFP vectors as per the manufacturer's protocol (Applied Biological Materials Inc). Briefly, iLenti-siRNA-

GFP vectors carrying *Htra3* siRNA sequences and scramble control siRNA sequence were transformed individually into DH5α cells and selected on Luria Bertani plates containing 50 µg/ml kanamycin. Single colonies were picked and grown overnight in Luria Bertani broth. Plasmid DNA was isolated from the respective cultures using endotoxin free plasmid DNA maxiprep kit (Qiagen). Restriction digestion of the plasmid DNA using *BamHI* was carried out for plasmid containing siRNA sequences and *NheI* and *XhoI* for the mock vector plasmid for the confirmation of the siRNA sequences.

293T cells were co-transfected with plasmid DNA and lentiviral packaging vectors pMD2.G and ps-PAX2 using polyethyleneimine (Addgene) and checked for the expression of GFP in the cells. Lentiviral particles collected after 48 h and 72 h were then concentrated by ultracentrifugation at 25,000 rpm for 2 h at 4°C in SW-25 rotor (Beckman). Lentiviral particles were then titrated using qPCR by a comparative Ct method (Applied Biological Materials Inc). Lentiviral particles were transduced in the palatal shelves in *in vitro* organ culture systems at various infection units (IU) and checked for the expression of GFP in the palatal shelves.

4.3.6 Isolation and primary culture of palatal epithelial cells

Palatal shelves from E13.5 C57BL/6J mice embryos were excised in Hank's balanced salt solution. Palatal shelves were treated using Dispase II (Stemcell technologies, BC) for 1 h at 37°C. Epithelial sheets were removed from the underlying mesenchyme using a fine needle. The epithelial sheets were then pipetted thoroughly and passed through 70 µm cell strainer (BD Falcon) and plated on poly-D-lysine (PDL) coated plates and grown on F12 media containing 10% FBS and 1% penicillin/streptomycin solution. Palatal epithelial cells were used for transduction of lentiviral particles containing *Htra3* siRNA sequences to test the efficiency in knockdown of *Htra3* mRNA.

4.4 Results

4.4.1 *Htra1* and *Htra3* are expressed in developing palatal shelves

HTRA1 and HTRA3 bind to TGFβ/BMP ligands such as TGFβ1, 2, Growth differentiation factor 5 (GDF5) and BMP4 and inhibit downstream signaling *in vitro* (Oka et al., 2004; Tochorus et al., 2004). Given the significant roles of TGFβ/BMP family members in palatal development, I investigated the expression of *Htra1* and *Htra3* in the developing palate. Due to alternative splicing, *Htra3* produces two forms of mRNAs, the long form which is the full-length form and the short form which lacks the c-terminal PDZ domain. Indeed, qPCR reveals that *Htra1* and *Htra3* mRNAs are endogenously expressed in palatal shelves throughout E12 to E15. mRNA expression of *Htra1*, *Htra3* long form and *Htra3* short form increases from E12 to E15 and are highest at E15 (Figure 4.1A-C) during which the palatal shelves fuse. *Tgfβ1* mRNA also increases from E12 to E15, whereas *Tgfβ3* mRNA increases from E12 to E14 and then slightly decreases at E15(data not significant) (Figure 4.2A, B).

Western blot analyses reveal that the expression of HTRA1 (Figure 4.3A, B) protein increases as palatogenesis proceeds from E12 to E15, analogous to the expression of *Htra1* mRNA. Interestingly, two bands of HTRA3 are observed in the immunoblots with a full-length isoform at ~55 kDa and a cleaved isoform at ~27 kDa. Both bands at ~55 kDa and ~27 kDa are upregulated from E12 to E15 in the developing palate (Figure 4.4A-C).

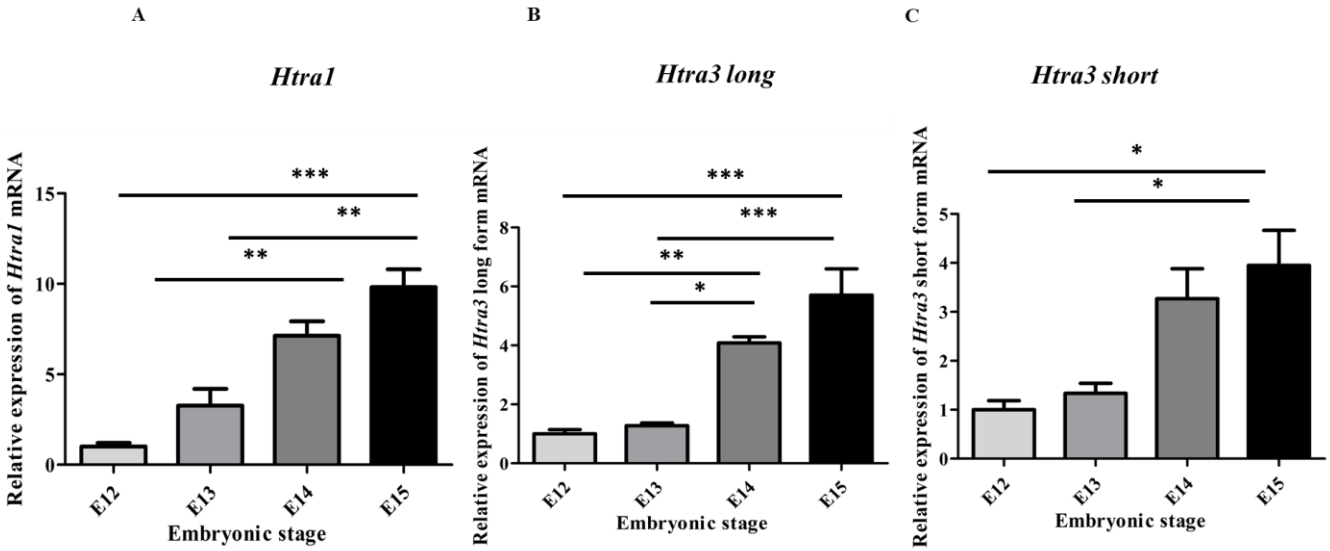

Figure 4.1 *Htra1* and *Htra3* mRNAs increase in developing palatal shelves from E12 to E15. Relative *Htra1* (A), *Htra3* short (B) and *Htra3* long form (C) mRNA expression levels in developing mouse palate were determined by qPCR using SYBR green assay normalized to β-actin. Graphs represent mean ± SEM, n=3. One-way ANOVA to calculate statistical significance and Bonferroni's multiple comparison test for comparison between the stages (* $P < 0.05$, ** $P < 0.01$, *** $P < 0.001$).

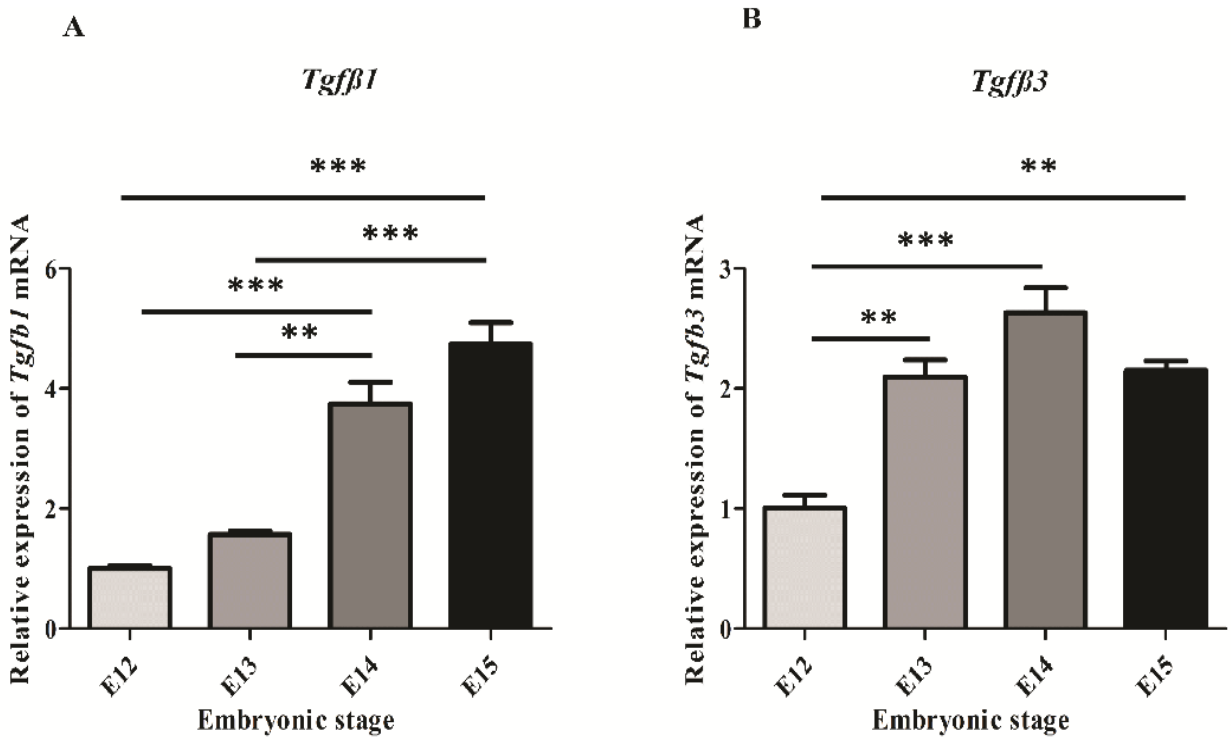

Figure 4.2 *Tgfβ1* mRNA increases from E12 to E15, whereas *Tgfβ3* mRNA increases from E12 to E14 and then decreases at E15. Relative *Tgfβ1* (A) and *Tgfβ3* (B) mRNA expression levels in developing mouse palate were determined by qPCR using Taqman FAM probes, normalized to labelled actin. Graphs represent mean ± SEM, n=3. One-way ANOVA to calculate statistical significance and Bonferroni's multiple comparison test for comparison between the stages (* $P < 0.05$, ** $P < 0.01$, *** $P < 0.001$).

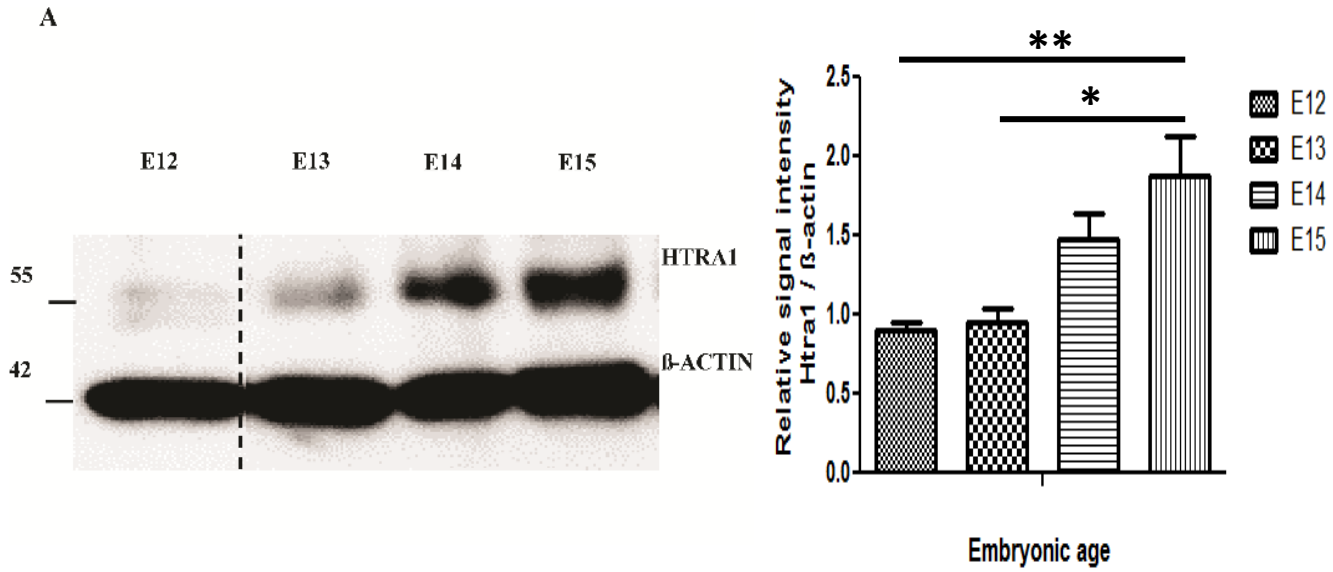

Figure 4.3 HTRA1 protein increases during palatal development from E12 to E15. Western blot analysis of proteins extracted from palatal shelves of E12 to E15 mouse embryos. Proteins (20 µg) were separated on 10% polyacrylamide-SDS gel and transferred to a PVDF membrane and probed with HTRA1 and β-ACTIN antibodies. Densitometry analysis was carried out using AlphaView software and one-way ANOVA to calculate statistical significance and Bonferroni's multiple comparison test for comparison between the stages (* $P < 0.05$, **$P < 0.01$).

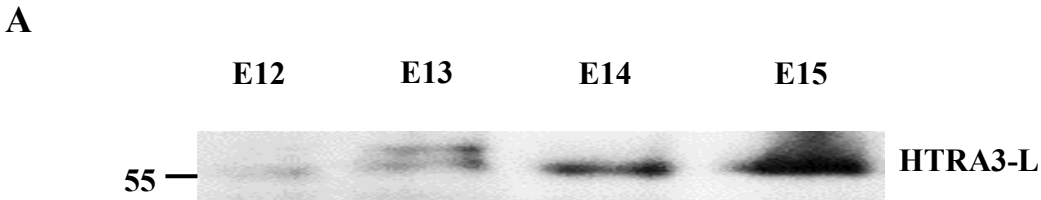

Figure 4.4 HTRA3 protein increases during palatal development from E12 to E15. Western blot analysis of proteins extracted from palatal shelves of E12 to E15 mouse embryos. Proteins (20 μg) were separated on 10% polyacrylamide-SDS gel and transferred to a PVDF membrane and probed with HTRA3 and β-ACTIN antibodies. Densitometry analyses were carried out using AlphaView software and one-way ANOVA to calculate statistical significance and Bonferroni's multiple comparison test for comparison between the stages (* $P < 0.05$, **$P < 0.01$).

4.4.2 HTRA3 and TGFβ3 are co-expressed mainly in the palatal epithelia

Immunohistochemistry shows that HTRA3 is expressed in the epithelia of the palatal shelves at E13.5 (Figure 4.5) and in the midline epithelial seam at E14.5 (Figure 4.6) along the anterior-posterior axis. HTRA3 colocalizes with the epithelial marker E-CADHERIN in the palatal epithelium at E13.5 and E14.5 and at the MES at E14.5 (Figure 4.5 and 4.6). This expression pattern is characteristic of TGFβ3

in the epithelia at E13.5 and in the MES at E14.5 (Figure 4.7). These results show that HTRA3 is expressed in the epithelia in the developing palate and its expression in the MES might be indicative of its role in palatal fusion. In addition, there is a strong staining for HTRA3 in the developing palatal process of the palatine bone at E14.5 (Figure 4.6), which indicates that HTRA3 could also play a role in the ossification of the palatal bones.

4.4.3 *Htra3* siRNA knockdown efficiency in palatal epithelial cells and transduction of lentiviral-GFP particles in palatal shelves organ culture *ex-vivo*

Four sets of lentiviral *Htra3* siRNA sequences in iLenti-siRNA-GFP vectors were purchased and lentiviral particles were produced in house by co-transfecting HEK 293T cells with individual lentiviral siRNA plasmids along with packing vectors pMD2.G and ps-PAX2 (Addgene). Four different siRNA sequences were evaluated for their efficiency to knockdown *Htra3* in palatal epithelial cells. Among the tested siRNAs, siRNA-A showed highest efficiency, with a knockdown of 90% of *Htra3* mRNA in palatal epithelial cells (Figure 4.8A).

Prior to evaluating the efficiency of lentiviral particles to knockdown *Htra3* in palatal shelves in organ culture *in vitro*, 10^7 infection units (IU) lentiviral particles expressing GFP (mock particles) were used to transduce the palatal shelves in organ culture system. After 48 h, the palatal shelves showed intense fluorescence of GFP expressing lentiviral particles (Figure 4.8B). However, repeated attempts of lentiviral siRNA transduction in the palatal fusion culture failed to efficiently silence *Htra3* mRNA in the organ culture. Therefore, the functional role of *Htra3* in the palatal epithelia remains to be characterized.

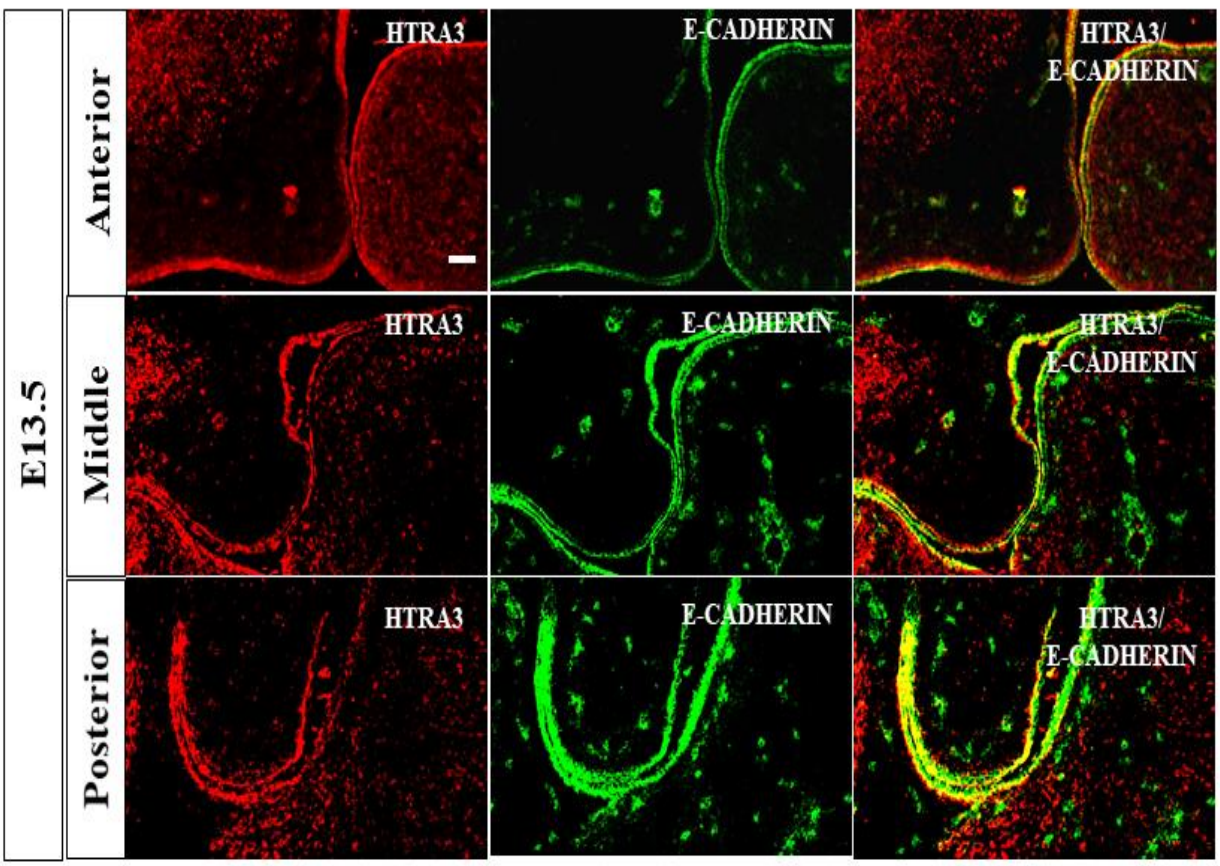
E13.5
Anterior
Middle
Posterior
HTRA3
E-CADHERIN
HTRA3/
E-CADHERIN

Figure 4.5 HTRA3 is expressed epithelia of the palatal shelves at E13.5. Immunohistochemistry staining of HTRA3 and E-CADHERIN in coronal sections of wild type embryonic heads at E13.5. Top row panels are in anterior region of the palate, bottom row panels are in the posterior region of the palate and middle rows are in the middle region of the palate. Scale bar, 50 μm.

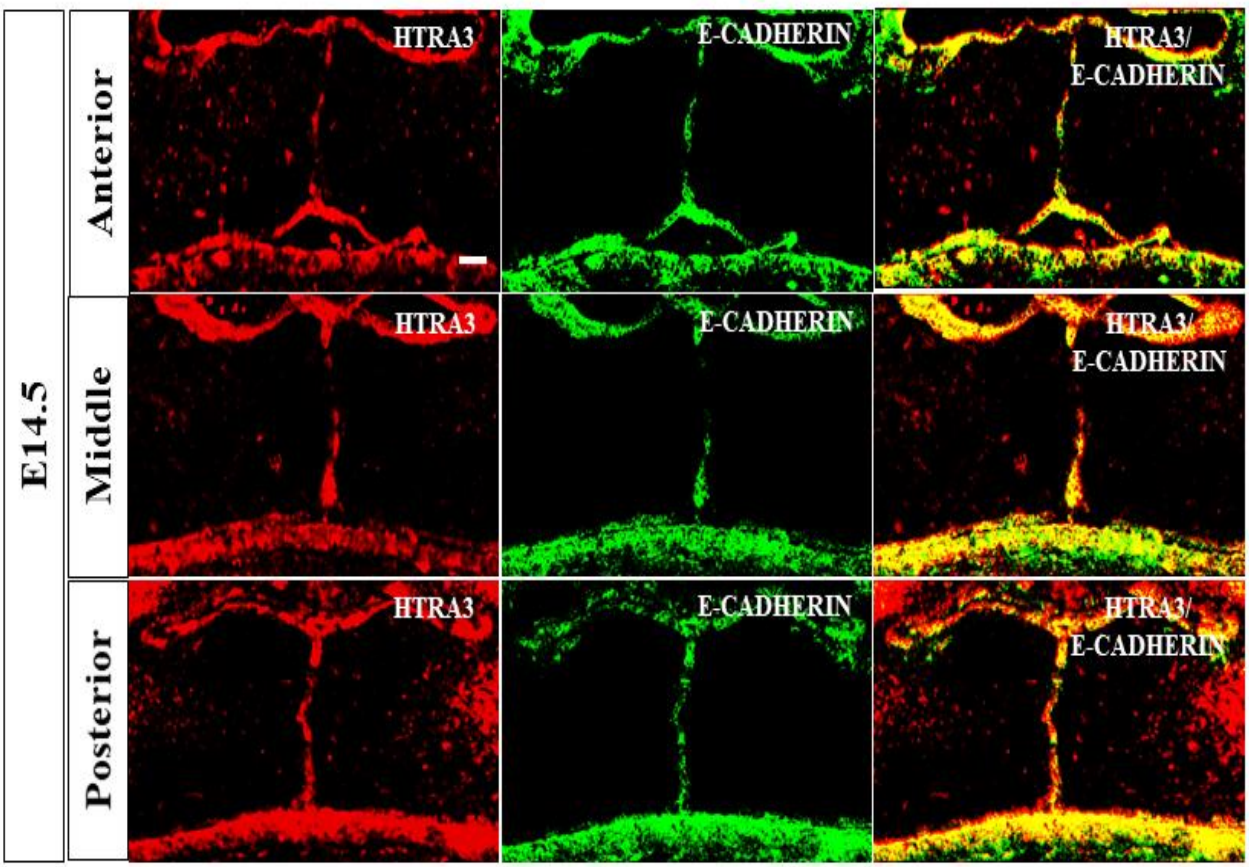

Figure 4.6 HTRA3 is expressed in MES during palatal fusion at E14.5. Immunohistochemistry staining of HTRA3 and E-CADHERIN in coronal sections of wild type embryonic heads at E14.5. Top row panels are in anterior region of the palate, bottom row panels are in the posterior region of the palate and middle rows are in the middle region of the palate. Scale bar, 50 μm.

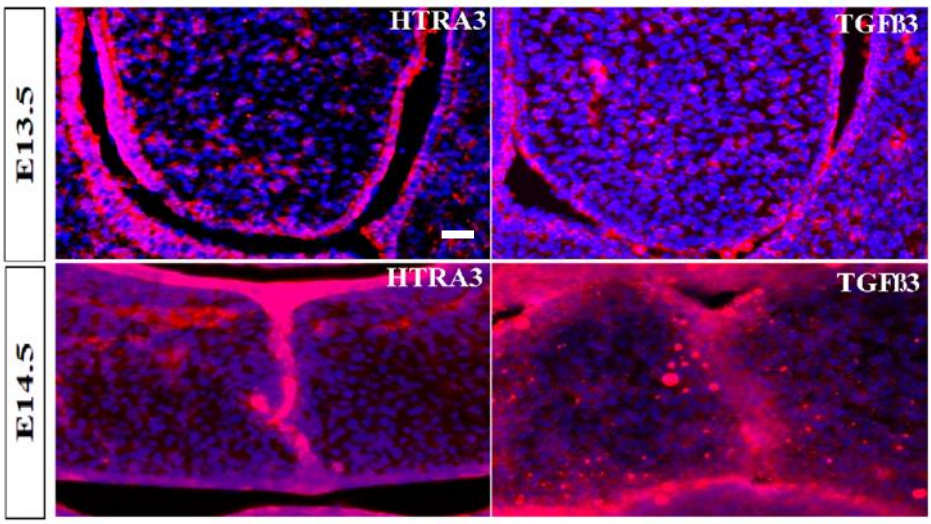

Figure 4.7 HTRA3 and TGFβ3 are co-expressed in the palatal epithelia and MES. Immunohistochemistry staining of HTRA3 and in coronal sections of wild type embryonic heads at E14.5. Top row panels are at the respective immunostaining at E13.5, bottom row panels are at E14.5. HTRA3-positive or TGFβ3-positive cells are stained in red and DAPI-positive nuclei are stained in blue.

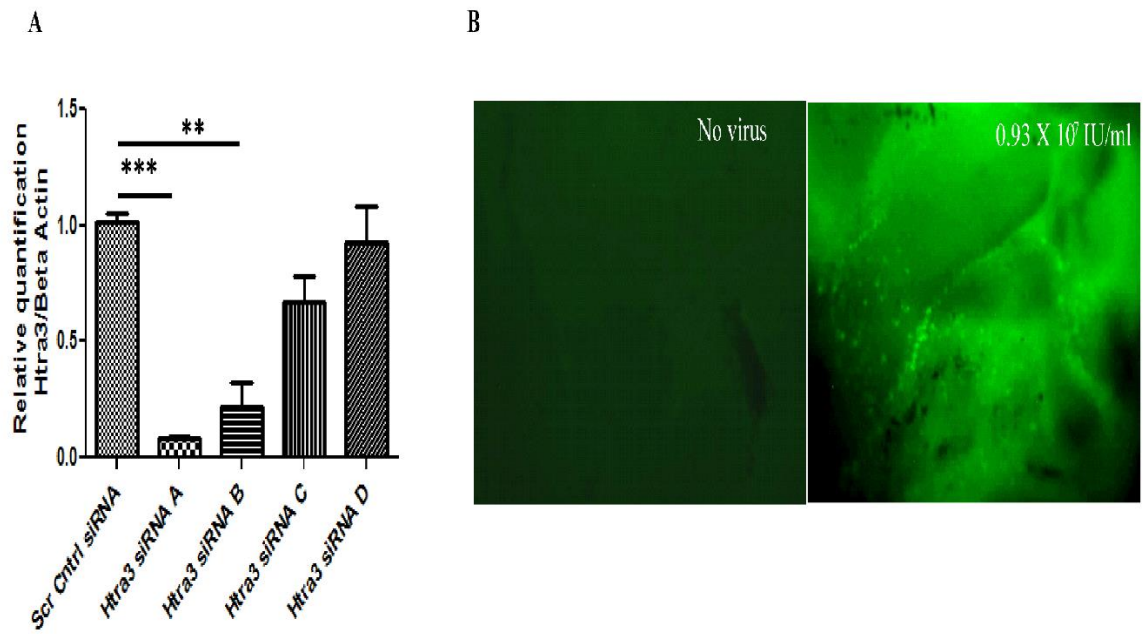

Figure 4.8 Efficiency of Lentiviral siRNA particles in palatal epithelial cells *in vitro* and in palatal shelves in *ex-vivo* organ culture. Palatal epithelial cells were transduced with scramble control siRNA or *Htra3* siRNA A, B, C or D. Relative *Htra3* mRNA expression levels in palatal epithelial cells were determined by qPCR using SYBR green assay normalized to *β-actin* 48 h after transfection. Graphs represent mean ± SEM. One-way ANOVA to calculate statistical significance and Bonferroni's multiple comparison test for comparison between the stages **P < 0.01, ***P < 0.001). E13.5 palatal shelves were transduced with around 10^7 lentiviral IU and grown on organ culture dish for 48 h and then evaluated for the GFP fluorescence. Palatal shelves not transduced with any lentiviral particles served as the control.

4.5 Discussion

The data in this chapter reveal a novel expression pattern of *Htra3* in the developing palate giving insight into the possible role of *Htra3* during palatogenesis. *Htra3* is expressed during the growth, elevation and fusion stages of palate development, with its expression highest during the fusion stages at E15. IHC analysis revealed that HTRA3 protein is expressed principally in the nasal side palatal epithelia, oral side palatal epithelia and in the MEE at E13.5. At E14.5, HTRA3 is expressed in the MES, which starts to degrade due to apoptosis (Cui et al., 2003). *Htra3* is known to induce apoptosis in lung cancer cells (Beleford et al., 2010). It would be interesting to double label activated-CASPASE3 and HTRA3 in the palatal sections at E14.5 to determine whether most of the HTRA3-positive cells are apoptotic in nature in the MES during palatal fusion at E14.5. HTRA3 is also expressed in the developing palatine bone. At E15.5, the palatal process of maxilla starts to ossify and *Htra3* is at its peak during this stage. It is plausible that *Htra3* could be involved in the osteogenic differentiation of the palatal mesenchyme.

The data here indicate that Htra family members- *Htra1* and *Htra3* share similar temporal expression patterns with TGFβ family members. TGFβ3 in the MEE in indispensable for the formation and degradation of MES (Cui et al., 2003). An existing hypothesis suggests that HTRA family members could facilitate TGFβ signaling by cleaving the latent TGFβ binding protein ligands (Beaufort et al., 2014). Therefore, it is possible that *Htra3* could be acting upstream of TGFβ3 to activate downstream signaling for the induction of apoptosis and palatal fusion. In the physiological cleft palate of the chick embryos, the developing palate is devoid of TGFβ3 (Sun et al., 1998). Addition of TGFβ3 to palatal explant cultures *ex-vivo* results in palatal fusion. It would be interesting to check if HTRA3 is expressed in the developing palatal shelves of the avian embryos and whether addition of HTRA3 protein could induce palatal fusion *ex-vivo*, which could be easier to do than lentiviral transduction to silence *Htra3* mRNA *ex-vivo*. The siRNA sequences were validated to silence *Htra3* mRNA *in vitro* in both MEPM (data not shown) and in palatal epithelial cells. Despite multiple attempts to transfect using duplex siRNA and to transduce using lentiviral particles, I failed to demonstrate a consistent knockdown of *Htra3* mRNA *ex-vivo*. This could

be due to the robust elevation in the expression of *Htra3* after E13.5, when the palatal explants are cultured *ex-vivo*. In addition, the expression of *Htra3* from the developing palatal bones could be a hindrance in knocking down *Htra3* expression in the palatal shelves. Furthermore, it is also possible that the multilayered tissue structure might have been a barrier in the diffusion of lentiviral particles along the epithelial layers.

TGFβ signaling inhibits osteogenic differentiation of the palatal mesenchyme (Iwata et al., 2010). The expression of *Htra3* in the osteogenic fronts could be indicative of its role in the osteogenic differentiation of the palatal mesenchyme. It is important to note that *Htra3*$^{-/-}$ mice do not show any bone related abnormalities (Filliat et al., 2017). Expression patterns of *Htra1* and *Htra3* show overlaps temporally across different stages of palate development. Hence, it is possible that *Htra1* and *Htra3* could be redundant in regulating osteogenic differentiation. However, it is also important to note that among the TGFβ ligands, knockin of *Tgfβ1* in the *Tgfβ3* locus could only partially rescue the cleft palate along the anterior-posterior axis in *Tgfβ3*$^{-/-}$ mice (Yang and Kaartinen, 2007). Therefore, it would be intriguing to identify if there is any functional redundancy between *Htra1* and *Htra3* in osteogenic differentiation of the palatal mesenchyme. In addition, the role of *Htra3* in palatal fusion and osteogenic differentiation remains to be characterized.

Preamble to Chapter 5: *Htra1* positively regulates osteogenic differentiation of the palatal mesenchyme and is a direct transcriptional target of *Runx2* during osteogenic differentiation

Rationale

Data emerged from the literature during the progress of this thesis indicating that *Htra1* may not be a direct downstream target of *Hoxa2* during craniofacial development. In addition, a recent report of genome-wide RUNX2 bound regions indicated that *Htra1* may be regulated by RUNX2 during osteogenic differentiation. In the previous chapter, I examined the quantitative mRNA and protein expression profile of Htra1 and Htra3, which increase from E12 to E15. In this chapter, I examine the localization of HTRA1

protein in the developing palate and the role of *Htra1* in osteogenic differentiation. Using pull-down and luciferase assays, I demonstrate the molecular interaction of *Htra1* and RUNX2.

Manuscript

Iyyanar, P. P. R*., Thangaraj, M. P., Eames, B. F., and Nazarali, A. J. *Htra1* is a novel direct downstream target of *Runx2* during osteogenic differentiation. Manuscript to be submitted to Osteoarthritis and Cartilage.

*Corresponding author

Contribution statement

Paul P. R. Iyyanar designed the study, performed experiments, analyzed data and wrote the manuscript. Adil J. Nazarali was the senior author who conceived, coordinated the study and after his passing away, Paul P. R. Iyyanar is responsible for the correspondence of the manuscript for publication. Merlin P. Thangaraj assisted in performing the luciferase assay and osteogenic arrays, while Paul P. R. Iyyanar carried out the experiments. B. Frank Eames was involved in conception of the study and critical analysis of the data and in manuscript revisions.

5. *HTRA1* POSITIVELY REGULATES OSTEOGENIC DIFFERENTIATION OF THE PALATAL MESENCHYME AND IS A DIRECT TRANSCRIPTIONAL TARGET OF *Runx2* DURING OSTEOGENIC DIFFERENTIATION

5.1 Summary

Craniofacial bones are mainly formed via intramembranous ossification. Transcription factor RUNX2 is a master regulator of osteoblast differentiation. The downstream targets of *Runx2* during osteoblastogenesis remain largely unknown. HTRA1 is a serine protease involved in cell survival, proliferation, and apoptosis. However, the role of *Htra1* during osteoblast differentiation remains elusive. In this chapter, I show that *Htra1* is expressed mainly in the ossifying matrix of the craniofacial region during development. Hence, I investigated the role of *Htra1* in osteogenic differentiation of MEPM cells and the regulation of *Htra1* by *Runx2*. The data here show that overexpression of *Htra1* increased the

matrix deposition and mineralization of MEPM cells at d15 and d21, respectively. In addition, overexpression of *Htra1* caused increased mRNA expression of osteoblast markers, *Alpl* and *Sp7* or *Osx* at d8 and d15. Overexpression of *Runx2* resulted in the upregulation of *Htra1* mRNA. Streptavidin agarose pulldown assay (SAPA) using biotin probes (-1000 bp and -400 bp upstream promoter of *Htra1*) showed that RUNX2 interacts with the *Htra1* promoter. Chromatin immunoprecipitation (ChIP) assay further confirmed that RUNX2 protein binds to the proximal -400 bp region of the *Htra1* promoter during osteoblast differentiation. Dual luciferase assay data revealed that *Runx2* significantly increased the luciferase reporter activity of the proximal *Htra1* promoter constructs. Mutation of the putative RUNX2 consensus binding sites revealed that RUNX2 interacts with the *Htra1* promoter at -252 bp and -84 bp to regulate the promoter activity of *Htra1*. These findings suggest that *Htra1* is a positive regulator of intramembranous osteoblast differentiation and is a direct downstream target of *Runx2* during osteoblast differentiation.

5.2 Introduction

Craniofacial bones are mainly formed via intramembranous ossification of cranial neural crest cells, which does not involve formation of an intermediate cartilaginous template (Jiang et al., 2002). The maxillary region comprises of six primordia, which includes pairs of premaxilla, maxilla, and palatine bones (Iwata et al., 2012). Transcription factor RUNX2 is a critical regulator of osteogenic differentiation and *Runx2 null* mutants exhibit complete lack of ossification (Komori et al., 1997). RUNX2 binds to the consensus RUNT binding site RCCRC(A/T) (Kamachi et al., 1990) to bind to the promoter region of several osteoblast regulators for their transcriptional regulation (Roca et al., 2005; Lamour et al., 2007; Li et al., 2011). Several transcriptional targets of RUNX2 during osteogenic differentiation are not yet known and remain to be characterized (Wu et al., 2014a).

HTRA1 is one of the four members of the HTRA family of serine proteases. HTRA1 is more known for its role in age-related macular degeneration (Yang et al., 2006) and cerebral autosomal recessive arteriopathy with subcortical infarcts and leukoencephalopathy (Hara et al., 2009; Mendioroz et al., 2010). HTRA1 is expressed in hypertrophic cartilage and osteoblasts in physiological conditions (Tocharus et al.,

2004) and in disease phenotypes like osteoarthritis bone regions (Tsuchiya et al., 2005) and fracture callus (Tiaden et al., 2012). Silencing of *Htra1* using siRNA inhibits all-trans retinoic acid (ATRA) induced osteogenic differentiation of adipose derived stromal cells (Glanz et al., 2016). Preliminary findings indicate that *Htra1* is a positive regulator of osteogenic differentiation, where it is involved in the lineage commitment of mesenchymal stem cells to form osteoblasts (Tiaden et al., 2012) at the expense of adipogenesis (Tiaden et al., 2016). In contrast, other studies have found *Htra1* as a negative regulator of osteogenesis (Hadfield et al., 2008; Wu et al., 2014). Therefore, the role of *Htra1* in osteogenesis remains unclear and there is limited evidence on the gene networks and signaling pathways both upstream and downstream of *Htra1* in osteogenic differentiation.

Here I investigated the role of *Htra1* in osteogenic differentiation of primary mesenchymal cells *in vitro*. I show that for the first time that RUNX2 binds to two putative consensus bindings sites on the proximal *Htra1* promoter to regulate its expression. In addition, the data show that *Htra1* as a positive regulator of osteogenic differentiation *in vitro*.

5.3 Materials and Methods

5.3.1 Primary cultured cells derived from mouse embryonic palatal mesenchyme (MEPM)

Primary MEPM cells were isolated from palatal shelves of wild type C57BL/6J mice embryos at E13.5. Briefly, palatal shelves were micro-dissected from the maxilla of E13.5 embryos and incubated with 0.25% trypsin (Sigma) for 15 min at 37°C (Iwata et al., 2012). Cells were gently pipetted up and down, passed through 70 µm cell strainer (BD Falcon) and plated on PDL coated T25 flasks. Cells were cultured in (DMEM): Ham's F12 (DMEM/F12) (1:1) media containing 10% FBS, 1% antibiotic-antimycotic solution (Sigma) and passaged three times or less. Osteogenic differentiation was carried out as described previously (Kwong et al., 2008) with minor modifications. Briefly, MEPM cells were seeded on PDL coated 24-well plates at a cell density of 5×10^4 cells per well in triplicate and cultured until they reached confluence. Osteogenic differentiation was induced with osteogenic differentiation media comprising of DMEM with 4,500 mg/L glucose, 10% FBS, 2 mM L-glutamine and 1% antibiotic-

antimycotic solution. Media was also supplemented with osteogenic inducing agents, including 50 µg/ml L-ascorbic acid 2-phosphate sesquimagnesium salt (Sigma), 10 mM β-glycerophosphate (Sigma) and 100 nM dexamethasone (Sigma). Media was changed every third day for up to 8, 14 or 21 days. In the case of all-trans retinoic acid (ATRA) treatment, MEPM cells were treated with 1 µM or 5 µM final concentration of ATRA or vehicle in osteogenic differentiation media with 0.5% FBS. Cells were harvested for RNA isolation or fixed for ALPL staining at day 8.

5.3.2 ALPL staining

MEPM cells were washed once with PBS, pH 7.4, followed by fixation in 4% paraformaldehyde for 15 min and then washed two times with PBS. Cells were subsequently washed with deionized water to remove excess PBS. Cells were then treated with ALPL buffer (100 mM NaCl, 100 mM Tris–HCl pH 9.5, 50 mM $MgCl_2$, 0.1% Tween-20) for 10 min prior to staining with 4.5 µl/ml of 5-Bromo-4-chloro-3-indolyl phosphate (Roche) and 3.5 µl/ml of nitro blue tetrazolium (Roche) in alkaline phosphatase buffer for 10 min. The reaction was stopped with PBS containing 20 mM EDTA buffer.

5.3.3 ARS staining and quantification

ARS staining and quantification was carried out as described in Gregory et al., 2004 with minor modifications. Briefly, monolayer MEPM cells were washed once with PBS, pH 7.4, followed by fixation in 4% paraformaldehyde for 15 min and then washed two times with PBS. Cells were subsequently washed with deionized water to remove excess PBS, prior to the addition of 250 µl of 40 mM ARS (Sigma) solution (pH 4.1). Cells were incubated at room temperature for 20 min with gentle shaking. Excess dye was aspirated and cells were washed with deionized water and imaged. For quantification of ARS, 400 µl of 10% acetic acid (Fisher Scientific) was added to each well and incubation proceeded for 30 min with shaking. The loosely attached monolayer cells were then dislodged using a cell scraper (Fisher Scientific) and transferred to a micro-centrifuge tube containing 10% acetic acid. After vortexing for 30 s, samples were heated at 85°C for 10 min and cooled on ice for another 5 min. The slurry was centrifuged at 15,000 g for 15 min and 300 µl of the supernatant transferred to a new micro-centrifuge tube followed by the

addition of 150 µl of 10% solution of ammonium hydroxide (Sigma). After vortexing, 150 µl was transferred from this mixture to an opaque walled 96-well plate for measurement of absorbance at 405 nm. Standard plot of ARS concentration was constructed by serially diluting 40 mM ARS in a buffer containing 10% (v/v) acetic acid and 10% (v/v) ammonium hydroxide. Absorbance values of standard concentrations were used to interpolate concentrations of the test sample.

5.3.4 Quantitative real-time polymerase chain reaction (qPCR)

Total RNA from the micro-dissected palatal shelves was isolated using RNA mini spin column as per the manufacturer's protocol (BioRad). First strand cDNA synthesis (Reverse transcription) was performed in 20 µl reactions with 500 ng of total RNA using High-Capacity cDNA Reverse Transcription Kit (Invitrogen). qPCR was carried out using SYBR green with the 7300-real time PCR system (Applied Biosystems) and the primers used for the qPCR assay are listed in Table 5.1.

Table 5.1 Primer sequences used for the relative quantification of the transcripts in palatal shelves by qPCR using SYBR green.

Transcript	Primer sequences	Length (bases)	Amplicon size (bp)
Alkaline phosphatase (*Alpl*)	CCTTGACTGTGGTTACTGCT	20	216
	CCTGGTAGTTGTTGTGAGCG	20	

High temperature requirement factor A1 (*Htra1*)	AGTTCTTGACAGAGTCCCACGA TATGCCCCAGAGAGCACATCC	22 21	154
Runt-related transcription factor 2 (*Runx2*)	TGCCTCCGCTGTTATGAAAA CTGTCTGTGCCTTCTTGGTT	20 20	187
Sp7 transcription factor (*Sp7*)	CACAAAGAAGCCATACGCTG CCAGGAAATGAGTGAGGGAAG	20 21	165
18s ribosomal RNA (18s rRNA)	CGCGGTTCTATTTTGTTGGT AGTCGGCATCGTTTATGGTC	20 20	219

5.3.5 *Htra1* overexpression transfections

Htra1-myc-ddk vector (Origene) was digested using *Sal*I and *Xho*I restriction enzymes to separate the *Htra1* cDNA, and the negative control vector was synthesized by self-ligation of *SalI* and *XhoI* compatible sticky ends. Site directed mutagenesis of *Htra1* on serine residue at 328 to alanine was carried out by PCR using QuikChange Lightning kit (Agilent Technologies) with the following primers: 5′CATCAATTATGGAAATGCCGGAGGCCCGTTAG 3′ and 5′GTAGTTAATACCTTTACGGCCTCCGGGCAATC 3′. MEPM cells were transfected with polyethylenimine (PEI) [Linear Mol. Wt 25,000, Polysciences, Inc.] at a ratio of 2.5:1 to the DNA concentration. For each well of a 24-well plate, 700 ng of *Htra1*-myc-ddk vector or the negative control vector was transfected with 1,750 ng of PEI every fourth day in the presence of serum and without antibiotics. After transfection, the media was changed after overnight incubation and fresh osteogenic media was added. Cells were either fixed for ALPL or ARS staining or lysed for RNA isolation. Similarly, *Runx2*-myc-ddk vector (Origene) was used for the overexpression of *Runx2* in MEPM cells.

5.3.6 Biotinylated probes

Biotinylated probes were synthesized by PCR amplification from mouse genomic DNA using 5' biotin labelled primers (Invitrogen). For synthesizing 1 kb *Htra1* promoter probe (-994 to +72 bp) the

primers used were forward primer 5'-biotin-TCCTCCTTGAGTCAGGGTCA-3' and reverse primer 5'-biotin-GCAGCAGTAGCAAAGACAGG-3'. The primers for the -400 bp probe were forward primer 5'-biotin-AAGTTCACAGCCACAGTCCC-3' and reverse primer 5'-biotin-TAGCAAAGACAGGAGCGTGG-3'. The annealing temperature for the primers was 60°C. All PCR amplified biotinylated probes were electrophoresed on an agarose gel and purified using gel extraction kit (Thermo Fisher).

5.3.7 Streptavidin agarose pull-down assay

The streptavidin agarose pull-down assay (SAPA) was carried out as previously described (Deng et al., 2006; Ji et al., 2011) with minor modifications. At d8 of osteogenic differentiation, MEPM cells were detached from the T75 flasks using 0.25% trypsin and centrifuged at 2,000 g for 5 min. To the cell pellet, 200 µl of RIPA buffer containing 50 mM Tris–HCl, pH 7.4, 1% NP-40, 0.25% Na deoxycholate,150 mM NaCl, 1 mM NaF, 1 mM Na_3VO_4, 1 mM EDTA, and 1% protease inhibitor cocktail (Sigma) was added to lyse the cells, vortexed and passed through 28-gauge needle and incubated on ice for a minimum of 30 min. The lysates were then centrifuged and the supernatant was collected. Protein concentration measured using the Bradford assay. 5 µg biotinylated DNA probe added to the cell lysates (250 µg) and incubated at 4°C overnight with rotational mixing. Streptavidin-agarose beads (20 µl) were added to each sample at 4°C for 4 h with rotational mixing. The beads were then washed and centrifuged four times in 1 ml RIPA buffer at 4°C. Beads were then suspended in 30 µl of 2X SDS loading buffer, boiled for 15 min at 95°C, centrifuged and collected supernatant used for Western blot analysis.

5.3.8 Chromatin immunoprecipitation assay

Chromatin immunoprecipitation (ChIP) assay was carried (Ji et al., 2011) out using a rabbit monoclonal antibody against RUNX2 (Cell Signaling). Briefly, MEPM cells were fixed with 0.75% formaldehyde in 1X PBS for 10 min and then blocked with 0.125 M glycine for 5 min at room temperature. After washing twice with ice cold PBS, cells were scraped in cold PBS and to the cell pellet 200 µl of cell lysis buffer containing 50 mM HEPES-KOH (pH 7.5), 140 mM NaCl, 1 mM EDTA (pH 8), 1% Triton X-

100, 0.1% sodium deoxycholate, 0.1% SDS, 1% protease inhibitors was added. Samples were then sonicated to shear the DNA with four rounds of 12 sec pulses each at 50% power output and 90% duty cycle using a Branson Sonicator 200. DNA samples were electrophoresed on a 1% agarose gel to ensure DNA shearing was between 400 bp to 1000 bp. Following sonication, 50 µl of the supernatant was stored as input and to measure DNA concentration of the sonicated samples. Protein A/G beads were washed and precleared with 50 µg of sonicated DNA in ChIP dilution buffer containing 1% Triton X-100, 2 mM EDTA (pH 8), 20 mM Tris-HCL (pH 8), 150 mM NaCl, 1% protease inhibitors for each immunoprecipitation for 1 h at 4°C and spun at 2,000 g for two min. The precleared supernatant was then mixed either the RUNX2 monoclonal antibody or the normal rabbit IgG and rotated at 4°C overnight. This was followed by addition of 40 µl of fresh protein A/G beads to the immunoprecipitated complex and further mixing by rotation at 4°C for 4 h. Beads were then washed four times with low salt wash buffer containing 0.1% SDS, 1% Triton X-100, 2 mM EDTA (pH 8), 20 mM Tris-HCL (pH 8), 150 mM NaCl and two times with high salt buffer containing 0.1% SDS, 1% Triton X-100, 2 mM EDTA (pH 8), 20mM Tris-HCL (pH 8), 500 mM NaCl at 4°C for 2 min each wash. The chromatin immunoprecipitant complex was eluted from the beads using 150 µl of elution buffer containing 1% SDS, 100 mM sodium bicarbonate at 30°C for 15 min with rotational mixing. The eluted DNA samples were treated with proteinase K and RNase A and incubated at 65°C for 2 h. Following incubation, DNA concentration was measured and PCR carried out using the primer set to amplify -295 to +72 bp region of *Htra1* promoter.

5.3.9 Cloning of 5' flanking region of *Htra1*

Five different regions of *Htra1* promoter were amplified by PCR using Phusion High-Fidelity DNA polymerase (NEB) using primers listed in Table 5.2. Annealing temperature used for all primers was 63°C. Using dATP, an A-overhang was introduced to the 3' end of the PCR amplicons by non-proof reading Taq DNA polymerase (Lucigen). The PCR products were then purified by gel extraction and cloned into pGEM-T easy vector (Promega). From the positive clones of the pGEM-T easy vector cloning, the respective *Htra1* promoter fragments were digested with *Kpn*I and *Xho*I for cloning into the destination

pGL3 promoter luciferase vector (Promega). All clones were verified by Sanger sequencing at National Research Council (NRC) sequencing facility (Saskatoon, SK) and found to match perfectly with the promoter region of *Htra1* (*M. musculus*|chr7|138078749-138079949).

Table 5.2 Primer sequences used for the cloning of *Htra1* promoter fragments into pGL3 promoter luciferase vector. The underlined are the sequences for restriction enzymes *Kpn*I and *Xho*I, which were used to clone the fragments into the destination vector. Sequences in red are the mutated putative RUNX2 binding sites.

***Htra1* promoter region**	**Primer sequences**
-994 to +72 bp	TAGGTACCTCCTCCTTGAGTCAGGGTCA TACTCGAGTAGCAAAGACAGGAGCGTGG
-399 to +72 bp	TAGGTACCAAGTTCACAGCCACAGTCC TACTCGAGTAGCAAAGACAGGAGCGTGG
-811 to -439 bp	TAGGTACCGGTGACAGTTGCTCTTCCTGA ATCTCGAGAAACCCAGTGCCCAGACCTA
-295 to +72 bp	AAGGTACCTTTCCAGGCGATTGCGCAGT TACTCGAGTAGCAAAGACAGGAGCGTGG
-199 to +72 bp	CCGGTACCGGTCTTCAATCTCTGAGGAAA TACTCGAGTAGCAAAGACAGGAGCGTGG
Site M1	GATTGAAGACCTTAAGACCAAAATAATACGTAACAGAGGGAAACCTGCCTAGCACTGCGC GCGCAGTGCTAGGCAGGTTTCCCTCTGTTACGTATTATTTTGGTCTTAAGGTCTTCAATC
Site M2	GGTTAAGCCCATTGGCCTAACAACAATGACGAAGCGCCAGGGGGA TCCCCCTGGCGCTTCGTCATTGTTGTTAGGCCAATGGGCTTAACC
Site M3	CGGCCACGGGCTGGATTATAGATGAAAAACCGCGCTCGGGA TCCCGAGCGCGGTTTTTCATCTATAATCCAGCCCGTGGCCG

5.3.10 Luciferase assay

Dual luciferase reporter assay (Promega) was carried out as previously described (Thangaraj et al., 2017). Briefly, 10^4 MEPM cells were seeded into white opaque 96-well plate. Next day, the cells were transfected using polyethylenimine (PEI) [Linear Mol. Wt 25,000, Polysciences, Inc.] with 100 ng of pGL3 firefly luciferase vector constructs, 100 ng of either the negative control or the *Runx2* expression vector and 40 ng of pRL-CMV renilla luciferase vector as the transfection control. After 48 h, cells were lysed with the passive lysis buffer and then firefly luciferase assay reagent II was added to measure the firefly luciferase activity. This was followed by the addition of Stop & Glo reagent and the renilla luciferase activity measured. The relative luciferase activity was calculated by normalizing the firefly luciferase activity values to the respective renilla luciferase values.

5.3.11 Statistical analyses

Statistical analyses were carried out by Prism5 software (Graphpad). Unpaired t-test was used in the case of two groups, one-way ANOVA or two-way ANOVA with Bonferroni multiple comparison test was used where applicable. Data were analyzed and represented as mean ± S.E.M relative to wild type. A p-value of <0.05 was considered significant.

5.4 Results

5.4.1 All-trans retinoic acid (ATRA) inhibits osteogenic differentiation of primary MEPM cells

ATRA is known to have a pleiotropic role in osteogenic differentiation and *Htra1* is shown to modulate osteogenic differentiation downstream of ATRA (Glanz et al., 2016). However, whether ATRA regulates *Htra1* expression during osteogenic differentiation is unknown. To answer this, MEPM cells were treated with 1 µM or 5 µM of ATRA during osteogenic differentiation. ALPL staining shows reduced osteogenic differentiation of MEPM after treatment with ATRA *in vitro* at d8 (Figure 5.1A-C). In addition, ATRA treatment decreased matrix mineralization stained by ARS at d21 (Figure 5.1D-F). Consistently,

ATRA treatment resulted in a complete downregulation of *Runx2*, a master regulator of osteogenic differentiation at d8 (Figure 5.1G). In contrast, *Hoxa2*, a negative regulator of osteogenic differentiation was upregulated ~1.67 and ~1.5-fold after treatment with ATRA 1 µM and 5 µM, respectively (Figure 5.1H). Interestingly, similar to the levels of *Runx2*, *Htra1* is significantly downregulated after treatment with ATRA during osteogenic differentiation at d8 (Figure 5.1I). These data indicate that ATRA inhibits osteogenic differentiation of primary mesenchymal cells from the palate potentially via downregulation of *Runx2* and *Htra1*.

5.4.2 *Htra1* expression is characteristic of osteogenic markers

Next, expression of HTRA1 was evaluated in the craniofacial region during development using IHC staining. HTRA1 is mainly expressed in ossifying matrix regions of the maxilla (Figure 5.2A), mandible (Figure 5.2B) and palatal bone (Figure 5.2C) regions in wild type embryos at E16.5. In the *Hoxa2*$^{-/-}$ palate, which exhibited increased osteoblast differentiation, HTRA1 is upregulated in the palatal process of maxilla at E16.5 (Figure 5.2D). In addition, *Htra1* mRNA is upregulated at stages E13.5 and E15.5 during palatogenesis, times when the palatal process of the palatine bone and the palatal process of maxilla are ossifying, respectively (Figure 5.2E). Intriguingly, *Htra1* follows a temporal pattern of expression comparable to *Runx2*, *Alpl* and *Sp7* (*Osx*) during osteogenic differentiation of the palatal mesenchyme *in vitro* (Figure 5.2F). These results show that *Htra1* is expressed osteogenic differentiation and might play role in osteogenic differentiation of MEPM cells.

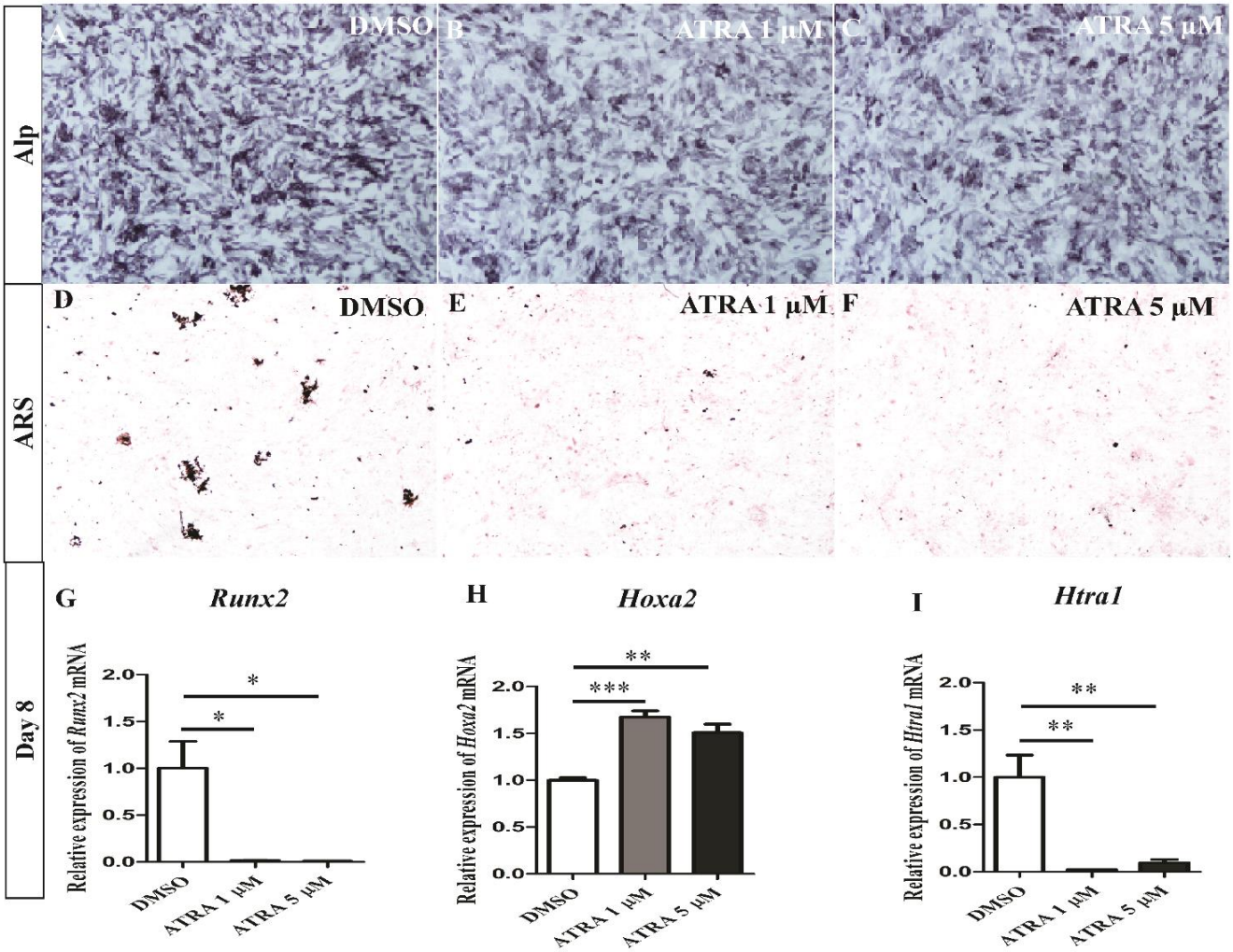

Figure 5.1 All-*trans* retinoic acid (ATRA) inhibits osteogenic differentiation of primary MEPM cells. (A-C) Alkaline phosphatase (Alpl) staining at d8 revealing osteogenic differentiation of MEPM cells treated with DMSO (A), ATRA 1 µM (B) and ATRA 5 µM (C) for 8 days. (D-F) Alizarin red (ARS) staining in MEPM cells after treatment with DMSO (D), ATRA 1 µM (E) and ATRA 5 µM (F) for 21 days during osteogenic differentiation. Gene expressions of *Runx2* (G), *Hoxa2* (H) and *Htra1* (H) at d8 of osteogenic differentiation with ATRA treatment. Data was normalized to *18s rRNA* (n=4 biological replicates; mean ± S.E.M; one-way ANOVA with Bonferroni post-hoc test, *, $p<0.05$; **, $p<0.01$; ***, $p<0.001$) and represented relative to DMSO control.

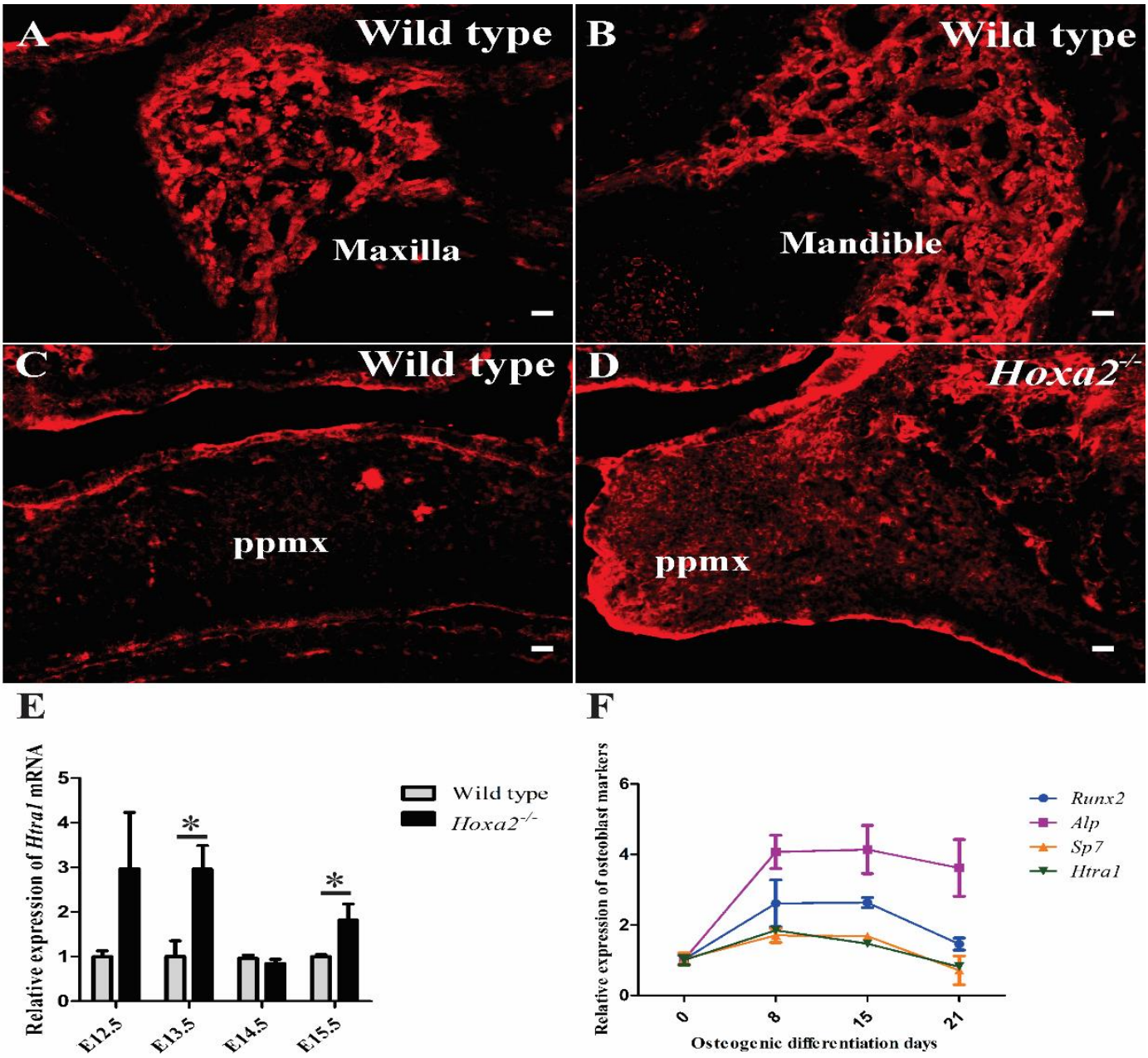

Figure 5.2 *Htra1* expression is characteristic of osteogenic markers. Immunohistochemical staining for HTRA1 in maxilla (A) and mandible (B) in wild type embryos at E16.5. HTRA1 protein expression in the palatal process of maxilla in wild type (C) and *Hoxa2*$^{-/-}$ embryos (D). Relative gene expression of *Htra1* in the developing palate from E12.5 to E15.5 in wild type and *Hoxa2*$^{-/-}$ embryos (E). Data was normalized to *18s rRNA* (n=4 biological replicates; mean ± S.E.M; unpaired t-test and represented relative to wild type controls at each stage. Relative gene expression of *Runx2*, *Alpl*, *Sp7* and *Htra1* during osteogenic differentiation of MEPM cells (F). Data was normalized to *18s rRNA* (n=4 biological replicates; mean ± S.E.M; one-way ANOVA with Bonferroni post-hoc test and represented relative to gene expression to d0.

5.4.3 *Htra1* positively regulates osteogenic differentiation *in vitro*

The role of *Htra1* in osteogenic differentiation is controversial, with reports indicating a role of *Htra1* as an inducer (Tiaden et al., 2012; Li and Zhang, 2015; Glanz et al., 2016) as well as an inhibitor (Hadfield et al., 2008; Graham et al., 2014; Wu et al., 2014b) of osteogenic differentiation. Hence, to investigate the role of *Htra1* in osteogenic differentiation in MEPM cells, *Htra1* was overexpressed using the pCMV-*Htra1*-myc-ddk vector and an inactive protease mutant of *Htra1* (*Htra1* S328A) generated by site directed mutagenesis was used as a control against the serine protease activity of active *Htra1*. At day 8, the ALPL staining revealed little difference between the *Htra1* overexpressed MEPM cells and that of the negative control (Figure 5.3A-C). However, overexpression of *Htra1* resulted in a clear increase in osteogenic differentiation of MEPM cells stained by ALPL at day 15 (Figure 5.3D-F). In addition, ARS staining exhibited increased mineralized matrix in MEPM cells overexpressed with *Htra1* compared to the negative control and the protease inactive *Htra1* mutant at day 15 (Figure 5.3G-I and M) and day 21 (Figure 5.3J-L and N). Furthermore, overexpression of *Htra1* increased the expression of osteoblast markers such as and *Alpl* to ~2.1-folds at d7 and d15 (Figure 5.4A) and *Sp7* (*Osx*) to ~1.7-fold at d7 and ~1.37-fold at d15 (Figure 5.4B). These results demonstrate that *Htra1* could be an inducer of osteogenic differentiation in primary mesenchymal progenitor cells.

To address the signaling mechanism downstream of *Htra1* during osteogenic differentiation, ossification and bone remodelling real-time PCR array (Bio-Rad) was utilized to identify differentially expressed genes upon overexpression of *Htra1*. In addition to *Alpl*, several other osteogenic related genes such as *Fgf9*, *Fgfr3*, *Ibsp*, *Vegfa*, *Mmp9* and *Esr2* were upregulated to ~1.98, 1.95, 2.97, 1.5, 2.33, 4.04 and 2-folds respectively, after overexpression of *Htra1* in differentiating mesenchymal progenitor cells at d7 (Figure 5.4C). In contrast, inhibitors of osteogenesis such as *Sost*, *Calca* and *Esr1* were downregulated to ~0.23, 0.6 and 0.51-fold, respectively, upon *Htra1* upregulation (Figure 5.4C). These data indicate that *Htra1* could regulate several osteogenesis related genes to positively modulate osteogenic differentiation.

RUNX2 is a key transcription factor that regulates several osteoblast specific gene expression (Roca et al., 2005; Lamour et al., 2007; Li et al., 2011). Given the similarity in the expression profile of

Htra1 and *Runx2 in vivo* and *in vitro*, next I investigated whether *Runx2* induces *Htra1* during osteoblast differentiation of MEPM cells. Indeed, *Htra1* was upregulated (Figure 5.5B) after the overexpression of *Runx2* (Figure 5.5A), similar to the levels of *Sp7* (*Osx*) (Figure 5.5C), a known transcriptional target of *Runx2*, at d8 during osteogenic differentiation. These results reveal that *Htra1* is a positive regulator of osteogenic differentiation of primary mesenchymal cells from the palate and is regulated by RUNX2 during osteogenic differentiation.

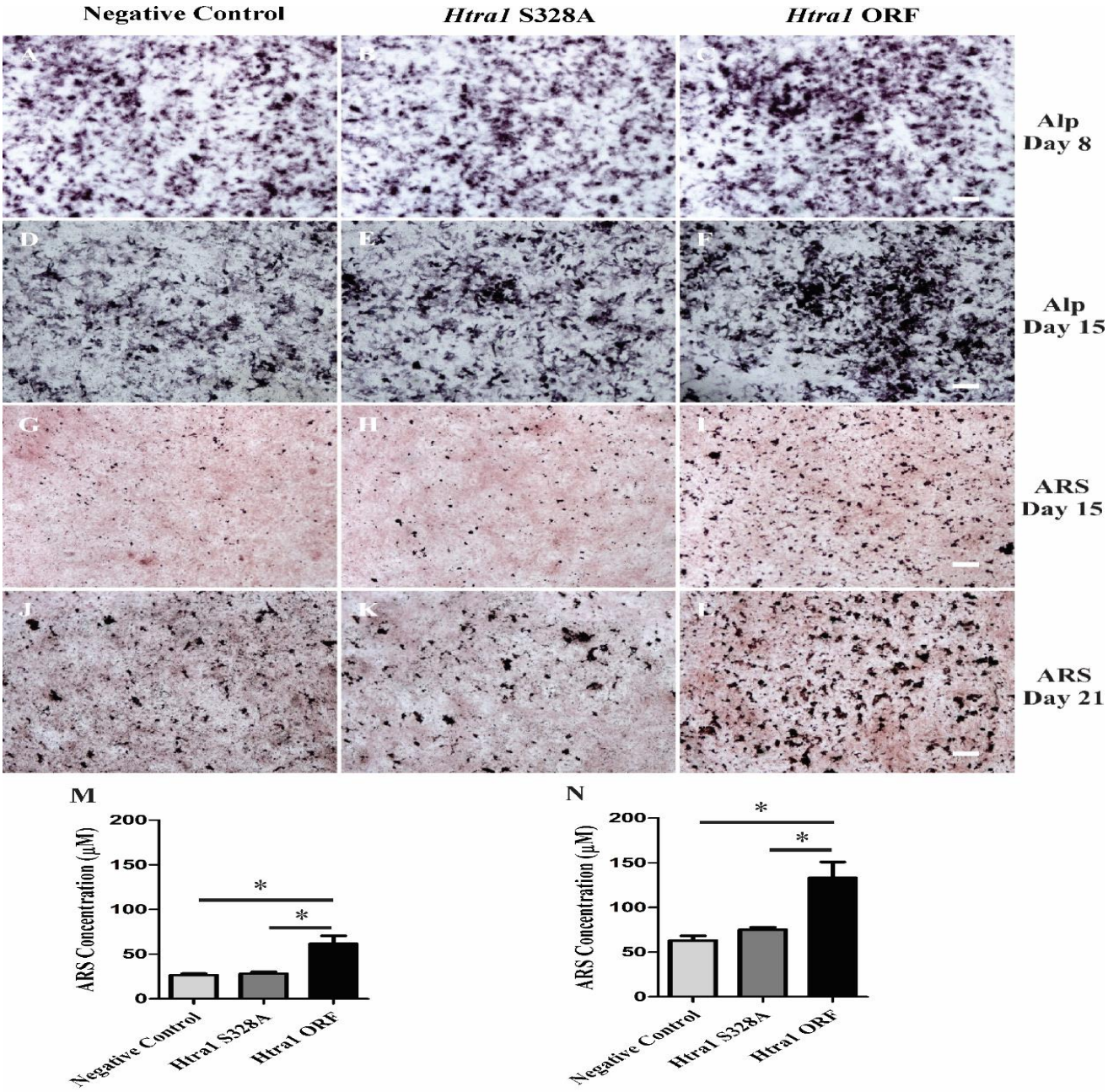

Figure 5.3 *Htra1* promotes osteogenic differentiation of MEPM cells *in vitro*. (A-F) ALPL staining in MEPM cells transfected with negative control-CMV-myc-ddk vector (A and D), *Htra1* S328A inactive mutant (B and E) and *Htra1*-CMV-myc-ddk vector (C and F) after day 8 (A-C) and day 15 (D-F) of osteoblast differentiation. (G-L) ARS staining in MEPM cells after *Htra1* overexpression at day 15 (G-I) and day 21 (J-L). Quantification of ARS stained osteoblast matrix after overexpression of *Htra1* at day 15 (M) and day 21 (N).

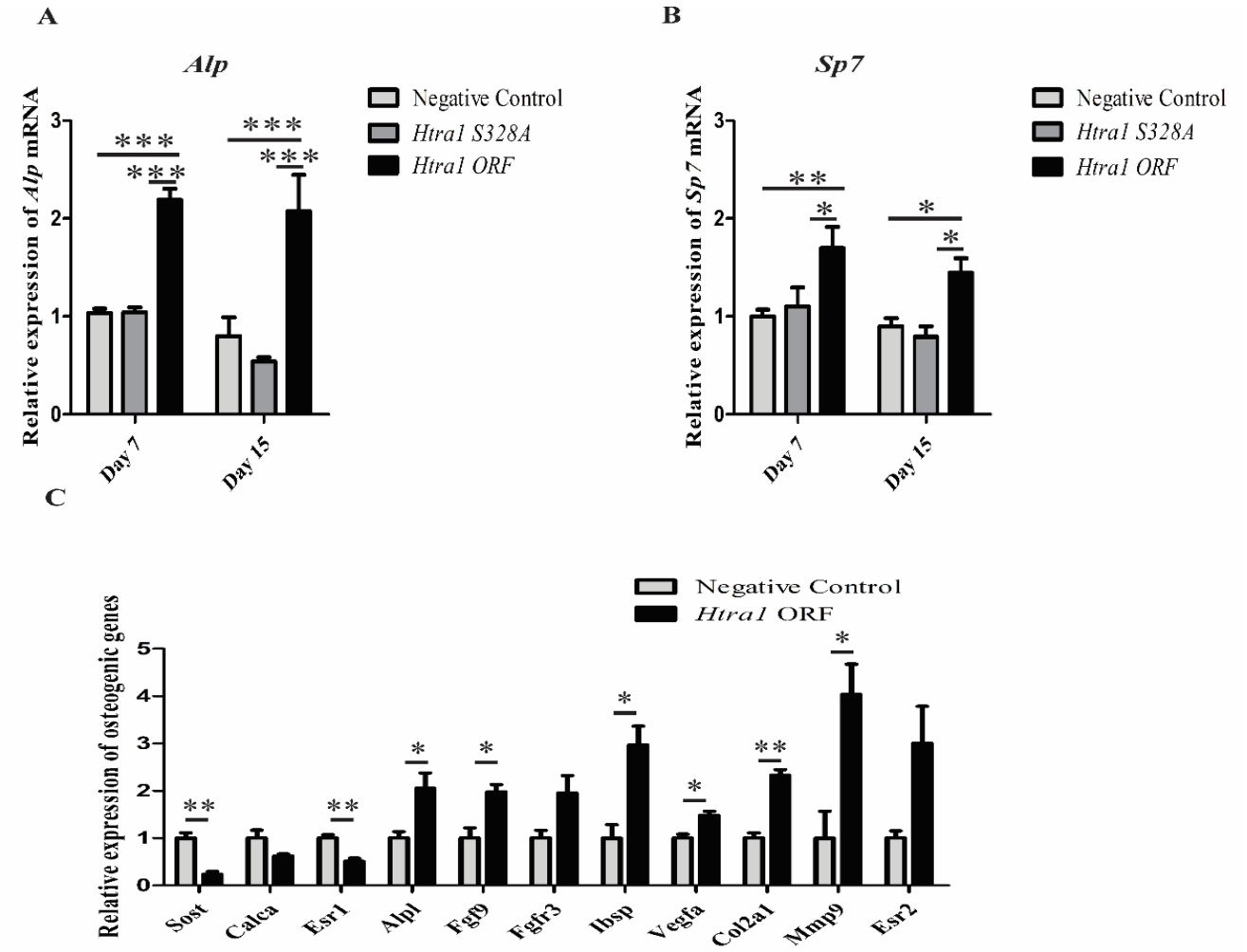

Figure 5.4 *Htra1* regulates the expression of osteogenesis related genes during differentiation of primary mesenchymal progenitor cells. Relative mRNA expression of osteoblast markers *Sp7* (*Osx*) (A) and *Alpl* (B) at d7 and d15 in primary mesenchymal progenitor cells after overexpression of *Htra1*. Data was normalized to *18s rRNA* (n=4 biological replicates; mean ± S.E.M; one-way ANOVA with Bonferroni post-hoc test, *, $p<0.05$; **, $p<0.01$; ***, $p<0.001$) and represented relative to cells transfected with negative control vector. Osteogenesis gene expression array was carried at d8 in primary mesenchymal progenitor cells transfected with negative control and *Htra1* overexpression vector during osteogenic differentiation. Differentially expressed genes between the negative control and *Htra1* overexpressing osteoblasts are plotted in the bar graph (C) (n=3 biological replicates) and the data were normalized to Glyceraldehyde 3-phosphate dehydrogenase (*Gapdh*) Ct values of the respective samples and analyzed using unpaired T-test, *, $p<0.05$; **, $p<0.01$.

5.4.4 RUNX2 interacts with the 5' flanking region of *Htra1* to induce *Htra1* expression during osteoblast differentiation

Runx2 is one of the master regulators of osteoblast differentiation. The targets of *Runx2* during osteoblast differentiation are still largely being explored (Wu et al., 2014). Analysis of the proximal 5' flanking region of *Htra1* (1 kb) revealed several putative binding sites of RUNX2 (Figure 5.5D). To test whether RUNX2 interacts with the 5' flanking region of *Htra1*, primers labelled with 5' biotin were used to amplify the 5' flanking region of region of *Htra1*. This 1 kb biotin probe was then used to pull-down proteins from the lysates of MEPM cells (d8 of osteogenic differentiation) using streptavidin agarose pull-down assay (SAPA). Results indicate that RUNX2 protein interacts with the 5' flanking region of of *Htra1* (Figure 5.5E). Similarly, the pull-down assay using a biotin probe of -400 bp from the transcription start site of *Htra1* (-399 bp to +72 bp) also showed an interaction of RUNX2 with the *Htra1* 5' flanking region (Figure 5.5E). In addition, ChIP analysis further confirmed that RUNX2 interacts within the proximal -400 bp of the *Htra1* 5' flanking region during osteoblast differentiation (Figure 5.5F). These results reveal that RUNX2 binds to the *Htra1* promoter during osteogenic differentiation.

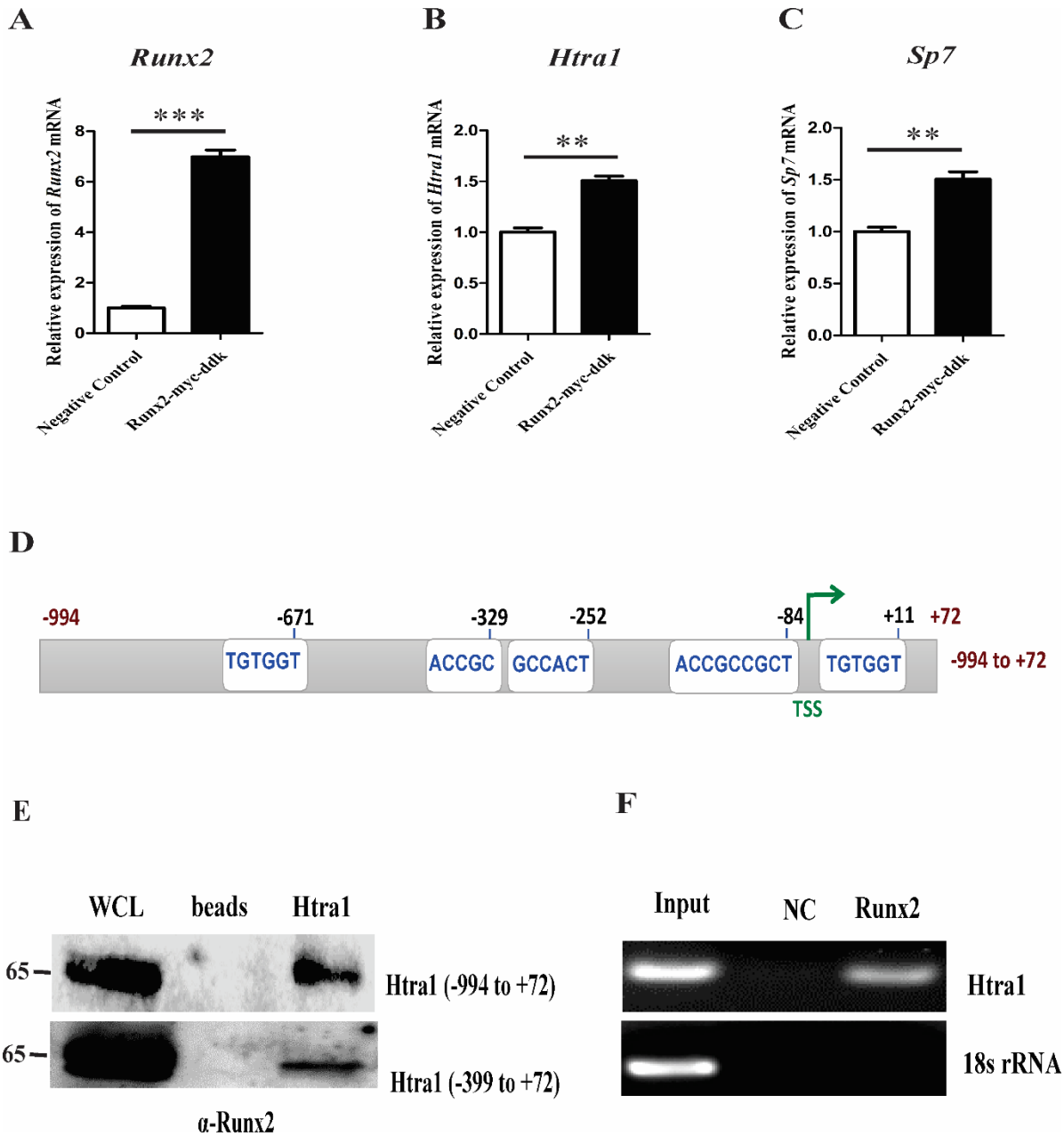

Figure 5.5 RUNX2 promotes the expression of *Htra1* and interacts with the *Htra1* proximal promoter in primary mesenchymal progenitor cells. (A-C) Relative mRNA expression of *Runx2* (A), *Htra1* (B) and *Sp7* (C) at d8 during osteogenic differentiation of primary mesenchymal progenitor cells

after over expression of *Runx2*. Data was normalized to *18s rRNA* (n=4 biological replicates; mean ± S.E.M; unpaired T-test, **, p<0.01; ***, p<0.001) and represented relative to cells transfected with negative control vector. Schematic diagram showing the 5' flanking region region of *Htra1* (-994 bp to +200 bp) with putative RUNX2 binding sites (D). RCCRC is the known RUNX2 consensus binding site and TGTGGT is the reverse complement of ACCACA (RCCRC). Western blot analyses (E) showing the interaction of RUNX2 with biotinylated *Htra1* promoter probes of length 1 kb (-994 to +72) (upper panel in E) and proximal (-399 to +72 bp) (lower panel in E) by streptavidin-agarose pull down assay (SAPA). (F) ChIP assay was performed in differentiating primary mesenchymal progenitor during osteoblast differentiation at d5. Cells were cross-linked with formaldehyde, lysed and the sonicated chromatin were immunoprecipitated with RUNX2 rabbit monoclonal antibody or normal rabbit IgG antibody. PCR was performed using the primers targeting the proximal -399 to +72 region of *Htra1* promoter (upper panel in F) and an unrelated control *18s rRNA* as a control. TSS, transcription start site; WCL, whole cell lysate; NC, negative control (rabbit IgG) antibody.

5.4.5 RUNX2 regulates the promoter activity of *Htra1*

Next, to determine whether the binding of RUNX2 to the *Htra1* promoter regulates its activity and to discover the RUNX2 binding region on the *Htra1* promoter, five different PCR amplified regions of *Htra1* promoter were cloned into the pGL3 promoter luciferase vector. The regions cloned into the pGL3 promoter luciferase vector were as follows: (i) -994 to +72 bp (ii) -399 to +72 bp (iii) -811 to -439 bp (iv) -295 to +72 bp (v) -199 to +72 (Figure 5.6A). All cloned constructs were sequenced using specific forward

and reverse primers for respective PCR fragments. Constructs were transfected individually along with either the negative control vector or the *Runx2* expression vector (*Runx2*-myc-ddk vector) into MEPM cells. The dual luciferase reporter assay was carried out after 48 h as per the manufacturer's protocol (Promega). The data showed that RUNX2 promotes luciferase reporter activity of the *Htra1* promoter. Amongst the different constructs of the *Htra1* promoter tested, *Runx2* overexpression increased the reporter activity of all the proximal promoter constructs as well as the full length 1 kb promoter construct, whereas it did not increase the reporter activity of the distal promoter construct (-811 to -439 bp) (Figure 5.6B). These results indicate that *Runx2* could induce the expression of *Htra1* during osteoblast differentiation of MEPM cells by interacting with the *Htra1* promoter and the putative binding site(s) for interaction could be between -399 to +72 bp.

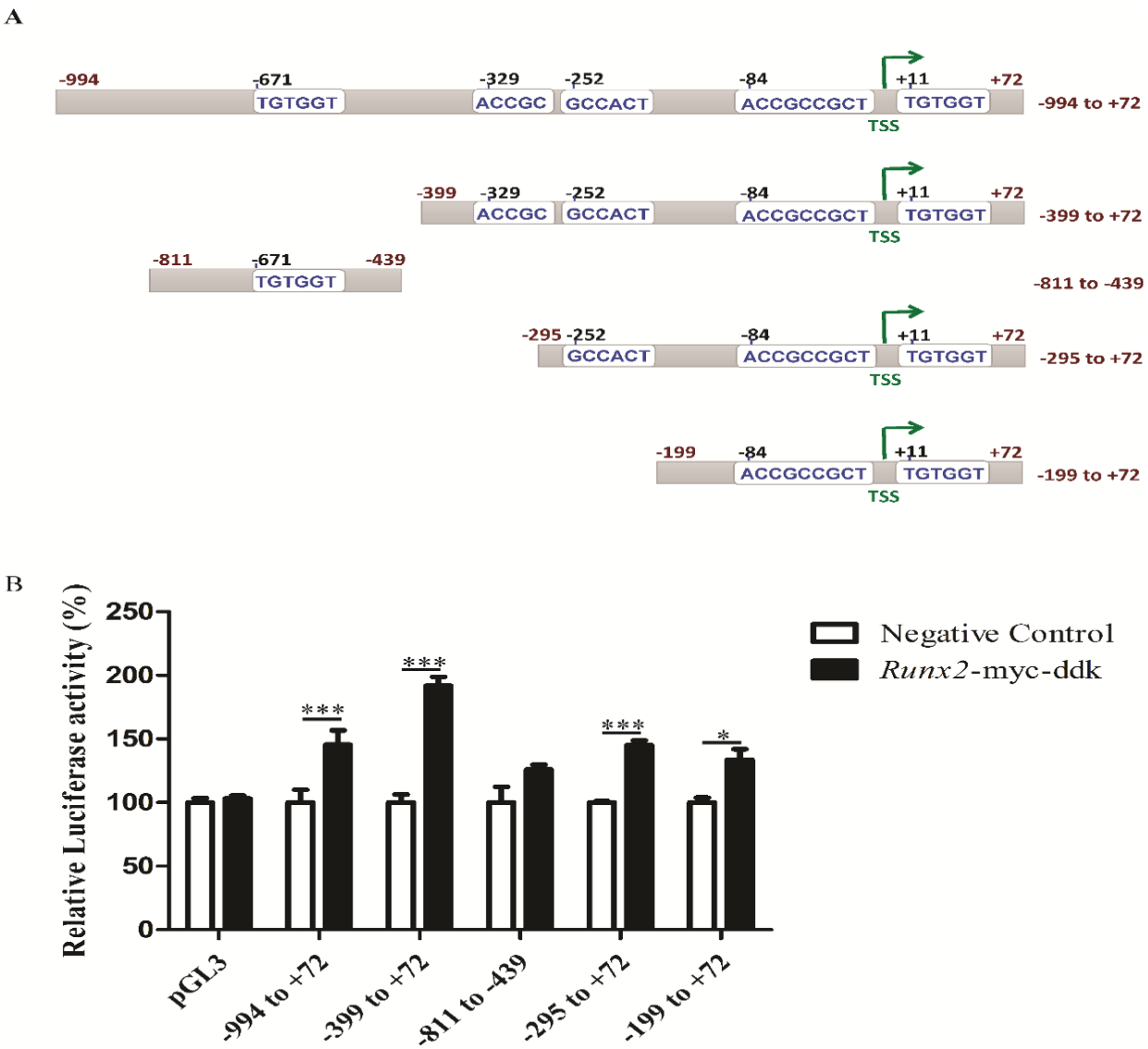

Figure 5.6 RUNX2 association increases the reporter activity of *Htra1* promoter. Five different lengths of *Htra1* promoter fragments were cloned into pGL3 promoter luciferase vector (A). Relative luciferase activity of the *Htra1* promoter fragments 48 h after transfection with *Runx2* overexpression vector. RUNX2 induces the luciferase activity of all the *Htra1* promoter fragments except the distal 373 bp (-811 to -439 bp) in MEPM cells.

5.4.6 RUNX2 interaction at the RUNX2 consensus binding sites at -252 bp and -84 bp in the proximal 5' flanking region of *Htra1* regulates *Htra1* promoter activity

The *Htra1* proximal 5' flanking region (-400 bp) contains four putative RUNX2 consensus binding sites. To investigate which one of the RUNX2 consensus binding sites is critical for *Htra1* promoter

activity, site directed mutagenesis was used to mutate these binding sites at -252 bp, -84 bp and +11 bp alone or in combination (Figure 5.7A) in the pGL3 promoter vector and carried out a luciferase assay after overexpression of *Runx2*. Mutations at site 1 (-252 bp) or site 2 (-84 bp) alone or in combination failed to increase the promoter activity of *Htra1* by RUNX2. In contrast, mutation at site 3 (+11 bp) increased the *Htra1* promoter activity after *Runx2* overexpression (Figure 5.7B). These results indicate that sites at -252 bp and -84 bp are critical for the inducing *Htra1* promoter activity for its expression by RUNX2.

In conclusion, the data show that *Htra1* is an inducer of osteogenic differentiation of primary mesenchymal cells and is a direct downstream target of *Runx2*. *Runx2* regulates *Htra1* expression through its interaction with the *Htra1* promoter at -252 bp and -84 bp.

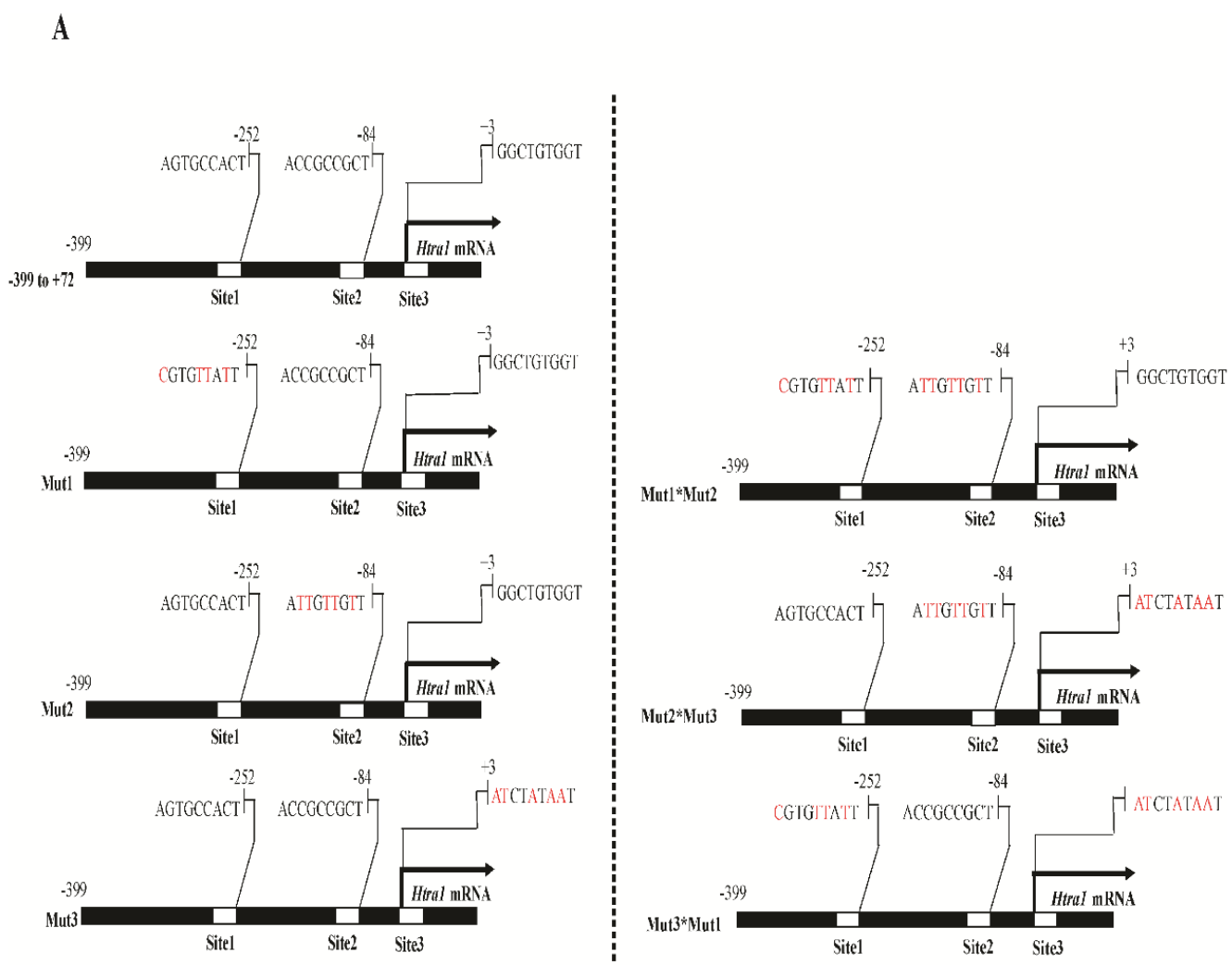

B

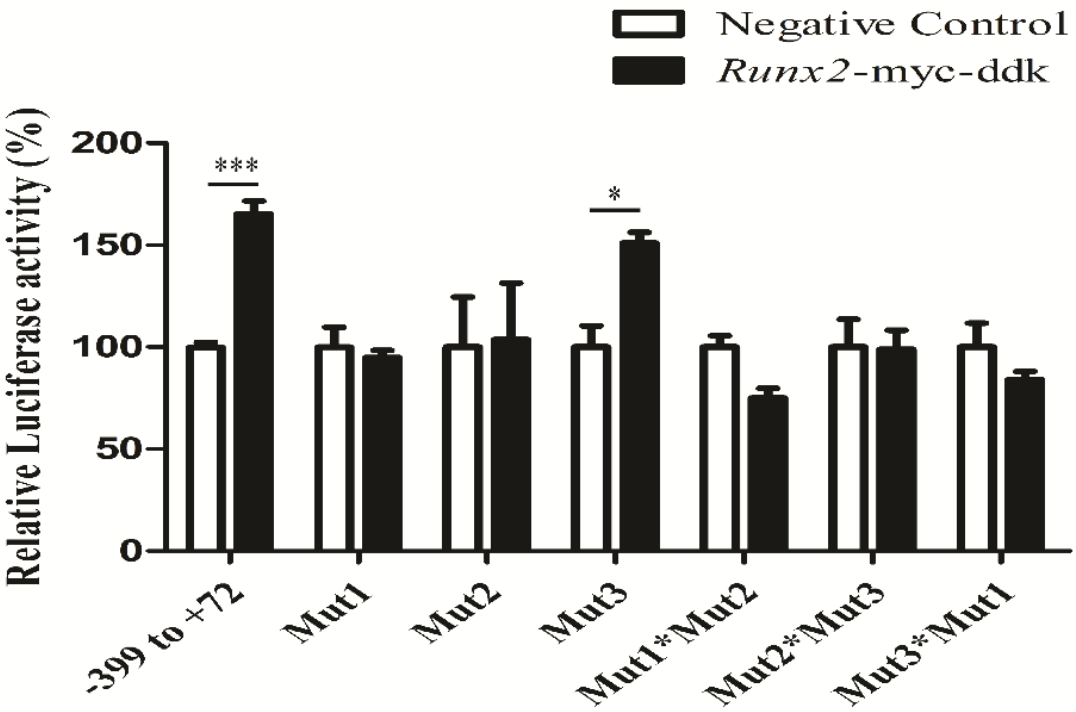

Figure 5.7 RUNX2 interaction at the RUNX2 consensus binding sites at -252 bp and -84 bp in the *Htra1* proximal promoter regulates *Htra1* promoter activity. Schematic diagram showing the three putative RUNX2 consensus binding sites on the *Htra1* promoter and site directed mutagenesis of binding sites alone or in combination in pGL3 promoter luciferase vector. Relative luciferase activity of the *Htra1* promoter fragment (-399 to +72 bp) with respective mutations after overexpression of *Runx2* for 48 h.

5.5 Discussion

In this chapter, I have demonstrated the role of serine protease HTRA1 as an inducer of osteogenic differentiation of primary mesenchymal progenitor cells. In addition, I have examined the specific molecular interaction between RUNX2 and *Htra1* during osteogenic differentiation delineating that RUNX2 binds to the *Htra1* proximal promoter to transactivate *Htra1* expression. Despite the advancements in the knowledge of the signaling mechanisms governing osteogenic differentiation, several interacting partners and their role in osteogenesis remain obscure. The data here significantly improve the understanding of the role of *Htra1* in osteogenic differentiation and unravel a novel interaction between *Htra1* and *Runx2*.

Htra1 expression follows the expression pattern of osteogenic markers such as *Runx2* in osteogenic fronts *in vivo* and during osteogenic differentiation *in vitro*. Using IHC, I have demonstrated that HTRA1 protein is expressed in the developing maxilla, mandible and in the palatal process of the maxilla. The expression pattern of HTRA1 in the developing jaw regions were similar to the previously reported expression profile of osteoblast markers such as *Runx2*, *Sp7* and *Alpl* (Baek et al., 2011). Similarly, there was a coordinated expression of *Htra1* along with other osteogenic markers including *Runx2* during osteogenic differentiation of primary mesenchymal progenitor cells. The pilot study indicated that ATRA inhibits osteogenic differentiation of primary mesenchymal progenitor cells. This is in agreement with previous reports on ATRA in osteogenesis of craniofacial mesenchyme (Chen et al., 2010; Morkmued et al., 2017). Interestingly, ATRA inhibited the expression of *Runx2* and *Htra1*, whereas it upregulated the expression of *Hoxa2*. *Hoxa2*$^{-/-}$ mice exhibit increased osteogenic differentiation of the palatal mesenchyme with increased expression of osteoblast markers including *Runx2* (Chapter 3). *Htra1* was upregulated in the palatal bones of the *Hoxa2*$^{-/-}$ mice during development. These findings lead to the hypothesis that *Htra1* may regulate osteogenic differentiation of the primary mesenchymal progenitor cells and it could be regulated by *Runx2* during osteogenesis.

Gain of function of *Htra1* in primary mouse mesenchymal progenitor cells results in enhanced osteogenesis and osteogenic marker expression. These findings are in line with the role of *Htra1* in

osteogenesis reported in human bone marrow-derived stem cells (Tiaden et al., 2012a), mouse adipose-derived stromal cells (Glanz et al., 2016) and periodontal ligament cells (Li and Zhang, 2015). Conversely, contradicting evidence suggest *Htra1* as an inhibitor of matrix mineralization in murine 2T3 and KusaO cell lines (Hadfield et al., 2008; Wu et al., 2014b). However, the expression of *Htra1* is significantly reduced in immortalized cell lines transformed with SV40 (Zumbrunn and Trueb, 1996) and the impeded osteogenesis by *Htra1* is considered to be due to the confounding effects of the transformed cell lines than the actual effect by *Htra1* (Filliat et al., 2017; Tiaden et al., 2012a). Therefore, the role of *Htra1* in osteogenesis is selectively dependent on the nature of the cells as primary or transformed. In addition, it is pertinent to note that these studies investigated the role of *Htra1* after stimulation with BMP2 in osteoblast cells (Hadfield et al., 2008; Wu et al., 2014b). Moreover, exogenous addition of recombinant BMP2 in C2C12 preosteoblasts results in upregulation of *Htra1* (Bustos-valenzuela et al., 2011). Hence, it is plausible that the role of *Htra1* could be surpassed by BMP2, a dominant inducer of osteogenesis and there might be a feedback mechanism preventing augmented osteogenesis in response to simultaneous stimulation with *Bmp2* and *Htra1*. *Htra1* deficient mice exhibit no obvious alteration in bone phenotype *in vivo* (Filliat et al., 2017). It is intriguing to note that HTRA3, which shares the highest homology with HTRA1, is also expressed in adjacent regions of bone formation (Filliat et al., 2017; Tocharus et al., 2004). The role of *Htra3* in osteogenic differentiation is unknown and it is possible that *Htra1* and *Htra3* could be functionally redundant in mediating osteogenesis of mesenchymal stem cells. Further work is needed to decipher the role and mechanism involving these two-family members in an osteoblast-specific compound mutant mice model.

The data here address the specific role of *Htra1* in osteogenesis of the mesenchymal progenitor cells during differentiation with insights into the molecular mechanisms both upstream and downstream of *Htra1*. Osteogenic gene expression array analysis revealed the upregulation of several ECM related genes namely, *Fgf9, Fgfr3*, *Ibsp*, *Vegfa, Col2a1* and *Mmp9*. In *Xenopus* embryo, the proteolytic cleavage of ECM proteins such as biglycan, syndecan-4 and glypican-4 by HTRA1 promotes FGF/ERK signaling. In turn, FGF signaling is necessary and sufficient for *Htra1* expression in chick facial and forelimb

mesenchyme (Ferrer-Vaquer et al., 2008). Consistent with our findings, previous studies have reported increased expression of *Ibsp* after overexpression of *Htra1* in human bone marrow-derived mesenchymal stem cells (Tiaden et al., 2012a). HTRA1 and IBSP co-localize during bone regeneration, in osteo-induced spheroid cultures, where HTRA1 is hypothesized to fragment IBSP for proper matrix mineralization (Tiaden et al., 2012a). *Htra1* induces osteogenesis over the expense of adipogenesis via MAP kinase-dependant MMP production in human mesenchymal stem cells (Tiaden et al., 2016). Proteolytic cleavage of ECM proteins such as fibronectin by HTRA1 induces the expression of MMPs during osteogenesis (Tiaden et al., 2016) and in other pathological conditions such as intervertebral disc degeneration (Tiaden et al., 2012b) and in age-related macular degeneration (Vierkotten et al., 2011). In this study, *Col2a1* is another gene that was upregulated in *Htra1* overexpressing primary mesenchymal progenitor cells. Yeast two-hybrid screening revealed the interaction of HTRA1 with procollagens including COL2A1 (Murwantoko et al., 2004). *Htra1* overexpression leads to downregulation of genes such as *Sost*, *Calca* and *Esr1*. Negative regulation of *Sost* by *Htra1* was reported in human bone marrow-derived mesenchymal stem cells (Tiaden et al., 2012a). The osteogenic array data also revealed some unreported putative downstream genes such as *Calca*, *Esr1, Esr2* and *Fgfr3.*

The findings here show that RUNX2 is recruited to the proximal *Htra1* promoter to transactivate *Htra1* gene expression during osteoblastogenesis. *Runx2* is a master regulator of osteogenic differentiation and plays a critical role in chondrocyte maturation and bone formation (Komori et al., 1997). RUNX2 binds to RUNT binding site RCCRC(A/T) (Kamachi et al., 1990) in the promoter region to drive osteoblast-specific gene expression (Lamour et al., 2007; Roca et al., 2005b). Several targets of RUNX2 during osteoblastogenesis are not yet functionally characterized (Wu et al., 2014a). The data from SAPA and ChIP assays revealed that RUNX2 interacts with the proximal -399 to +72 bp region of the *Htra1* promoter during osteogenic differentiation. Luciferase reporter assay using different regions of *Htra1* promoter also revealed the interaction of RUNX2 between -399 to +72 bp. Mutation analysis revealed two critical RUNX2 binding sites at -252 bp and -84 bp for the transactivation of *Htra1* osteoblastogenic expression. This region of interaction, close to the transcription start site, is comparable to the promoter

interaction of RUNX2 with other target genes such as *Col10a1* (Li et al., 2011), *Ibsp* (Roca et al., 2005a) and *Mmp9* (Pratap et al., 2005). To my knowledge, the nucleotide sequences, GCCACT (-252 bp) and GCCGCT, are the two novel RUNX2 binding sites that were not reported previously with any other target genes. The data here uncovers a previously unknown functional interaction between RUNX2 and *Htra1*. *Htra1* has been recently reported to promote osteoclastogenesis in bone marrow macrophages (Wu et al., 2014b). *Runx2* null mice exhibit complete lack of osteoclast cells in the calvarial region. Therefore, *Htra1* could act downstream of RUNX2 during osteoclastogenesis in addition to osteogenesis. *Runx2* is a negative regulator of cell proliferation and suppression of *Runx2* expression is linked to tumorigenesis (Kilbey et al., 2007; Zaidi et al., 2007). Moreover, forced expression of *Runx2* inhibits osteosarcoma cell proliferation (Lucero et al., 2013). *Htra1* is also a tumor suppressor gene, which inhibits cancer cell proliferation (Baldi et al., 2002; Chien et al., 2004a). Transactivation of *Mmp9* by *Runx2* has been observed in osteoblast lineage cells and in cancer cells (Pratap et al., 2007). Therefore, considering the role of *Htra1* as a tumor suppressor along with its potential in modulating the expression of MMPs, the regulation of *Htra1* by *Runx2* identified here in osteoblast cells might have physiological and pathological relevance in other cell lineages. Further studies are needed to address the interaction of RUNX2 and *Htra1* in other systems including tumor where these two molecules have significant roles.

In conclusion, my data here show that *Htra1* is a direct downstream target of *Runx2* and is an inducer of osteogenic differentiation of primary mesenchymal progenitor cells. *Runx2* regulates *Htra1* expression through its interaction with the *Htra1* promoter at -252 bp and -84 bp.

6. GENERAL DISCUSSION

In this thesis, I have demonstrated the role of *Hoxa2* as an inhibitor of osteogenic differentiation by restricting the BMP signaling dependent osteogenic markers spatially and temporally. This study deepens the current understanding on the role of *Hoxa2* in palatogenesis shedding light on the signaling mechanisms downstream of *Hoxa2*.

Hoxa2 was previously identified to be expressed in the developing palate (Nazarali et al., 2000), regulating palate development intrinsically (Smith et al., 2009); however, the mechanisms remained largely unknown. My findings here reveal that *Hoxa2* controls the expression domain of preosteoblast markers by inhibiting osteoprogenitor commitment and osteoprogenitor proliferation on the nasal side of the palate and the loss of *Hoxa2* leads to accelerated osteogenic signaling in the developing palate. The greater cell proliferation rate and osteogenic differentiation on the nasal side of the palate highlights the regional heterogeneity on the role played by *Hoxa2* in this region. The greater cell proliferation in the nasal side of the *Hoxa2*$^{-/-}$ palatal shelves is reaffirmed by a parallel study carried out in our group (Okello et al., 2017). Until recently, improper palatal osteogenesis as a causative agent in the pathogenesis of cleft palate received little attention (Wu et al., 2008; Fu et al., 2017; Jia et al., 2017 a, b), despite mutants of several osteoblast markers known to develop cleft palate (Aberg et al., 2004; Dobreva et al., 2006; Han et al., 2009). IHC analyses *in vivo* evidently revealed augmented bone differentiation and proliferation (Smith et al., 2017; Okello et al., 2017) in the *Hoxa2*$^{-/-}$ palatal shelves at stage E13.5 prior to the elevation, which could be responsible for the cleft palate pathogenesis. However, further investigations using gene ablations of osteoblast-specific specific mutants such as *Runx2*$^{-/-}$ or *Satb2*$^{-/-}$ to test if these mutants could

rescue the cleft palate phenotype in the *Hoxa2*$^{-/-}$ mice are necessary. Such an approach may also directly answer the role of osteogenic differentiation in cleft palate pathogenesis in the *Hoxa2*$^{-/-}$ mice.

The role of *Htra1* in osteogenic differentiation remained controversial and the study here is the first one to exemplify molecular regulation of *Htra1* in osteogenic differentiation. Evidence demonstrated in this study may possibly have placed *Htra1* as an osteoblast marker and a key target of the master regulator, *Runx2*.

In this thesis, I have demonstrated that *Htra1* promotes osteogenic differentiation of palatal mesenchymal cells *in vitro*, and that it is regulated transcriptionally by *Runx2*. Luciferase experiments revealed that RUNX2 binds to *Htra1* proximal promoter at -252 bp and -84 bp to transactivate *Htra1* expression. In addition, *Htra1* induces MMPs possibly via degradation of ECM proteins like biglycan and syndecan to activate FGF signaling (Hou et al., 2007). Although the evidence provided here makes a strong case for *Htra1* as an osteogenic inducer, *Htra1*$^{-/-}$ mice reported elsewhere display very few abnormalities in bone formation (Filliat et al., 2017). This could be due to the functional redundancy of other members of the HTRA family. IHC analyses here revealed that *Htra3* is expressed in similar regions in the palate and in other craniofacial regions. Indeed, *Htra3* shares the highest homology with *Htra1* and a functional redundancy may not be surprising. It remains to be identified whether *Htra3* also promotes osteogenic differentiation and whether *Runx2* regulates *Htra3* expression during osteogenic differentiation.

Htra family members are putative targets of *Hoxa2* in embryonic spinal cord and my initial hypothesis was to test if *Htra1* is a direct downstream target of *Hoxa2* during palate development. IHC and qPCR analyses revealed upregulation of *Htra1* in the *Hoxa2*$^{-/-}$ palatal shelves. In addition, the upregulated *Htra1* expression corroborates with the enhanced osteogenesis in the *Hoxa2*$^{-/-}$ palatal mesenchyme. During the progress of this work, a report on HOXA2 bound regions on the genome in the developing second pharyngeal arch revealed several previously known as well as novel targets of HOXA2 (Donaldson et al., 2012). The report did not show any of the promoters of the *Htra* family members bound by HOXA2. Although the possibility of *Htra1* as a direct transcriptional target of *Hoxa2* cannot be ignored,

it is highly unlikely considering several other known targets have been demonstrated to be bound by HOXA2. It remains to be tested whether *Htra1* is a direct downstream target of *Hoxa2* in osteoblast lineage determination.

In summary, the data here unravels a deeper understanding on the signaling mechanisms downstream of *Hoxa2* in palate development. The regulation of BMP signaling-dependent osteogenic differentiation by *Hoxa2* is a novel finding in understanding the cleft palate pathogenesis of *Hoxa2*$^{-/-}$ mice (Figure 6.1). The direct transcriptional regulation of *Htra1* by *Runx2* is a novel finding in bone development research and it is the first study to reveal any specific molecular regulation of *Htra1* during osteogenesis (Figure 6.1).

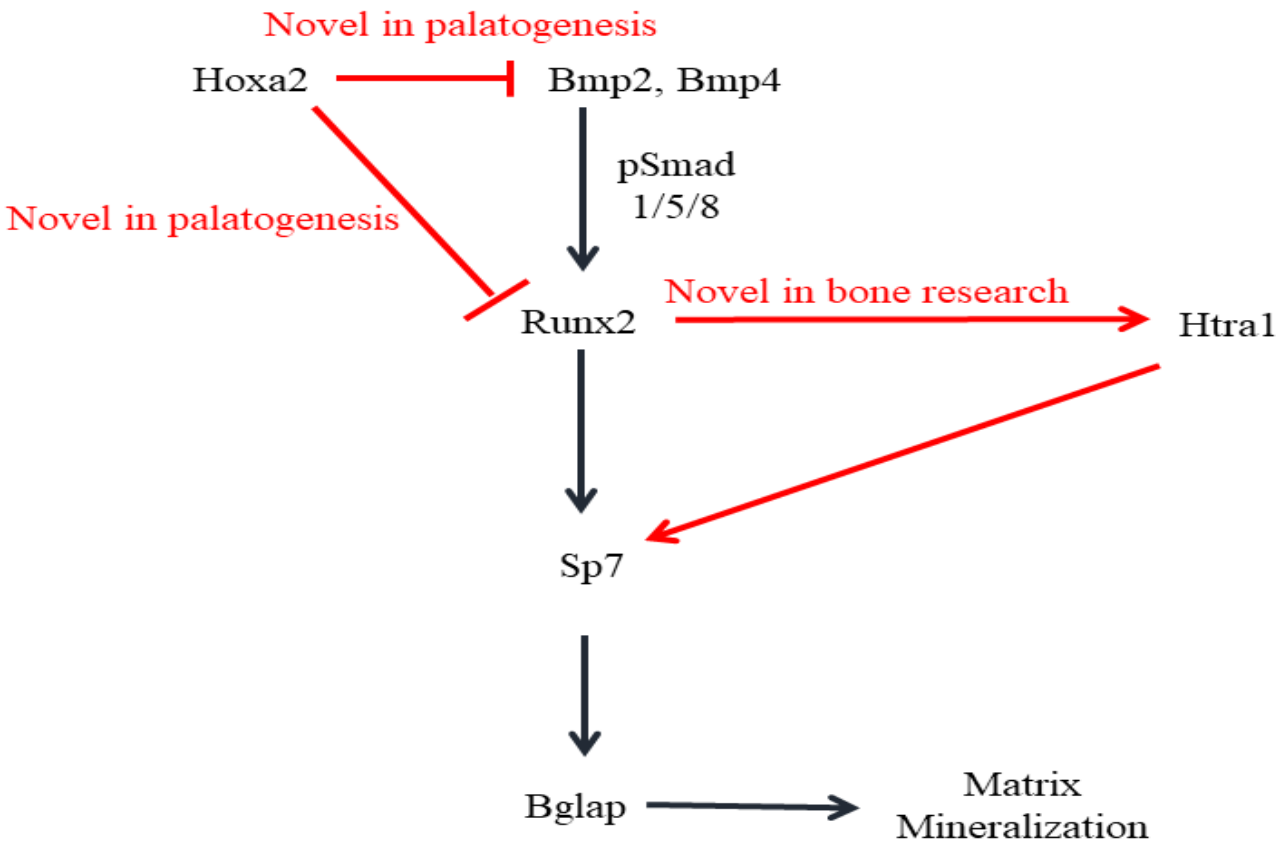

Figure 6.1 Novel insights from the thesis on the molecular mechanism governing palatogenesis and osteogenesis. Schematic diagram showing key findings from this thesis work deciphering gene networks and signaling mechanisms in palatogenesis and osteogenesis. This thesis work explored the role of *Hoxa2* and its putative downstream target *Htra1* in osteogenic differentiation of the palatal mesenchyme. The findings on *Hoxa2* inhibiting BMP signaling and *Runx2*-dependent transcriptional program to control osteogenic domain in the palatal mesenchyme is a new finding on the signaling mechanism in palatogenesis. In addition, the data on the involvement of *Htra1* in as part of the *Runx2* governed transcriptional program of osteogenesis is a new finding in bone development research, which for the first time puts *Htra1* into context in molecular mechanism of osteogenesis.

7. FUTURE DIRECTIONS

7.1 *Hoxa2* in palatogenesis

Although several lines of evidence indicate that *Hoxa2* plays an intrinsic role during palatogenesis, the use of a palatal mesenchyme specific deletion of *Hoxa2* using *Osr2*^{cre} will aid in deciphering the comprehensive cell autonomous requirement of *Hoxa2* in palate development. Furthermore, increased osteogenesis during early palate development could be responsible for the cleft palate pathogenesis. However, further evidence is needed using a compound mutant of *Hoxa2* and *Runx2* or *Stab2*, which would give insight into the specific role of osteogenic differentiation in cleft palate pathogenesis and whether the cleft palate in the *Hoxa2*$^{-/-}$ due to accelerated osteogenic differentiation can be rescued by the genetic ablation of the critical osteoblast markers, which also develop cleft palate. In addition, if the cleft palate phenotype is recued in the compound mutant mouse, it could lead to future therapy work for cleft palate. This thesis work provided some insights into the signaling mechanisms downstream of *Hoxa2*, yet major targets of *Hoxa2* in palate development remain unknown. RNA-seq and ChIP-seq analyses using some elegant genetic tools like *Osr2*$^{RFP/+}$ knockin mice, which could be used to isolate RNA from RFP^{+} *Hoxa2* deleted cells would give insights into the downstream targets of *Hoxa2* in palatogenesis. From the list of differentially regulated targets from the RNA-seq data and genes that are known to cause cleft palate in mouse and humans (Funato et al., 2015), some possible downstream targets of *Hoxa2* that could have a role in palate development, could be chosen for further exploration using genetic tools to address functional targets of *Hoxa2* to better fill the gaps in the existing knowledge. During this thesis work, I was also involved in using X-ray fluorescence imaging at the Canadian Light Source, Saskatoon, Canada, to identify the metal distributions across different stages of palate development. Although we identified some interesting patterns of metal distribution across palatogenesis, we have not identified the metal distribution in the palatal shelves of *Hoxa2* mutants that develop cleft palate, which has elevated cell proliferation and osteogenic differentiation. Metal distribution during palatogenesis is unknown and comparative metal distribution between wild type and *Hoxa2*$^{-/-}$ would give insights into the influence of key chemical

elements in cell proliferation and osteogenic differentiation during palatal shelf elevation and fusion. Understanding the metal distribution using XRF imaging could give information on the abundance of critical elements that could influence palatogenesis, which could open new avenues of an unexplored interactions between metal elements and genetic elements during palatogenesis.

7.2 *Htra1* and *Htra3*

The role of *Htra3* in osteogenic differentiation remains unknown. A preliminary investigation using *Htra3* siRNA in primary mesenchymal cells to identify the role of *Htra3* in osteogenic differentiation is warranted. As *Htra3 null* mice do not show any abnormal bone phenotype, a compound mutant of *Htra1* and *Htra3* could be useful in understanding the redundant role during development. In particular, a compound preosteoblast-specific deletion of *Htra1* and *Htra3* using *Runx2*-cre would reveal the role and redundancy of these serine proteases in osteogenic differentiation. In order to decipher the role in palatal fusion, chick embryonic palatal explants in culture which do not fuse naturally could be exploited to exogenously add HTRA3 protein along with pro-TGFβ3 to check if *Htra3* aids in palatal fusion via aiding the activation of mature TGFβ3 by cleaving the inactive form. This could be more successful than the usage of lentiviral particles. In addition, an epithelial specific *K14*-Cre compound deletion of *Htra1* and *Htra3* could reveal the role and redundancy of these two serine proteases in palatal fusion during development. Although it is plausible that the regulation of *Htra1* by *Hoxa2* is indirectly through *Runx2*, the hypothesis of a direct regulation of *Htra3* and/or *Htra1* by *Hoxa2* cannot be neglected. Therefore, an in-silico analysis of *Htra1* and *Htra3* promoter could indicate whether there are any putative binding sites of *Hoxa2* in the promoter regions of *Htra1* and *Htra3*. In addition, ChIP analysis or ChIP-seq analysis using wild type and *Hoxa2*$^{-/-}$ palatal mesenchymal cells will shed further light into any possible interaction between *Hoxa2* and these two serine protease genes *Htra1* and *Htra3*.

8. CONCLUSIONS

The data presented in this thesis is the first to show that *Hoxa2* inhibits BMP signaling to regulate osteoprogenitor commitment and proliferation unraveling a possible mechanism for the cleft pathogenesis

in the *Hoxa2*$^{-/-}$ mice. This study is also one of the very few studies to show that controlled osteogenic differentiation in the palatal mesenchyme could be critical for the palatal shelf elevation. *Htra1* acts downstream of *Runx2* to promote bone matrix mineralization. This study also identified *Htra1* as a novel direct downstream target of *Runx2* during osteogenic differentiation.

9. REFERENCES

1. Aberg, T., Cavender, A., Gaikwad, J.S., Bronckers, A.L.J.J., Wang, X., Waltimo-Sirén, J., Thesleff, I., and D'Souza, R.N. (2004) Phenotypic changes in dentition of Runx2 homozygote-null mutant mice. *J. Histochem. Cytochem.*, **52** (1), 131–39.
2. Acampora, D., Merlo, G.R., Paleari, L., Zerega, B., Postiglione, M.P., Mantero, S., Bober, E., Barbieri, O., Simeone, a, and Levi, G. (1999) Craniofacial, vestibular and bone defects in mice lacking the Distal-less-related gene Dlx5. *Development*, **126**, 3795–809.
3. Alappat, S.R., Zhang, Z., Suzuki, K., Zhang, X., Liu, H., Jiang, R., Yamada, G., and Chen, Y. (2005) The cellular and molecular etiology of the cleft secondary palate in Fgf10 mutant mice. *Dev. Biol.*, **277** (1), 102–13.
4. Alasti, F., Sadeghi, A., Sanati, M.H., Farhadi, M., Stollar, E., Somers, T., and Van Camp, G. (2008) A Mutation in HOXA2 Is Responsible for Autosomal-Recessive Microtia in an Iranian Family. *Am. J. Hum. Genet.*, **82** (4), 982–91.

5. Baek, J., Lan, Y., Liu, H., Maltby, K.M., Mishina, Y., and Jiang, R. (2011) Bmpr1a signaling plays critical roles in palatal shelf growth and palatal bone formation. *Dev. Biol.*, **350** (2), 520–531.

6. Baldi, A., De Luca, A., Morini, M., Battista, T., Felsani, A., Baldi, F., Catricalà, C., Amantea, A., Noonan, D.M., Albini, A., Natali, P.G., Lombardi, D., Paggi, M.G. (2002) The HtrA1 serine protease is down-regulated during human melanoma progression and represses growth of metastatic melanoma cells. *Oncogene*, **21**, 6684–88.

7. Barlow, a J., Bogardi, J.P., Ladher, R., and Francis-West, P.H. (1999) Expression of chick Barx-1 and its differential regulation by FGF-8 and BMP signaling in the maxillary primordia. *Dev. Dyn.*, **214** (4), 291–302.

8. Barrow, J.R., and Capecchi, M.R. (1999) Compensatory defects associated with mutations in Hoxa1 restore normal palatogenesis to Hoxa2 mutants. *Development*, **126** (22), 5011-26.

9. Beaufort, N., Scharrer, E., Kremmer, E., Lux, V., Ehrmann, M., Huber, R., Houlden, H., Werring, D., Haffner, C., and Dichgans, M. (2014) Cerebral small vessel disease-related protease HtrA1 processes latent TGF-β binding protein 1 and facilitates TGF-β signaling. *Proc. Natl. Acad. Sci.*, **111**, 16496–501.

10. Beleford, D., Liu, Z., Rattan, R., Quagliuolo, L., Boccellino, M., Baldi, A., Maguire, J., Staub, J., Molina, J., and Shridhar, V. (2010a) Methylation induced gene silencing of HtrA3 in smoking-related lung cancer. *Clin. Cancer Res.*, **16** (2), 398–409.

11. Beleford, D., Rattan, R., Chien, J., and Shridhar, V. (2010b) High temperature requirement A3 (HtrA3) promotes etoposide- and cisplatin-induced cytotoxicity in lung cancer cell lines. *J. Biol. Chem.*, **285** (16), 12011–27.

12. Blavier, L., Lazaryev, a, Groffen, J., Heisterkamp, N., DeClerck, Y. a, and Kaartinen, V. (2001) TGF-beta3-induced palatogenesis requires matrix metalloproteinases. *Mol. Biol. Cell*, **12** (5), 1457–66.

13. Brown, G.D., and Nazarali, A.J. (2010) Matrix metalloproteinase-25 has a functional role in mouse secondary palate development and is a downstream target of TGF-β3. *BMC Dev. Biol.*, **10** (1), 93.

14. Bush, J.O., and Jiang, R. (2012) Palatogenesis: morphogenetic and molecular mechanisms of secondary palate development. *Development*, **139** (4), 231–43.

15. Bustos-valenzuela, J.C., Fujita, A., Halcsik, E., Granjeiro, J.M., and Sogayar, M.C. (2011) Unveiling novel genes upregulated by both rhBMP2 and rhBMP7 during early osteoblastic transdifferentiation of C2C12 cells. *BMC Res. Notes*, 4, 370

16. Campioni, M., Severino, A., Manente, L., Tuduce, I.L., Toldo, S., Caraglia, M., Crispi, S., Ehrmann, M., He, X., Maguire, J., De Falco, M., De Luca, A., Shridhar, V., and Baldi, A. (2010) The serine protease HtrA1 specifically interacts and degrades the tuberous sclerosis complex 2 protein. *Mol. Cancer Res.*, **8** (9), 1248–60.

17. Chai, Y., Ito, Y., and Han, J. (2003) Tgf- Signaling and Its Functional Significance in Regulating the Fate of Cranial Neural Crest Cells. *Crit. Rev. Oral Biol. Med.*, **14** (2), 78–88.

18. Chen, M., Huang, H-Z., Wang, M., and Wang, A-X. (2010) Retinoic Acid Inhibits Osteogenic Differentiation of Mouse Embryonic Palate Mesenchymal Cells. *Birth Defects Res. A Clin. Mol. Teratol.*, **88**, 965-70.

19. Chien, J., He, X., and Shridhar, V. (2009) Identification of tubulins as substrates of serine protease HtrA1 by mixture-based oriented peptide library screening. *J. Cell. Biochem.*, **107** (2), 253–63.

20. Chien, J., Staub, J., Hu, S., Erickson-johnson, M.R., Couch, F.J., Smith, D.I., Crowl, R.M., Kaufmann, S.H., and Shridhar, V. (2004) A candidate tumor suppressor HtrA1 is downregulated in ovarian cancer. *Oncogene*, 1636–44.

21. Choi, J., Pratap, J., Javed, A., Zaidi, S.K., Xing, L., Balint, E., Dalamangas, S., Wijnen, J. Van, Lian, J.B., Stein, J.L., Jones, S.N., Stein, G.S., and Boyce, B. (2001) Subnuclear targeting of Runx/ Cbfa/ AML factors is essential for tissue-specific differentiation during embryonic development. *Proc. Natl. Acad. Sci. U. S. A.*, *98*(15), 8650-55.

22. Clawson, G. a, Bui, V., Xin, P., Wang, N., and Pan, W. (2008) Intracellular localization of the tumor suppressor HtrA1/Prss11 and its association with HPV16 E6 and E7 proteins. *J. Cell. Biochem.*, **105** (1), 81–8.

23. Cui, X.M., and Shuler, C.F. (2000) The TGF-beta type III receptor is localized to the medial edge epithelium during palatal fusion. *Int. J. Dev. Biol.*, **44** (4), 397–402.

24. Cui, X.-M., Chai, Y., Chen, J., Yamamoto, T., Ito, Y., Bringas, P., and Shuler, C.F. (2003) TGF-beta3-dependent SMAD2 phosphorylation and inhibition of MEE proliferation during palatal fusion. *Dev. Dyn.*, **227** (3), 387–94.

25. Cui, X.-M., Shiomi, N., Chen, J., Saito, T., Yamamoto, T., Ito, Y., Bringas, P., Chai, Y., and Shuler, C.F. (2005) Overexpression of Smad2 in Tgf-beta3-null mutant mice rescues cleft palate. *Dev. Biol.*, **278** (1), 193–202.

26. Cui, X.M., Warburton, D., Zhao, J., Crowe, D.L., and Shuler, C.F. (1998) Immunohistochemical localization of TGF-beta type II receptor and TGF-beta3 during palatogenesis in vivo and in vitro. *Int. J. Dev. Biol.*, **42** (6), 817–20.

27. Deng, W.G., Zhu, Y., Montero, A., and Wu, K.K. (2003) Quantitative analysis of binding of transcription factor complex to biotinylated DNA probe by a streptavidin-agarose pulldown assay. *Anal. Biochem.*, **323** (1), 12–18.

28. Deprez, P.M.L., Nichane, M.G., Rousseaux, P., Devogelaer, J.-P., Chappard, D., Lengelé, B.G., Rezsöhazy, R., and Nyssen-Behets, C. (2012) Postnatal growth defect in mice upon persistent Hoxa2 expression in the chondrogenic cell lineage. *Differentiation*, **83** (3), 158–67.

29. Dixon, M.J., Marazita, M.L., Beaty, T.H., and Murray, J.C. (2011) Cleft lip and palate: understanding genetic and environmental influences. *Nat. Rev. Genet.*, **12** (3), 167–78.

30. Dobreva, G., Chahrour, M., Dautzenberg, M., Chirivella, L., Kanzler, B., Fariñas, I., Karsenty, G., and Grosschedl, R. (2006) SATB2 is a multifunctional determinant of craniofacial patterning and osteoblast differentiation. *Cell*, **125** (5), 971–86.

31. Donaldson, I.J., Amin, S., Hensman, J.J., Kutejova, E., Rattray, M., Lawrence, N., Hayes, A., Ward, C.M., and Bobola, N. (2012) Genome-wide occupancy links Hoxa2 to Wnt-β-catenin signaling in mouse embryonic development. *Nucleic Acids Res.*, **40** (9), 3990–4001.

32. Dudas, M., Nagy, A., Laping, N.J., Moustakas, A., and Kaartinen, V. (2004) Tgf-β3-induced palatal fusion is mediated by Alk-5/Smad pathway. *Dev. Biol.*, **266** (1), 96–108.

33. Ferguson, M.W. (1988) Palate development. *Development*, **103**, 41–60.

34. Ferrer-Vaquer, A., Maurey, P., Werzowa, J., Firnberg, N., Leibbrandt, A., and Neubüser, A. (2008) Expression and regulation of HTRA1 during chick and early mouse development. *Dev. Dyn.*, **237** (7), 1893–900.

35. Filliat, G., Mirsaidi, A., Tiaden, A.N., Kuhn, G.A., Weber, F.E., Oka, C., and Richards, P.J. (2017) Role of HTRA1 in bone formation and regeneration: In vitro and in vivo evaluation. *PLoS One*, **12** (7), e0181600.

36. Fu, X., Xu, J., Chaturvedi, P., Liu, H., Jiang, R., and Lan, Y. (2017). Identification of Osr2 transcriptional target genes in palate development. *J. Dent. Res.*, **96**, 1451–58.

37. Fuchs, A., Inthal, A., Herrmann, D., Cheng, S., Nakatomi, M., Peters, H., and Neubüser, A. (2010) Regulation of Tbx22 during facial and palatal development. *Dev. Dyn.*, **239**, 2860–74.

38. Funato, N., Nakamura, M., and Yanagisawa, H. (2015). Molecular basis of cleft palates in mice. *World J. Biol. Chem.*, **6**, 121–38.

39. Gammill, L. S. and Bronner-Fraser, M. (2003). Neural crest specification: migrating into genomics. *Nat. Rev. Neurosci.*, **4** (10), 795-805.

40. Gato, a, Martinez, M., Tudela, C., Alonso, I., Moro, J., Formoso, M., Ferguson, M., and Martinezalvarez, C. (2002) TGF-β3-Induced Chondroitin Sulphate Proteoglycan Mediates Palatal Shelf Adhesion. *Dev. Biol.*, **250** (2), 393–405.

41. Gendron-Maguire, M., Mallo, M., Zhang, M., and Gridley, T. (1993) Hoxa-2 mutant mice exhibit homeotic transformation of skeletal elements derived from cranial neural crest. *Cell*, **75** (7), 1317–31.

42. Glanz, S., Filliat, G., Mirsaidi, A., Tiaden, N., and Richards, P.J. (2016) Loss-of-function of HtrA1 abrogates all-trans retinoic acid-induced osteogenic differentiation of mouse adipose-derived stromal cells through deficiencies in p70S6K activation. *Stem Cells Dev.*, **25**, 687–98.

43. Gordon, J. a R., Hassan, M.Q., Saini, S., Montecino, M., van Wijnen, A.J., Stein, G.S., Stein, J.L., and Lian, J.B. (2010) Pbx1 represses osteoblastogenesis by blocking Hoxa10-mediated recruitment of chromatin remodeling factors. *Mol. Cell. Biol.*, **30** (14), 3531–41.

44. Graham, A., Heyman, I., and Lumsden, A. (1993). Even-numbered rhombomeres control the apoptotic elimination of neural crest cells from odd numbered rhombomeres in the chick hindbrain. *Development*, **119** (1), 233-45.

45. Graham, J.R., Chamberland, A., Lin, Q., Li, X.J., Dai, D., Zeng, W., Flannery, C.R., Yang, Z., and Ryan, M.S. (2013) Serine protease HTRA1 antagonizes transforming growth factor-β signaling by cleaving its receptors and loss of HTRA1 in vivo enhances bone formation. **8** (9), e74094.

46. Grammatopoulos, G.A., Bell, E., Toole, L., Lumsden, A., and Tucker, A.S. (2000) Homeotic transformation of branchial arch identity after Hoxa2 overexpression. *Development*, **127**, 5355–65.

47. Grau, S., Richards, P.J., Kerr, B., Hughes, C., Caterson, B., Williams, A.S., Junker, U., Jones, S. A, Clausen, T., and Ehrmann, M. (2006) The role of human HtrA1 in arthritic disease. *J. Biol. Chem.*, **281** (10), 6124–9.

48. Gregory, C. a, Gunn, W.G., Peister, A., and Prockop, D.J. (2004) An Alizarin red-based assay of mineralization by adherent cells in culture: comparison with cetylpyridinium chloride extraction. *Anal. Biochem.*, **329** (1), 77–84.

49. Hadfield, K.D., Rock, C.F., Inkson, C.A, Dallas, S.L., Sudre, L., Wallis, G.A, Boot-Handford, R.P., and Canfield, A.E. (2008) HtrA1 inhibits mineral deposition by osteoblasts: requirement for the protease and PDZ domains. *J. Biol. Chem.*, **283** (9), 5928–38.

50. Han, J., Mayo, J., Xu, X., Li, J., Bringas, P., Maas, R.L., Rubenstein, J.L.R., and Chai, Y. (2009) Indirect modulation of Shh signaling by Dlx5 affects the oral-nasal patterning of palate and rescues cleft palate in Msx1-null mice. *Development*, **136** (24), 4225–33.

51. Hara, K., Shiga, A., Fukutake, T., Nozaki, H., Miyashita, A., Yokoseki, A., Kawata, H., Koyama, A., Arima, K., Takahashi, T., Ikeda, M., Shiota, H., Tamura, M., Shimoe, Y., Hirayama, M., Arisato, T., Yanagawa, S., Tanaka, A., Nakano, I., Ikeda, S., Yoshida, Y.,

Yamamoto, T., Ikeuchi, T., Kuwano, R., Nishizawa, M., Tsuji, S., and Onodera, O. (2009) Association of HTRA1 mutations and familial ischemic cerebral small-vessel disease. *N. Engl. J. Med.*, **360** (17), 1729–39.

52. He, F., Xiong, W., Wang, Y., Matsui, M., Yu, X., Chai, Y., Klingensmith, J., and Chen, Y. (2010) Modulation of BMP signaling by Noggin is required for the maintenance of palatal epithelial integrity during palatogenesis. *Dev. Biol.*, **347** (1), 109–21.
53. He, X., Khurana, A., Maguire, J.L., Chien, J., and Shridhar, V. (2012) HtrA1 sensitizes ovarian cancer cells to cisplatin-induced cytotoxicity by targeting XIAP for degradation. *Int. J. Cancer*, **130** (5), 1029–35.
54. He, X., Ota, T., Liu, P., Su, C., Chien, J., and Shridhar, V. (2010) Downregulation of HtrA1 promotes resistance to anoikis and peritoneal dissemination of ovarian cancer cells. *Cancer Res.*, **70** (8), 3109–18.
55. Herr, A., Meunier, D., Müller, I., Rump, A., Fundele, R., Ropers, H.-H., and Nuber, U. a. (2003) Expression of mouse Tbx22 supports its role in palatogenesis and glossogenesis. *Dev. Dyn.*, **226** (4), 579–86.
56. Hill, C.R., Yuasa, M., Schoenecker, J., and Goudy, S.L. (2014) Jagged1 is essential for osteoblast development during maxillary ossification. *Bone*, **62**, 10–21.
57. Hilliard, S. A, Yu, L., Gu, S., Zhang, Z., and Chen, Y.P. (2005) Regional regulation of palatal growth and patterning along the anterior-posterior axis in mice. *J. Anat.*, **207** (5), 655–67.
58. Hosokawa, R., Deng, X., Takamori, K., Xu, X., Urata, M., Bringas, P., and Chai, Y. (2009) Epithelial-specific requirement of FGFR2 signaling during tooth and palate development. *J. Exp. Zool. B. Mol. Dev. Evol.*, **312B** (4), 343–50.
59. Hou, S., Maccarana, M., Min, T.H., Strate, I., and Pera, E.M. (2007) The secreted serine protease xHtrA1 stimulates long-range FGF signaling in the early Xenopus embryo. *Dev. Cell*, **13** (2), 226–41.
60. Hu, R., Liu, W., Li, H., Yang, L., Chen, C., Xia, Z.-Y., Guo, L.-J., Xie, H., Zhou, H.-D., Wu, X.-P., and Luo, X.-H. (2011) A Runx2/miR-3960/miR-2861 regulatory feedback loop during mouse osteoblast differentiation. *J. Biol. Chem.*, **286** (14), 12328–39.
61. Hu, R., Liu, W., Li, H., Yang, L., Chen, C., Xia, Z.-Y., Guo, L.-J., Xie, H., Zhou, H.-D., Wu, X.-P., and Luo, X.-H. (2011) A Runx2/miR-3960/miR-2861 regulatory feedback loop during mouse osteoblast differentiation. *J. Biol. Chem.*, **286** (14), 12328–39.
62. Hunter, M.P., and Prince, V.E. (2002) Zebrafish hox paralogue group 2 genes function redundantly as selector genes to pattern the second pharyngeal arch. *Dev. Biol.*, **247** (2), 367–89.

63. Ito, Y., Yeo, J.Y., Chytil, A., Han, J., Bringas, P., Nakajima, A., Shuler, C.F., Moses, H.L., and Chai, Y. (2003) Conditional inactivation of Tgfbr2 in cranial neural crest causes cleft palate and calvaria defects. *Development*, **130** (21), 5269–80.

64. Iwata, J., Hacia, J.G., Suzuki, A., Sanchez-Lara, P. a, Urata, M., and Chai, Y. (2012a) Modulation of noncanonical TGF-β signaling prevents cleft palate in Tgfbr2 mutant mice. *J. Clin. Invest.*, **122** (3), 873–85.

65. Iwata, J., Hosokawa, R., Sanchez-Lara, P. A, Urata, M., Slavkin, H., and Chai, Y. (2010) Transforming growth factor-beta regulates basal transcriptional regulatory machinery to control cell proliferation and differentiation in cranial neural crest-derived osteoprogenitor cells. *J. Biol. Chem.*, **285** (7), 4975–82.

66. Iwata, J., Parada, C., and Chai, Y. (2011) The mechanism of TGF-β signaling during palate development. *Oral Dis.*, **17** (8), 733–44.

67. Iwata, J., Suzuki, A., Pelikan, R.C., Ho, T.V., Sanchez-Lara, P. a., and Chai, Y. (2014) Modulation of lipid metabolic defects rescues cleft palate in tgfbr2 mutant mice. *Hum. Mol. Genet.*, **23** (1), 182–193.

68. Iwata, J.I., Tung, L., Urata, M., Hacia, J.G., Pelikan, R., Suzuki, A., Ramenzoni, L., Chaudhry, O., Parada, C., Sanchez-Lara, P.A., and Chai, Y. (2012b) Fibroblast growth factor 9 (FGF9)-pituitary homeobox 2 (PITX2) pathway mediates transforming growth factorβ (TGFβ) signaling to regulate cell proliferation in palatal mesenchyme during mouse palatogenesis. *J. Biol. Chem.*, **287** (4), 2353–63.

69. Iyyanar, P.P.R., and Nazarali, A.J. (2017) Hoxa2 inhibits bone morphogenetic protein signaling during osteogenic differentiation of the palatal mesenchyme. *Front. Physiol.*, **8**, 929.

70. Javed, A., Chen, H., and Ghori, F.Y. (2010) Genetic and transcriptional control of bone formation. *Oral Maxillofac. Surg. Clin. North Am.*, **22** (3), 283–93.

71. Ji, S., Doucette, J.R., and Nazarali, A.J. (2011) Sirt 2 is a novel in vivo downstream target of Nkx 2.2 and enhances oligodendroglial cell differentiation. *J. Mol. Cell Biol.*, **3**, 351–59.

72. Jia, S., Zhou, J., Fanelli, C., Wee, Y., Bonds, J., Schneider, P., Mues, G., Souza, R.N.D. (2017a). Small molecule Wnt agonists correct cleft palates in Pax9 mutant mice in utero. *Development*, **144**, 3819–28.

73. Jia, S., Zhou, J., Wee, Y., Mikkola, M.L., Schneider, P., and Souza, R.N.D. (2017b). Anti-EDAR agonist antibody therapy resolves palate defects in Pax9−/− Mice. *J. Dent. Res.*, **96** (11), 1282–89.

74. Jin, J.-Z., and Ding, J. (2006) Analysis of Meox-2 mutant mice reveals a novel post fusion-based cleft palate. *Dev. Dyn.*, **235** (2), 539–46.

75. Kaartinen, V., Voncken, J.W., Shuler, C.F., Warburton, D., Bu, D., Heisterkamp, N. and Groffen, J. (1995). Abnormal lung development and cleft palate in mice lacking Tgf-Beta3 indicates defects of epithelial-mesenchymal interactions. *Nat. Genet.*, **11**, 415-21.

76. Kamachi, Y., Ogawa, E., Asano, M., Ishida, S., and Murakami, Y. (1990) Purification of a mouse nuclear factor that binds to both the A and B cores of the polyomavirus enhancer. *J. Virol.*, **64** (10), 4808–19.

77. Kanzler, B., Kuschert, S.J., Liu, Y., and Mallo, M. (1998) Hoxa-2 restricts the chondrogenic domain and inhibits bone formation during development of the branchial area. *Development*, **125**, 2587–97.

78. Kilbey, A., Blyth, K., Wotton, S., Terry, A., Jenkins, A., Bell, M., Hanlon, L., Cameron, E.R., Neil, J.C. (2007) Runx2 disruption promotes immortalization and confers resistance to oncogene-induced senescence in primary murine fibroblasts. *Cancer Res.*, **67**, 11263–71.

79. Kim, G.-Y., Kim, H.-Y., Kim, H.-T., Moon, J.-M., Kim, C.-H., Kang, S., and Rhim, H. (2012) HtrA1 is a novel antagonist controlling fibroblast growth factor (FGF) signaling via cleavage of FGF8. *Mol. Cell. Biol.*, **32** (21), 4482–92.

80. Komori, T. (2010) Regulation of bone development and extracellular matrix protein genes by RUNX2. *Cell Tissue Res.*, **339**, 189–195.

81. Komori, T., Yagi, H., Nomura, S., Yamaguchi, a, Sasaki, K., Deguchi, K., Shimizu, Y., Bronson, R.T., Gao, Y.H., Inada, M., Sato, M., Okamoto, R., Kitamura, Y., Yoshiki, S., and Kishimoto, T. (1997) Targeted disruption of Cbfa1 results in a complete lack of bone formation owing to maturational arrest of osteoblasts. *Cell*, **89** (5), 755–64.

82. Köntges, G., and Lumsden, A. (1996) Rhombencephalic neural crest segmentation is preserved throughout craniofacial ontogeny. *Development*, **122**, 3229–42.

83. Krumlauf, R. (1993) Hox genes and pattern formation in the branchial region of the vertebrate head. *Trends Genet.*, **9** (4), 106–12.

84. Kwong, F.N.K., Richardson, S.M., and Evans, C.H. (2008) Chordin knockdown enhances the osteogenic differentiation of human mesenchymal stem cells. *Arthritis Res. Ther.*, **10** (3), R65.

85. Lamour, V., Sanchez, C., Henrotin, Y., Castronovo, V., and Bellahce, A. (2007) Runx2- and Histone deacetylase 3-mediated repression is relieved in differentiating human osteoblast cells to allow high bone sialoprotein expression. *J. Biol. Chem.*, **282** (50), 36240–49.

86. Lan, Y., and Jiang, R. (2009) Sonic hedgehog signaling regulates reciprocal epithelial-mesenchymal interactions controlling palatal outgrowth. *Development*, **136** (8), 1387–96.

87. Lan, Y., Ovitt, C.E., Cho, E.-S., Maltby, K.M., Wang, Q., and Jiang, R. (2004) Odd-skipped related 2 (Osr2) encodes a key intrinsic regulator of secondary palate growth and morphogenesis. *Development*, **131** (13), 3207–16.

88. Le Douarin, N. M. and Kalcheim, C. (1999). *The Neural Crest.* Cambridge, UK: Cambridge University Press.

89. Lee, J.-M., Kim, J.-Y., Cho, K.-W., Lee, M.-J., Cho, S.-W., Kwak, S., Cai, J., and Jung, H.-S. (2008) Wnt11/Fgfr1b cross-talk modulates the fate of cells in palate development. *Dev. Biol.*, **314** (2), 341–50.

90. Lee, Y.H., and Saint-Jeannet, J.P. (2011) Sox9 function in craniofacial development and disease. *Genesis*, **49** (4), 200–08.

91. Levi, G., Mantero, S., Barbieri, O., Cantatore, D., Paleari, L., Beverdam, A., Genova, F., Robert, B., and Merlo, G.R. (2006) Msx1 and Dlx5 act independently in development of craniofacial skeleton, but converge on the regulation of Bmp signaling in palate formation. *Mech. Dev.*, **123** (1), 3–16.

92. Li, C., Lan, Y., Krumlauf, R., and Jiang, R. (2017) Modulating Wnt Signaling Rescues Palate Morphogenesis in Pax9 Mutant Mice. *J. Dent. Res.*, **96** (11), 1273-81.

93. Li, F., Lu, Y., Ding, M., Napierala, D., Abbassi, S., Chen, Y., Duan, X., Wang, S., Lee, B., and Zheng, Q. (2011) Runx2 contributes to murine Col10a1 gene regulation through direct interaction with its cis-enhancer. *J Bone Miner Res.*, **26**, 2899–910.

94. Li, L., Lin, M., Wang, Y., Cserjesi, P., Chen, Z., and Chen, Y. (2011) BmprIa is required in mesenchymal tissue and has limited redundant function with BmprIb in tooth and palate development. *Dev. Biol.*, **349** (2), 451–61.

95. Li, L., Wang, Y., Lin, M., Yuan, G., Yang, G., Zheng, Y., and Chen, Y.P. (2013) Augmented BMPRIA-mediated BMP signaling in cranial neural crest lineage leads to cleft palate formation and delayed tooth differentiation. *PLoS One*, **8** (6), e66107.

96. Li, R., and Zhang, Q. (2015) HtrA1 may regulate the osteogenic differentiation of human periodontal ligament cells by TGF-β1. *J. Mol. Histol.*, **46** (2), 137–44.

97. Liu, W. (2005) Distinct functions for Bmp signaling in lip and palate fusion in mice. *Development*, **132** (6), 1453–61.

98. Liu, W., Lan, Y., Pauws, E., Meester-Smoor, M. A, Stanier, P., Zwarthoff, E.C., and Jiang, R. (2008) The Mn1 transcription factor acts upstream of Tbx22 and preferentially regulates posterior palate growth in mice. *Development*, **135** (23), 3959–68.

99. Lou, Y., Javed, A., Hussain, S., Colby, J., Frederick, D., Pratap, J., Xie, R., Gaur, T., van Wijnen, A.J., Jones, S.N., Stein, G.S., Lian, J.B., and Stein, J.L. (2009) A Runx2 threshold for the cleidocranial dysplasia phenotype. *Hum. Mol. Genet.*, **18** (3), 556–68.

100. Lucero, C.M., Vega, O.A., Osorio, M.M., Tapia, J.C., Antonelli, M., Stein, G.S, van Wijnen A.J., Galindo, M.A. (2013) The cancer-related transcription factor Runx2 modulates cell

proliferation in human osteosarcoma cell lines. *J Cell Physiol*., **228**, 714–23.

101. Lumsden, A., and Keynes, R. (1989). Segmental patterns of neuronal development in the chick hindbrain. *Nature*, 337 (6206), 424-28.

102. Martins, L.M., Morrison, A., Klupsch, K., Fedele, V., Moisoi, N., Teismann, P., Abuin, A., Grau, E., Geppert, M., George, P., Creasy, C.L., Martin, A., Hargreaves, I., Heales, S.J., Okada, H., Brandner, S., Schulz, B., Mak, T., Downward, J., and Livi, G.P. (2004) Neuroprotective role of the reaper-related serine protease HtrA2 / Omi revealed by targeted deletion in mice. *Molecular and Cell. Biol.*, ***24***(22), 9848–62.

103. Mendioroz, M., Ferna´ndez-Cadenas, I., del Río-Espinola, A., Rovira, A., Sole´,E., Ferna´ndez-Figueras, M. T., García-Patos, V., Sastre-Garriga, J., Domingues-Montanari, S., A´ lvarez-Sabín, J., Montaner, J. (2010) A missense HTRA1 mutation expands CARASIL syndrome to the Caucasian population. *Neurology*. 75, 2033-2035

104. Minoux, M., and Rijli, F. M. (2010). Molecular mechanisms of cranial neural crest cell migration and patterning in craniofacial development. *Development*, ***137*** (16), 2605–21.

105. Minoux, M., and Rijli, F.M. (2010) Molecular mechanisms of cranial neural crest cell migration and patterning in craniofacial development. *Development*, **137**, 2605–21.

106. Morales, A. V., Barbas, J. A. and Nieto, M. A. (2005). How to become neural crest: from segregation to delamination. *Semin. Cell Dev. Biol.*, **16** (6), 655-62.

107. Morkmued, S., Laugel-Haushalter, V., Mathieu, E., Schuhbaur, B., Hemmerlé, J., Dollé, P., Bloch-Zupan, A., and Niederreither, K. (2017) Retinoic acid excess impairs amelogenesis inducing enamel defects. *Front. Physiol.*, **7**, 673.

108. Mullany, S. a, Moslemi-Kebria, M., Rattan, R., Khurana, A., Clayton, A., Ota, T., Mariani, A., Podratz, K.C., Chien, J., and Shridhar, V. (2011) Expression and functional significance of HtrA1 loss in endometrial cancer. *Clin. Cancer Res.*, **17** (3), 427–36.

109. Murray, J.C., and Schutte, B.C. (2004). Cleft palate: players, pathways, and pursuits. *J. Clin. Invest.* 113, 1676–78.

110. Murwantoko, Yano, M., Ueta, Y., Murasaki, A., Kanda, H., Oka, C., and Kawaichi, M. (2004) Binding of proteins to the PDZ domain regulates proteolytic activity of HtrA1 serine protease. *Biochem. J.*, **381**, 895–904.

111. Nakajima, A., Ito, Y., Asano, M., Maeno, M., Iwata, K., Mitsui, N., Shimizu, N., Cui, X.-M., and Shuler, C.F. (2007) Functional role of transforming growth factor-beta type III receptor during palatal fusion. *Dev. Dyn.*, **236** (3), 791–801.

112. Narkiewicz, J., Klasa-Mazurkiewicz, D., Zurawa-Janicka, D., Skorko-Glonek, J., Emerich, J., and Lipinska, B. (2008) Changes in mRNA and protein levels of human HtrA1, HtrA2 and HtrA3 in ovarian cancer. *Clin. Biochem.*, **41**, 561–9.

113. Nazarali, A., Puthucode, R., Leung, V., Wolf, L., Hao, Z., and Yeung, J. (2000) Temporal and Spatial Expression of Hoxa-2 During Murine Palatogenesis. *Cell. Mol. Neurobiol.*, **20** (3), 269–90.

114. Nelson, E.R., Levi, B., Sorkin, M., James, A.W., Liu, K.J., Quarto, N., and Longaker, M.T. (2011) Role of GSK-3β in the osteogenic differentiation of palatal mesenchyme. *PLoS One*, **6** (10), e25847.

115. Nie, G., Hampton, A., Li, Y., Findlay, J.K., and Salamonsen, L.A. (2003) comparison of its tissue distribution with HtrA1 and HtrA2. *Biochem. J.*, **371**, 39-48.

116. Nik, A.M., Johansson, J.A., Ghiami, M., Ravahi, A., and Carlsson, P. (2016) Foxf2 is required for secondary palate development and Tgfβ signaling in palatal shelf mesenchyme. *Dev. Biol.*, **415**, 14-23.

117. Noden, D. M. (1983). The role of the neural crest in patterning of avian cranial skeletal, connective and muscle tissues. *Dev. Biol.*, 96, 144-65.

118. Oka, C., Tsujimoto, R., Kajikawa, M., Koshiba-Takeuchi, K., Ina, J., Yano, M., Tsuchiya, A., Ueta, Y., Soma, A., Kanda, H., Matsumoto, M., and Kawaichi, M. (2004) HtrA1 serine protease inhibits signaling mediated by Tgfbeta family proteins. *Development*, **131** (5), 1041–53.

119. Okello, D.O., Iyyanar, P.P.R., Kulyk, W.M., Smith, T.M., Lozanoff, S., Ji, S., and Nazarali, A.J. (2017) Six2 plays an intrinsic role in regulating proliferation of mesenchymal cells in the developing palate. *Front. Physiol.*, **8**, 955.

120. Pasqualetti, M., Ori, M., Nardi, I., and Rijli, F.M. (2000) Ectopic Hoxa2 induction after neural crest migration results in homeosis of jaw elements in Xenopus. *Development*, **127**, 5367–78.

121. Pauws, E., Hoshino, A., Bentley, L., Prajapati, S., Keller, C., Hammond, P., Moore, G.E., and Stanier, P. (2009) Tbx22 null mice have a submucous cleft palate due to reduced palatal bone formation and also display ankyloglossia and choanal atresia phenotypes. *Hum. Mol. Genet.*, **18** (21), 4171–79.

122. Pratap, J., Javed, A., Languino, L.R., Andre, J., Wijnen, V., Stein, J.L., Stein, G.S., and Lian, J.B. (2005) The Runx2 osteogenic transcription factor regulates matrix metalloproteinase 9 in bone metastatic cancer cells and controls cell invasion. *Mol. Cell. Biol.*, **25** (19), 8581–8591.

123. Prince, V., and Lumsden, a (1994) Hoxa-2 expression in normal and transposed rhombomeres: independent regulation in the neural tube and neural crest. *Development*, **120** (4), 911–23.

124. Proetzel, G., Pawlowski, S.A., Wiles, M.V., Yin, M., Boivin, G.P., Howles, P.N., Ding, J., Ferguson, M.W.J. and Doetschman, T. (1995). Transforming growth factor-beta 3 is required for secondary palate fusion. *Nat. Genet.*, **11**, 409-14.

125. Rice, R., Connor, E., and Rice, D.P.C. (2006) Expression patterns of Hedgehog signalling pathway members during mouse palate development. *Gene Expr. Patterns*, **6** (2), 206–12.

126. Rice, R., Spencer-dene, B., Connor, E.C., Gritli-linde, A., Mcmahon, A.P., Dickson, C., Thesleff, I., and Rice, D.P.C. (2004) Disruption of Fgf10 / Fgfr2b -coordinated epithelial-mesenchymal interactions causes cleft palate. *J. Clin. Invest.*, **113** (12), 1692–700.

127. Rijli, F.M., Mark, M., Lakkaraju, S., Dierich, a, Dollé, P., and Chambon, P. (1993) A homeotic transformation is generated in the rostral branchial region of the head by disruption of Hoxa-2, which acts as a selector gene. *Cell*, **75** (7), 1333–49.

128. Roca, H., Phimphilai, M., Gopalakrishnan, R., Xiao, G., and Franceschi, R.T. (2005) Cooperative interactions between RUNX2 and homeodomain protein-binding sites are critical for the osteoblast-specific expression of the bone sialoprotein gene. *J. Biol. Chem.*, **280** (35), 30845–55.

129. Sanford, L.P., Ormsby, I., Groot, A.C.G., Sariola, H., Friedman, R., Boivin, G.P., Cardell, E. Lou, and Doetschman, T. (1997) TGFβ2 knockout mice have multiple developmental defects that are non-overlapping with other TGFβ knockout phenotypes. *Development*, **124**, 2659–70.

130. Santagati, F. and Rijli, F. (2003). Cranial neural crest and the building of the vertebrate head. *Nat. Rev. Neurosci*., **4** (10), 806-18.

131. Santagati, F., Minoux, M., Ren, S., and Rijli, F.M. (2005) Temporal requirement of Hoxa2 in cranial neural crest skeletal morphogenesis. *Development*, **132**, 4927–36.

132. Shiga, A., Nozaki, H., Yokoseki, A., Nihonmatsu, M., Kawata, H., Kato, T., Koyama, A., Arima, K., Ikeda, M., Katada, S., Toyoshima, Y., Takahashi, H., Tanaka, A., Nakano, I., Ikeuchi, T., Nishizawa, M., and Onodera, O. (2011) Cerebral small-vessel disease protein HTRA1 controls the amount of TGF-β1 via cleavage of proTGF-β1. *Hum. Mol. Genet.*, **20** (9), 1800–10.

133. Shiomi, N., Cui, X.-M., Yamamoto, T., Saito, T., and Shuler, C.F. (2006) Inhibition of SMAD2 expression prevents murine palatal fusion. *Dev. Dyn.*, **235** (7), 1785–93.

134. Singh, H., Endo, Y., and Nie, G. (2011) Decidual HtrA3 negatively regulates trophoblast invasion during human placentation. *Hum. Reprod.*, **26** (4), 748–57.

135. Singh, H., Makino, S., Endo, Y., and Nie, G. (2010) Inhibition of HTRA3 stimulates trophoblast invasion during human placental development. *Placenta*, **31** (12), 1085–92.

136. Smith, T., Lozanoff, S., Iyyanar, P., and Nazarali, A.J. (2013) Molecular signaling along the anterior–posterior axis of early palate development. *Front. Physiol.*, **3**, 488.

137. Smith, T.M., Wang, X., Zhang, W., Kulyk, W., and Nazarali, A.J. (2009) Hoxa2 plays a direct role in murine palate development. *Dev. Dyn.*, **238** (9), 2364–73.

138. Steventon, B., Carmona-Fontaine, C. and Mayor, R. (2005). Genetic network during neural crest induction: from cell specification to cell survival. *Semin. Cell Dev. Biol.*, **16** (6), 647-54.

139. Sun, D., Vanderburg, C.R., Odierna, G.S., and Hay, E.D. (1998) TGFbeta3 promotes transformation of chicken palate medial edge epithelium to mesenchyme in vitro. *Development*, **125** (1), 95–105.

140. Tang, W., Li, Y., Osimiri, L., and Zhang, C. (2011) Osteoblast-specific transcription factor Osterix (Osx) is an upstream regulator of Satb2 during bone formation. *J. Biol. Chem.*, **286** (38), 32995–3002.

141. Taya, Y., O'Kane, S., and Ferguson, M.W.J. (1999) Pathogenesis of cleft palate in TGF-β3 knockout mice. *Development*, **126**, 3869–79.

142. Thangaraj, M.P., Furber, K.L., Gan, J.K., Ji, S., Sobchishin, L., Doucette, J.R., and Nazarali, A.J. (2017) RNA binding protein Quaking stabilizes Sirt2 mRNA during oligodendroglial differentiation. *J. Biol. Chem.*, **292**, 5166–82.

143. Tiaden, A.N., Bahrenberg, G., Mirsaidi, A., Glanz, S., BluÈher, M., and Richards, P. J. (2016) Novel function of serine protease HTRA1 in inhibiting adipogenic differentiation of human mesenchymal stem cells via MAP kinase-mediated MMP upregulation. *Stem Cells*, **34**, 1601-14

144. Tiaden, A.N., Breiden, M., Mirsaidi, A., Weber, F. a, Bahrenberg, G., Glanz, S., Cinelli, P., Ehrmann, M., and Richards, P.J. (2012a) Human serine protease HTRA1 positively regulates osteogenesis of human bone marrow-derived mesenchymal stem cells and mineralization of differentiating bone-forming cells through the modulation of extracellular matrix protein. *Stem Cells*, **30** (10), 2271–82.

145. Tiaden, A.N., Klawitter, M., Lux, V., Mirsaidi, A., Bahrenberg, G., Glanz, S., Quero, L., Liebscher, T., Wuertz, K., Ehrmann, M., and Richards, P.J. (2012b) Detrimental role for human high temperature requirement serine protease A1 (HTRA1) in the pathogenesis of intervertebral disc (IVD) degeneration. *J. Biol. Chem.*, **287** (25), 21335–45.

146. Tocharus, J., Tsuchiya, A., Kajikawa, M., Ueta, Y., Oka, C., and Kawaichi, M. (2004) Developmentally regulated expression of mouse HtrA3 and its role as an inhibitor of TGF-beta signaling. *Dev. Growth Differ.*, **46** (3), 257–74.

147. Tsuchiya, A., Yano, M., Tocharus, J., Kojima, H., Fukumoto, M., Kawaichi, M., and Oka, C. (2005) Expression of mouse HtrA1 serine protease in normal bone and cartilage and its upregulation in joint cartilage damaged by experimental arthritis. *Bone*, **37** (3), 323–36.

148. Valcourt, U., Thuault, S., Pardali, K., Heldin, C.-H., and Moustakas, A. (2007) Functional role of Meox2 during the epithelial cytostatic response to TGF-beta. *Mol. Oncol.*, **1** (1), 55–71.

149. Wang, N., Eckert, K. A, Zomorrodi, A.R., Xin, P., Pan, W., Shearer, D. A, Weisz, J., Maranus, C.D., and Clawson, G. A (2012) Down-regulation of HtrA1 activates the epithelial-mesenchymal transition and ATM DNA damage response pathways. *PLoS One*, **7** (6), e39446.

150. Welsh, I.C., and O'Brien, T.P. (2009) Signaling integration in the rugae growth zone directs sequential SHH signaling center formation during the rostral outgrowth of the palate. *Dev. Biol.*, **336** (1), 53–67.

151. Welsh, I.C., Hagge-Greenberg, A., and O'Brien, T.P. (2007) A dosage-dependent role for Spry2 in growth and patterning during palate development. *Mech. Dev.*, **124**, 746–61.

152. Wu, H., Whitfield, T.W., Gordon, J.A.R., Dobson, J.R., Tai, P.W.L., van Wijnen, A.J., Stein, J.L., Stein, G.S., and Lian, J.B. (2014a) Genomic occupancy of Runx2 with global expression profiling identifies a novel dimension to control of osteoblastogenesis. *Genome Biol.*, **15** (3), R52.

153. Wu, M., Li, J., Engleka, K.A., Zhou, B., Min, M.L., Plotkin, J.B., and Epstein, J.A. (2008) Persistent expression of Pax3 in the neural crest causes cleft palate and defective osteogenesis in mice. *J. Clin. Invest.*, **118** (6), 2076–87.

154. Wu, X., Chim, S.M., Kuek, V., Lim, B.S., Chow, S.T., Zhao, J., Yang, S., Rosen, V., Tickner, J., and Xu, J. (2014b) HtrA1 is upregulated during RANKL-induced osteoclastogenesis, and negatively regulates osteoblast differentiation and BMP2-induced Smad1/5/8, ERK and p38 phosphorylation. *FEBS Lett.*, **588** (1), 143–50.

155. Xia, J., Wang, F., Wang, L., and Fan, Q. (2013) Elevated serine protease HtrA1 inhibits cell proliferation, reduces invasion, and induces apoptosis in esophageal squamous cell carcinoma by blocking the nuclear factor-κB signaling pathway. *Tumour Biol.*, **34** (1), 317–28.

156. Xiong, W., He, F., Morikawa, Y., Yu, X., Zhang, Z., Lan, Y., Jiang, R., Cserjesi, P., and Chen, Y. (2009) Hand2 is required in the epithelium for palatogenesis in mice. *Dev. Biol.*, **330** (1), 131–41.

157. Xu, J., Liu, H., Lan, Y., Aronow, B.J., Kalinichenko, V. V., and Jiang, R. (2016) A Shh-Foxf-Fgf18-Shh molecular circuit regulating palate development. *PLoS Genet.*, **12** (1), e1005769.

158. Xu, X., Han, J., Ito, Y., Bringas, P., Deng, C., and Chai, Y. (2008) Ectodermal Smad4 and p38 MAPK are functionally redundant in mediating TGF-beta/BMP signaling during tooth and palate development. *Dev. Cell*, **15** (2), 322–29.

159. Xu, X., Han, J., Ito, Y., Bringas, P., Urata, M.M., and Chai, Y. (2006) Cell autonomous requirement for Tgfbr2 in the disappearance of medial edge epithelium during palatal fusion. *Dev. Biol.*, **297** (1), 238–48.

160. Yamamoto, T., Cui, X. and Shuler, C. F. (2003). Role of ERK1/2 signaling during EGF-induced inhibition of palatal fusion. *Dev. Biol.*, **260** (2), 512-21.

161. Yan, X. (2008) Characterization of the Hoxa2 binding site in dual specificity tyrosine kinase 4 (*Dyrk4*) and High temperature requirement factor A 3 (*Htra3*) genes. Master's thesis, University of Saskatchewan, Saskatoon, SK, Canada.

162. Yang, F., Tang, W., So, S., de Crombrugghe, B., and Zhang, C. (2010) Sclerostin is a direct target of osteoblast-specific transcription factor osterix. *Biochem. Biophys. Res. Commun.*, **400** (4), 684–8.

163. Yang, L.-T., and Kaartinen, V. (2007) Tgfb1 expressed in the Tgfb3 locus partially rescues the cleft palate phenotype of Tgfb3 null mutants. *Dev. Biol.*, **312** (1), 384–95.

164. Yang, Z., Camp, N.J., Sun, H., Tong, Z., Gibbs, D., Cameron, D.J., Chen, H., Zhao, Y., Pearson, E., Li, X., Chien, J., Dewan, A., Harmon, J., Bernstein, P.S., Shridhar, V., Zabriskie, N. a, Hoh, J., Howes, K., and Zhang, K. (2006) A variant of the HTRA1 gene increases susceptibility to age-related macular degeneration. *Science*, **314** (5801), 992–3.

165. Yu, K., Deng, M., Naluai-cecchini, T., Glass, I.A., and Cox, T.C. (2017) Differences in oral structure and tissue interactions during mouse vs. human palatogenesis: implications for the translation of findings from mice. *Front. Physiol***. 8**:154.

166. Yu, L., Gu, S., Alappat, S., Song, Y., Yan, M., Zhang, X., Zhang, G., Jiang, Y., Zhang, Z., Zhang, Y., and Chen, Y. (2005) Shox2-deficient mice exhibit a rare type of incomplete clefting of the secondary palate. *Development*, **132** (19), 4397–406.

167. Zaidi, S.K., Pande, S., Pratap, J., Gaur, T., Grigoriu, S., Ali, S.A., Stein, J.L., Lian, J.B., van Wijnen, A.J., Stein, G.S. (2007) Runx2 deficiency and defective subnuclear targeting bypass senescence to promote immortalization and tumorigenic potential. *Proc Natl Acad Sci*., **104**, 19861–66.

168. Zhang, C. (2010) Transcriptional regulation of bone formation by the osteoblast-specific transcription factor Osx. *J. Orthop. Surg. Res.*, **5** (1), 37.

169. Zhang, C., Cho, K., Huang, Y., Lyons, J.P., Zhou, X., Sinha, K., McCrea, P.D., and de Crombrugghe, B. (2008) Inhibition of Wnt signaling by the osteoblast-specific transcription factor Osterix. *Proc. Natl. Acad. Sci. U. S. A.*, **105** (19), 6936–41.

170. Zhang, C., Tang, W., and Li, Y. (2012) Matrix metalloproteinase 13 (MMP13) is a direct target of osteoblast-specific transcription factor osterix (Osx) in osteoblasts. *PLoS One*, **7** (11), e50525.

171. Zhang, Z., Song, Y., Zhao, X., Zhang, X., Fermin, C., and Chen, Y. (2002) Rescue of cleft palate in Msx1-deficient mice by transgenic Bmp4 reveals a network of BMP and Shh signaling in the regulation of mammalian palatogenesis. *Development*, **129**, 4135–46.

172. Zhou, J., Gao, Y., Lan, Y., Jia, S., and Jiang, R. (2013) Pax9 regulates a molecular network involving Bmp4, Fgf10, Shh signaling and the Osr2 transcription factor to control palate morphogenesis. *Development*, **140** (23), 4709–18.

173. Zumbrunn, J., and Trueb, B. (1996) Primary structure of a putative serine protease specific for IGF-binding proteins. *FEBS Lett.*, **398**, 187–92.

174. Zuo, C., Huang, Y., Bajis, R., Sahih, M., Li, Y.-P., Dai, K., and Zhang, X. (2012) Osteoblastogenesis regulation signals in bone remodeling. *Osteoporos. Int.*, **23** (6), 1653–63.

10. Appendix: Published manuscripts

published: 14 November 2017
doi: 10.3389/fphys.2017.00929

Hoxa2 Inhibits Bone Morphogenetic Protein Signaling during Osteogenic Differentiation of the Palatal Mesenchyme

Paul P. R. Iyyanar* and Adil J. Nazarali †

Laboratory of Molecular Cell Biology, College of Pharmacy and Nutrition and Neuroscience Research Cluster, University of Saskatchewan, Saskatoon, SK, Canada

OPEN ACCESS

Edited by:
Thimios Mitsiadis, University of Zurich, Switzerland

Reviewed by:
Alexandre Rezende Vieira, University of Pittsburgh, United States
David Clouthier, University of Colorado Anschutz Medical Campus, United States

****Correspondence:***
Paul P. R. Iyyanar paul.iyyanar@usask.ca

†Deceased.

Specialty section:
This article was submitted to Craniofacial Biology and Dental Research, a section of the journal Frontiers in Physiology

Received: *01 September 2017*
Accepted: *02 November 2017*
Published: *14 November 2017*

Citation:
Iyyanar PPR and Nazarali AJ (2017) Hoxa2 Inhibits Bone Morphogenetic Protein Signaling during Osteogenic Differentiation of the Palatal Mesenchyme. Front. Physiol. 8:929. doi: 10.3389/fphys.2017.00929

Cleft palate is one of the most common congenital birth defects worldwide. The homeobox (*Hox*) family of genes are key regulators of embryogenesis, with *Hoxa2* having a direct role in secondary palate development. *Hoxa2*$^{-/-}$ mice exhibit cleft palate; however, the cellular and molecular mechanisms leading to cleft palate in *Hoxa2*$^{-/-}$ mice is largely unknown. Addressing this issue, we found that *Hoxa2* regulates spatial and temporal programs of osteogenic differentiation in the developing palate by inhibiting bone morphogenetic protein (BMP) signaling dependent osteoblast markers. Expression of osteoblast markers, including *Runx2*, *Sp7*, and *AlpI* were increased in *Hoxa2*$^{-/-}$ palatal shelves at embryonic day (E) 13.5 and E15.5. *Hoxa2*$^{-/-}$ mouse embryonic palatal mesenchyme (MEPM) cells exhibited increased bone matrix deposition and mineralization *in vitro*. Moreover, loss of *Hoxa2* resulted in increased osteoprogenitor cell proliferation and osteogenic commitment during early stages of palate development at E13.5. Consistent with upregulation of osteoblast markers, *Hoxa2*$^{-/-}$ palatal shelves displayed higher expression of canonical BMP signaling *in vivo*. Blocking BMP signaling in *Hoxa2*$^{-/-}$ primary MEPM cells using dorsomorphin restored cell proliferation and osteogenic differentiation to wild-type levels. Collectively, these data demonstrate for the first time that *Hoxa2* may regulate palate development by inhibiting osteogenic differentiation of palatal mesenchyme via modulating BMP signaling.

Keywords: Hoxa2, cleft palate, bone morphogenetic protein (BMP), osteoblast, osteoprogenitor, proliferation, RUNX2

INTRODUCTION

Cleft palate is one of the most common structural birth defects in humans with an incidence of 1 in 700–1,000 live births (Dixon et al., 2011). Studies using mouse model which has a high similarity to human palate development helped to identify several key stages and cellular processes during palate formation (Yu et al., 2017). In mice, secondary palate development begins at embryonic day (E)11.5 and is completed with palatal fusion by E15.5 (Ferguson, 1988). During palate development, the

Abbreviations: AlpI, alkaline phosphatase I; ARS, Alizarin red S; BMP, bone morphogenetic protein; CNCC, cranial neural crest cells; d, day; E, embryonic day; MEPM, mouse embryonic palatal mesenchyme; pSMAD 1/5/8, phosphorylated SMAD 1/5/8; qRT-PCR, quantitative real-time PCR; Runx2, runt-related transcription factor 2.

vertical palatal shelves grow downward along the sides of the tongue until E13.5 and then elevate above the tongue at E14. The palatal shelves on either side contact each other forming midline epithelial seam at E14.5, which eventually disintegrates leading to palatal fusion by E15.5 (Kaufman, 1992). Impairment in any of these distinct stages during palatogenesis may result in cleft palate. The palate is comprised of the palatal process of the maxilla and the palatal process of the palatine bone derived from the cranial neural crest cells (CNCC) (Iwata et al., 2010), constituting the anterior and posterior part of the hard palate, respectively (Baek et al., 2011). While the structural changes during palate development are well defined, there is a scarcity of knowledge on the molecular mechanisms governing the patterning of the palate.

In murine models, deletion of about 280 genes are known to cause cleft palate (Funato et al., 2015). Among these genes, mutations of 55 genes are associated with cleft palate in humans (Funato et al., 2015). Mutation in the *Hoxa2* gene is associated with cleft palate in humans (Alasti et al., 2008) and mouse models (Gendron-Maguire et al., 1993; Rijli et al., 1993). In *Hoxa2*$^{-/-}$ mice, the cleft palate phenotype was initially attributed to the physical obstruction of the tongue preventing the palatal shelves to elevate and fuse (Barrow and Capecchi, 1999). However, our group has previously demonstrated that *Hoxa2* is expressed in the palatal shelves (Nazarali et al., 2000) and plays an intrinsic role in palatogenesis (Smith et al., 2009). The palatal shelves from *Hoxa2*$^{-/-}$ mouse embryonic maxilla devoid of tongue grown in rolling bottle cultures failed to fuse (Smith et al., 2009). Hence, tongue musculature may not be the principal reason for the cleft palate phenotype in *Hoxa2*$^{-/-}$ mice. *Hoxa2* appears to be a key regulator of palatogenesis, yet the molecular signaling pathways downstream of *Hoxa2* remain largely unknown.

Bone morphogenetic protein (BMP) signaling plays a critical role in palate development regulating cell proliferation (Zhang et al., 2002). *Bmp4* is upstream of *Bmp2* to induce proliferation in the palatal mesenchyme and is able to reverse the reduced cell proliferation and cleft palate phenotype in the *Msx1*$^{-/-}$ mice (Zhang et al., 2002). Defective cell proliferation observed in *Pax9*$^{-/-}$ embryos is consistent with the reduced *Bmp4* expression in the palatal mesenchyme at E13.5 (Zhou et al., 2013). Similarly, reduced expression of *Bmp2* is associated with reduced cell proliferation in the palatal shelves of *Hand2* hypomorphic mice (*Hand2*$^{LoxP/-}$) (Xiong et al., 2009). In addition, growing evidence highlight the importance of osteogenic differentiation in the elevation of palatal shelves and abnormal osteogenic differentiation could lead to cleft palate manifestations (Wu et al., 2008; Fu et al., 2017; Jia et al., 2017a,b). BMP signaling is critical for osteogenic differentiation in the palatal mesenchyme (Wu et al., 2008; Baek et al., 2011; Hill et al., 2014), where it is required for the expression of osteoblast markers such as *Runx2*, *Sp7*, and *AlpI* (Baek et al., 2011). During craniofacial development, *Hoxa2* restricts the bone mineralization in the calvaria (Dobreva et al., 2006). Moreover, *Hoxa2*$^{-/-}$ mice exhibit ectopic *Runx2*-positive osteogenic center in the second pharyngeal arch that results in duplication of tympanic ring (Kanzler et al., 1998).

In this study, we tested the hypothesis that *Hoxa2* inhibits osteogenic differentiation of the palatal mesenchyme *in vivo* and *in vitro* using *Hoxa2*$^{-/-}$ mice. Our findings reveal that *Hoxa2* plays a critical role in the spatial and temporal regulation of osteogenic differentiation via modulating BMP signaling pathway in the developing palate.

MATERIALS AND METHODS

Animals

Wild-type and *Hoxa2*$^{-/-}$ embryos were obtained from timed pregnant *Hoxa2*$^{+/-}$ (heterozygous) mice. Genotype was confirmed using PCR as previously described (Gendron-Maguire et al., 1993). This research was approved by the University of Saskatchewan's Animal Research Ethics Board and adhered to the Canadian Council on Animal Care guidelines for humane animal use.

Primary Mouse Embryonic Palatal Mesenchyme (MEPM) Cell Culture and Osteogenic Induction

Primary MEPM cells were isolated from micro-dissected palatal shelves of wild-type and *Hoxa2*$^{-/-}$ mouse embryos at E13.5. The palatal shelves were treated with 0.25% trypsin-EDTA for 15 min, passed through a 70 µm cell strainer and cultured as monolayer cells (Iwata et al., 2012) in DMEM: Ham's F12 (1:1) media containing 10% FBS, 1% antibiotic-antimycotic solution (Sigma). Osteogenic differentiation was carried out as described previously (Kwong et al., 2008) with minor modifications. Briefly, MEPM cells were seeded on 0.1% gelatin or poly-D-lysine coated plates at a cell density of 5×10^4 cells per well in 24 well plates and cultured until they reached confluence. Osteogenic differentiation was induced with differentiation media (DMEM, 10% FBS, 2 mM L-glutamine and 1% antibiotic-antimycotic solution) supplemented with osteogenic inducing agents, including 50 µg/ml L-ascorbic acid 2-phosphate sesquimagnesium salt (Sigma), 10 mM β-glycerophosphate (Sigma), and 100 nM dexamethasone (Sigma). Cells were differentiated for up to 21 days (d) and samples were collected at d8, d15, or d21. To assess the impact of BMP signaling, MEPM cells were treated with dorsomorphin (5 µM) or DMSO and were harvested at d8 for further experiments.

Alkaline Phosphatase I (ALPI) Staining

ALPI staining in the palatal shelves *in vivo* was carried out as previously described (Baek et al., 2011). Embryonic mouse heads were fixed overnight in freshly prepared 4% paraformaldehyde at 4°C and rehydrated in 30% sucrose at 4 °C. Frozen coronal sections (10 µm) were prepared on slides coated with 0.5% gelatin. The sections were air dried for at least 2 h and then rehydrated with TBS with 0.08% tween-20 two times for 10 min each. Subsequently, the sections were treated with alkaline phosphatase buffer (100 mM NaCl, 100 mM Tris-HCl pH 9.5, 50 mM $MgCl_2$, 0.1% Tween-20) for 20 min and stained with alkaline phosphatase buffer containing 4.5 µl/ml of 5-bromo-4-chloro-3-indolyl phosphate (Roche) and 3.5 µl/ml of nitro blue tetrazolium (Roche) for 10 min. The reaction was stopped with PBS containing 20 mM EDTA buffer and counter stained with nuclear fast red. The stained sections were dehydrated in

a series of PBS/ethanol, ethanol/xylene and finally mounted in DPX mounting media (Sigma). For osteoblast differentiation in primary MEPM cells, ALPI staining was carried out following the aforementioned protocol after fixing the cells with 4% paraformaldehyde for 15 min.

Alizarin Red S (ARS) Staining and Quantification

ARS staining and quantification was carried out as previously described (Gregory et al., 2004) with minor modifications. Briefly, monolayer MEPM cells were fixed with 4% paraformaldehyde for 15 min and stained with 250 µl of 40 mM ARS (Sigma) solution (pH 4.1) at room temperature for 20 min with gentle shaking. Excess dye was aspirated and washed with deionized water before imaging. ARS quantification was carried using an acid extraction method (Gregory et al., 2004). Standard plot of ARS concentration was constructed by serially diluting the 40 mM ARS in the buffer containing 10% (v/v) acetic acid and 10% (v/v) ammonium hydroxide. The absorbance values of the standard concentrations were used to interpolate the concentrations of the test samples.

Quantitative Real-Time Polymerase Chain Reaction (qRT-PCR)

Total RNA was isolated from the micro-dissected palatal shelves using RNA mini spin column (Bio-Rad) as per the manufacturer's protocol. First strand complementary DNA synthesis (reverse transcription) was performed in 20 µl reactions with 500 ng of total RNA using High-Capacity complementary DNA Reverse Transcription Kit (Invitrogen). qRT-PCR was carried out as described in our previous study (Thangaraj et al., 2017) using SYBR green assay (Applied Biosystems) in 7300-real time PCR system (Applied Biosystems) with primers listed in **Table 1**.

Western Blotting

Western bot analyses were carried out as previously described (Brown and Nazarali, 2010). Briefly, palatal tissues were homogenized in RIPA buffer. Total protein content was quantified using the Bradford assay and proteins were separated in 10% SDS-PAGE. Primary antibodies used were: RUNX2 (1:500; Abcam ab102711), SP7 (1:1500; Abcam ab22552), phosphorylated SMAD 1/5/8 (pSMAD 1/5/8) (1:500; Cell signaling 9511S), SMAD 1/5/8 (1:500; Santa Cruz Biotechnology sc-6031-R), and β-ACTIN (1:2,000; Developmental Studies Hybridoma JLA20). Densitometric analyses were carried out using AlphaView software.

Immunohistochemistry

Embryonic mouse heads were fixed overnight with freshly-prepared 4% paraformaldehyde and rehydrated in 30% sucrose at 4°C. Frozen coronal sections (10 µm) were rehydrated with PBS for 45 min, permeabilized with 0.1% Triton X-100 and blocked with 3% skim milk containing 0.1% Triton X-100 in 1X PBS for 1 h at room temperature. Sections were then incubated overnight with the following primary antibodies: RUNX2 (1:200; Abcam ab23981) or SP7 (1:800; Abcam ab22552) in 1X PBS with 0.1% Triton X-100 at 4°C. Double labeling was carried out by co-incubating: Ki67 (1:100; eBioscience 14569882) and RUNX2 (1:200; Abcam ab23981) overnight at 4°C. Sections were then washed three times and treated with secondary antibodies conjugated with Alexa Fluor R 488 (1:200) or Alexa Fluor R 594 (1:400) in 1X PBS with 0.1% Triton X-100 at room temperature for 1.5 h. Cell counting analyses were carried out manually using ImageJ software platform (NIH).

TABLE 1 | Primer sequences used for the relative quantification of the transcripts by qRT-PCR.

Transcript	Primer sequences	Length (bases)	Amplicon size (bp)
Alkaline phosphatase *(AlpI)*	CCTTGACTGTGGTTACTGCT	20	216
	CCTGGTAGTTGTTGTGAGCG	20	
Bone morphogenic protein 2 (*Bmp2*)	CAGTAGTTTCCAGCACCGAA	20	199
	CACTTCCACCACAAACCCAT	20	
Bone morphogenic protein 4 (*Bmp4*)	AGGAAGGAGTAGATGTGAGAG	21	158
	AGGGACGGAGACCAGATAC	19	
Bone carboxy-glutamic acid containing protein (*Bglap*)	GCAGGAGGGCAATAAGGTAG	20	159
	ATGCGTTTGTAGGCGGTC	18	
CyclinD1 (*Ccnd1*)	ACCCTGACACCAATCTCCTC	20	214
	AAGCGGTCCAGGTAGTTCAT	20	
Sp7 transcription factor (*Sp7*)	CACAAAGAAGCCATACGCTG	20	165
	CCAGGAAATGAGTGAGGGAAG	21	
Runt-related transcription factor 2 (*Runx2*)	TGCCTCCGCTGTTATGAAAA	20	187
	CTGTCTGTGCCTTCTTGGTT	20	

Cell Proliferation Assay

Cell proliferation assay was carried out in MEPM cells using cell-counting kit-8 (Dojindo) as previously described (Iwata et al., 2010). MEPM cells were incubated with CCK-8 reagent for 1 h and the absorbance measured at 450 nm was plotted to calculate the relative cell proliferation rate.

Statistical Analyses

Statistical analyses were carried out using unpaired *t*-test in the case of two groups. One-way ANOVA or two-way ANOVA with Bonferroni multiple comparison test was used for one or two variate analyses, respectively. A p-value of <0.05 was considered significant.

RESULTS

Hoxa2$^{-/-}$ Mice Exhibit Increased Expression of Osteoblast Markers during Palate Development *in Vivo*

To investigate the role of *Hoxa2* in osteogenesis of the palatal mesenchyme, we first examined changes in osteogenic differentiation in the embryonic palatal shelves of *Hoxa2*$^{-/-}$ mice at E16.5, a stage when both the prospective palatal process of the maxilla and the palatal process of the palatine

bone evidently ossify (Baek et al., 2011). Staining for ALPI, a marker of osteoblast differentiation showed an expansion in ALPI expression domain in the *Hoxa2*$^{-/-}$ palatal mesenchyme compared to wild-type (**Figures 1A–H**). At the anterior region of the hard palate, ALPI staining was restricted to the nasal half in two condensations of the prospective palatal process of the maxilla on either side of the degraded midline epithelial seam in wild-type embryos (**Figures 1A,E**). In contrast, the domain of ALPI positive preosteoblast area was increased and expanded toward the oral side covering oral-nasal axis in *Hoxa2*$^{-/-}$ palatal shelves (**Figures 1B,F**). In the posterior region of the hard palate, ALPI staining was present in the ossifying centers of the palatal process of the palatine bone in wild-type embryos (**Figures 1C,G**), whereas there was an expansion in the expression domain of ALPI positive preosteoblasts toward the oral side in *Hoxa2*$^{-/-}$ embryos (**Figures 1D,H**).

Two well-known regulators of osteogenic differentiation RUNX2 (Komori et al., 1997) and SP7 (previously known as Osterix; Nakashima et al., 2002) have been implicated in the patterning of the palatal bones (Baek et al., 2011).

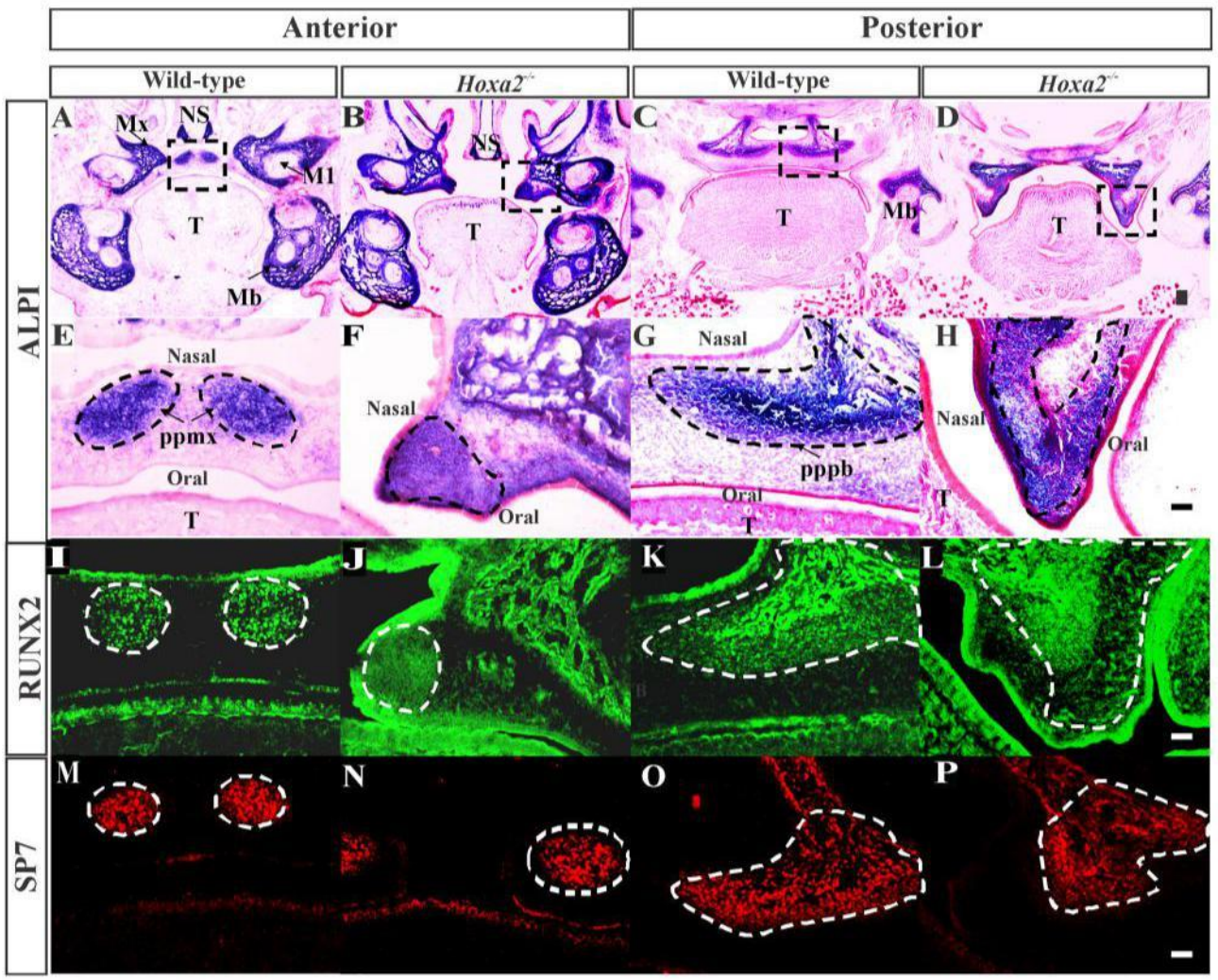

FIGURE 1 | Loss of *Hoxa2* leads to increased osteogenic differentiation of the palatal mesenchyme at E16.5. Position matched coronal sections of wild-type and *Hoxa2*$^{-/-}$ embryos at E16.5 were stained for ALPI **(A–H),** RUNX2 **(I–L),** and SP7 **(M–P).** Sections in the anterior region **(A,B,E,F,I,J,M,N)** were through the middle of the first molar tooth bud to detect osteogenic condensation of the palatal process of the maxilla. Sections in the posterior region **(C,D,G,H,K,L,O,P)** were through the osteogenic centers of the developing palatal process of the palatine bone. **(A–D)** ALPI staining (blue) counterstained with nuclear fast red. Scale bar, 100 µm. Boxed regions in **(A–D)** highlighting the palate are enlarged **(E–H)**. Scale bar, 50 µm. **(E,F)** In the anterior hard palate, ALPI staining in the two condensations of the palatal process of the maxilla (marked in black dotted lines) was evidently increased in the *Hoxa2*$^{-/-}$ embryos **(F)** compared to wild-type **(E)**. **(G,H)** In the posterior hard palate, ALPI stained developing palatal process of the palatine bone (marked in black dotted lines) in the *Hoxa2*$^{-/-}$ embryos **(H)** was increased compared to the wild-type **(G)**, $n = 5$ biological replicates. **(I–P)** Immunohistochemical analyses of RUNX2 (green; **I–L)** and SP7 (red; **M–P)** in wild-type and *Hoxa2*$^{-/-}$ palate at E16.5. RUNX2 was increased in both anterior **(J)** and posterior regions **(L)** of the *Hoxa2* null hard palate, whereas SP7 was increased only in the anterior hard palate **(N),** $n = 4$ biological replicates. Scale bar, 50 µm. M1, first molar; Mb, mandible; Mx, maxilla; NS, nasal septum; pppb, the palatal process of the palatine bone; ppmx, the palatal process of the maxilla; T, tongue.

To elucidate the spatial mis-regulation of palatal bone formation in *Hoxa2*$^{-/-}$ mice, expression pattern of these two osteoblast-specific transcription factors were assessed at E16.5. Immunohistochemical analyses revealed that RUNX2 (**Figure 1I**) and SP7 (**Figure 1M**) expressions were confined to the condensations of the palatal process of the maxilla at the anterior hard palate in wild-type embryos at E16.5, whereas RUNX2 (**Figure 1J**) and SP7 (**Figure 1N**) expression domains were increased in *Hoxa2*$^{-/-}$ embryos. In the posterior region, along the developing palatal process of the palatine bone, the expression of RUNX2 (**Figure 1L**) was increased in *Hoxa2*$^{-/-}$ embryos compared to wild-type (**Figure 1K**). In this region, the expression of SP7, a downstream target of RUNX2 and a marker of mature osteoblasts, was not evidently increased in the *Hoxa2*$^{-/-}$ palate (**Figure 1P**) compared to wild-type (**Figure 1O**). This suggests that cells toward the oral side of the palatal process of the palatine bone are at immature osteoblast stage and may not have developed bone matrix by E16.5. Collectively, these data indicate that *Hoxa2* could be a potential inhibitor of osteogenic differentiation in the palatal mesenchyme, which may serve to spatially restrict the expression of osteoblast-specific proteins during palate development *in vivo*.

Furthermore, gene expression profiles of osteoblast markers were evaluated during the initiation of ossification of the palatal process of the palatal bone and the palatal process of the maxilla at E13.5 and E15.5, respectively. The loss of *Hoxa2* in the developing palate resulted in an increase in mRNA expression of osteoblast markers such as *Runx2*, *AlpI* and *Sp7* at both E13.5 (**Figures 2A–D**) and E15.5 (**Figures 2E–H**). At E13.5, mRNA expression of *Runx2*, *AlpI* and *Sp7* were increased to ∼6.36-, ∼9.65-, and ∼2.62-fold, respectively, in *Hoxa2*$^{-/-}$ palate compared to wild-type (**Figures 2A–C**). At E13.5, mRNA expression of *Bglap* (previously known as *Ocn*) was not significantly altered (**Figure 2D**). At E15.5, mRNA expression of *Runx2*, *AlpI*, *Sp7*, and *Bglap* were upregulated ∼1.86-, ∼2.29-, ∼1.42-, ∼3.27-folds, respectively, in *Hoxa2*$^{-/-}$ palate compared to wild-type (**Figures 2E–H**). Consistent with this, protein expression of RUNX2 was upregulated at E13.5 and E15.5 to ∼1.4-fold (**Figures 2I,J**). SP7 protein expression, both long (**Figures 2I,K**) and short isoforms (**Figures 2I,L**) were upregulated at E15.5 to ∼1.4-fold. These data reveal that along with regulating the spatial patterning of osteogenic differentiation, *Hoxa2* also regulates the expression of osteogenic markers at the molecular level in the developing palate.

Hoxa2 Inhibits Osteoblast Differentiation of Mouse Embryonic Palatal Mesenchymal (MEPM) Cells *in Vitro*

To evaluate the potential of *Hoxa2* in regulating the temporal pattern of osteogenesis, the primary mesenchyme cells from the wild-type and *Hoxa2*$^{-/-}$ palatal shelves were differentiated *in vitro* for up to 21 days (d). Osteogenesis of mesenchymal cells involves sequential stages of proliferation, osteogenic commitment around day8 (∼d8) followed by matrix deposition (∼d15) and mineralization (∼d21) (Gordon et al., 2010). Differentiating cells were stained for ALPI at d8 and Alizarin Red S (ARS) at d15 and d21. ALPI staining showed an increased osteoblast differentiation at d8 in *Hoxa2*$^{-/-}$ MEPM cells compared to the wild-type MEPM cells (**Figures 3A,B**). In addition, ARS staining followed by quantification of ARS extracted matrix showed that *Hoxa2*$^{-/-}$ MEPM cells exhibited increased extracellular matrix deposition ∼2-fold at d15 (**Figures 3C,D,G**) and increased mineralization ∼1.5-fold at d21 (**Figures 3E,F,H**) compared to the wild-type MEPM cells.

Next, the gene expression profiles of osteogenic markers were examined in wild-type and *Hoxa2*$^{-/-}$ MEPM cells during osteogenic differentiation *in vitro*. *Runx2* mRNA expression was increased to ∼1.9-fold in the *Hoxa2*$^{-/-}$ MEPM cells compared to the wild-type during osteoblast commitment stage at d8 (**Figure 3I**). *AlpI* and *Sp7* mRNA expression were increased ∼2.85 and ∼3.37-fold, respectively, during matrix deposition stage at d15 in the *Hoxa2*$^{-/-}$ MEPM cells (**Figures 3J,K**). *Bglap* mRNA expression was increased ∼6.37-fold during matrix deposition at d15 and ∼8.09-fold during matrix mineralization at d21 in the *Hoxa2*$^{-/-}$ MEPM cells (**Figure 3L**). Thus, loss of *Hoxa2* results in upregulation of osteogenic marker expression in a stage-specific manner as early as d8 (osteogenic commitment stage). These data indicate that *Hoxa2* may play a role in early osteoblast differentiation by inhibiting the transcription factors regulating osteogenic fate specification.

Increased Osteoprogenitor Proliferation and Commitment in the *Hoxa2*$^{-/-}$ Palatal Mesenchyme during Early Palate Development

Hoxa2 peaks in its expression in the developing palate at E13.5 (Smith et al., 2009), a stage when the mesenchymal cells simultaneously proliferate and commit to form preosteoblasts of the prospective palatal process of the palatine bone. This suggests that the cleft palate phenotype in *Hoxa2*$^{-/-}$ mice, due to the failure of palatal shelves to elevate and reorient horizontally above the tongue after E13.5 (Barrow and Capecchi, 1999), may be a consequence of abnormal cell proliferation (Smith et al., 2013) and osteogenic differentiation (Wu et al., 2008; Fu et al., 2017; Jia et al., 2017a,b). To gain further insight into the role of *Hoxa2* during this early stage of palate development, the rate of mesenchymal cell proliferation and the commitment of mesenchymal cells to osteoprogenitor fate was investigated *in vivo* at E13.5. Immunohistochemical staining of RUNX2 (**Figures 4A,B**) was used to evaluate osteoprogenitor commitment in the wild-type and *Hoxa2*$^{-/-}$ palatal shelves at E13.5. RUNX2 (**Figure 4A**) expression in the wild-type was restricted to the bend region in the nasal side of the palatal shelves, whereas the expression domain of RUNX2 (**Figure 4B**) was increased spatially toward the medial edge of the palate as well as to the oral side of the palate in the *Hoxa2*$^{-/-}$ mutants. This is similar to the aberrant expression patterns of RUNX2 observed at E16.5 in the *Hoxa2*$^{-/-}$ palatal shelves. In addition, the number of RUNX2-positive osteoprogenitor cells on the nasal side of the palatal shelves were significantly higher in

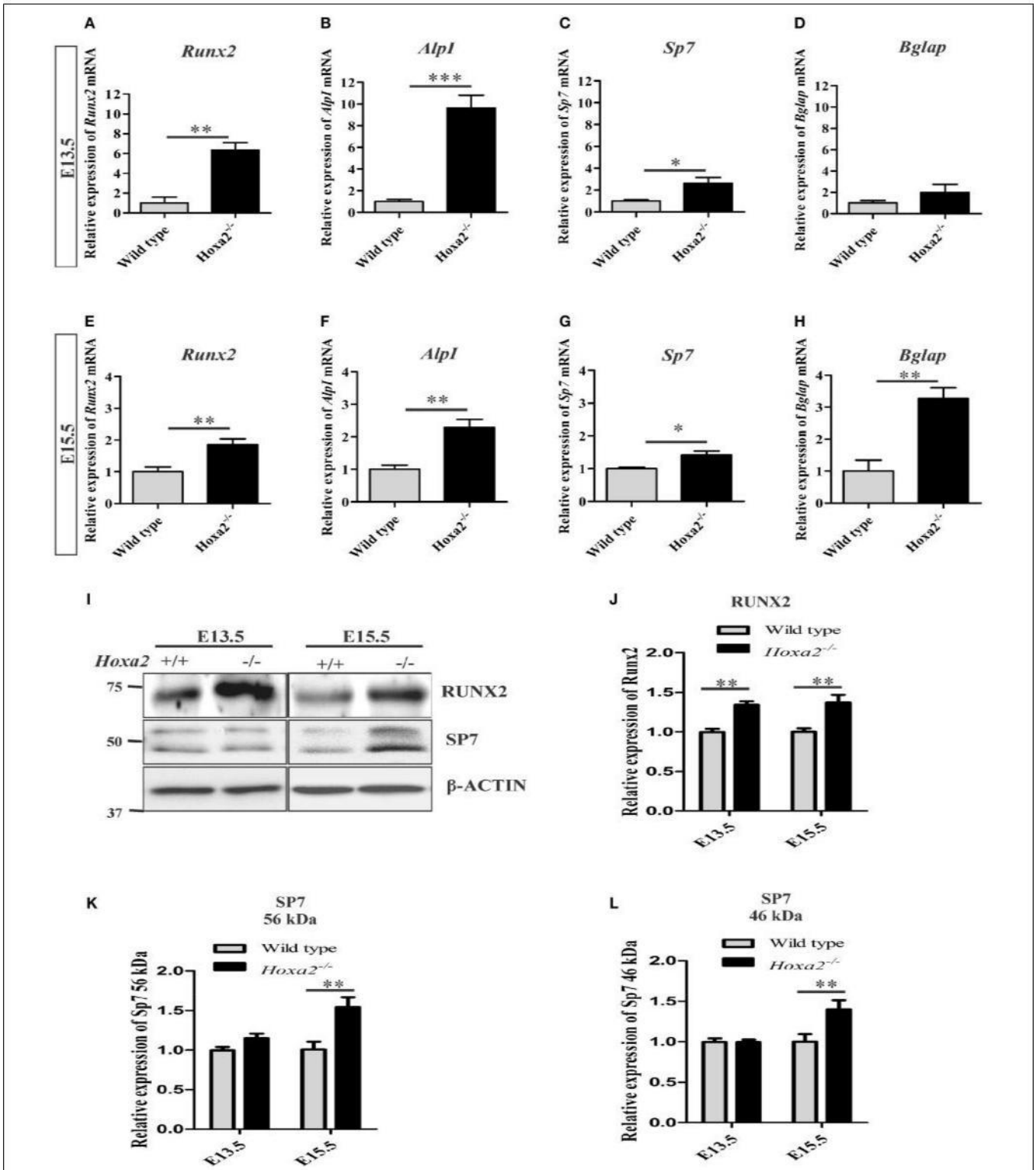

FIGURE 2 | Loss of *Hoxa2* leads to increased expression of osteogenic markers in the developing palate at E13.5 and E15.5. Quantitative real-time PCR (qRT-PCR) analyses indicate that the gene expression profile of osteogenic markers such as *Runx2* **(A,E)**, *Alp1* **(B,F),** and *Sp7* **(C,G)** were upregulated in the developing *Hoxa2*$^{-/-}$ palatal shelves at E13.5 **(A–C)** and E15.5 **(E–G).** Gene expression of *Bglap* was upregulated at E15.5 **(H)** but not at E13.5 **(D).** qRT-PCR data (n = 5 biological replicates) were normalized to β -*actin* and represented relative to wild-type (mean ± S.E.M; unpaired t-test, *$p < 0.05$; **$p < 0.01$; ***$p < 0.001$). Western blot analyses of RUNX2 **(I,J)** and SP7 **(I,K,L)** were carried out using the microdissected palatal shelves from wild-type and *Hoxa2*$^{-/-}$ mice at E13.5 and E15.5. RUNX2 protein expression was upregulated in the *Hoxa2*$^{-/-}$ palate at E13.5 and E15.5 **(I,J)**, whereas SP7 isoforms were upregulated at E15.5 **(I,K,L)**. Densitometric analyses (n = 4 biological replicates) were normalized to β-ACTIN and represented relative to wild-type (mean ± S.E.M; unpaired t-test, **$p < 0.01$).

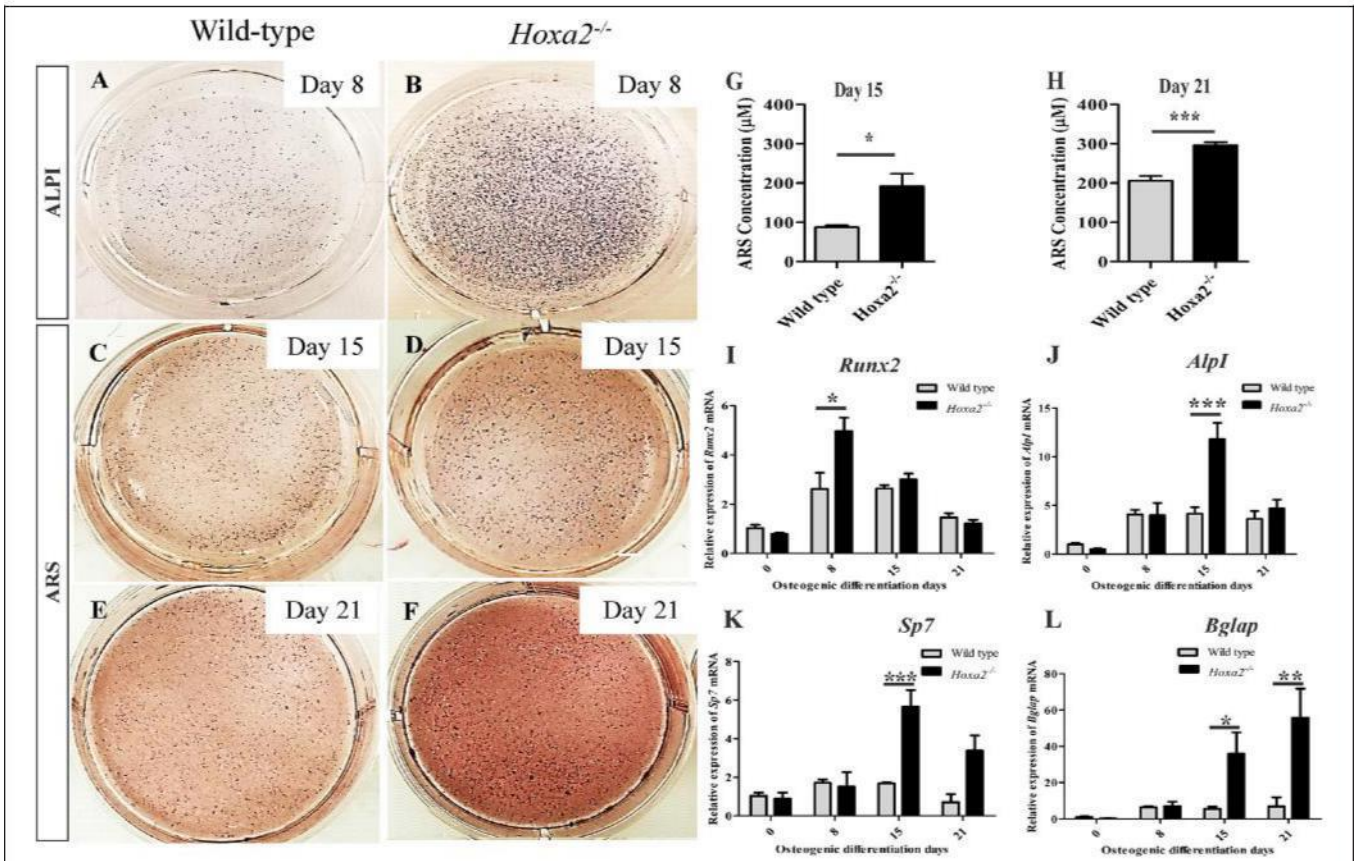

FIGURE 3 | *Hoxa2* inhibits osteoblast differentiation of MEPM cells *in vitro*. Wild-type and *Hoxa2*$^{-/-}$ MEPM cells were subjected to osteogenic differentiation *in vitro* for up to 21 days (d). The differentiated cells were stained for ALPI at d8 **(A,B)**, ARS at d15 **(C,D),** and d21 **(E,F).** ARS stained osteocyte matrices from wild-type and *Hoxa2*$^{-/-}$ MEPM cells were extracted and quantified at d15 **(G)** and d21 **(H).** Experiment was carried out three times and the data shown here are from a representative experiment with n = 3 biological replicates; mean ± S.E.M; unpaired t-test, $*p < 0.05$; $***p < 0.001$). *Hoxa2*$^{-/-}$ MEPM cells displayed increased matrix deposition and mineralization at d15 **(G)** and d21 **(H),** respectively. **(I–L)** qRT-PCR analyses revealed that gene expression profile of osteogenic markers such as *Runx2* **(I),** *AlpI* **(J),** *Sp7* **(K),** and *Bglap* **(L)** were upregulated in the *Hoxa2*$^{-/-}$ MEPM cells in a stage-specific manner during osteoblast differentiation. Data was normalized to β -*actin* and represented relative to wild-type at d0 (n = 3 biological replicates; mean ± S.E.M; two-way ANOVA with Bonferroni post-hoc test, $*p < 0.05$; $**p < 0.01$; $***p < 0.001$).

the *Hoxa2*$^{-/-}$ mutants (~64%) compared to wild-type (~33%; **Figure 4C**).

Next, the rate of cell proliferation was assessed at E13.5 using Ki67 immunostaining. The percentage of Ki67-positive cells was significantly increased in the *Hoxa2*$^{-/-}$ palatal mesenchyme (~50%) compared to wild-type (~26%; **Figures 4D–F**). In the nasal side of the palatal shelves, the percentage of Ki67-positive cells was ~53% in *Hoxa2*$^{-/-}$ embryos compared to ~26% in the wild-type (**Figure 4F**). Interestingly, the nasal side mesenchyme displayed a higher proliferation rate of ~53% compared to the oral side of ~23% in *Hoxa2*$^{-/-}$ palatal shelves (**Figure 4F**). In addition, the percentage of proliferating osteoprogenitor cells (RUNX2-positive/Ki67-positive) in the nasal side of the *Hoxa2*$^{-/-}$ palatal shelves was higher (~20%) compared to ~11% in wild-type (**Figures 4G–I**). Furthermore, mRNA expression of cyclin D1 (*Ccnd1*), a critical G1 phase cell cycle regulator was also upregulated in the *Hoxa2*$^{-/-}$ palatal shelves from E12.5 to E14.5 (**Figure 4J**). These results indicate that *Hoxa2* plays a critical role by inhibiting osteoprogenitor commitment and osteoprogenitor proliferation prior to the elevation and fusion of the palatal shelves.

Increased Canonical BMP Signaling Pathway in the *Hoxa2*$^{-/-}$ Palatal Shelves

To understand the molecular signaling pathways underlying the aberrant cell proliferation and osteogenic differentiation in the *Hoxa2*$^{-/-}$ palatal shelves, BMP signaling was investigated as it is critical for cell proliferation (Zhang et al., 2002) and expression of osteogenic markers in the developing palate (Baek et al., 2011). First, the mRNA expression of BMP ligands critical for osteoblast differentiation such as *Bmp2* and *Bmp4* in the developing palatal shelves was examined. *Bmp2* expression was upregulated to ~3.57-fold at E13.5 and ~1.96-fold at E15.5 in *Hoxa2*$^{-/-}$ palatal shelves compared to wild-type (**Figure 5A**). Similarly, *Bmp4* expression was upregulated to ~3.42-fold at E13.5 and to ~1.81-fold at E15.5

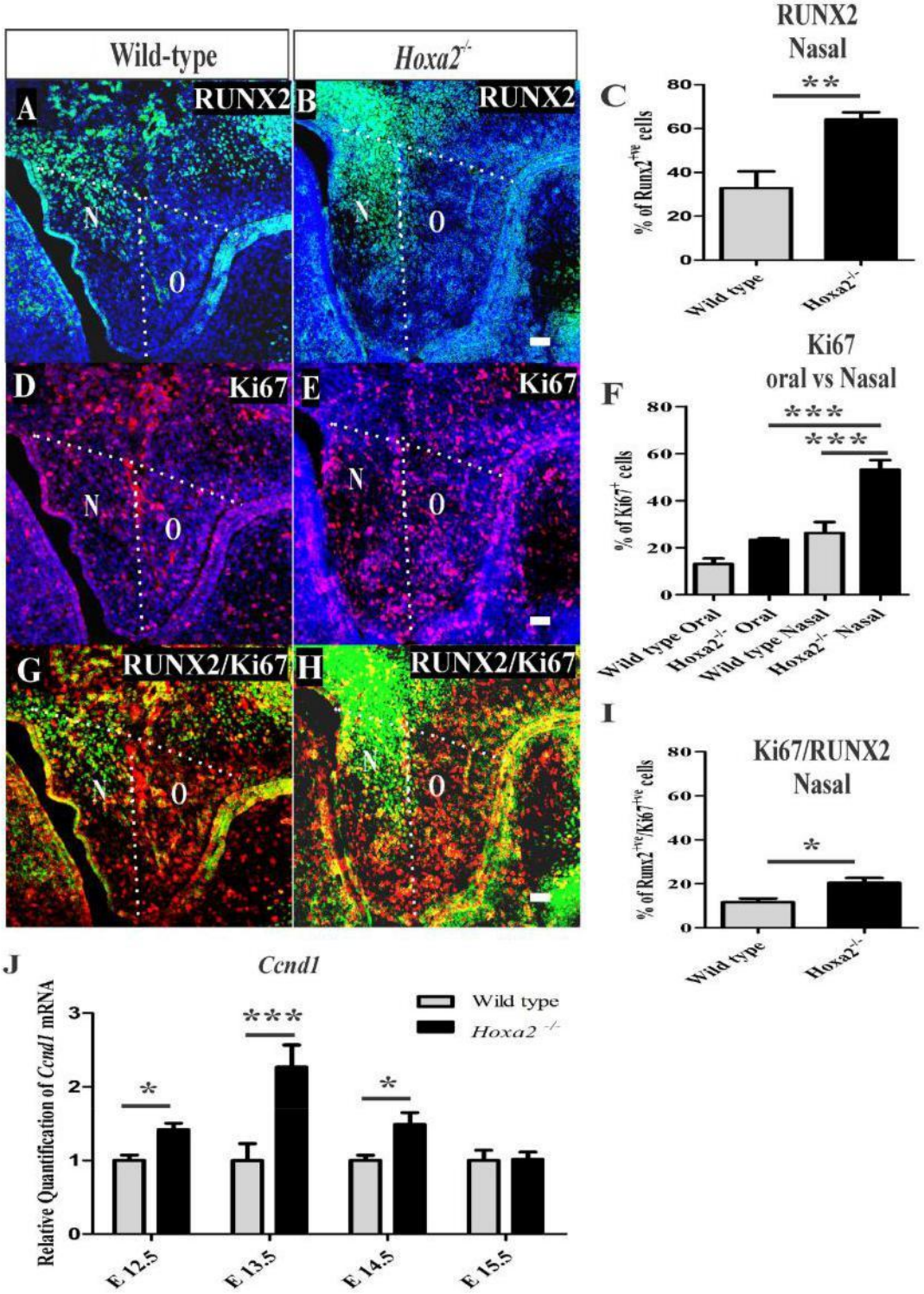

FIGURE 4 | *Hoxa2*$^{-/-}$ palatal shelves exhibit increased osteoprogenitor proliferation and commitment at E13.5. Osteoprogenitor cells in the developing palatal shelves of wild-type and *Hoxa2*$^{-/-}$ embryos were evaluated using RUNX2 immunostaining **(A,B)** and RUNX2-positive cells were counted manually using ImageJ platform **(C).** Proliferation rate was assessed using Ki67 immunostaining **(D–F)** at E13.5. Scale bar, 50 µm; N, nasal; O, oral. Proliferating osteoprogenitor cells (cellspositive for both RUNX2 and Ki67) (Runx2 /Ki67) **(G,H)** relative to the total number of mesenchymal cells (DAPI-positive) from wild-type and *Hoxa2*$^{-/-}$ palatal shelves were counted in the nasal side **(I)**. *Hoxa2*$^{-/-}$ embryos exhibited increased RUNX2-positive **(C)**, Ki67-positive **(F)** and RUNX2/Ki67-double positive **(I)** cells in the nasal side of the palatal shelves ($n = 5$ biological replicates; mean ± S.E.M; unpaired *t*-test, *$p < 0.05$; **$p < 0.01$; ***$p < 0.001$). Expression of cell cycle regulator *Cyclin D1* (*Ccnd1*) mRNA was upregulated in the *Hoxa2*$^{-/-}$ palatal shelves **(J)** from E12.5 to E14.5. qRT-PCR data was normalized to β -*actin* and represented relative to wild-type at respective embryonic stages ($n = 6$ biological replicates; mean ± S.E.M; unpaired *t*-test, *$p < 0.05$; ***$p < 0.001$).

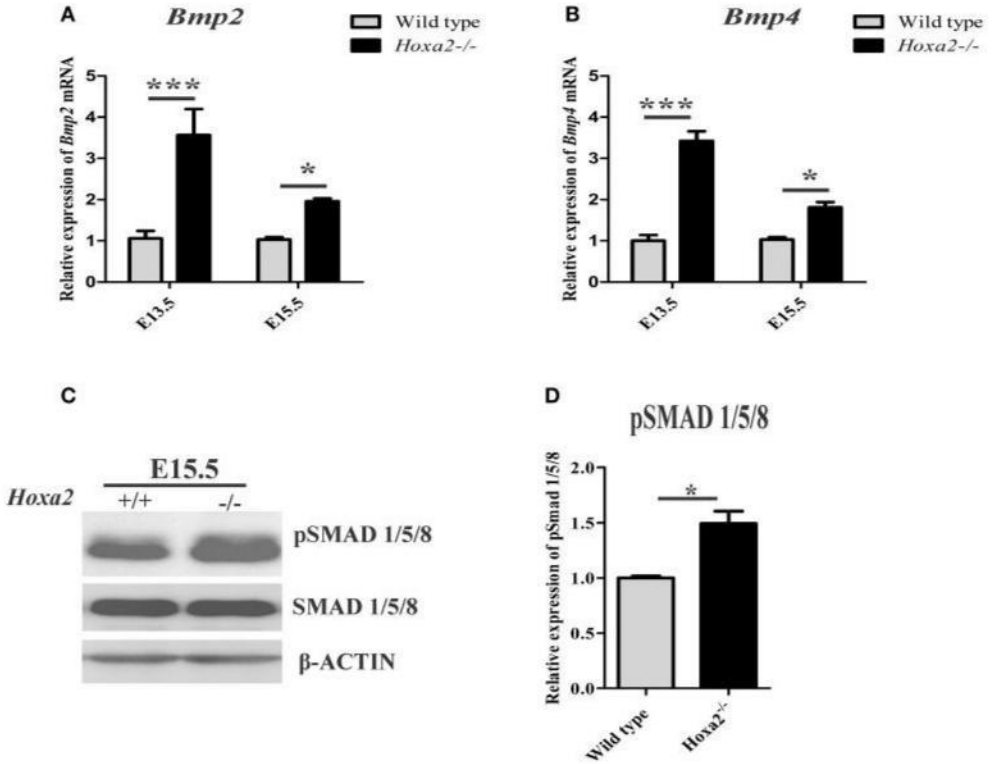

FIGURE 5 | *Hoxa2* regulates canonical BMP signaling in the developing palate. Gene expression of BMP ligands, *Bmp2* **(A)** and *Bmp4* **(B)** were upregulated in $Hoxa2^{-/-}$ palatal shelves at E13.5 and E15.5. qRT-PCR data (n = 4 biological replicates) were normalized to β *-actin* (mean ± S.E.M; unpaired *t*-test, $*p < 0.05$; $***p < 0.001$). Representative immunoblot **(C)** of pSMAD 1/5/8 from the developing palate of wild-type and $Hoxa2^{-/-}$ embryos at E15.5. **(D)** Densitometric analysis represents the relative expression of pSMAD 1/5/8 normalized to SMAD 1/5/8 and represented relative to wild-type (n = 4 biological replicates; mean ± S.E.M; unpaired *t*-test, $*p < 0.05$).

(**Figure 5B**). Immunoblotting analyses revealed that canonical BMP signaling mediated by pSMAD 1/5/8 was also upregulated to ∼1.5-fold in the $Hoxa2^{-/-}$ palate at E15.5 (**Figures 5C,D**). These results indicate that canonical BMP signaling pathway may be downstream of the *Hoxa2* gene network in palate development.

Blocking Canonical BMP Signaling Rescues the Aberrant Cell Proliferation and Osteogenic Differentiation in $Hoxa2^{-/-}$ MEPM Cells

To determine if the upregulated canonical BMP signaling is functionally responsible for the increased mesenchymal cell proliferation and osteogenic differentiation observed in the $Hoxa2^{-/-}$ palate, dorsomorphin was used to inhibit BMP signaling during osteogenic differentiation of MEPM cells *in vitro*. Although at higher doses dorsomorphin (10–20 μM) inhibits AMPK signaling (Zhou et al., 2001) and mTOR signaling (Vucicevic et al., 2011), it selectively inhibits BMP signaling at lower doses (Yu et al., 2008). Upon 5 μM dorsomorphin treatment, upregulated mRNA expressions of *Bmp2* (**Figure 6A**), *Bmp4* (**Figure 6B**) and *Runx2* (**Figure 6C**) in the $Hoxa2^{-/-}$ MEPM cells were restored to the wild-type levels. Moreover, increased protein expression of RUNX2 and pSMAD 1/5/8 (**Figure 6D**) in the $Hoxa2^{-/-}$ MEPM cells were reduced after dorsomorphin treatment. The increased cell proliferation (**Figure 6E**) and osteogenic differentiation (**Figure 6F**) in the $Hoxa2^{-/-}$ MEPM cells were also reduced after dorsomorphin treatment. These results indicate that the upregulated canonical BMP signaling is functionally responsible for the increased cell proliferation and osteogenic differentiation during palate development in $Hoxa2^{-/-}$ embryos. Altogether, the findings reveal that *Hoxa2* inhibits osteoprogenitor proliferation and commitment, via BMP signaling, to control the spatial and temporal expression of osteoblast markers for proper palatogenesis.

DISCUSSION

Mice lacking *Hoxa2* exhibit cleft palate (Gendron-Maguire et al., 1993; Rijli et al., 1993; Barrow and Capecchi, 1999) and microtia (Minoux et al., 2013), which are consistent with *Hoxa2* mutations in humans (Alasti et al., 2008). We have previously shown that *Hoxa2* is expressed in the palatal shelves during development (Nazarali et al., 2000) reaching a maximal expression at E13.5 and regulates cell proliferation in the

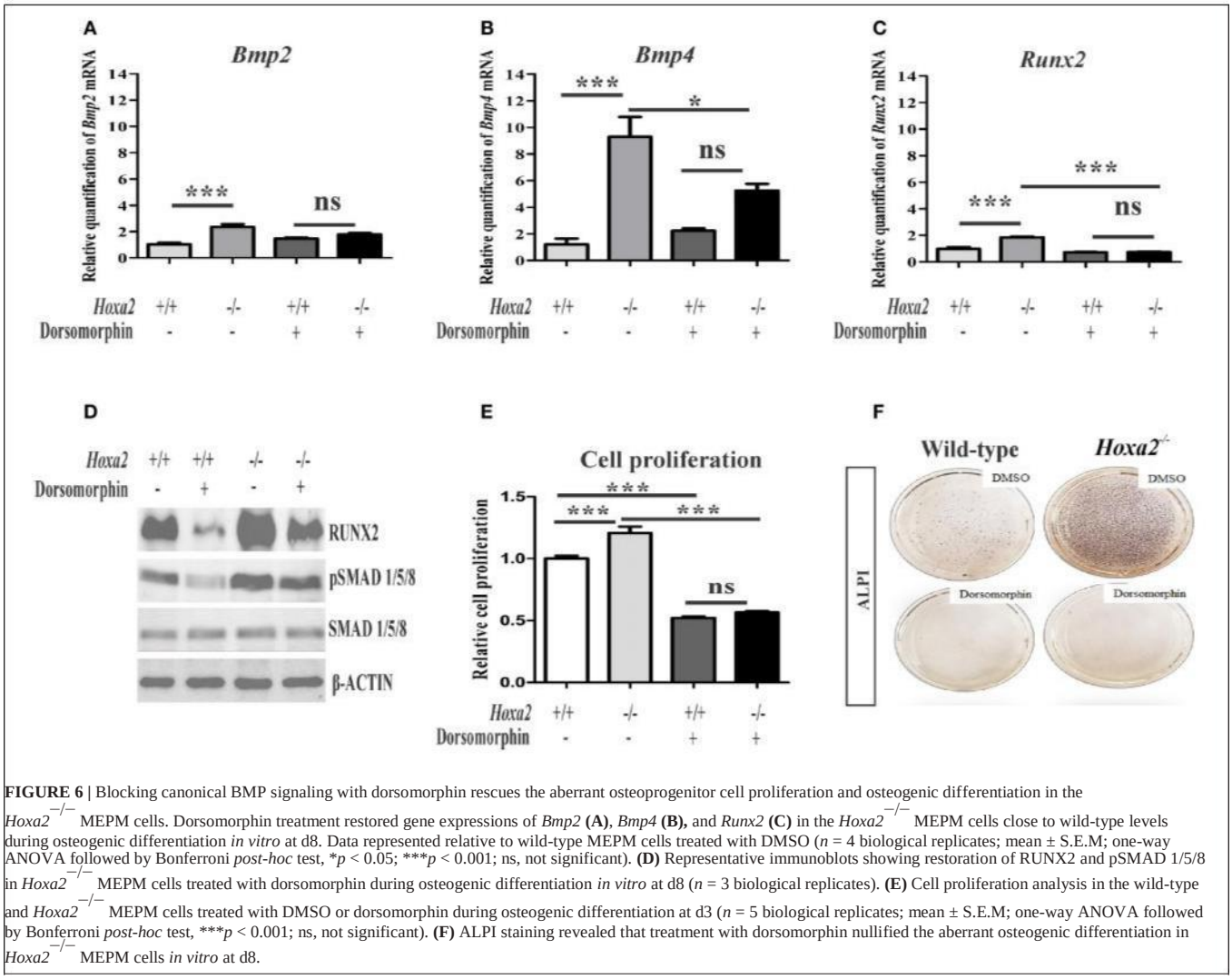

FIGURE 6 | Blocking canonical BMP signaling with dorsomorphin rescues the aberrant osteoprogenitor cell proliferation and osteogenic differentiation in the *Hoxa2*$^{-/-}$ MEPM cells. Dorsomorphin treatment restored gene expressions of *Bmp2* **(A)**, *Bmp4* **(B),** and *Runx2* **(C)** in the *Hoxa2*$^{-/-}$ MEPM cells close to wild-type levels during osteogenic differentiation *in vitro* at d8. Data represented relative to wild-type MEPM cells treated with DMSO (n = 4 biological replicates; mean ± S.E.M; one-way ANOVA followed by Bonferroni *post-hoc* test, *p < 0.05; ***p < 0.001; ns, not significant). **(D)** Representative immunoblots showing restoration of RUNX2 and pSMAD 1/5/8 in *Hoxa2*$^{-/-}$ MEPM cells treated with dorsomorphin during osteogenic differentiation *in vitro* at d8 (n = 3 biological replicates). **(E)** Cell proliferation analysis in the wild-type and *Hoxa2*$^{-/-}$ MEPM cells treated with DMSO or dorsomorphin during osteogenic differentiation at d3 (n = 5 biological replicates; mean ± S.E.M; one-way ANOVA followed by Bonferroni *post-hoc* test, ***p < 0.001; ns, not significant). **(F)** ALPI staining revealed that treatment with dorsomorphin nullified the aberrant osteogenic differentiation in *Hoxa2*$^{-/-}$ MEPM cells *in vitro* at d8.

developing palate (Smith et al., 2009). There are several lines of evidence that *Hoxa2* regulates palate development intrinsically (Smith et al., 2009), yet the mechanism is largely unknown. In this study, we have found that *Hoxa2* inhibits BMP signaling dependent osteogenic differentiation spatially and temporally to regulate palate formation. The present study deepens the current understanding of the role of *Hoxa2* in palate formation and the mechanisms underlying the cleft palate phenotype in *Hoxa2*$^{-/-}$ mice linking *Hoxa2*, BMP signaling and osteogenesis.

Our findings here reveal that *Hoxa2* controls the temporal and spatial expression pattern of osteoblast markers in the developing palatal mesenchyme. Ossifying domains characterized by RUNX2 and ALPI were increased in the palatal process of the maxilla and in the palatal process of the palatine bone in *Hoxa2*$^{-/-}$ mice. In contrast, SP7 a marker of mature osteoblasts was expanded only in the palatal process of the maxilla and not in the palatal process of the palatine bone at E16.5. This suggests that cells toward the oral side of the palatal process of the palatine bone are at immature osteoblast stage and may not have developed bone matrix by E16.5. Patterning of the palatal process of the palatine bone and of the maxilla are through independent skeletogenic processes (Baek et al., 2011). The palatal process of the palatine bone ossifies at E13.5, whereas the ossification of the palatal process of the maxilla begins only at E15.5. Consistent with this, qRT-PCR and immunoblot analyses revealed a corresponding upregulation of osteogenic markers in the *Hoxa2*$^{-/-}$ palate at these two critical stages E13.5 and E15.5. In addition, primary *Hoxa2*$^{-/-}$ MEPM cells displayed an increase in osteogenic differentiation and a stage-specific increase in the expressions of the osteoblast-specific transcripts indicating that *Hoxa2* regulates temporal differentiation of mesenchyme cells to osteoblasts in the palate. Together, our results reveal that *Hoxa2* functions as an inhibitor of osteogenic differentiation in the palatal mesenchyme during development. Our findings are in agreement with previous studies showing the role of *Hoxa2* as an inhibitor of bone formation in other craniofacial regions (Kanzler et al., 1998; Dobreva et al., 2006).

Very little is known about the signaling network downstream of *Hoxa2* during palatogenesis. Here, we have demonstrated that *Hoxa2*$^{-/-}$ palatal shelves exhibit upregulated canonical

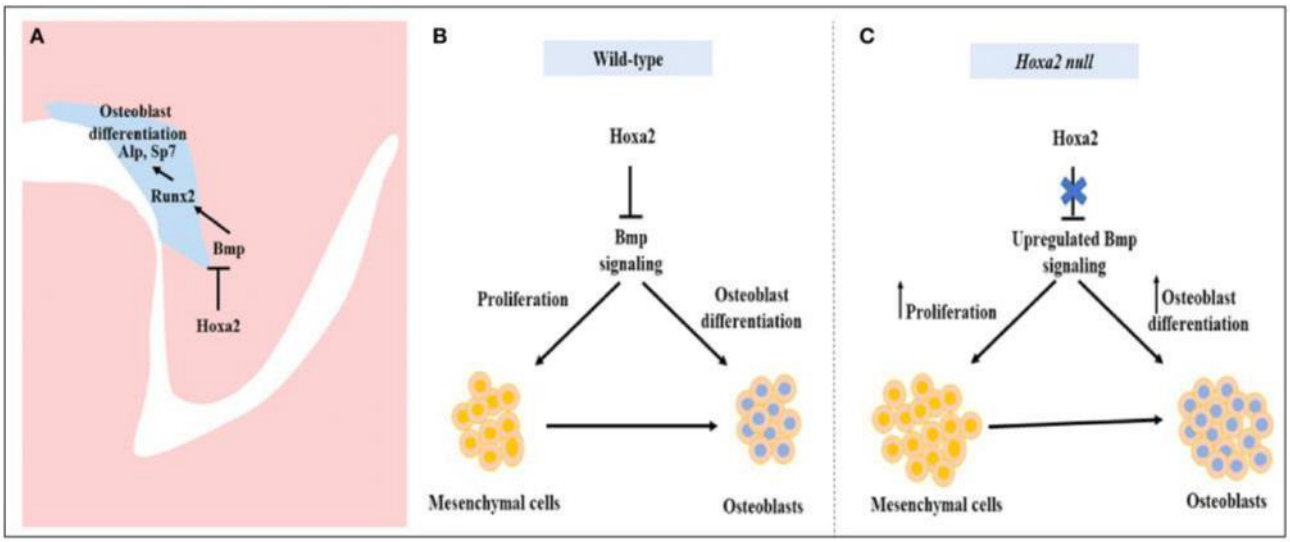

FIGURE 7 | Schematic diagram depicting the role of *Hoxa2* in proliferation and osteogenic differentiation of the palatal mesenchyme. **(A)** *Hoxa2* inhibits canonical BMP signaling in the developing palate, which in turn restricts the expression domain of osteogenic markers such as *Runx2*, *AlpI*, and *Sp7*. **(B)** In wild-type, *Hoxa2* expression peaks during early palatogenesis to control cell proliferation and to maintain mesenchymal cells in an undifferentiated stage by regulating BMP signaling pathway. **(C)** Loss of *Hoxa2* leads to upregulation of BMP signaling resulting in increased osteoprogenitor cell proliferation and osteogenic differentiation, possibly accounting for the failure in the elevation of palatal shelves resulting in manifestation of cleft palate.

BMP signaling mediated by pSMAD 1/5/8. In addition, the expression of BMP ligands such as *Bmp2* and *Bmp4* are upregulated in *Hoxa2*$^{-/-}$ palatal shelves *in vivo* and in *Hoxa2*$^{-/-}$ MEPM cells *in vitro*. BMP signaling plays a critical role in proliferation (Zhang et al., 2002; Baek et al., 2011) and osteogenic differentiation of the palatal mesenchyme (Wu et al., 2008; Han et al., 2009; Baek et al., 2011). Importantly, abnormal BMP signaling in the palatal mesenchyme leads to cleft palate manifestation (Zhang et al., 2002; He et al., 2008). Inactivation of *Bmpr1a* in the palatal mesenchyme (*Osr2-IresCre; Bmpr1a*$^{f/f}$) results in submucous cleft palate, absence in the patterning of the palatal process of the maxilla and defective palatal process of the palatine bone (Baek et al., 2011). Genome-wide mapping revealed that *Bmp2*, *Bmp4* and *Bmpr1a* are possible targets of *Hoxa2* (Donaldson et al., 2012) and HOXA2 protein binds to the intronic region of *Bmp4* (Minoux et al., 2013) in the developing pharyngeal arch2. In this study, dorsomorphin was used to inhibit BMP signaling in the wild-type and *Hoxa2*$^{-/-}$ primary palatal mesenchymal cells during osteogenic differentiation. Dorsomorphin selectively inhibits BMP signaling at lower doses (Yu et al., 2008) and at higher doses dorsomorphin (10–20 μM) also inhibits AMPK signaling (Zhou et al., 2001) and mTOR signaling (Vucicevic et al., 2011). In our study, dorsomorphin treatment not only rescued the upregulated gene expression of osteogenic factors such as *Bmp2*, *Bmp4*, and *Runx2* but also the aberrant cell proliferation and osteogenic differentiation in the *Hoxa2*$^{-/-}$ MEPM cells. These experiments highlight the involvement of BMP signaling in the abnormal osteoprogenitor cell proliferation and osteogenic differentiation in the *Hoxa2*$^{-/-}$ palate, which could attribute to the cleft palate phenotype in these mutants.

To our knowledge, there is no report available on the characterization of osteoprogenitor cell proliferation and commitment in the palatal mesenchyme during development. In this study, we have unraveled the role of *Hoxa2* in maintaining the palatal mesenchymal cells in an undifferentiated stage by inhibiting osteoprogenitor proliferation and commitment preventing abnormal ossification in the developing palate. Palatal mesenchymal cells derived from CNCC undergo osteogenic proliferation and commit to form osteoblasts (Iwata et al., 2010). Double immunolabeling analyses of RUNX2 and Ki67 at E13.5 revealed that among the total population of mesenchyme cells, there was a significantly higher number of (i) proliferating cells (Ki67-positive cells), (ii) osteoprogenitor cells (RUNX2-positive cells), and (iii) proliferating osteoprogenitor cells (RUNX2-positive /Ki67-positive cells) in the nasal side of the *Hoxa2*$^{-/-}$ palatal shelves compared to the wild-type. In the palatal mesenchyme, increased or decreased cell proliferation could result in failure of the palatal shelves to elevate and reorient above the tongue leading to cleft palate (Bush and Jiang, 2012; Smith et al., 2013). Recent studies show evidence for abnormal osteogenic signaling prior to the elevation of palatal shelves in several well-studied cleft palate mutant mice models including *Pax9*$^{-/-}$ mice (Jia et al., 2017a,b) and *Osr2*$^{-/-}$ mice (Fu et al., 2017). Consistent with our findings here in the *Hoxa2*$^{-/-}$ mice, *Osr2*$^{-/-}$ exhibit increased osteogenic centers of the palatal process of the palatine bone prior to the elevation of the palatal shelves at E13.5 and in addition to defective cell proliferation, enhanced osteogenesis could contribute to cleft palate phenotype in *Osr2*$^{-/-}$ mice (Fu et al., 2017). In addition, RNA-Seq data from *Osr2*$^{-/-}$ palatal shelves revealed upregulation of several positive regulators of osteogenesis including *Runx2*, *Runx3*,

Sp7, and Bmp ligands- *Bmp3*, *Bmp5*, and *Bmp7*. Furthermore, *Pax9*$^{-/-}$ mice exhibit reduced cell proliferation and osteogenesis in the developing palate (Jia et al., 2017a). Restoration of reduced cell proliferation and osteogenesis by Wnt agonists (Dkk inhibitors) rescued the cleft palate phenotype in *Pax9*$^{-/-}$ mice (Jia et al., 2017a). The increase in cell proliferation in the nasal side of the *Hoxa2*$^{-/-}$ palate indicates a strong role for *Hoxa2* in the spatial maintenance of mesenchymal cells in an undifferentiated state for temporal coordination of osteoblast differentiation (**Figure 7**). Our findings here exemplify the regional heterogeneity in proliferation and osteogenic differentiation by *Hoxa2* along the oral-nasal axis in the palatal mesenchyme prior to the elevation of palatal shelves. Our data argue that improper BMP signaling leading to the increased osteoprogenitor cell proliferation and commitment could be a reason for the cleft palate pathogenesis in the *Hoxa2*$^{-/-}$ mice. Further studies are needed to address if the cleft palate phenotype in the *Hoxa2*$^{-/-}$ mice could be rescued using other mutant mice with impaired osteogenesis.

Our data demonstrate that *Hoxa2* inhibits osteoprogenitor cell proliferation and osteogenic commitment via modulating BMP signaling in the mouse embryonic palatal mesenchyme. *Hoxa2* regulates spatial and temporal programs of osteogenesis by maintaining mesenchymal cells in an undifferentiated stage until osteogenic clues arrive. In conclusion, our findings provide new insights into the signaling mechanism underlying the role of *Hoxa2* during embryonic palate development.

AUTHOR CONTRIBUTIONS

AN conceived and coordinated the study. PI designed the study, performed experiments, analyzed data and wrote the manuscript. AN and PI proofed, revised the manuscript for critical content and interpretation of data.

FUNDING

This work was supported by discovery grant 171317–2012 from the Natural Sciences and Engineering Research Council of Canada (NSERC) to AN and in part by Subtelny Orthodontic Clinical Research Grant from American Cleft Palate-Craniofacial Association (ACPA-CPF), USA to PI.

ACKNOWLEDGMENTS

PI acknowledges the Apotex Graduate Scholarship Award from the College of Pharmacy and Nutrition, University of Saskatchewan; Graduate Research fellowship and Saskatchewan Innovation and Opportunity Scholarships from the College of Graduate and Postdoctoral studies, University of Saskatchewan. Authors thank Drs. Brian F. Eames and Kendra L. Furber for critical suggestions on the manuscript and Larhonda Sobchishin for providing technical expertise. This manuscript is dedicated to the memory of our colleague and mentor, Dr. Adil J. Nazarali, who passed away before the submission of the manuscript.

REFERENCES

Alasti, F., Sadeghi, A., Sanati, M. H., Farhadi, M., Stollar, E., Somers, T., et al. (2008). A mutation in HOXA2 is responsible for autosomal-recessive microtia in an Iranian family. *Am. J. Hum. Genet.* 82, 982–991. doi: 10.1016/j.ajhg.2008.02.015

Baek, J., Lan, Y., Liu, H., Maltby, K. M., Mishina, Y., and Jiang, R. (2011). Bmpr1a signaling plays critical roles in palatal shelf growth and palatal bone formation. *Dev. Biol.* 350, 520–531. doi: 10.1016/j.ydbio.2010. 12.028

Barrow, J. R., and Capecchi, M. R. (1999). Compensatory defects associated with mutations in Hoxa1 restore normal palatogenesis to Hoxa2 mutants. *Development* 126, 5011–5026. Available online at: http://dev.biologists.org/content/126/22/5011.abstract

Brown, G. D., and Nazarali, A. J. (2010). Matrix metalloproteinase-25 has a functional role in mouse secondary palate development and is a downstream target of TGF-β3. *BMC Dev. Biol.* 10:93. doi: 10.1186/1471-213X-10-93

Bush, J. O., and Jiang, R. (2012). Palatogenesis: morphogenetic and molecular mechanisms of secondary palate development. *Development* 139, 231–243. doi: 10.1242/dev.067082

Dixon, M. J., Marazita, M. L., Beaty, T. H., and Murray, J. C. (2011). Cleft lip and palate: understanding genetic and environmental influences. *Nat. Rev. Genet.* 12, 167–178. doi: 10.1038/nrg2933

Donaldson, I. J., Amin, S., Hensman, J. J., Kutejova, E., Rattray, M., Lawrence, N., et al. (2012). Genome-wide occupancy links Hoxa2 to Wnt-β-catenin signaling in mouse embryonic development. *Nucleic Acids Res.* 40, 3990–4001. doi: 10.1093/nar/gkr1240

Dobreva, G., Chahrour, M., Dautzenberg, M., Chirivella, L., Kanzler, B., Karsenty, G., et al. (2006). SATB2 is a multifunctional determinant of craniofacial patterning and osteoblast differentiation. *Cell* 125, 971–986. doi: 10.1016/j.cell.2006.05.012

Ferguson, M. W. J. (1988). Palate development. *Development* 103(Suppl.), 41–60.

Fu, X., Xu, J., Chaturvedi, P., Liu, H., Jiang, R., and Lan, Y. (2017). Identification of Osr2 transcriptional target genes in palate development. *J. Dent. Res.* 96, 1451–1458. doi: 10.1177/0022034517719749

Funato, N., Nakamura, M., and Yanagisawa, H. (2015). Molecular basis of cleft palates in mice. *World J. Biol. Chem.* 6, 121–138. doi: 10.4331/wjbc.v6.i3.121

Gendron-Maguire, M., Mallo, M., Zhang, M., and Gridley, T. (1993). Hoxa-2 mutant mice exhibit homeotic transformation of skeletal elements derived from cranial neural crest. *Cell* 75, 1317–1331. doi: 10.1016/0092-8674(93)90619-2

Gordon, J. A., Hassan, M. Q., Saini, S., Montecino, M., van Wijnen, A. J., Stein, G. S., et al. (2010). Pbx1 represses osteoblastogenesis by blocking Hoxa10-mediated recruitment of chromatin remodeling factors. *Mol. Cell. Biol.* 30, 3531–3541. doi: 10.1128/MCB.00889-09

Gregory, C. A., Grady Gunn, W., Peister, A., and Prockop, D. J. (2004). An Alizarin red-based assay of mineralization by adherent cells in culture: comparison with cetylpyridinium chloride extraction. *Anal. Biochem.* 329, 77–84. doi: 10.1016/j.ab.2004.02.002

Han, J., Mayo, J., Xu, X., Li, J., Bringas, P., Maas, R. L., et al. (2009). Indirect modulation of Shh signaling by Dlx5 affects the oral-nasal patterning of palate and rescues cleft palate in Msx1 -null mice. *Development* 136, 4225–4233. doi: 10.1242/dev.036723

He, F., Xiong, W., Yu, X., Espinoza-Lewis, R., Liu, C., Gu, S., et al. (2008). Wnt5a regulates directional cell migration and cell proliferation via Ror2-mediated noncanonical pathway in mammalian palate development. *Development* 135, 3871–3879. doi: 10.1242/dev.025767

Hill, C. R., Yuasa, M., Schoenecker, J., and Goudy, S. L. (2014). Jagged1 is essential for osteoblast development during maxillary ossification. *Bone* 62, 10–21. doi: 10.1016/j.bone.2014.01.019

Iwata, J., Hosokawa, R., Sanchez-lara, P. A., Urata, M., Slavkin, H., and Chai, Y. (2010). Transforming growth factor- β regulates basal transcriptional regulatory machinery to control cell proliferation and differentiation in cranial neural crest-derived osteoprogenitor cells. *J. Biol. Chem.* 285, 4975–4982. doi: 10.1074/jbc.M109.035105

Iwata, J., Tung, L., Urata, M., Hacia, G., Pelikan, R., Suzuki, A., et al. (2012). Fibroblast Growth Factor 9 (FGF9) -Pituitary Homeobox 2 (PITX2) pathway mediates Transforming Growth Factor β (TGFβ) signaling to regulate cell proliferation in palatal mesenchyme during mouse palatogenesis. *J. Biol. Chem.* 287, 2353–2363. doi: 10.1074/jbc.M111.280974

Jia, S., Zhou, J., Fanelli, C., Wee, Y., Bonds, J., Schneider, P., et al. (2017a). Small-molecule Wnt agonists correct cleft palates in Pax9 mutant mice in utero. *Development* 144, 3819–3828. doi: 10.1242/dev.157750

Jia, S., Zhou, J., Wee, Y., Mikkola, M. L., Schneider, P., and Souza, R. N. D. (2017b). Anti-EDAR agonist antibody therapy resolves palate defects in Pax9$^{-/-}$ Mice. *J. Dent. Res.* 96, 1282–1289. doi: 10.1177/0022034517726073

Kanzler, B., Kuschert, S. J., Liu, Y., and Mallo, M. (1998). Hoxa-2 restricts the chondrogenic domain and inhibits bone formation during development of the branchial area. *Development* 125, 2587–2597.

Kaufman, M. H. (1992). *The Atlas of Mouse Development*. Academic Press. Available online at: https://books.google.ca/books?id=Lo5pAAAAMAAJ

Komori, T., Yagi, H., Nomura, S., Yamaguchi, A., Sasaki, K., Deguchi, K., et al. (1997). Targeted disruption of Cbfa1 results in a complete lack of bone formation owing to maturational arrest of osteoblasts. *Cell* 89, 755–764. doi: 10.1016/S0092-8674(00)80258-5

Kwong, F. N., Richardson, S. M., and Evans, C. H. (2008). Chordin knockdown enhances the osteogenic differentiation of human mesenchymal stem cells. *Arthritis Res. Ther*. 10:R65. doi: 10.1186/ar2436

Minoux, M., Kratochwil, C. F., Ducret, S., Amin, S., Kitazawa, T., Kurihara, H., et al. (2013). Mouse Hoxa2 mutations provide a model for microtia and auricle duplication. *Development* 140, 4386–4397. doi: 10.1242/dev.098046

Nakashima, K., Zhou, X., Kunkel, G., Zhang, Z., Deng, J. M., Behringer, R. R., et al. (2002). The novel zinc finger-containing transcription factor osterix is required for osteoblast differentiation and bone formation. *Cell* 108, 17–29. doi: 10.1016/S0092-8674(01)00622-5

Nazarali, A., Puthucode, R., Leung, V., Wolf, L., Hao, Z., and Yeung, J. (2000). Temporal and spatial expression of Hoxa-2 during murine palatogenesis. *Cell. Mol. Neurobiol*. 20, 269–290. doi: 10.1023/A:10070060 24407

Rijli, F. M., Mark, M., Lakkaraju, S., Dierich, A., Doll, P., Chambon, P., et al. (1993). A homeotic transformation is generated in the rostra1 branchial region of the head by disruption of Hoxa-2, which acts as a selector gene. *Cell* 75, 1333–1349. doi: 10.1016/0092-8674(93)90620-6

Smith, T. M., Lozanoff, S., Iyyanar, P. P., and Nazarali, A. J. (2013). Molecular signaling along the anterior-posterior axis of early palate development. *Front. Physiol.* 3:488. doi: 10.3389/fphys.2012.00488

Smith, T. M., Wang, X., Zhang, W., Kulyk, W., and Nazarali, A. J. (2009). Hoxa2 plays a direct role in murine palate development. *Dev. Dyn*. 238, 2364–2373. doi: 10.1002/dvdy.22040Thangaraj, M. P., Furber, K. L., Gan, J. K., Ji, S., Sobchishin, L., Doucette, J. R., et al. (2017). RNA binding protein Quaking stabilizes Sirt2 mRNA during oligodendroglial differentiation. *J. Biol. Chem.* 292, 5166–5182. doi: 10.1074/jbc.M117.775544

Vucicevic, L., Misirkic, M., Janjetovic, K., Vilimanovich, U., Sudar, E., Isenovic, E., et al. (2011). Compound C induces protective autophagy in cancer cells through AMPK inhibition-independent blockade of Akt/mTOR pathway. *Autophagy* 7, 40–50. doi: 10.4161/auto.7.1.13883

Wu, M., Li, J., Engleka, K. A., Zhou, B., Lu, M. M., Plotkin, J. B., et al. (2008). Persistent expression of Pax3 in the neural crest causes cleft palate and defective osteogenesis in mice. *J. Clin. Invest.* 118, 2076–2087. doi: 10.1172/JCI33715

Xiong, W., He, F., Morikawa, Y., Yu, X., Zhang, Z., Lan, Y., et al. (2009). Hand2 is required in the epithelium for palatogenesis in mice. *Dev. Biol*. 330, 131–141. doi: 10.1016/j.ydbio.2009.03.021

Yu, K., Deng, M., Naluai-cecchini, T., Glass, I. A., and Cox, T. C. (2017). Differences in oral structure and tissue interactions during mouse vs. Human palatogenesis: implications for the translation of findings from mice. *Front. Physiol.* 8:154. doi: 10.3389/fphys.2017.00154

Yu, P. B., Hong, C. C., Sachidanandan, C., Babitt, J. L., Deng, D. Y., Hoyng, S. A., et al. (2008). Dorsomorphin inhibits BMP signals required for embryogenesis and iron metabolism. *Nat. Chem. Biol.* 4, 33–41. doi: 10.1038/nchembio.2007.54 Zhang, Z., Song, Y., Zhao, X., Zhang, X., Fermin, C., and Chen, Y. (2002). Rescue of cleft palate in Msx1-deficient mice by transgenic Bmp4 reveals a network of BMP and Shh signaling in the regulation of mammalian palatogenesis.

Development 129, 4135–4146.

Zhou, G., Myers, R., Li, Y., Chen, Y., Shen, X., Fenyk-melody, J., et al. (2001). Role of AMP-activated protein kinase in mechanism of metformin action role of AMP-activated protein kinase in mechanism of metformin action. *J. Clin. Invest.* 108, 1167–1174. doi: 10.1172/JCI13505

Zhou, J., Gao, Y., Lan, Y., Jia, S., and Jiang, R. (2013). Pax9 regulates a molecular network involving Bmp4, Fgf10, Shh signaling and the Osr2 transcription factor to control palate morphogenesis. *Development* 140, 4709–4718. doi: 10.1242/dev.099028

Conflict of Interest Statement: The authors declare that the research was conducted in the absence of any commercial or financial relationships that could be construed as a potential conflict of interest.

frontiers in Physiology

ORIGINAL RESEARCH
published: 23 November 2017
doi: 10.3389/fphys.2017.00955

Six2 Plays an Intrinsic Role in Regulating Proliferation of Mesenchymal Cells in the Developing Palate

Dennis O. Okello [1†], Paul P. R. Iyyanar [1†], William M. Kulyk [2*], Tara M. Smith [1, 3], Scott Lozanoff [4], Shaoping Ji [1, 5] and Adil J. Nazarali [1‡]

[1] *Laboratory of Molecular Cell Biology, Neuroscience Research Cluster, College of Pharmacy and Nutrition, University of Saskatchewan, Saskatoon, SK, Canada,* [2] *Department of Anatomy and Cell Biology, College of Medicine, University of Saskatchewan, Saskatoon, SK, Canada,* [3] *Med-life Discoveries LP, Saskatoon, SK, Canada,* [4] *Department of Anatomy, Biochemistry and Physiology, John A. Burns School of Medicine, University of Hawaii, Honolulu, HI, United States,* [5] *Department of Biochemistry and Molecular Biology, Medical School, Henan University, Kaifeng, China*

OPEN ACCESS

Edited by:
David P. Rice,
University of Helsinki, Finland

Reviewed by:
Amel Gritli-Linde,
University of Gothenburg, Sweden
Frank Wagener,
Radboud Institute for Molecular Life Sciences, Netherlands

****Correspondence:***
William M. Kulyk william.kulyk@usask.ca

[†]*These authors have contributed equally to this work.*

[‡]*Passed away on April 27, 2017.*

Specialty section:
This article was submitted to Craniofacial Biology and Dental Research, a section of the journal Frontiers in Physiology

Received: *21 September 2017*
Accepted: *09 November 2017*
Published: *23 November 2017*

Citation:
Okello DO, Iyyanar PPR, Kulyk WM, Smith TM, Lozanoff S, Ji S and Nazarali AJ (2017) Six2 Plays an Intrinsic Role in Regulating Proliferation of Mesenchymal Cells in the Developing Palate. Front. Physiol. 8:955. doi: 10.3389/fphys.2017.00955

Cleft palate is a common congenital abnormality that results from defective secondary palate (SP) formation. The *Sine oculis-related homeobox 2* (*Six2*) gene has been linked to abnormalities of craniofacial and kidney development. Our current study examined, for the first time, the specific role of *Six2* in embryonic mouse SP development. *Six2* mRNA and protein expression were identified in the palatal shelves from embryonic days (E)12.5 to E15.5, with peak levels during early stages of palatal shelf outgrowth. Immunohistochemical staining (IHC) showed that Six2 protein is abundant throughout the mesenchyme in the oral half of each palatal shelf, whereas there is a pronounced decline in Six2 expression by mesenchyme cells in the nasal half of the palatal shelf by stages E14.5–15.5. An opposite pattern was observed in the surface epithelium of the palatal shelf. Six2 expression was prominent at all stages in the epithelial cell layer located on the nasal side of each palatal shelf but absent from the epithelium located on the oral side of the palatal shelf. *Six2* is a putative downstream target of transcription factor *Hoxa2* and we previously demonstrated that *Hoxa2* plays an intrinsic role in embryonic palate formation. We therefore investigated whether *Six2* expression was altered in the developing SP of *Hoxa2* null mice. Reverse transcriptase PCR and Western blot analyses revealed that *Six2* mRNA and protein levels were upregulated in *Hoxa2*$^{-/-}$ palatal shelves at stages E12.5–14.5. Moreover, the domain of Six2 protein expression in the palatal mesenchyme of *Hoxa2*$^{-/-}$ embryos was expanded to include the entire nasal half of the palatal shelf in addition to the oral half. The palatal shelves of *Hoxa2*$^{-/-}$ embryos displayed a higher density of proliferating, Ki-67 positive palatal mesenchyme cells, as well as a higher density of Six2/Ki-67 double-positive cells. Furthermore, *Hoxa2*$^{-/-}$ palatal mesenchyme cells in culture displayed both increased proliferation and elevated *Cyclin D1* expression relative to wild-type cultures. Conversely, siRNA-mediated *Six2* knockdown restored proliferation and *Cyclin D1* expression in *Hoxa2*$^{-/-}$ palatal mesenchyme cultures to near wild-type levels. Our findings demonstrate that *Six2* functions downstream of *Hoxa2* as a positive regulator of mesenchymal cell proliferation during SP development.

Keywords: *Six2*, palate, *Hoxa2*, craniofacial development, cell proliferation, *Cyclin D1*

INTRODUCTION

Cleft palate is a common congenital malformation in humans, with a complex etiology (Vanderas, 1987). The palate separates the nasal and oral cavities, allowing for proper respiration, feeding and phonation. Both genetic and environmental factors have been implicated in the causation of cleft palate (Dixon et al., 2011). However, the molecular mechanisms involved in the pathogenesis of cleft palate are poorly understood.

Mouse secondary palate (SP) development begins around embryonic day (E) 11.5, with the emergence of paired palatal shelf outgrowths from the maxillary prominences. From E12.0–13.5, the palatal shelves grow vertically downwards on either side of the developing tongue. At E14.0, the tongue depresses, allowing the two palatal shelves to re-orient horizontally above the tongue. The elevated palatal shelves grow horizontally toward each other, establishing contact to form the midline epithelial seam (MES) at E14.5. The MES degrades by E15.5, creating a confluent SP. The SP then fuses anteriorly with the primary palate, a derivative of the converged medial nasal processes, to complete the formation of the roof of the oral cavity by E16.5 (Ferguson, 1988; Kaufman, 1992). In addition, mesenchymal cells located in the anterior portion of the SP ossify to form the palatine bone. Disruptions in the growth, elevation or fusion of the palatal shelves can lead to congenital cleft palate defects (Ferguson, 1988; Gritli-Linde, 2007; Smith et al., 2013).

Sine oculis-related homeobox 2 (*Six2*) is a member of the vertebrate *Six* gene family which encode homeobox transcription factors homologous to the *Drosophila* Sine oculis protein (Kawakami et al., 2000). *Six* family genes have been reported to promote cell proliferation and survival during embryogenesis (Kawakami et al., 2000). *Six2* is expressed primarily in the cranial base, midface, facial prominences, first pharyngeal arch, and in the urogenital region of the developing embryo (Fogelgren et al., 2008). *Six2* null mice die at birth exhibiting renal hypoplasia (Self et al., 2006) and a shorter cranial base (He et al., 2010). In these mice, chondrocyte differentiation in the cranial base is abnormal, with decreased cell proliferation and increased terminal differentiation leading to premature fusion of the cranial base (He et al., 2010).

Downregulation of *Six2* by microRNAs miR-181b or miR-181c inhibits cell proliferation and promotes apoptosis in metanephric kidney mesenchymal cells *in vitro* (Lyu et al., 2013; Lv et al., 2014). Transcription factor Zeb1, a marker of epithelial-mesenchymal transitions during embryogenesis and cancer metastasis, regulates cell proliferation in metanephric mesenchymal cells by binding to the *Six2* promoter and upregulating its expression (Gu et al., 2016). Additionally, *Six2* promotes metastasis of breast cancer cells by repressing E-cadherin expression via mechanisms involving miR-200b downregulation, Zeb 2 upregulation, and *E-cadherin* promoter methylation (Wang et al., 2014).

Abbreviations: ddPCR, digital droplet PCR; E, embryonic day; IHC, immunohistochemical; MEE, medial edge epithelium; MEPM, mouse embryonic palatal mesenchyme; MES, midline epithelial seam; O-N, oro-nasal, qRT-PCR, quantitative real-time PCR; SP, secondary palate.

In the radiation-induced mouse mutant *brachyrrhine* (*Br/Br*), prenatal deficiency of *Six2* leads to frontonasal dysplasia, cleft palate (Singh et al., 1998; McBratney et al., 2003) and renal hypoplasia (McBratney et al., 2003; Fogelgren et al., 2008, 2009). Moreover, investigations have linked *Six2* deletion in humans to an autosomal dominant frontonasal dysplasia syndrome that has similarities to the murine *Br* mutant phenotype (Hufnagel et al., 2016).

Deletions of the *Hoxa2* gene in mice also lead to cleft palate defects, together with altered morphogenesis of second pharyngeal arch structures (Rijli et al., 1993 and Gendron-Maguire et al., 1993). Investigations in our laboratory have previously demonstrated that *Hoxa2* is expressed intrinsically within the palatal shelves of wild-type mouse embryos (Nazarali et al., 2000), where it inhibits proliferation of the palatal mesenchyme cells (Smith et al., 2009). The possibility that *Six2* plays a specific role in SP development has not been previously examined. In our present study we demonstrate, for the first time, that *Six2* is expressed intrinsically in both the palatal shelf mesenchyme and palatal shelf epithelium of wild-type mouse embryos, and further show that *Six2* mRNA and protein are upregulated in the palatal shelves of *Hoxa2*$^{-/-}$ mice. In addition, we provide evidence that *Six2* functions downstream of *Hoxa2* to regulate mesenchymal cell proliferation within the developing secondary palate.

MATERIALS AND METHODS

Hoxa2 Transgenic Mice

Hoxa2$^{+/-}$ mice were maintained by backcrossing to C57BL/6J wild-type mice and the heterozygous mice were intercrossed to generate *Hoxa2*$^{+/+}$ and *Hoxa2*$^{-/-}$ embryos for analysis in this study (Smith et al., 2009). Pregnant mice were sacrificed by isoflurane inhalation followed by cervical dislocation. Embryos were staged according to Kaufman (1992) and were considered E0 on the day the vaginal plug was found. Genotypes were confirmed by PCR analyses as described in Gendron-Maguire et al. (1993). The protocol for the use of animals was approved by the University of Saskatchewan's Animal Research Ethics Board and adhered to Canadian Council on Animal Care guidelines for humane animal use.

Immunohistochemistry

Embryos were harvested from timed-pregnant mice and the heads were fixed with 4% paraformaldehyde in phosphate buffered saline, pH 7.4 (PBS) for 24 h. Embryo heads were placed in 30% sucrose in PBS for at least 24 h, followed by embedding in optimal cutting temperature compound (OCT; Tissue-Tek ^{R}) and serially sectioned at 10 µm thickness. Histological sections taken anterior or posterior to the first molar tooth bud were designated as anterior and posterior palate sections, respectively, and sections taken at the plane of the first molar tooth bud were designated as middle palate sections (Welsh and O'Brien, 2009; Smith et al., 2013). Tissue sections were placed on 0.5% gelatin-coated glass slides, air-dried at room temperature for at least 2 h, rehydrated for 30 min in PBS, and blocked for 30 min at room temperature in PBS containing 4% skim milk and 0.1%

Triton X-100. Sections were then incubated overnight at 4°C with primary antibody diluted in PBS. The antibodies used were: Six2 rabbit polyclonal antibody (Proteintech ® ; 1:500 dilution), E-cadherin rat monoclonal antibody (Sigma; 1:200 dilution) and Ki-67 rat monoclonal antibody (Affymetrix eBioscience ® ; 1:100 dilution). Sections were rinsed twice for 5 min in PBS followed by incubation with secondary antibody for 1 h at room temperature (anti-IgG Alexa fluor 488 antibody, 1:200 dilution or anti-IgG Alexa fluor 594, 1:400 dilution; Molecular Probes ®). Finally, sections were rinsed twice in PBS and mounted in ProLong ® Gold antifade reagent with DAPI (Molecular Probes ®).

RNA Isolation and Reverse Transcription

Total RNA was isolated from excised palatal shelves of wild-type and *Hoxa2*$^{-/-}$ embryos at stages E12.5, E13.5, E14.5, and E15.5 using Aurum Total RNA mini kit (BioRad ®) as per the manufacturer's protocol. First-strand cDNA synthesis was performed using SuperScript reverse transcriptase (Invitrogen ®) with 1 µg of total RNA as per the manufacturer's protocol (Smith et al., 2009).

Quantitative Real Time PCR (qRT-PCR)

Gene expression analysis was performed on palatal shelf cDNA samples as described in our previous study (Thangaraj et al., 2017). Briefly, a TaqMan ® gene expression assay was used for qRT-PCR analysis of relative *Six2* mRNA expression levels. All qRT-PCR reactions were performed using 25 ng of template cDNA, TaqMan Universal Master Mix, FAM-labeled TaqMan Gene Expression assay Mm03003557_S1 for *Six2* (Applied Biosystems ®), and VIC-labeled endogenous control TaqMan assay for β *-actin* (Applied Biosystems ® assay 4352341E). *Cyclin D1* expression was quantified by SYBR Green assay using forward primer 5′-ACCCTGACACCAATCTCCTC-3′ and reverse primer 5′-AAGCGGTCCAGGTAGTTCAT-3′. All reactions were run in biological replicates of 5. Thermocycling parameters were: 2 min at 50°C, 10 min at 95°C, followed by 40 cycles of 95°C for 15 s and 60°C for 70 s. The C_T values obtained were analyzed using the 2^{-11CT} method to determine the relative expression of target genes in wild-type and *Hoxa2* null samples.

Droplet Digital PCR (ddPCR)

To independently confirm the results of our qRT-PCR analyses, we also performed ddPCR gene expression analyses on palatal shelf cDNA samples, following established protocols (Hindson et al., 2013). Briefly, oil-emulsified PCR reaction mixtures containing palatal shelf cDNA were amplified in 96-well plates on a Bio-Rad Tetrad 2 Peltier Thermal Cycler under the following conditions: 95°C for 10 min then 40 cycles of 95 °C for 15 s and 60°C for 1 min (2.5°C/s ramp rate) with a final 10 min hold at 98°C. After amplification, the plates were transferred to a Bio-Rad QX 100 Droplet Reader, which aspirated oil-emulsified PCR products from each well and counted numbers of FAM-positive and VIC-positive droplets, sampling at 100 kHz. Discrimination between droplets containing amplified target (positives) from those which did not (negatives) was achieved by applying a global fluorescence amplitude threshold. Gene transcript concentrations for each palatal RNA sample were calculated using dedicated ddPCR Poisson distribution computational modeling software (Bio-Rad ®). We employed the same *Six2* and β*-actin* TaqMan assays for our ddPCR analyses as described in our qRT-PCR protocol.

Western Blot Analysis

Palatal shelves were dissected from wild-type or *Hoxa2*$^{-/-}$ embryos and homogenized in RIPA Buffer (150 mM NaCl, 10 mM Tris, 0.1%-SDS, 1% Triton X-100, 1% deoxycholate, 5 mM EDTA) supplemented with a protease inhibitor cocktail (Sigma ®) as previously described (Brown and Nazarali, 2010). Sample aliquots containing equal total protein were loaded onto 10% polyacrylamide-SDS gels. Following electrophoresis, the proteins were transferred to Immunoblot PVDF membranes (Bio-Rad ®). The membranes were blocked overnight at 4°C in PBS containing 4% skim milk, followed by incubation for 1 h at room temperature with rabbit polyclonal Six2 primary antibody (Proteintech ® ; diluted 1:2,000 in PBS containing 4% skim milk). This was followed by four 15 min washes in PBST (PBS containing 0.08% Tween-20) and incubation for 1 h at room temperature with horseradish peroxidase-conjugated anti-rabbit secondary antibody (Bio-Rad ® ; diluted 1:3,000 in PBS containing 4% skim milk). After four 15 min washes in PBST, the membranes were incubated with Clarity ® Western ECL substrate (Bio-Rad ®) and the signal detected using a SYNGENE ® image analyzer. As a control for equal protein loading, the membranes were subsequently washed overnight at 4°C in PBS, followed by incubation with anti-β-tubulin (Developmental Studies Hybridoma Bank) at 1:2,000 dilution for 1 h at room temperature. Subsequently, membranes were washed with PBST, incubated with anti-mouse IgG horseradish peroxidase conjugate (Bio-Rad ® ; 1:2,000 dilution), and processed for chemiluminescence protein detection as described above. After imaging, semi-quantitative densitometry was performed using AlphaView ® software to generate an integrated density value for each Six2 protein band, which was normalized to the β-tubulin density value from the same sample. Four separate Western blots, each having both wild-type and *Hoxa2*$^{-/-}$ samples from E12.5, E13.5, E14.5, E15.5 palatal shelves, were performed. For each blot, the normalized Six2 expression values in the various samples (wild-type and *Hoxa2*$^{-/-}$ palates at E12.5, E13.5, E14.5, E15.5 stages) were compared to the value of the E12.5 wild-type sample on the same blot, which was arbitrarily assigned a relative expression level of

1. A total of four blots (n = 4) were analyzed using two-way ANOVA to compare Six2 protein expression in wild-type and *Hoxa2*$^{-/-}$ samples.

Culture of Mouse Embryonic Palate Mesenchymal (MEPM) Cells

Primary cultures of MEPM cells were established as previously described (Iwata et al., 2012; Iyyanar and Nazarali, 2017). Briefly, palatal shelves from E13.5 embryos were aseptically micro-dissected and placed in Hank's balanced salt solution. The palatal shelves were then incubated with 0.25% trypsin/EDTA in Ca^{+}/Mg^{++}-free PBS for 20 min at 37°C, briefly triturated,

and passed through a 70 µm cell strainer (BD Falcon ®) to generate a dissociated mesenchymal cell suspension. Trypsin action was terminated by adding complete DMEM/F-12 medium (Dulbecco's Modified Eagle's Medium/Ham's medium F12 [1:1] supplemented with 10% fetal bovine serum, 1% antibiotic/antimycotic solution [Sigma ®], and L-glutamate) to the cell suspension. The cells were plated on poly-D-lysine coated plates and cultured at 37°C in 5% CO_2 incubator.

siRNA Treatment and Cell Proliferation Analysis

A pre-designed *Six2* siRNA (Invitrogen ® Silencer Select assay s73795) and a negative control siRNA (Invitrogen ®) were utilized. MEPM cells (5×10^3) were plated in a 96-well plate until they reached 60–80% confluency. Aliquots of 50 nM siRNA were mixed with Lipofectamine 3000 (Invitrogen ®) according to the manufacturer's protocol. The siRNA-Lipofectamine complex (10 µl) was added to each well of MEPM cells containing 100 µl of serum free medium. Following incubation at 37°C for 12 h, the transfection medium was replaced with fresh medium. MEPM cells were analyzed for cellular DNA content after 48 h from the time of transfection using the CyQUANT NF cell proliferation assay kit (Life Technologies ®) following the manufacturer's protocol. Briefly, the transfected MEPM cells were incubated with 1X dye binding solution at 37°C for 45 min in the dark. Fluorescence was measured with a BioTek ® microplate reader at 485 nm excitation and 530 nm emission wavelengths.

Cell Density Determination

Following IHC staining of histological sections, the number of Ki-67 positive mesenchymal cells in the palatal shelf were counted manually using Image J software and this number was divided by the total cross-sectional area (mm^2) of the palatal mesenchyme. Additionally, the numbers of Ki-67 positive mesenchyme cells in the nasal vs. oral halves of the sectioned palatal shelves were counted and divided by their respective areas (mm^2); $n = 4$.

Statistical Analyses

All statistical analyses and graph construction were performed using GraphPad ® Prism 5.0 software. The Western blot, gene expression, and cell count data were evaluated using two-way analysis of variance (ANOVA) followed by Bonferroni *post-hoc* tests.

RESULTS

Six2 mRNA and Protein Are Expressed in the Developing Palate and Upregulated in *Hoxa2*$^{-/-}$ Mice

Our qRT-PCR analyses revealed that *Six2* mRNA is expressed in the developing palatal shelves of wild-type mouse embryos from E12.5 to E15.5, with highest expression at E12.5 and E13.5 (**Figure 1A**). The palatal shelves of *Hoxa2*$^{-/-}$ null embryos showed a significant upregulation of *Six2* mRNA levels relative to wild-type palates at stages E12.5 to E14.5 (**Figure 1A**).

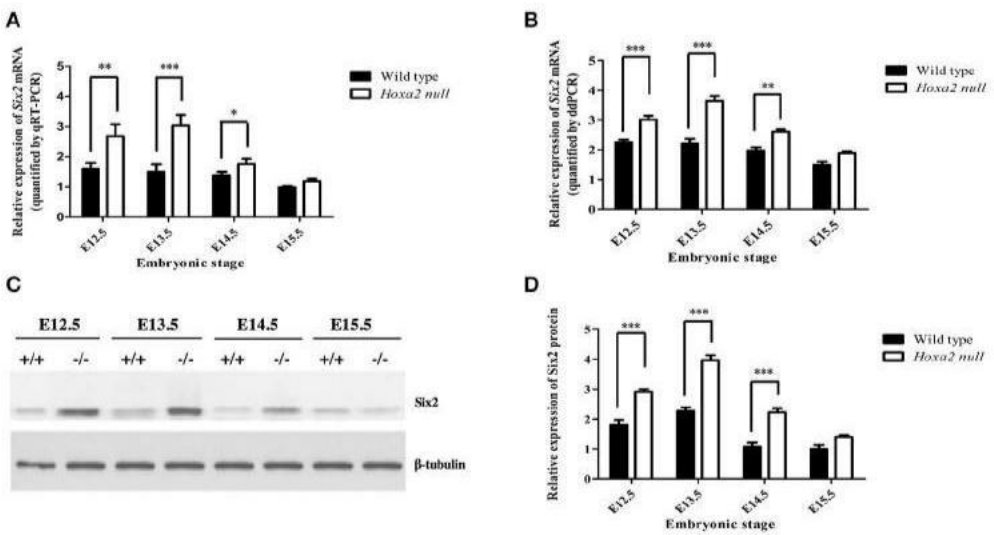

FIGURE 1 | Temporal changes in *Six2* mRNA **(A,B)** and Six2 protein **(C,D)** levels in the palatal shelves of wild-type and *Hoxa2*$^{-/-}$ mouse embryos at developmental stages E12.5-E15.5. **(A)** qRT-PCR analysis of relative levels of *Six2* mRNA expression in the palatal shelves of wild-type and *Hoxa2*$^{-/-}$ mouse embryos at developmental stages E12.5-E15.5. The *Six2* mRNA expression values are normalized against expression levels of the β *-actin* reference gene ($n = 5$ biological replicates). Note that *Six2* mRNA levels were significantly higher in *Hoxa2*$^{-/-}$ palatal shelves compared to wild-type from stages E12.5 to E14.5. **(B)** Droplet digital PCR (ddPCR) quantification of relative *Six2* mRNA levels in palatal shelves of wild-type and *Hoxa2*$^{-/-}$ embryos at stages E12.5–E15.5 ($n = 5$ biological replicates). Western blots **(C)** and corresponding densitometric measurements **(D)** of temporal changes in Six2 protein levels in wild-type and *Hoxa2*$^{-/-}$ palatal shelves during palatogenesis ($n = 4$ biological replicates). Note that Six2 protein is significantly upregulated in palatal shelves of *Hoxa2*$^{-/-}$ embryos from E12.5 to E14.5. Two-way ANOVA followed by Bonferroni *post-hoc* test was performed for each analysis. Bars represent mean ± SEM. *$p < 0.05$, **$p < 0.01$, ***$p < 0.001$.

These trends were confirmed on independent biological samples using the ddPCR technique as an alternate method to quantify *Six2* gene transcript levels (**Figure 1B**). Consistent with the *Six2* mRNA expression profiles, Western blot analysis revealed that Six2 protein is present in the developing palatal shelves from E12.5 to E15.5, with peak expression at E13.5 in wild-type embryos (**Figures 1C,D**). At stages E12.5 to E14.5, Six2 protein levels were significantly higher in *Hoxa2*$^{-/-}$ palatal shelves compared to wild-type palatal shelves (**Figure 1D**). These results demonstrate that *Six2* is expressed intrinsically in the developing palate and is negatively regulated by *Hoxa2* during palatogenesis.

Six2 Protein Distribution in the Developing Secondary Palate Exhibits Temporal and Spatial Variations

We next examined the spatial distribution of Six2 protein in the developing SP. IHC analyses of mid-coronal sections of heads from wild-type mouse embryos revealed abundant Six2 protein expression in the mesenchyme of the palatal shelves from stages E12.5 to E15.5 (**Figures 2A–D**). The intensity of Six2 immunostaining in the palatal shelf mesenchyme of wild-type embryos appeared higher at earlier stages of palatogenesis (E12.5–E13.5) (**Figures 2A,B**) compared to later stages (E14.5– E15.5) (**Figures 2C,D**). At stages E12.5 and E13.5, prior to palatal shelf elevation, Six2 protein was observed throughout the palatal mesenchyme in both the prospective "nasal half " of the palatal shelf (located nearest the tongue at these pre-elevation stages) as well as in the "oral half " of the palatal shelf (located furthest from the tongue) (**Figures 2A,B**). However, by E14.5 to E15.5, after the wild-type palatal shelves have reoriented to a horizontal position above the tongue, there was a conspicuous loss of Six2 immunostaining within a layer of palatal mesenchyme located in the nasal half of the palatal shelf, immediately subjacent to the surface palatal epithelium (**Figures 2C,D**). In contrast, Six2 protein expression persisted throughout the palatal mesenchyme in the oral half of the palatal shelf in wild type embryos (**Figures 2C,D**).

The palatal shelves of *Hoxa2* null embryos, unlike those of wild-type embryos, fail to elevate and instead remain oriented vertically downward on either side of the developing tongue (**Figures 2E–H**). Within these *Hoxa2*$^{-/-}$ palatal shelves, Six2 protein expression persisted through stage E15.5 in palatal mesenchyme cells of both the nasal half of the palatal shelf (positioned nearest the tongue) as well as the oral half of the palatal shelf (located furthest from the tongue) (**Figures 2E–H**). Therefore, in comparison to wild-type embryos, the loss of *Hoxa2* function expands the spatial domain of Six2 expression within the palatal mesenchyme at stages E14.5–E15.5 (compare **Figures 2A–D** to **Figures 2E–H**).

The outer epithelial cell layer that coats the nasal and oral surfaces of the palatal shelf displayed a strikingly different pattern of Six2 protein distribution. In wild-type palatal shelves, Six2 immunostaining was prominent in the surface epithelium located on the nasal side of the palatal shelf at both pre-elevation and post-elevation stages (**Figures 2A–D**; **Figures 3A,B**). Conversely, Six2 protein was undetectable in the surface epithelium located

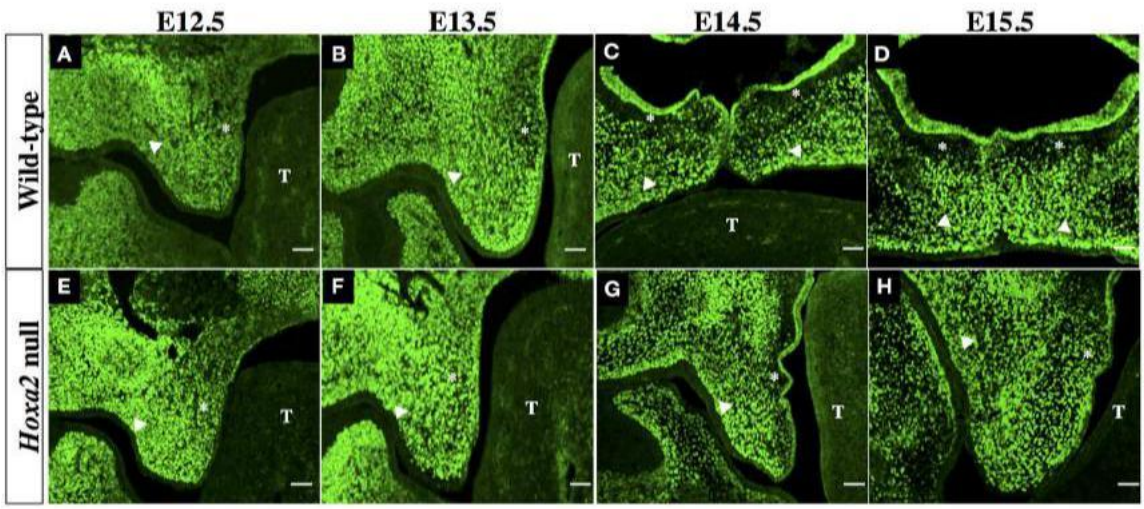

FIGURE 2 | Immunohistochemical (IHC) analysis of Six2 localization in the palatal shelves of wild-type **(A–D)** and *Hoxa2* null embryos **(E–H)** at developmental stages E12.5 **(A,E)**, E13.5 **(B,F)**, E14.5 **(C,G)**, and E15.5 **(D,H)**. Photomicrographs are mid-coronal sections, and are representative of a minimum of 5 biological replicates per stage. In each photograph, the asterisk indicates the nasal half of the palatal shelf and the arrow head indicates the oral half of the palatal shelf. T, identifies the developing tongue. Six2 immunostaining in the mesenchyme of wild-type palatal shelves appeared most intense at stages E12.5 **(A)** and E13.5 **(B),** and was uniformly distributed throughout the palatal shelf at these early stages. However, by stages E14.5 **(C)** to E15.5 **(D)** there was a pronounced decline in Six2 expression by a layer of mesenchyme cells in the nasal half of the palatal shelf lying immediately beneath the palatal epithelium. In *Hoxa2*$^{-/-}$ embryos **(E–H)**, Six2 immunostaining persisted throughout the palatal mesenchyme within the nasal half as well as the oral half of the palatal shelf at all stages from E12.5-15.5 **(E–H)**. Note that the palatal shelves of *Hoxa2* null embryos fail to elevate and remain oriented vertically alongside the tongue **(G,H)**. Scale bar, 50 µm.

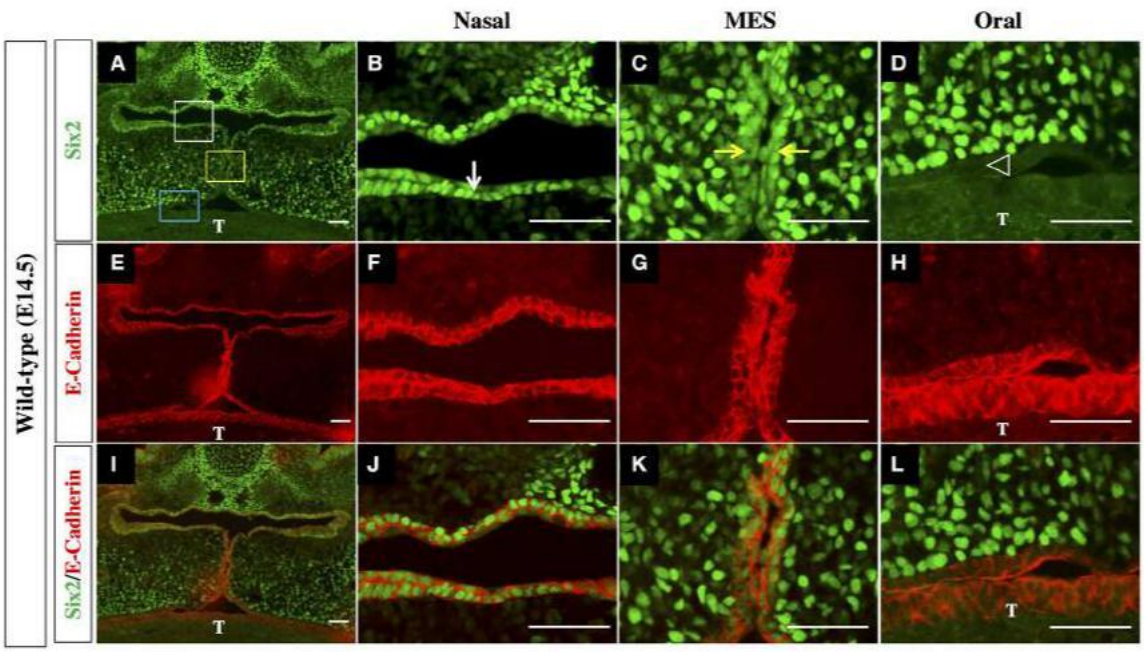

FIGURE 3 | Six2 protein is differentially expressed by epithelium on the nasal side vs. the oral side of the palatal shelf in wild-type mice. IHC staining of mid-coronal sections of wild-type palatal shelves at E14.5 for Six2 **(A–D)** and E-Cadherin **(E–H)**. Panels I-L are the Six2 immunofluorescence images overlaid with the E-Cadherin immunofluorescence images to identify cells co-expressing the two proteins. Six2 protein expression is prominent in epithelial cells located on nasal side of the palatal shelf (marked by the white rectangle in panel **(A),** and by the white arrow in panel **(B),** where it is co-expressed with the epithelial marker E-cadherin **(E,F,I,J)**. Six2 is also expressed in epithelial cells of the MES (marked by yellow rectangle in panel A, and by yellow arrows in panel **(C),** which is the point of contact between the apical tips of the two elevated palatal shelves. In contrast, Six2 protein is absent from the epithelium on the oral side of the palatal shelf [marked by the blue rectangle in panel **(A)** and by position of the arrowhead in panel **(D)**], which expresses E-cadherin alone **(E,H,I,L)**. MES, midline epithelial seam; T, tongue. Scale bars, 50 μm. The IHC staining images shown are representative of palatal sections from a minimum of 5 embryos.

on the oral side of the palatal shelf (**Figures 2A–D**, **3A,D**). The pattern of Six2 expression within the palatal epithelium was largely unaffected by loss of *Hoxa2* function. In *Hoxa2*$^{-/-}$ embryos, like wild-type embryos, Six2 expression was prominent in epithelial cells located on the nasal side of the palatal shelf (facing the tongue), with little or no Six2 protein detectable in the epithelium covering the oral side of the palatal shelf (located furthest from the tongue) (**Figures 2E–H**, **4A,B,D**). These findings were confirmed by co-staining palatal sections from wild-type (**Figure 3**) and *Hoxa2*$^{-/-}$ embryos (**Figure 4**) with an antibody for E-cadherin, a characteristic epithelial marker (**Figures 3E–L**, **4E–L**). Examination of the palatal sections at high magnification revealed that the surface epithelium on the nasal side of the palatal shelf co-expressed both Six2 and E-cadherin proteins in wild-type embryos (**Figures 3B,F,J**) as well as in *Hoxa2*$^{-/-}$ mutants (**Figures 4B,F,J**). By contrast, epithelial cells on the oral side of the palatal shelf were positive for E-cadherin alone in both wild-type (**Figures 3D,H,L**) and *Hoxa2*$^{-/-}$ embryos (**Figures 4D,H,L**).

Interestingly, in the palatal shelves of E14.5 wild-type embryos, we also observed prominent expression of Six2 together with E-cadherin within cells of the MES, the point of contact/adhesion between the apical tips of the two horizontally elevated palatal shelves (**Figures 3C,G,K**). However, Six2 immunostaining was only faintly visible in medial edge epithelium (MEE) cells located at the apical tips of the *Hoxa2*$^{-/-}$ palatal shelves, which fail to elevate and make midline contact (**Figures 4C,G,K**).

Expression of the Ki-67 Cell Proliferation Marker Is Enhanced in the *Hoxa2*$^{-/-}$ Palatal Shelves

To explore the relationships between *Six2*, *Hoxa2* and cell proliferation during SP development, we performed double immunofluorescence staining on histological sections from the anterior, middle, and posterior regions of E13.5 wild-type and *Hoxa2* null palatal shelves using Six2 antibody in combination with an antibody for Ki-67, a nuclear protein expressed exclusively in proliferating cells (**Figure 5**).

We observed that the mesenchyme of both wild-type and *Hoxa2*$^{-/-}$ palatal shelves contained large numbers of proliferating, Ki-67 positive cells (**Figures 5C,D**). Cell counts performed on the immunostained sections revealed that the number of Ki-67 positive palatal mesenchyme cells per unit area was significantly higher in *Hoxa2*$^{-/-}$ palatal shelves compared to wild-type in both the anterior and posterior regions of the palate (**Figure 6A**). This trend was also observed in the middle region of the palate, although the difference there was not statistically significant. Interestingly, in all three regions along the A-P axis

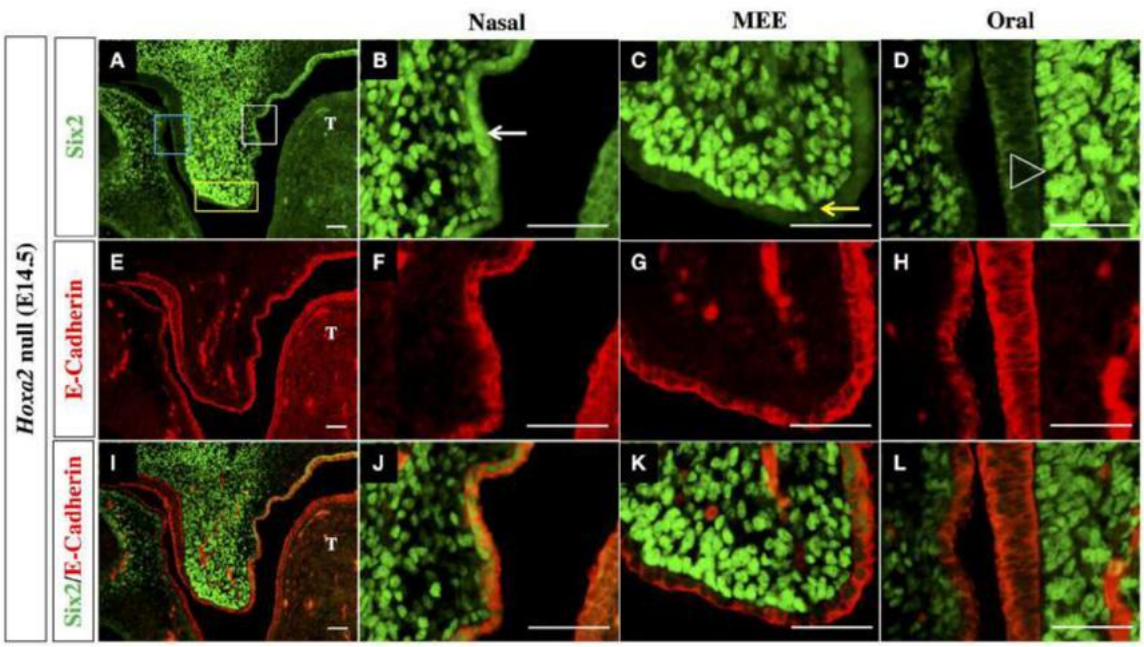

FIGURE 4 | Six2 protein is exclusively expressed in epithelium on the nasal side of the palatal shelf in *Hoxa2*$^{-/-}$ mice**.** IHC staining of mid-coronal sections of *Hoxa2* null palatal shelves at E14.5 for Six2 **(A–D)**, E-Cadherin **(E–H)**, and overlays of the Six2 and E-Cadherin immunofluorescence images **(I–L)**. Expression of Six2 protein within the palatal epithelium is restricted to epithelial cells located on the nasal side of the palatal shelf (marked by white rectangle in panel **(A)**, and by white arrow in the higher magnification image **(B)**. Six2 is absent from epithelial cells located on the oral side of the palatal shelf (marked by blue rectangle in **A**, and by position of arrowhead in higher magnification image **D**). Within *Hoxa2*$^{-/-}$ embryos, Six2 is also absent from cells of the medial edge epithelium (MEE) which is located at the apical tip of the palatal shelf (marked by yellow rectangle in **(A),** and by yellow arrow in higher magnification image **(C).** Because palatal shelves of *Hoxa2*$^{-/-}$ fail to elevate and make contact, they do not form an MES. The entire surface epithelium of *Hoxa2*$^{-/-}$ palatal shelves (on both its nasal and oral sides, as well as within the MEE) expresses E-cadherin **(E–H, I–L).** MEE, medial edge epithelium; T, tongue. Scale bars, 50 μm. The IHC staining images shown are representative of palatal sections from a minimum of 5 embryos.

of the palate (anterior, middle, and posterior), the density of proliferating Ki-67 positive mesenchyme cells was significantly higher in the nasal half of the palatal shelf compared to its oral half (**Figure 6B**). This was the case for both wild-type as well as *Hoxa2* null embryos (**Figure 6B**).

Many Six2-expressing palatal mesenchyme cells in both wild-type and *Hoxa2* null embryos were actively proliferating, as evidenced by Ki-67 co-expression (**Figures 5E, F**). Cell counts revealed that the numbers of these Six2/Ki-67 double-positive palatal mesenchyme cells per unit area were significantly higher in *Hoxa2*$^{-/-}$ mice compared to wild-type in all three regions along the A-P axis of the palate (anterior, middle, and posterior) (**Figure 6C**).

Six2 Knockdown Reduces Cell Proliferation and *Cyclin D1* Expression in MEPM Palatal Mesenchyme Cell Cultures

We next investigated whether *Six2* is a positive regulator of cell proliferation in the palatal mesenchyme and whether upregulation of *Six2* is responsible for the increased cell proliferation in *Hoxa2*$^{-/-}$ palatal mesenchyme. Primary cultures of MEPM cells were transfected with siRNA targeting *Six2* mRNA to determine the effects of *Six2* knockdown on proliferation of palatal mesenchyme cells *in vitro*. As shown in **Figure 7A**, treatment with *Six2* siRNA resulted in ∼90% reduction in *Six2* mRNA expression in MEPM cultures when compared to cultures administered either siRNA delivery vehicle alone (mock treatment) or a non-targeting negative control siRNA. Importantly, siRNA-mediated *Six2* knockdown decreased cell proliferation in both wild-type and *Hoxa2*$^{-/-}$ MEPM cultures (**Figure 7B**) and also reduced mRNA levels of *Cyclin D1*, a cell cycle regulator (**Figure 7C**). In the *Hoxa2*$^{-/-}$ MEPM cultures, *Six2* knockdown restored both cell proliferation and *Cyclin D1* expression down to levels approximating those of wild-type control MEPM cultures treated with either siRNA delivery vehicle alone or the negative control siRNA (**Figures 7B,C**).

DISCUSSION

Previous studies have established that the *Six2* gene is expressed within multiple regions and tissues of vertebrate embryos, including the developing head, pharyngeal arches, and kidneys (Oliver et al., 1995; Kutejova et al., 2005; Fogelgren et al., 2008). Furthermore, *Six2* mutations are linked to embryonic craniofacial and renal malformations (Singh et al., 1998; McBratney et al., 2003; Self et al., 2006; Fogelgren et al., 2008, 2009), which appear to result in part from reduced cell proliferation during organogenesis (Self et al.,

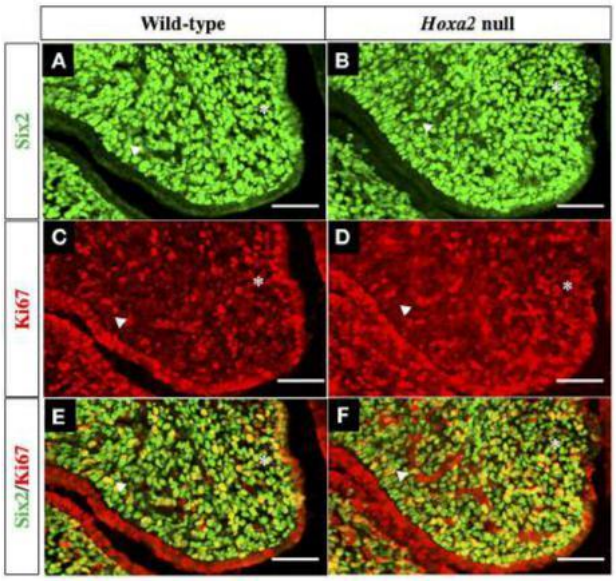

FIGURE 5 | Double IHC staining of wild-type and *Hoxa2*$^{-/-}$ palatal shelves with antibodies for Six2 as well as Ki-67, a marker of proliferating cells. Representative coronal sections from the middle region of E13.5 wild-type palatal shelves **(A,C,E)** and *Hoxa2*$^{-/-}$ palatal shelves **(B,D,F)**. Green fluorescence in panels **(A,B)** identifies Six2 expressing cells, whereas red fluorescence in panels **(C,D)** identifies all cells expressing proliferation marker Ki-67. Panels **(E,F)** are overlays of the Six2 **(A,B)** and Ki-67 **(C,D)** immunofluorescence images to identify cells that co-expressed Six2 together with Ki-67. Both wild-type **(E)** and *Hoxa2*$^{-/-}$ **(F)** palatal shelves contained numerous Six2/Ki-67 double-positive mesenchyme cells, which appear yellow in these image overlays. Six2/Ki-67 double-positive cells appear higher in the *Hoxa2*$^{-/-}$ palate. Asterisk indicates the nasal half of the palatal shelf and the arrowhead indicates the oral half of the palatal shelf. Scale bars, 50 μm. The IHC staining images shown are representative of palatal sections from a minimum of four wild-type and four *Hoxa2* null embryos.

2006; He et al., 2010). Our present study demonstrates, for the first time, that *Six2* transcripts and Six2 protein are expressed endogenously within the palatal shelves of wild-type mouse embryos throughout the period of normal SP formation. Moreover, we found that Six2 expression within the palatal primordia is both temporally modulated and spatially heterogeneous.

Our gene expression and Western blot data indicate that *Six2* mRNA and protein levels are quantitatively highest during the early stages of SP formation (E12.5–13.5), when the palatal shelves emerge as paired outgrowths of the two maxillary prominences and grow vertically downwards on either side of the developing tongue. *Six2* mRNA and protein expression persist, albeit at quantitatively lower levels, within the palatal processes during the subsequent phases of palatal shelf elevation, contact, and fusion (at E14.5–E15.5) which culminate in the separation of the oral and nasal cavities. The lateral palatine processes undergo progressive enlargement during early phases of palatogenesis, suggesting the possibility that the Six2 transcription factor may assist in promoting palatal shelf tissue growth. Supporting this possibility, we have demonstrated that siRNA-mediated knockdown of *Six2* mRNA expression in cultures of palatal shelf mesenchyme cells resulted in reduced mesenchymal cell proliferation as well as reduced mRNA levels of the cell cycle regulator, *Cyclin D1*.

In addition to the temporal variation in *Six2* expression levels during SP development, our IHC analyses revealed intriguing heterogeneity in its spatial distribution within the mesenchyme and epithelium of the growing palatal shelves. Within the palatal mesenchyme of wild-type embryos, Six2 protein was expressed uniformly throughout mesenchymal cells located in the prospective oral half of the palate, at stages both prior to and following palatal shelf elevation. By contrast, palatal shelf elevation in wild-type embryos was accompanied by a marked loss of Six2 expression by a band of palatal mesenchyme cells located in the nasal half of the palatal shelf. Interestingly, a somewhat converse pattern of Six2 distribution was observed in the surface epithelium of the palatal shelves, such that Six2 expression was prominent within epithelial cells located on the nasal side of each palatal shelf, whereas little or no Six2 protein was detectable within epithelial cells on the oral side of the palatal shelves. Several other genes have been previously shown to exhibit differential expression along the oro-nasal (O-N) axis of the developing SP. Like *Six2*, the *Fgf10* (Rice et al., 2004), *Foxf1* (Lan and Jiang, 2009; Xu et al., 2016), *Gli1* (Han et al., 2009; Lan and Jiang, 2009), *Osr2* (Lan and Jiang, 2009), and *Ptch1* (Lan and Jiang, 2009) genes are all predominantly expressed in the oral half of the palatal mesenchyme (reviewed in Bush and Jiang, 2012). Conversely, *Pax9* exhibits higher expression in mesenchyme in the nasal half of palatal shelf (Lan et al., 2004; Zhou et al., 2013). It remains to be explored whether the localized expression of *Six2* along the O-N axis in the palatal mesenchyme or the palatal epithelium either regulates or is regulated by, the domains of expression of any of these other genes. Alternatively, the loss of Six2 expression by a population of mesenchymal cells in the nasal half of the palatal shelf might be a consequence of the onset of osteogenic differentiation in this location, since bone formation during SP development is confined to the nasal half of the palatal shelves (Han et al., 2009; Baek et al., 2011). A number of transcription factors and signaling molecules also demonstrate gradations in their expression levels along the A-P (anterior-posterior) axis of the developing SP including *Msx1*, *Bmp4*, *Bmp2*, *Shh*, *Spry2*, *Fgf10*, *Fgf7*, *Shox2*, *Meox2*, *Tbx22*, and *Barx1* (reviewed in Bush and Jiang, 2012; Smith et al., 2013). However, our study revealed no significant quantitative differences in Six2 expression levels between anterior, middle and posterior regions of the palate.

Our study also examined the relationship between *Hoxa2* function within the developing palatal shelves and the regulation of *Six2* expression therein. Our gene expression and Western blot analyses revealed that *Six2* mRNA and Six2 protein levels are significantly elevated in palatal shelves of *Hoxa2*$^{-/-}$ mouse mutants, and our IHC data demonstrate that the domain of Six2 expression in *Hoxa2*-null palatal shelf mesenchyme is ectopically expanded to include the entire nasal half of the palatal shelf in addition to the oral half. These findings suggest that *Hoxa2* acts as a negative regulator of *Six2* expression within palatal shelf mesenchyme. Consistent with our observations, earlier studies by Kutejova et al. (2005, 2008) showed that the *Six2* gene is an

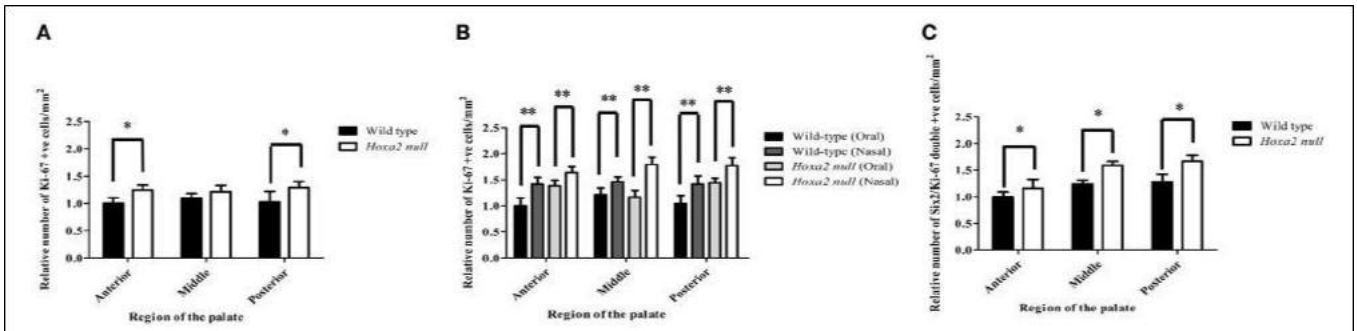

FIGURE 6 | The densities of proliferating, Ki-67 positive and Six2/Ki-67 double-positive mesenchyme cells are elevated in *Hoxa2*$^{-/-}$ palatal shelves compared to wild-type. **(A)** Relative numbers of Ki-67 positive palatal mesenchyme cells per mm^2 in coronal sections taken from anterior, middle and posterior regions of E13.5 wild-type and *Hoxa2*$^{-/-}$ palatal shelves. In the anterior and posterior regions, the density of proliferating palatal mesenchyme cells was significantly higher in *Hoxa2*$^{-/-}$ palatal shelves compared to wild-type. **(B)** In both wild-type and *Hoxa2*$^{-/-}$ palatal shelves, the density of proliferating palatal mesenchyme cells was consistently higher in the nasal half vs. the oral half of the palatal shelf. **(C)** Relative numbers of Six2-positive mesenchyme cells that co-expressed Ki-67 (i.e., were actively proliferating) in the anterior, middle and posterior regions of *Hoxa2*$^{-/-}$ palatal shelves compared to wild-type. Bar graphs represent mean ± SEM; $n = 4$ biological replicates. *$p < 0.05$, **$p < 0.01$.

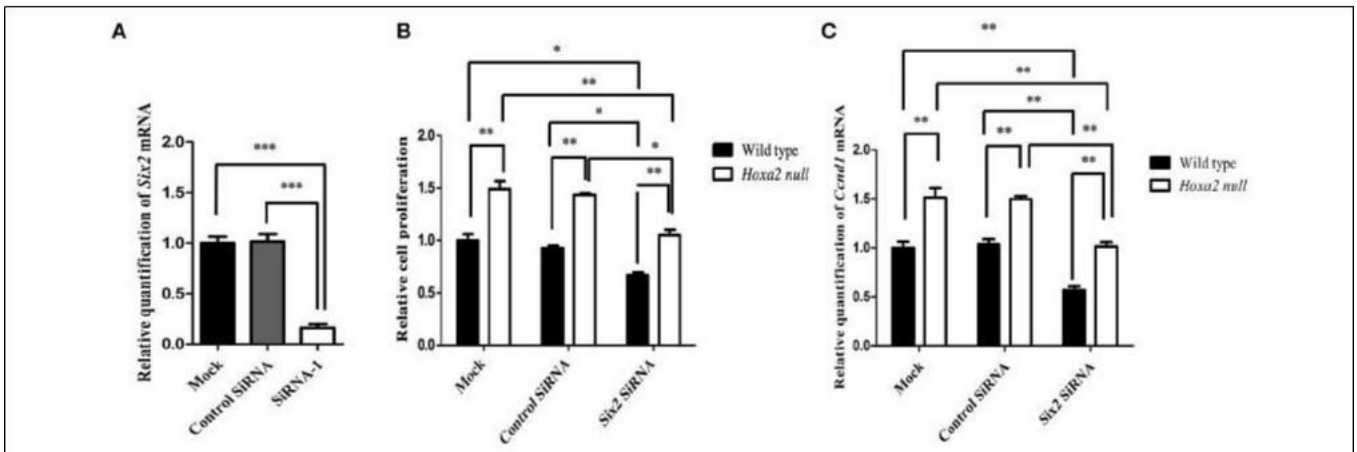

FIGURE 7 | *Six2* knockdown in wild-type and *Hoxa2*$^{-/-}$ mouse embryonic palate mesenchyme (MEPM) cultures reduces cell proliferation and *Cyclin D1* expression. **(A)** Treatment of MEPM cultures with *Six2* siRNA decreased *Six2* mRNA expression by 90% compared to cultures administered either a negative control siRNA or siRNA delivery-vehicle alone (mock treatment). **(B)** *Six2* siRNA treatment significantly decreased cell proliferation in both wild-type MEPM and *Hoxa2*$^{-/-}$ MEPM cultures and also reduced expression of *Cyclin D1* mRNA **(C)**. Note that levels of cell proliferation **(B)** and *Cyclin D1* expression **(C)** in *Hoxa2*$^{-/-}$ MEPM cultures were consistently higher than those of parallel wild-type cultures in all three treatment groups. Also, *Six2* knockdown restored cell proliferation and *Cyclin D1* expression in *Hoxa2*$^{-/-}$ MEPM cultures to levels approximating those of control wild-type MEPM cultures. Bars represent mean ± SEM; $n = 4$ biological replicates. *$p < 0.05$, **$p < 0.01$, ***$p < 0.001$.

immediate downstream target of transcription factor Hoxa2 in the second pharyngeal arch which, through negative regulation, confines Six2 expression to the more anterior first pharyngeal arch. Previous investigations in our own laboratory have shown that the *Hoxa2* gene is expressed endogenously in the epithelium and mesenchyme of the developing palatal shelves (Nazarali et al., 2000; Smith et al., 2009). However, unlike Six2, we have observed no conspicuous difference in Hoxa2 expression levels between the oral and nasal halves of the palate. Therefore, other genes in addition to *Hoxa2* must regulate *Six2* expression domains within the palatal mesenchyme of wild-type embryos to account for the greater Six2 protein abundance in the oral half of the palatal shelf vs. the nasal half. Moreover, within the outer epithelium layer of the palate, the spatial expression pattern of Six2 must be independent of Hoxa2 function, since Six2 protein remains confined to epithelial cells on the nasal side of the palatal shelf in *Hoxa2*$^{-/-}$ mutants, as it is in wild-type embryos.

The palatal shelves originate from outgrowths of the maxillary prominence derivatives of pharyngeal arch 1. However, somewhat paradoxically, *Hoxa2* expression is normally absent from tissue of the first pharyngeal arch itself, and the loss of *Hoxa2* function in *Hoxa2*$^{-/-}$ mutant mice leads to ectopic formation of arch 1 skeletal structures in place of arch 2 elements (Gendron-Maguire et al., 1993; Rijli et al., 1993). Studies from several labs have shown that *Hoxa2* null mice develop cleft palate defects *in vivo* (Gendron-Maguire et al., 1993; Rijli et al., 1993; Barrow and Capecchi, 1999). We have previously demonstrated that *Hoxa2* knockdown in whole

palatal organ culture explants resulted in failure of the palatal shelves to fuse *ex vivo* (Smith et al., 2009). We have now extended those findings by showing that the cleft palate defects in *Hoxa2*$^{-/-}$ palatal shelves are accompanied by elevated levels and spatially expanded expression of Six2 protein, as well as increased proliferation of the palatal mesenchyme cells. This suggests the possibility that *Six2* expression within the normally developing SP may positively regulate palatal mesenchyme cell proliferation and, furthermore, that the increased mesenchymal cell proliferation observed in *Hoxa2* null palatal mesenchyme may result from increased expression of endogenous *Six2*. This is supported by our observation that, *in vivo*, the numbers of palatal mesenchyme cells that co-express Six2 together with the cell proliferation marker Ki-67 are higher in *Hoxa2*$^{-/-}$ palatal shelves than wild-type palatal shelves. Moreover, we demonstrated that treatment of wild-type palate mesenchymal cell cultures with *Six2* siRNA to knockdown *Six2* expression led to significant reductions in both cell proliferation and *Cyclin D1* mRNA levels. Indeed, whereas *Hoxa2*$^{-/-}$ MEPM cultures otherwise displayed enhanced cell proliferation, *Six2* knockdown in the *Hoxa2* null cultures restored mesenchymal proliferation to wild-type levels.

From our findings, it appears likely that increased Six2 expression leading to a rise in the level of palatal mesenchyme proliferation is responsible, at least in part, for the generation of cleft palate defects in *Hoxa2*$^{-/-}$ embryos. This is consistent with studies from other laboratories that have implicated increased mesenchymal proliferation as contributing to cleft palate formation in *Wnt5a*$^{-/-}$ (He et al., 2008) and *Sprouty2*$^{-/-}$ mice (Welsh et al., 2007; Matsumura et al., 2011), as well as in embryos expressing *Fgf8* ectopically in palatal mesenchyme (Wu et al., 2015). Apparently, rates of mesenchymal cell proliferation must be tightly regulated for normal growth, morphogenesis and elevation of the palatal shelves, with either increased or decreased proliferation of palatal mesenchyme potentially leading to cleft palate defects (reviewed in Smith et al., 2013).

In summary, our study is the first to specifically investigate the expression and cell proliferation function of *Six2* in the developing SP. We have demonstrated that *Six2* mRNA and protein exhibit dynamic temporal and spatial expression profiles within the mouse SP from embryonic stages E12.5 through to E15.5. We observed that Six2 protein is present within both the mesenchyme and epithelium of the developing SP; however, its spatial distribution within these two cell populations displays an intriguing pattern of complementarity along the O-N axis of the palatal shelf. Additionally, we demonstrated that *Six2* functions downstream of *Hoxa2*, which negatively regulates *Six2* expression. Finally, we provide new evidence supporting a role for *Six2* as a positive regulator of mesenchymal cell proliferation in the developing SP.

AUTHOR CONTRIBUTIONS

AN conceived and coordinated the study, with assistance from WK. DO together with PI designed and performed experiments, analyzed the data, and prepared initial manuscript drafts. AN and WK extensively revised subsequent versions of the manuscript contents and interpretations of results. TS performed pilot experiments that laid the foundation for this investigation. SL was involved in the initial study design and critically reviewed the manuscript. SJ assisted with experimental design and data analysis. All authors approved the final manuscript version for submission.

FUNDING

This work was supported by Discovery Grant 171317-2012 to AN from the Natural Sciences and Engineering Research Council of Canada (NSERC) and, in part, by NSERC Discovery Grant 121407-2012 to WK.

ACKNOWLEDGMENTS

DO was supported in part by graduate funding from the University of Saskatchewan, College of Pharmacy and Nutrition. PI was the recipient of an Apotex Graduate Scholarship Award from the College of Pharmacy and Nutrition, University of Saskatchewan, as well as a Graduate Research Fellowship and a Saskatchewan Innovation and Opportunity Scholarship from the College of Graduate and Postdoctoral Studies, University of Saskatchewan. TS was recipient of an NSERC Postgraduate Scholarship. The authors thank L. Sobschishin and K. Schroeder for their technical expertise. This manuscript is dedicated to the memory of our esteemed colleague and mentor, Dr. Adil J. Nazarali, who was the lead investigator on this study.

REFERENCES

Baek, J. A., Lan, Y., Liu, H., Maltby, K. M., Mishina, Y., and Jiang, R. (2011). Bmpr1a signaling plays critical roles in palatal shelf growth and palatal bone formation. *Dev. Biol.* 350, 520–531. doi: 10.1016/j.ydbio.2010.12.028

Barrow, J. R., and Capecchi, M. R. (1999). Compensatory defects associated with mutations in Hoxa1 restore normal palatogenesis to Hoxa2 mutants. *Development* 126, 5011–5026.

Brown, G. D., and Nazarali, A. J. (2010). Matrix metalloproteinase-25 has a functional role in mouse secondary palate development and is a downstream target of TGF-β3. *BMC Dev. Biol.* 10:93. doi: 10.1186/1471-213X-10-93

Bush, J. O., and Jiang, R. (2012). Palatogenesis: morphogenetic and molecular mechanisms of secondary palate development. *Development* 139, 231–243. doi: 10.1242/dev.067082

Dixon, M. J., Marazita, M. L., Beaty, T. H., and Murray, J. C. (2011). Cleft lip and palate: understanding genetic and environmental influences. *Nat. Rev. Genet.* 12, 167–178. doi: 10.1038/nrg2933

Ferguson, M. W. (1988). Palate development. *Development* 103(Suppl.), 41–60. Fogelgren, B., Kuroyama, M. C., McBratney-Owen, B., Spence, A. A., Malahn,

L. E., Anawati, M. K., et al. (2008). Misexpression of Six2 is associated with heritable frontonasal dysplasia and renal hypoplasia in 3H1 Br mice. *Dev. Dyn.* 237, 1767–1779. doi: 10.1002/dvdy2.1587

Fogelgren, B., Yang, S., Sharp, I. C., Huckstep, O. J., Ma, W., Somponpun, S. J., et al. (2009). Deficiency in Six2 during prenatal development is associated with reduced nephron number, chronic renal failure, and hypertension in Br/+ adult mice. *Am. J. Physiol. Renal Physiol.* 296, F1166–F1178. doi: 10.1152/ajprenal.90550.2008

Gendron-Maguire, M., Mallo, M., Zhang, M., and Gridley, T. (1993). Hoxa-2 mutant mice exhibit homeotic transformation of skeletal elements derived from cranial neural crest. *Cell* 75, 1317–1331. doi: 10.1016/0092-8674(93)90619-2

Gritli-Linde, A. (2007). Molecular control of secondary palate development. *Dev. Biol.* 301, 309–326. doi: 10.1016/j.ydbio.2006.07.042

Gu, Y., Zhao, Y., Zhou, Y., Xie, Y., Ju, P., Long, Y., et al. (2016). Zeb1 Is a potential regulator of six2 in the proliferation, Apoptosis and migration of metanephric mesenchyme Cells. *Int. J. Mol. Sci.* 17:1283. doi: 10.3390/ijms17081283

Han, J., Mayo, J., Xu, X., Li, J., Bringas, P., Maas, R. L., et al. (2009). Indirect modulation of Shh signaling by Dlx5 affects the oral-nasal patterning of palate and rescues cleft palate in Msx1-null mice. *Development* 136, 4225–4233. doi: 10.1242/dev.036723

He, F., Xiong, W., Yu, X., Espinoza-Lewis, R., Liu, C., Gu, S., et al. (2008). Wnt5a regulates directional cell migration and cell proliferation via Ror2-mediated noncanonical pathway in mammalian palate development. *Development* 135, 3871–3879. doi: 10.1242/dev.025767

He, G., Tavella, S., Hanley, K. P., Self, M., Oliver, G., Grifone, R., et al. (2010). Inactivation of Six2 in mouse identifies a novel genetic mechanism controlling development and growth of the cranial base. *Dev. Biol.* 344, 720–730. doi: 10.1016/j.ydbio.2010.05.509

Hindson, C. M., Chevillet, J. R., Briggs, H., A, Gallichotte, E. N., Ruf, I. K., Hindson, B. J., et al. (2013). Absolute quantification by droplet digital PCR versus analog real-time PCR. *Nat. Methods* 10, 1003–1005. doi: 10.1038/nmeth.2633

Hufnagel, R. B., Zimmerman, S. L., Krueger, L. A., Bender, P. L., Ahmed, Z. M., and Saal, H. M. (2016). A new frontonasal dysplasia syndrome associated with deletion of the SIX2 gene. *Am. J. Med. Genet. Part A* 170, 487–491. doi: 10.1002/ajmg.a.37441

Iwata, J., Tung, L., Urata, M., Hacia, J. G., Pelikan, R., Suzuki, A., et al. (2012). Fibroblast growth factor 9 (FGF9)-pituitary homeobox 2 (PITX2) pathway mediates transforming growth factor β (TGFβ) signaling to regulate cell proliferation in palatal mesenchyme during mouse palatogenesis. *J. Biol. Chem.* 287, 2353–2363. doi: 10.1074/jbc.M111.280974

Iyyanar, P. P. R., and Nazarali, A. J. (2017). Hoxa2 inhibits bone morphogenetic protein signaling during osteogenic differentiation of palatal mesenchyme. *Front. Physiol.* 8:929. doi: 10.3389/fphys.2017.00929

Kaufman, M. H. (1992). *The Atlas of Mouse Development*. New York, NY: AcademicPress.

Kawakami, K., Sato,S., Ozaki, H., and Ikeda, K. (2000). Six family genes-structure and function as transcription factors and their rolesin development. *BioEssays* 22, 616–626. doi: 10.1002/1521-1878(200007)22:7<616::AID-BIES4>3.0.CO;2-R Kutejova, E., Engist, B., Mallo, M., Kanzler, B., and Bobola, N. (2005). Hoxa2

downregulates Six2 in the neural crest-derived mesenchyme. *Development* 132, 469–478. doi: 10.1242/dev.01536

Kutejova, E., Engist, B., Self, M., Oliver, G., Kirilenko, P., and Bobola, N. (2008). Six2 functions redundantly immediately downstream of Hoxa2. *Development* 135, 1463–1470. doi: 10.1242/dev.017624

Lan, Y., and Jiang, R. (2009). Sonic hedgehog signaling regulates reciprocal epithelial-mesenchymal interactions controlling palatal outgrowth. *Development* 136, 1387–1396. doi: 10.1242/dev.028167

Lan, Y., Ovitt, C. E., Cho, E.-S., Maltby, K. M., Wang, Q., and Jiang, R. (2004). Odd-skipped related 2 (Osr2) encodes a key intrinsic regulator of secondary palate growth and morphogenesis. *Development* 131, 3207–3216. doi: 10.1242/dev.01175

Lv, X., Mao, Z., Lyu, Z., Zhang, P., Zhan, A., Wang, J., et al. (2014). miR181c promotes apoptosis and suppresses proliferation of metanephric mesenchyme cells by targeting Six2 *in vitro*. *Cell Biochem. Funct.* 32, 571–579. doi: 10.1002/cbf.3052

Lyu, Z., Mao, Z., Wang, H., Fang, Y., Chen, T., Wan, Q., et al. (2013). MiR-181b targets Six2 and inhibits the proliferation of metanephric mesenchymal cells *in vitro*. *Biochem. Biophys. Res. Commun.* 440, 495–501. doi: 10.1016/j.bbrc.2013.09.059

Matsumura, K., Taketomi, T., Yoshizaki, K., Arai, S., Sanui, T., Yoshiga, D., et al. (2011). Sprouty2 controls proliferation of palate mesenchymal cells via fibroblast growth factor signaling. *Biochem. Biophys. Res. Commun.* 404, 1076–1082. doi: 10.1016/j.bbrc.2010.12.116

McBratney, B. M., Margaryan, E., Ma, W., Urban, Z., and Lozanoff, S. (2003). Frontonasal dysplasia in 3H1 Br/Br mice. *Anat. Rec. A Discov. Mol. Cell. Evol. Biol.* 271, 291–302. doi: 10.1002/ar.a.10034

Nazarali, A., Puthucode, R., Leung, V., Wolf, L., Hao, Z., and Yeung, J. (2000). Temporal and spatial expression of Hoxa-2 during murine palatogenesis. *Cell. Mol. Neurobiol.* 20, 269–290. doi: 10.1023/A:10070060 24407

Oliver, G., Wehr, R., Jenkins, N. A., Copeland, N. G., Cheyette, B. N., Hartenstein, V., et al. (1995). Homeobox genes and connective tissue patterning. *Development* 121, 693–705.

Rice, R., Spencer-dene, B., Connor, E. C., Gritli-linde, A., McMahon, A. P., Dickson, C., et al. (2004). Disruption of Fgf10 / Fgfr2b -coordinated epithelial-mesenchymal interactions causes cleft palate. *J. Clin. Invest.* 113, 1692–1700. doi: 10.1172/JCI20384

Rijli, F. M., Mark, M., Lakkaraju, S., Dierich, A., Dollé, P., Chambon, P., et al. (1993). A homeotic transformation is generated in the rostra1 branchial region of the head by disruption of Hoxa-2, which acts as a selector gene. *Cell* 75, 1333–1349. doi: 10.1016/0092-8674(93) 90620-6

Self, M., Lagutin, O. V., Bowling, B., Hendrix, J., Cai, Y., Dressler, G. R., et al. (2006). Six2 is required for suppression of nephrogenesis and progenitor renewal in the developing kidney. *EMBO J.* 25, 5214–5228. doi: 10.1038/sj.emboj.7601381

Singh, G. D., Johnston, J., Ma, W., and Lozanoff, S. (1998). Cleft palate formation in fetal Br mice with midfacial retrusion: tenascin, fibronectin, laminin, and type IV collagen immunolocalization. *Cleft Palate-Craniofacial J.* 35, 65–76. doi: 10.1597/1545-1569(1998)035<0065:CPFIFB>2.3.CO;2

Smith, T. M., Lozanoff, S., Iyyanar, P. P., and Nazarali, A. J. (2013). Molecular signaling along the anterior-posterior axis of early palate development. *Front. Physiol.* 3:488. doi: 10.3389/fphys.2012.00488

Smith, T. M., Wang, X., Zhang, W., Kulyk, W., and Nazarali, A. J. (2009). Hoxa2 plays a direct role in murine palate development. *Dev. Dyn.* 238, 2364–2373. doi: 10.1002/dvdy.22040

Thangaraj, M. P., Furber, K. L., Gan, J. K., Ji, S., Sobchishin, L., Doucette, J. R., et al. (2017). RNA binding protein Quaking stabilizes Sirt2 mRNA during oligodendroglial differentiation. *J. Biol. Chem.* 292, 5166–5182. doi: 10.1074/jbc.M117.775544

Vanderas, A. P. (1987). Incidence of cleft lip, cleft palate, and cleft lip and palate among races: a review. *Cleft Palate J.* 24, 216–225.

Wang, C. A., Drasin, D., Pham, C., Jedlicka, P., Zaberezhnyy, V., Guney, M., et al. (2014). Homeoprotein Six2 promotes breast cancer metastasis via transcriptional and epigenetic control of E-cadherin expression. *Cancer Res.* 74, 7357–7370. doi: 10.1158/0008-5472.CAN-14-0666

Welsh, I. C., and O'Brien, T. P. (2009). Signaling integration in the rugae growth zone directs sequential SHH signaling center formation during the rostral outgrowth of the palate. *Dev. Biol.* 336, 53–67. doi: 10.1016/j.ydbio.2009. 09.028

Welsh, I. C., Hagge-Greenberg, A., and O'Brien, T. P. (2007). A dosage-dependent role for Spry2 in growth and patterning during palate development. *Mech. Dev.* 124, 746–761. doi: 10.1016/j.mod.2007.06.007

Wu, W., Gu, S., Sun, C., He, W., Xie, X., Li, X., et al. (2015). Altered FGF signaling pathways impair cell proliferation and elevation of palate shelves. *PLoS ONE* 10, 1–17. doi: 10.1371/journal.pone.0136951

Xu, J., Liu, H., Lan, Y., Aronow, B. J., Kalinichenko, V. V., and Jiang, R. (2016). A Shh-Foxf-Fgf18-Shh molecular circuit regulating palate development. *PLoS Genet.* 12:e1005769. doi: 10.1371/journal.pgen.1005769

Zhou, J., Gao, Y., Lan, Y., Jia, S., and Jiang, R. (2013). Pax9 regulates a molecular network involving Bmp4, Fgf10, Shh signaling and the Osr2 transcription factor to control palate morphogenesis. *Development* 140, 4709–4718. doi: 10.1242/dev.099028

Conflict of Interest Statement: The authors declare that the research was conducted in the absence of any commercial or financial relationships that could be construed as a potential conflict of interest.

frontiers in PHYSIOLOGY
published: 07 January 2013
doi: 10.3389/fphys.2012.00488

REVIEW ARTICLE

Molecular signaling along the anterior–posterior axis of early palate development

Tara M. Smith[1], Scott Lozanoff[2], Paul P. Iyyanar [1] and Adil J. Nazarali [1]*

[1] *Laboratory of Molecular Cell Biology, College of Pharmacy and Nutrition, University of Saskatchewan, Saskatoon, SK, Canada*
[2] *Department of Anatomy, Biochemistry and Physiology, University of Hawaii School of Medicine, Honolulu, HI, USA*

Edited by:
Daniel Graf, University of Zurich, Switzerland

Reviewed by:
Daniel Graf, University of Zurich, Switzerland
*Claire A. Canning, A*STAR Agency for Science Technology and Research, Singapore*
Carolina Parada, University of Southern California, USA

****Correspondence:***
Adil J. Nazarali, Laboratory of Molecular Cell Biology, College of Pharmacy and Nutrition, University of Saskatchewan, 116 Thorvaldson Building, 110 Science Place, Saskatoon, SK S7N 5C9, Canada. e-mail: aj.nazarali@usask.ca

Cleft palate is a common congenital birth defect in humans. In mammals, the palatal tissue can be distinguished into anterior bony hard palate and posterior muscular soft palate that have specialized functions in occlusion, speech or swallowing. Regulation of palate development appears to be the result of distinct signaling and genetic networks in the anterior and posterior regions of the palate. Development and maintenance of expression of these region-specific genes is crucial for normal palate development. Numerous transcription factors and signaling pathways are now recognized as either anterior- (e.g., *Msx1*, *Bmp4*, *Bmp2*, *Shh*, *Spry2*, *Fgf10*, *Fgf7*, *and Shox2*) or posterior-specific (e.g., *Meox2*, *Tbx22*, *and Barx1*). Localized expression and function clearly highlight the importance of regional patterning and differentiation within the palate at the molecular level. Here, we review how these molecular pathways and networks regulate the anterior–posterior patterning and development of secondary palate. We hypothesize that the anterior palate acts as a signaling center in setting up development of the secondary palate.

Keywords: anterior–posterior axis, secondary palate, development, signaling, migration, growth factors

INTRODUCTION

Cleft palate is one of the most common congenital birth defects in humans, occurring with a frequency of 1:700 to 1:1000 live births (Gorlin et al., 2001). A cleft secondary palate can occur as an iso-lated birth defect (non-syndromic), in conjunction with a cleft lip, or as a part of another syndrome. Both genetic and environ-mental factors play roles in the development of cleft palate (Dixon et al., 2011).

During mammalian embryogenesis, the development of the secondary palate is regulated by a number of complex networks of growth factors and transcription factors. These molecular networks and pathways work together to tightly regulate criti-cal cellular processes in the palate including cell proliferation, apoptosis, migration, and epithelial-mesenchymal transdifferen-tiation. The secondary palate originates from first branchial arch neural-crest derived mesenchymal cells covered by a multi-layer sheet of cells derived from the facial ectoderm (Noden, 1983). In the mouse, bilateral palate shelves first develop as outgrowths from the maxillary processes at embryonic day 11.5 (E11.5). The shelves then grow vertically down either side of the tongue until E14.0 (Ferguson, 1988), after which the shelves undergo a rapid elevation to become horizontally oriented toward one another above the tongue. Growth of the stomodeum as well as jaw joint activity and neuromuscular function make it possible for the embryo to have mouth-opening reflexes. These movements allow the tongue to flatten and depress, and the downward positioned palate shelves to reorient (Humphrey, 1969; Diewert, 1980). A number of changes occur within the palate shelves to facilitate the rapid movement of the shelves from a vertical to a horizontal position starting at the anterior end and proceeding posteriorly, however, a clear understanding of how elevation occurs has yet to be achieved. Ultimately, the elevated palatal shelves then grow toward one another until the medial edge epithelium from each shelf contacts to form the midline epithelial seam (MES) at E14.5. In addition to growth of the palate shelves, a change in the relative dimensions of the head (vertical dimensions of the head increase while the lateral maxillary width remains constant) allows the palate shelves to contact one another at the midline (Diewert, 1978, 1983). Epithelial cells from opposing palate shelves adhere to one another through glycoproteins on their surface (Greene and Kochhar, 1974; Pratt and Hassell, 1975; Souchon, 1975; Greene and Pratt, 1977) as well as through desmosomes (De Angelis and Nalbandian, 1968; Morgan and Pratt, 1977). Contact and subsequent fusion begins in the anterior mid-palate regions and proceeds in both the anterior and posterior directions like a zipper (Morgan and Pratt, 1977; Ferguson, 1988). The MES then undergoes a rapid degradation to form a secondary palate with complete mesenchymal confluence (Ferguson, 1988; Berkovitz et al., 2009). Numerous mechanisms for the degradation of the MES have been proposed, including epithelial apoptosis (Pourtois, 1966; Saunders, 1966; Farbman, 1968; Shuler, 1995; Martínez-Álvarez et al., 2000a; Xu et al., 2006), migration (Carette and Ferguson, 1992; Shuler et al., 1992; Martínez-Álvarez et al., 2000a), and epithelial-mesenchymal transformation (Fitchett and Hay, 1989; Griffith and Hay, 1992; Shuler et al., 1992; Kaartinen et al., 1995; Proetzel et al., 1995; Sun et al., 1998; Cui et al., 2005). Epithelial-mesenchymal transformation has been ruled out based on fate-maps (Vaziri Sani et al., 2005), but this theory is still

unsettled. Mesenchymal confluence signals the end of palatoge-nesis at E15.5 (Ferguson, 1988). Finally, the anterior secondary palate fuses to the primary palate and the dorsal portions of the secondary palate fuse with the nasal septum marking the comple-tion of proper palatal development. Distinct pathways/networks regulate development at each stage of palatogenesis, with defects at any stage capable of resulting in cleft palate. In addition to problems with development of the palate proper, defects in the development of other craniofacial elements including the tongue and mandible can result in a cleft palate (Ferguson, 1987).

Analysis of the literature on regionally expressed genes can be difficult since a standardized method of determining the anterior, medial, and posterior regions of the palate is not in place. Many authors fail to indicate how they define the region of the palate that they are examining making comparison difficult between articles. It is important for the field to adopt a standard con-vention for defining the anterior, medial, and posterior palate to ensure that these comparisons can be made. In the past, the anterior and posterior have been described in a number of ways. We propose that the convention can be followed such that the tissue anterior or posterior to the first molar tooth bud be con-sidered the anterior or posterior palate, respectively. The medial palate would be considered palate tissue in the plane of the molar tooth bud (**Figure 1**). The rationale is that the first formed palatal rugae (R1) demarcates the expression boundary of anterior (e.g., *Msx1, Shox2, and Fgf10*) and posterior (e.g., *Meox2, Tbx22*) spe-cific genes (Zhang et al., 2002; Yu et al., 2005; Li and Ding, 2007; Pantalacci et al., 2008; Welsh and O'Brien, 2009; Bush and Jiang, 2012). The first molar tooth bud lies immediately ante-rior to the R1, which forms the posterior boundary for anterior *Fgf10* expression (Welsh et al., 2007). On the structural basis, the anterior two-thirds of the palate is the future hard palate. During rostral extension of the anterior palate from E11.5 to E14.5, the spatial relationship between R1 and the developing molar tooth bud remains unchanged (Welsh et al., 2007; Welsh and O'Brien, 2009), making the molar tooth bud an ideal convention to delineate the two structurally distinct regions of palate.

This review will provide an in depth look at the molecular processes involved in regulating the patterning and early devel-opment of the secondary palate. Genes known to be involved in the fusion of the palate processes will not be discussed in detail; see Nawshad (2008) for a comprehensive review. The major focus here will be to summarize both current information and devel-oping new connections between the factors and genes involved in specifying and maintaining the A–P axis. We hypothesize that the anterior palate acts as a signaling center for secondary palate patterning and development.

ANTERIOR-SPECIFIC GENE EXPRESSION

A large number of anterior-specific genes specifically expressed and active within the anterior palate (**Figure 2**) compared to the posterior palate highlights the importance of the anterior region during secondary palate development (Zhang et al., 2002; Rice et al., 2004; Alappat et al., 2005; Yu et al., 2005; Levi et al., 2006; Lee et al., 2007, 2008; Welsh et al., 2007; He et al., 2008; Liu et al., 2008).

Msx1 NETWORK

The first network described to play an anterior-specific role in the developing palate involves the homeobox transcription fac-tor *Msx1*. Mutations in the human *MSX1* gene have been linked

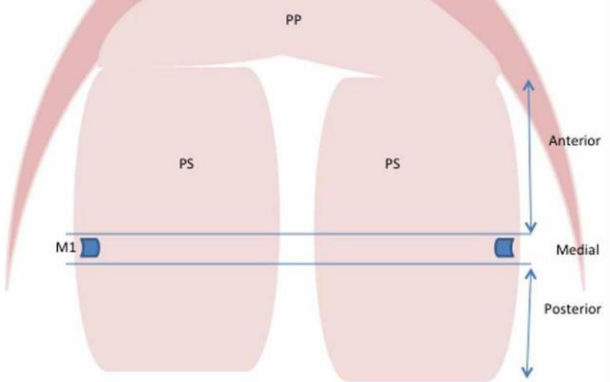

FIGURE 1 | Schematic representation for defining anterior, medial, and posterior regions of palatal shelves. Tissue anterior or posterior to first molar tooth is considered anterior or posterior palate, respectively. The palatal tissue in the region of first molar tooth bud is considered medial. Abbreviations: PP, primary palate; PS, palatal shelves; M1, first molar tooth bud.

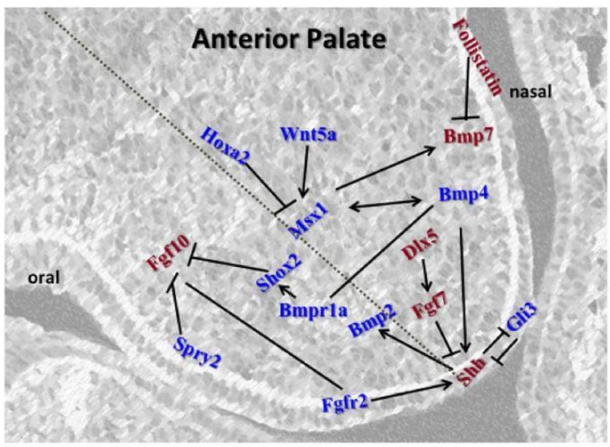

FIGURE 2 | Schematic representation of the key regulators in the anterior palate. *Msx1* and *Bmp4* function in an autoregulatory loop mechanism in the mesenchyme. *Bmp4* induces *Shh* expression in the epithelium which signals backs to the mesenchyme to positively regulate *Bmp2* to enhance cell proliferation in the mesenchyme. *Msx1* expression is controlled by Hoxa2 in early palatal development. *Fgfs* and their receptors are regulated by *Spry*2 for proper balance of proliferation and prevention of premature apoptosis in the epithelium. *Fgf10* induces *Shh* whereas *Fgf* 7 acts as an antagonist. *Msx1* also maintains proliferation by inducing *Bmp*7 in the mesenchyme along the nasal epithelium. Genes represented in red are restricted to either oral or nasal side of the palate, whereas those represented in blue are present across the shelf.

to isolated non-syndromic cleft palate (Vastardis et al., 1996; Lidral et al., 1998; Van den Boogaard et al., 2000; Suzuki et al., 2004; Tongkobpetch et al., 2006; Otero et al., 2007). *Msx1*-deficient mice display neonatal lethality due to a wide open cleft secondary palate (Satokata and Maas, 1994; Houzelstein et al., 1997). Expression of *Msx*1 is localized exclusively to the anterior mesenchyme during the early stages of palate development from E12.5 to E13.5 (Zhang et al., 2002; Alappat et al., 2003) and functions through regulating the expression of *Bmp4*, *Shh*, and *Bmp2* at E12.5–E13.5 in the anterior palate (Zhang et al., 2002). *Msx1* appears to regulate *Bmp4* expression in the ante-rior mesenchyme, which subsequently signals to the epithelium and regulates *Shh* expression; from the epithelium *Shh* then sig-nals back to the mesenchyme and regulates *Bmp2* expression (Zhang et al., 2002). In addition to this linear network, *Bmp4* is involved in a reciprocal regulatory cycle controlling the expres-sion of *Msx1*. The main function of *Msx1* and its subsequent network appears to be regulation of cell proliferation within the anterior mesenchyme (Zhang et al., 2002). It has been demon-strated that although exogenous BMP is capable of inducing *Msx1* expression and increasing cell proliferation in the anterior palate it has no effect on the posterior palate (Zhang et al., 2002; Hilliard et al., 2005). Since first reported, numerous studies have investigated the expression and function of the genes in this net-work. All studies performed to date (see below) confirm that this network is important in anterior mesenchyme proliferation; how-ever, the regulation of each of these genes is far more complex than suggested originally.

The regulation of *Msx*1 expression has been linked to many other factors in the palate. *Msx1* was shown to be downstream of the *Foxe1* gene with *Foxe1* null mice having very low expression of palatal *Msx1* and *Tgf*-β*3* at E14 (Venza et al., 2011). Loss of the Fgf antagonist *Spry2* in the piebald deletion animal model (discussed in more details in the section "Fgf Signaling Pathway") results in increased *Msx1* expression as well as a posterior expansion of its expression border at E13.5 and E14.5; this increased expres-sion leads to an increase in proliferation within the palate (Welsh et al., 2007). *Msx1* is Fgf-responsive in other regions of cranio-facial development (Bei and Maas, 1998; Alappat et al., 2003), although *Fgf10* null palates do not exhibit altered *Msx1* expres-sion (Alappat et al., 2005). These data suggest other Fgfs may be acting in the palate to regulate *Msx1* expression (other pos-sible explanations are discussed in subsequent sections below). *Fgf9* may play an active role in palate development (Colvin et al., 1999, 2001) and loss of *Spry*2 may relieve the antagonism of *Fgf9* resulting in the observed upregulated and expanded *Msx1* expres-sion (Welsh et al., 2007). Recently, *Fgf9* was shown to regulate cell proliferation in palatal mesenchyme via *Pitx2*-dependent induc-tion of cyclin D1 and cyclin D3 in the *Tgfbr2*$^{fl/fl}$; *Wnt1-Cre* mice (Iwata et al., 2012a), however, expression of *Msx1* was not exam-ined in this study. *Fgf7* is expressed within the palate mesenchyme (Rice et al., 2004) and may also be involved in regulating *Msx1* expression and affected by loss of *Spry2*, although this has not been investigated.

Hoxa2, another homeobox gene, has recently been shown to regulate palatal *Msx1* expression (Smith et al., 2009). *Hoxa*2 null mice exhibit an 81% penetrance of cleft palate (Gendron-Maguire et al., 1993; Rijli et al., 1993; Barrow and Capecchi, 1999), which appears to result from increased cell proliferation where expres-sion levels of both *Msx1* and its known down-stream target *Bmp4* are up-regulated during the early stages of palate development (Smith et al., 2009). Genetic studies in humans have also linked mutations in the *HOXA2* gene with a cleft secondary palate (Alasti et al., 2008). *Hoxa*2 acts upstream of *Msx1* in the second branchial arch neural crest cells (Santagati et al., 2005). This new gene tar-get provides additional insight, as *Hoxa2* is known to be absent from the migrating first branchial arch from which the palate shelves arise (Prince and Lumsden, 1994). Clearly expression in the branchial arches prior to overt palate growth is not a pre-requisite of genes that are important in regulating palatogenesis. Whether *Hoxa*2 and Fgfs represent distinct regulatory network of *Msx1* or are part of the same regulatory network remains to be determined. Strict regulation of *Msx1* expression in the palate is probably due to its importance in regulating proliferation in the anterior palate.

The transcriptional activity of *Msx1* can also be altered by other proteins in the palate. *Msx1* undergoes post-translation modification by sumoylation *in vivo* in a region of the protein that is responsible for regulating *Msx1* interactions with other proteins (Gupta and Bei, 2006). Thus, sumoylation of *Msx1* may help facilitate its ability to interact with other transcription fac-tors and therefore control its ability to regulate the expression of other genes. Haploinsufficiency of the SUMO1 gene has been reported to lead to cleft palate through altering the sumoyla-tion status of various proteins (*Eya1*, *Pax9*, and *Msx1*) in the palate (Alkuraya et al., 2006). However, it has also been sug-gested that SUMO1 expression is not necessary for normal mouse development (Zhang et al., 2008). Debates also exist on whether polymorphisms of the SUMO1 gene in humans are linked to cleft palate (Song et al., 2008; Almeida de Assis et al., 2011). What role SUMO1 plays in palate development is therefore unclear at this time.

In addition to regulating *Bmp4* and *Bmp2*, *Msx1* regulates the expression of Bmp7 and its antagonist Follistatin (Levi et al., 2006). Loss of *Msx1* leads to a decrease in the anterior palatal expression of *Bmp7* but an increase in its expression in the pos-terior palate (Levi et al., 2006). The Bmp antagonist Follistatin is expressed throughout the palatal epithelium; in the anterior palate it is primarily expressed in a restricted dorsal domain that does not overlap the regions of *Bmp4* and *Bmp2* expression (Levi et al., 2006). *Msx1* null mice also exhibit a decrease in the level of anterior palatal Follistatin expression (Levi et al., 2006). Together, these data highlight the important role of *Msx*1 in the regula-tion of the Bmp family and their antagonists in the palate, and provide another mechanism by which it may regulate the level of proliferation in the anterior palate.

*Dlx*5 is expressed in the anterior mesenchyme of the palate and mutations in the *Dlx5* gene result in a cleft secondary palate (Levi et al., 2006; Han et al., 2009). Furthermore, loss of the transcription factor MEF2C consequently leads to loss of *Dlx*5 expression in the branchial arches resulting in a cleft palate (Verzi et al., 2007). Although *Dlx5* and *Msx1* share similar expres-sion domains it is unlikely that they are involved in regulating each others expression as *Msx1* expression is not altered in *Dlx5* null palates and vice versa (Han et al., 2009). *Dlx5/Msx1* double knockouts show a rescue of the *Msx1* null cleft palate phenotype

(Levi et al., 2006; Han et al., 2009). Loss of *Dlx5* in *Msx*1 null embryos alters the expression of *Shh*, *Bmp7*, and *Follistatin* in the palate. Bmp7 expression in these double knockouts is increased throughout the palate, while expression of Follistatin is decreased (Levi et al., 2006; Han et al., 2009). *Shh* expression is decreased in *Msx1* null palates but its domain is expanded in the double knockouts suggesting that both *Msx1* and *Dlx5* are involved in determining the area of *Shh* expression (Han et al., 2009). *Dlx5* and *Fgf7* share the same expression region in the anterior palate mesenchyme on the nasal side. *Fgf7* region of expression is lim-ited in *Dlx5* null mutants as well as in the *Msx1/Dlx5* double knockouts (Han et al., 2009). These data point toward a sys-tem where *Dlx5* regulates the expression of *Fgf7*, which in turn represses *Shh*. It has also been demonstrated that a feedback loop and cross talk exists between *Bmp7* and *Shh*, which plays a role in refining the expression domain of both genes (Han et al., 2009). Therefore, in the *Msx1/Dlx5* double knockouts the limited *Bmp7* expression allows an increase in *Shh* expression, which likely leads to the observed increase in cell proliferation and rescues the *Msx1*-induced cleft palate.

BONE MORPHOGENIC PROTEIN SIGNALING PATHWAYS

Bmp4 is known to be downstream of *Msx*1 in the palate (Zhang et al., 2002). However, similar to *Msx1*, many alternative regula-tory pathways for *Bmp4* have been described in recent years. The transcription factor *Tbx3* shows an overlapping expression pat-tern with *Bmp4* in the developing anterior palate mesenchyme (Lee et al., 2007). These two genes regulate each other's expression in the palate whereby *Tbx3* inhibits the expression of *Bmp4* while *Bmp4* induces *Tbx3* expression (Lee et al., 2007). As expected and based on the previously reported role of *Bmp4* in the palate, this regulatory loop acts by regulating the levels of cell prolifer-ation in the anterior palatal mesenchyme (Lee et al., 2007). In the limb, *Tbx3* expression is dependent on *Bmp4* (Tümpel et al., 2002) and plays an important role in maintaining normal prolif-eration in the region (Davenport et al., 2003). *Tbx3* null embryos however, do not exhibit a cleft palate (Davenport et al., 2003) and therefore the ability of *Tbx3* to regulate *Bmp4* expression and subsequently proliferation may be redundant with another regulatory mechanism in the palate.

At the onset of palate development, the transcription factor *Tp63* regulates the expression of *Bmp4* in the anterior palate. Loss of the *Tp63* gene leads to cleft palate through altering the expression of a variety of genes (including *Bmp4*) in the max-illary processes from which the palatal shelves emanate. This altered gene expression results in defects of the A–P axis as well as the onset of palate development (Thomason et al., 2008). These observations indicate regulation of gene expression during and prior to the overt growth of the palate shelves can influence palate development and patterning.

Bmp4 acts upstream of *Shh* and *Bmp2* within the palate (Zhang et al., 2002). New studies detail the importance of the *Wnt5a* sig-naling molecule in regulating the A–P axis in the palate including the expression of *Bmp4* (He et al., 2008). In the absence of *Wnt5a* signaling, *Bmp4* expression is down-regulated in the anterior palate at E13.5, while being ectopically up-regulated in the pos-terior palate (He et al., 2008). As predicted, *Shh* expression in the anterior palate and posterior palate correspondingly decreases and increases, respectively. Surprisingly, *Bmp2* expression was unaltered in the *Wnt5a* null mutants (He et al., 2008), imply-ing *Bmp2* expression in the palate is regulated by an additional mechanism. Despite a decrease in *Bmp4* and *Shh* expression, pro-liferation was increased in the anterior mesenchyme, which is contrary to what would normally be expected (He et al., 2008).

Noggin is a polypeptide that binds to members of the Bmp family preventing them from signaling. Noggin null mice show that without Noggin's repression of Bmp signaling, palate devel-opment does not proceed normally, with fusion between the palate and mandible ultimately leading to a cleft palate pheno-type. Although Noggin null mice did not have changes in the expression of *Msx1*, *Bmp4*, or *Shh* they did have reduced *Shox2* and *Bmp2* expression in the anterior palate and an ectopic exten-sion of *Bmp2* expression into the posterior region of the palate. In addition, decreased proliferation rates were seen exclusively in the anterior mesenchyme of Noggin null palate which suggests that loss of *Bmp2* in the anterior palate effects proliferation and sup-ports the theory that posterior cells are not receptive to ectopic Bmp expression (Hilliard et al., 2005; He et al., 2010).

The Bmp family plays an important role in maintaining the A–P axis of the palate shelves as well as regulating proliferation (Nie, 2005). *Bmp* ligands regulate down-stream gene expres-sion and cell processes through activation of cellular receptors. *Bmpr1a* and *Bmpr1b* are expressed in an overlapping pattern in the anterior palate. The Bmp receptor Bmpr1a is essential in the regulation of proliferation and patterning in the palate; a total loss of the *Bmpr1a* gene in all craniofacial cells leads to decreased proliferation as well as an anterior shift in the expression pat-terns of the posterior-specific genes *Pax9* and *Barx*1 (Liu et al., 2005). Conditional loss of *Bmpr1a* in the neural crest and deriva-tives (*Wnt1-Cre*; *Bmpr1a* $^{f/-}$ mice) leads to an anterior clefting of the secondary palate resulting from decreased mesenchymal pro-liferation (Li et al., 2011). The significantly reduced expression of *Msx1*, *Bmp4*, *Pax9*, and *Shox2* may be responsible for the defective cell proliferation. These results indicate that although Bmpr1b has a common expression pattern it is not able to compensate for the loss of epithelial Bmpr1a expression (Li et al., 2011). Interestingly when Bmpr1a is deleted from all craniofacial tissue the expres-sion of *Msx1* is unaltered (Liu et al., 2005). Together these data show that the role and number of Bmp receptors in the palate is complex and yet to be fully understood. This could also imply a novel role for *Bmp4* and potentially other Bmps acting through the Bmpr1a receptor in regulation of the spatial expression of posterior-specific genes.

SONIC HEDGEHOG SIGNALING

Sonic hedgehog *(Shh)* is expressed in the epithelium through-out palatogenesis (Paiva et al., 2010) and proper regulation of the *Shh* signal is crucial for normal palate development to occur. Expression is restricted to a striped pattern that corresponds to the rugae (Rice et al., 2006). Rugae develop through the thick-ening of the epithelium and condensation of the underlying mesenchyme. These rugae are suggested to act as centers that coordinate patterning within the palate implying an important role for *Shh* in the patterning of the developing palate (Rice et al.,

2004; Lin et al., 2011). The epithelial cells expressing *Shh* are not actively proliferating, whereas the mesenchymal cells underly-ing these regions are more highly proliferative than mesenchymal cells in other areas of the palate (Han et al., 2009). Loss of rugae and rugae-specific morphogens has been suggested to hamper the molecular guidance necessary to regulate the growth of the palate. For example, loss of Wnt signaling in the palate epithelium blocks the formation of the rugae and altered *Shh* expression which in turn results in abnormal extension along the A–P axis and a unique anterior only cleft palate phenotype (Lin et al., 2011). *Shh* is also a down-stream target of the *Msx1* network that regulates cell proliferation in the anterior palate (Zhang et al., 2002). Loss of the *Spry2* gene also leads to a disorganization in the expres-sion pattern of *Shh*, which ultimately leads to deformities in the rugae in the palate of these knockout animals (Welsh et al., 2007). Double null mutants of Fgf intracellular antagonists $Spry2^{-/-}$ act as Fgf gain-of-function mutant with highly disorganized palatal rugae. Similar rugae disorganization was also observed in the con-ditional deletion of *Shh* (*K14-Cre*; $Shh^{fl/fl}$ *mice*) (Economou et al., 2012). Their analyses suggests that Fgf acts as an activating factor and *Shh* acts like *Spry*, functioning as an inhibitor of Fgf signaling and of rugae development.

Gli3, a protein expressed in the epithelium and mesenchyme along the entire A–P axis of the palate, is capable of acting as both an activator and repressor of *Shh* signaling (Huang et al., 2008). In the absence of the *Shh* signal, the Gli3 protein is processed by protein kinase A allowing it to enter the nucleus and repress the expression of *Shh* target genes. Presence of the *Shh* signal pre-vents the processing of the Gli3 protein, and therefore prevents Gli3 from repressing the expression of the *Shh* target genes (Wang et al., 2000; Litingtung et al., 2002). In the limb, an antagonis-tic relationship between *Shh* and Gli3 is crucial in setting up the A–P axis. Gli3 is expressed in the anterior region of the devel-oping limb, where it represses the expression of *Shh*. dHAND is a posterior-specific protein in the limb that is also repressed by Gli3 but is a known activator of *Shh* expression. Together, this pathway sets up an A–P axis in the limb that ensures proper development (Niswander, 2003). This important interaction between Gli3 and *Shh* in the limb in combination with the expression of both genes in the palate suggests a role for Gli3 in the palate. Not surpris-ingly, *Gli3* null mice display a cleft secondary palate; however, the cleft palate phenotype was not due to changes within the palate itself, but rather due to defective growth of the tongue (Huang et al., 2008). These results demonstrate that regional differences and signaling pathways are not conserved between areas of the developing embryos. Hence, simply lining up the expression of all of the players in a pathway within the palate does not necessar-ily imply they function by a similar mechanism as described for other areas of the developing embryo.

Fgf SIGNALING PATHWAY

Mutations in numerous members of the Fgf family have been linked to cleft palate in the human population (Riley et al., 2007). The best understood Fgf-dependent pathway in the palate involves *Fgf10* and its receptor *Fgf2rb*. *Fgf10* null mice exhibit a wide open cleft palate that is due to abnormal palate shelf morphology and size, preventing the shelves from contacting at the MES (Rice et al., 2004; Alappat et al., 2005). In addi-tion, ectopic fusion of the palate shelves to the oral epithelium is observed in some animals, preventing normal shelf eleva-tion (Alappat et al., 2005). Similar to *Msx*1 expression, *Fgf10* is expressed primarily in the anterior palate mesenchyme at the early stages (E12–E13) of palatogenesis (Rice et al., 2004). The *Fgf10* ligand acts through the receptor *Fgfr2b*, which also shows an anterior-specific expression pattern in areas of epithelium adjacent to mesenchyme expressing *Fgf10* (Rice et al., 2004). *Shh* expression is down-regulated in the epithelium of both *Fgf10* and *Fgfr2b* null embryos, leading directly to a severe reduction in epithelial cell proliferation and a consequently thin epithelial layer. Mesenchymal cell proliferation also significantly decreases due to a lack of reciprocal *Shh* signaling through its receptor *Ptc*1 (Rice et al., 2004). As discussed above, *Msx*1 expression is not altered in *Fgf10* null mutants (Alappat et al., 2005), nor is *Bmp4* expression. However, the Bmp antagonist Sostdc1 does have reduced expression levels in *Fgf10* null palates (Welsh and O'Brien, 2009). Therefore the altered *Shh* expression in the *Fgf10* or *Fgfr2b* null mice may be due to the decreased antagonism on Bmp signaling or directly due to loss of Fgf signaling and not through alterations in the *Msx*1 network. Conditionally knocking out all *Fgfr*2 isoforms exclusively in the epithelium also lead to a cleft palate. Once again *Shh* expression is disordered and there is a lack of clearly defined rugae during the time palatogenesis nor-mally occurs. In this instance however, cell proliferation is only decreased within the epithelium, suggesting that *Fgfr*2 receptors must exist in mesenchymal cells, and be responsible for regulat-ing cell proliferation in these cells (Hosokawa et al., 2009). Loss of *Fgf* 10 signaling alters cellular processes including apoptosis, suggesting it plays a role in cell survival. *Fgf10* null mice exhibit premature and ectopic fusion indicating that *Fgf10* also has a role in ensuring proper fusion (Rice et al., 2004).

While *Fgf10* regulates cell proliferation within the anterior palate, ectopic exposure to *Fgf10* does not bring about a notice-able effect on the level of proliferation in the posterior palate (Yu et al., 2005), implying the down-stream effectors of *Fgf10* expression must not be present within the posterior region of the palate. This provides further evidence the anterior and pos-terior regions of the palate are distinct cell populations with very different regulatory mechanisms for the same cellular processes.

In addition to regulating proliferation, apoptosis, and fusion, *Fgf10* can also induce cell migration within the anterior palate. *Fgf10* expression is not only localized to the anterior mesenchyme but is also higher in the oral region of the anterior mesenchyme (Rice et al., 2004). *Fgf10* acts as a chemoattractant and induces the migration of anterior mesenchyme cells from the nasal to the oral side of the palate (He et al., 2008). The loss of *Fgf10* causes palate shelves to assume an abnormal shape (Alappat et al., 2005), which could in part be explained by the loss of oral cell migration.

The Fgf receptor *Fgfr1b* has also been described as having an anterior and nasal specific expression pattern within the devel-oping palate (Lee et al., 2008). As with other members of the Fgf family, its expression is linked to the regulation of prolifer-ation within the anterior palate. Expression of *Fgfr1b* is negatively regulated by the *Wnt11* signaling molecule. In return, *Fgfr1b*

negatively regulates the expression of *Wnt11* (Lee et al., 2008). At early stages (E13.5) of palate development, the balance is tilted toward *Fgfr1b* allowing the palate to undergo cell proliferation. However, as palate development proceeds (E14), the expression balance is shifted away from *Fgfr1b*. At this stage proliferation must temporarily halt in order for the individual palate shelves to fuse and form a complete palate (Lee et al., 2008). Thus, although the most obvious role for the Fgf family is in regulating the level of proliferation within the palate, the Fgf family also plays a role in regulating events such as fusion by maintaining minimal expression of certain genes until the appropriate time.

As discussed above, one specific animal model showed that loss of the Fgf antagonist *Spry2* leads to a cleft palate due to alterations in the level of cell proliferation within the palate as well as the expression profiles of numerous genes including *Msx1* (Welsh et al., 2007; Matsumura et al., 2011). *Spry2* is expressed in the epithelium and mesenchyme at consistent levels through-out palatogenesis (Matsumura et al., 2011). The animal model discussed above has a piebald deletion, which is a collection of overlapping Mb-scale chromosomal deficiencies which includes the *Spry2* gene (Welsh et al., 2007), while another is a single specific knockout of the *Spry2* gene (Matsumura et al., 2011). Earlier reports from the group that developed the animal model lacking exclusively *Spry2* indicated that animals were not shown to have a cleft palate (Shim et al., 2005; Taketomi et al., 2005), however more recent reports have shown a prevalence for cleft palate (Matsumura et al., 2011). The piebald deletion led to a high incidence of cleft palate while the targeted deletion of *Spry2* only displayed the cleft palate phenotype in approximately 20% of animals. The differences in incidence rates are likely due to other defects resulting from the Mb-scale of the piebald deletion. Both mutants showed that a loss of *Spry2* expression leads to an increase in the level of cell proliferation in the palate (Welsh et al., 2007; Matsumura et al., 2011) which could be expected since its absence relieves inhibition on Fgf signaling which has been reported to control proliferation rates (Rice et al., 2004; Alappat et al., 2005). Also seen in both mutant animal models was altered *Msx1* expression. The true knockout model showed an increase in the level of *Msx1* expression, although region specific expression was not investigated (Matsumura et al., 2011). The piebald muta-tion initiates a posterior expansion of *Msx*1 coinciding with a loss of the anterior expansion of the posterior-specific transcription factor *Tbx22*. While *Tbx22* expression fails to reach its normal anterior expression boundary, *Etv5* and *Barx1*, which are primar-ily expressed in the posterior palate, expand their domains to the anterior (Welsh et al., 2007). These results suggest antagonism of Fgfs by *Spry2* affects a number of networks in the palate lead-ing to gross changes in their expression patterns. Further analysis will be required to determine, which other factors are involved with the high rate of cleft palate in the piebald deletion mice. Although Fgf signaling is necessary for palate development, its action appears to require fine-tuning by repressors for normal palatogenesis to occur.

Shox2 NETWORK

Fgf10 expression is down-stream of the homeobox transcrip-tion factor *Shox2* (Yu et al., 2005). The *Shox2* gene is expressed exclusively in the anterior mesenchyme region of the developing secondary palate, with its highest expression occurring during the early stages of palate development. Mice deficient in the *Shox2* gene exhibit a rare form of cleft palate where the cleft only occurs in the anterior part of the secondary palate. Expression of a number of genes critical for palatogenesis such as *Jag2*, *Lhx8*, *Osr2*, *Pax9*, *Tgfb3*, and *Msx1* and its down-stream target *Bmp4* do not change in the *Shox2*$^{-/-}$ palatal shelves (Yu et al., 2005). However, expression domains of both *Fgf10* and *Fgfr2c* are altered, which corresponds with altered proliferation and apop-tosis within the anterior palate in the *Shox2* null mice (Yu et al., 2005). These data indicate altering the expression of genes only in one area of the palate can lead to clefting only in that spe-cific area. However, *Msx1* is also expressed in the very anterior region of the palatal shelves and yet in *Msx1* null mice a com-plete cleft of the secondary palate is observed (Zhang et al., 2002) as it is in the *Fgf10* $^{-/-}$ mice (Rice et al., 2004; Alappat et al., 2005). It is not known precisely why *Shox2* exhibits this unusual anterior cleft. It may be that increased *Fgf10* expres-sion is sending a signal to the posterior palate to fuse (Yu et al., 2005).

While regulation of the *Shox2* gene has been the subject of recent investigations in palate development, a complete under-standing of *Shox2* regulation remains elusive (Yu et al., 2005). Blocking of Bmp signaling with the antagonist Noggin results in a down-regulation of *Shox2* expression within the exposed anterior mesenchyme at E12.5. Exposure of palatal mesenchyme to Bmp4, Bmp2, and Shh in culture is not sufficient to induce *Shox2* expres-sion. These data suggest Bmp signaling is not capable of inducing *Shox2* expression on its own but is necessary for normal *Shox2* gene expression (Yu et al., 2005).

EPHRIN SIGNALING

Ephrin-B1 belongs to the transmembrane B-type subfamily of Eph/Ephrin signaling molecules (Davy and Soriano, 2005). These signaling molecules have the ability to carry out bidirectional sig-naling. Hence, cells expressing the Eph receptor tyrosine kinase can receive a forward signal whereas cells expressing ephrin (Efn) can be transduced to receive the reverse signal (Bush and Jiang, 2012). The *Efnb1* gene is expressed in the mesenchyme of the anterior palate throughout the secondary palate devel-opment. *Efnb1* forward signals to regulate anterior palatal shelf outgrowth by promoting cell proliferation through the activa-tion of ERK/MAP pathway (Bush and Soriano, 2010). Both *Efnb1* null mice and *Efnb1*$^{+/-}$ heterozygous female mice develop cleft palate with decreased cell proliferation in the anterior palatal mes-enchyme (Bush and Soriano, 2010). The *Efnb1* gene is X-linked and the *Efnb1*$^{+/-}$ heterozygous embryos exhibit mosaic pattern of *Efnb1* expression in the palate that correlates with a mosaic pat-tern of proliferation and hence a more severe dysmorphogenesis of the palatal shelves compared to *Efnb*$^{-/-}$ null mice. *Efnb1* is pri-marily expressed in the anterior mesenchyme, although the cleft palate phenotype was along the entire axis (Bush and Soriano, 2010). In contrast, loss of *Shox2* (described above) which is also anteriorly restricted in the palate, induces a unique anterior-delimited cleft palate (Yu et al., 2005). Hence, reduced *Efnb1* signaling in the anterior palatal mesenchyme in *Efnb*$^{-/-}$ null

or *Efnb1*$^{+/-}$ heterozygous embryos may cross a threshold A–P position at which initiation of fusion is required (Bush and Soriano, 2010).

Tgf-β PATHWAY

The role of *Tgf* -β family members in palatal shelf growth and fusion is an area that has been well-studied. Loss ofxd func-tion of *Tgf*-β*2* (Sanford et al., 1997), *Tgf*-β*3* (Kaartinen et al., 1995; Proetzel et al., 1995; Martínez-Álvarez et al., 2000b), and *Tgf*-β receptors *Tgfbr1* (Dudas et al., 2006), *Tgfbr2* (Ito et al., 2003; Xu et al., 2006) are known to cause cleft palate. More detailed information on this pathway was reviewed recently in Bush and Jiang (2012). In the context of this review, we will only highlight the anterior and posterior-specific roles of these pathway members. The *Tgf* type I receptor *Alk5* is expressed exclusively in the anterior palatal epithelium and its activation in *Tgf* -β3$^{-/-}$ palatal epithelium rescues palatal fusion, whereas loss of *Alk5* function in epithelium of wild-type palatal shelves prevents palatal fusion (Dudas et al., 2004). Interestingly, fusion of the posterior parts of palates is predominant following acti-vation of *Alk5* at E14 whereas its activation at E13.5 also facil-itates fusion in the anterior region (Dudas et al., 2004). Thus, there appears to be an anterior to posterior direction of palatal fusion (Taya et al., 1999) with *Tgf* -β*3* signaling mediated by Alk5 in the anterior epithelium (Dudas et al., 2004). The homozy-gous knock-in of *Tgf*-β*1* in the *Tgf*-β*3* locus partially rescues the cleft palate phenotype of *Tgf*-β*3*$^{-/-}$ mice in the anterior palate (Yang and Kaartinen, 2007). Since *Tgf*-β*1* is expressed in the palatal epithelium along the A–P axis (Yang and Kaartinen, 2007), its partial rescue of anterior palatal fusion may also be mediated via Alk5 signaling in *Tgf*-β*3*$^{-/-}$ mice. Recent find-ings show that craniofacial abnormalities in *Tgfbr2* $^{-/-}$ mice is prevented following genetic manipulation of an alternative non-canonical *TGF*-β signaling pathway through Alk5/*Tgf* type

III receptor complex and SMAD-independent TRAF6/TAK1/p38 signaling (Iwata et al., 2012b). The role of *Tgf*-β*3* in apoptosis of medial edge epithelium (MEE) is well-established (Martínez-Álvarez et al., 2000a,b) and *Tgf*-β*3* synthesized at the MEE facilitates accumulation of chondroitin sulfate proteoglycans at apical surface of MEE (Gato et al., 2002). Loss of *Tgf*-β*3* dis-rupts the normal distribution of E-cadherin, α-, and β-catenins in MEE and impairs cell-cell adhesion (Tudela et al., 2002). Conditional deletion of β-catenin in the epithelium in K14-Cre transgenic mice suppresses canonical Wnt signaling giving rise to an abnormal and persistent MES. Loss of β-catenin also induces down-regulation of *Tgf*-β*3* and inhibition of apoptosis in MEE that subsequently leads to a cleft palate phenotype (He et al., 2011). Hence, region specific expression of *Tgf*-β*3* is essen-tial for proper palate development and these findings highlight the interplay between the various pathways that govern palate development.

POSTERIOR-SPECIFIC GENE EXPRESSION

Although many genes important in palate development have regional specific expression and are expressed predominantly in the anterior palate, several genes are also important in the posterior region (**Figure 3**).

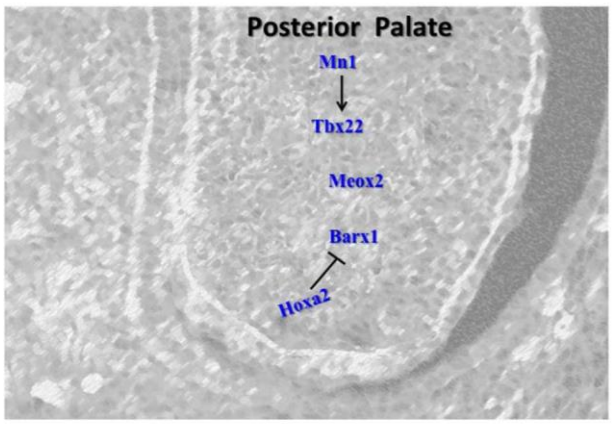

FIGURE 3 | Schematic representation of the key regulators in the posterior palate. Barx1 and Tbx22 induce cell proliferation in the posterior palate. Hoxa2 also controls the expression of Barx1 in the early stage of palatogenesis. Mn1 positively regulates Tbx22 and represents the first network determined to specifically regulate the level of proliferation in the posterior palate. Meox2 plays role in fusion of the posterior palate.

Meox2 NETWORK

Meox2 is a homeobox transcription factor with a posterior-specific expression pattern that becomes increasingly localized to the extreme posterior region of the palate as development pro-ceeds (Jin and Ding, 2006; Li and Ding, 2007). Mice lacking the *Meox2* gene exhibit a low penetrance of cleft palate that results from a novel mechanism. Palate shelves grow, elevate and fuse; however, fusion is weak and as the craniofacial region expands the palate shelves pull apart from one another leading to a cleft palate specifically in the posterior region. Histological analysis of the cleft palates clearly show the palate shelves were completely absent of the medial epithelial edge and were composed solely of mes-enchyme. The mechanism responsible for the post-fusion cleft palate is not completely clear, but may involve a palatal growth defect in the posterior palate that prevents the palates from being able to keep up with the rest of craniofacial development (Jin and Ding, 2006). Alternatively, the loss of *Meox2* may lead to improper palatal fusion and a weak seam that does not stand up to the mechanical forces of craniofacial development (Jin and Ding, 2006). *Meox2* has been reported to be *Tgf*-β responsive in the mammary epithelial cells by inhibiting epithelial cell proliferation by binding to the promoter of p21 through *Tgf*- β/Smad signal-ing pathway (Valcourt et al., 2007). Interestingly, Xu et al. (2008) showed that p21 is required for Smad4 mediated p38 MAPK path-way for apoptosis and MES degeneration. These works suggest that *Meox2* could play a role in *Tgf*-β3 mediated fusion. However, these mechanisms need to be investigated further.

Tbx22 NETWORK

Tbx22 also has a posterior-specific expression profile within the developing palate (Herr et al., 2003). The *Tbx22* gene is a T-box protein that acts as a transcription factor regulating the expres-sion of down-stream genes. Alterations in the *Tbx22* gene are a common single cause of cleft palate in humans (Marçano et al., 2004). A missense mutation in the *Tbx22* gene is responsible for

X-linked cleft palate (Marçano et al., 2004), whereby the mis-sense mutation affects the ability of Tbx22 to bind DNA and subsequently act as a transcriptional repressor (Andreou et al., 2007). This mutation is believed to prevent the SUMO-1 enzyme from sumoylating the Tbx22 protein. In the absence of this post-translational modification, Tbx22 has a much lower affinity for its DNA binding sequence (Andreou et al., 2007), cannot recognize the DNA sequence and bind appropriately, and does not per-form its normal repressor functions. Notably, SUMO-1 is again implicated in regulating palatogenesis. Based on the number of important genes known to require sumoylation to function prop-erly, haploinsufficiency of SUMO-1 is not surprisingly linked to cleft palate phenotype (Alkuraya et al., 2006).

Tbx22 expression in *Spry2* piebald mutants is affected as dis-cussed above. In the absence of this Fgf antagonist, the expression of *Tbx22* fails to expand from the most posterior regions of the palate at E14.5. This altered expression profile coincides with a posterior shift in the expression of *Msx*1 as well as an increase in proliferation throughout the palate shelves (Welsh et al., 2007). The 5 regulatory region of the *Tbx22* gene contains putative *Msx1* binding sites (Herr et al., 2003), however, *Msx1* null mice do not show an expansion of the *Tbx22* expression domain (Fuchs et al., 2010), and *Tbx22* null mice are not reported to have increased *Msx1* expression (Pauws et al., 2009). Palatal *Tbx22* expression has been demonstrated to be independent of Fgf signaling, but was reported to be repressed in culture by exogenous *Bmp4* (Fuchs et al., 2010). Taken together this suggests a system whereby *Msx1* is involved in regulating *Bmp4* expression which subsequently plays a role in the repression of Tbx22 expression, leading to a posterior-specific expression pattern.

Liu et al. describe a novel molecular network involving the *Tbx22* (Liu et al., 2008). The transcription factor Mn1 has a medial-posterior-specific expression profile that generally over-laps the *Tbx22* expression profile. Loss of one or more copies of *Mn1* leads to craniofacial abnormalities including a cleft secondary palate. In the *Mn1* null embryos, *Tbx22* expression decreases in the posterior region of the palate, and Mn1 directly regulates the expression of *Tbx22* in the palate (Liu et al., 2008). A marked decrease in proliferation in the medial and posterior palate shelves also occurs, and is believed to be due in part to the regulation of a separate gene target (*Ccnd2*) by Mn1 (Liu et al., 2008). This represents the first network determined to specifically regulate the level of proliferation in the posterior palate. Tbx22 expression appears to be regulated by at least two factors; *Msx*1 acts as a repressor, while Mn1 acts as an activator, and together they determine the specific expression domain of Tbx22 in the posterior region of the palate.

Barx1 NETWORK

Barx1 expression has a predominantly posterior expression pro-file that is complementary to the anterior expression of *Msx1* (Barlow et al., 1999; Welsh and O'Brien, 2009). This region-specific expression is initially set up in the branchial arches where *Msx1* expression is localized to the distal regions of the first brachial arch and *Barx1* expression is localized proximally (Barlow et al., 1999). The A–P axis derived from the regional expression of *Msx1* and *Barx1* is believed to result from the relative strength of Bmp and Fgf signaling (Welsh et al., 2007). The expression of *Barx1* is altered in a number of knockout mouse lines. Loss of *Spry2* via the piebald deletion not only affects *Msx*1 and *Tbx22* expression, but also leads to an anterior expansion of *Barx1* expression that may be involved in the increased cell proliferation seen in these palates (Welsh et al., 2007). The loss of the Bmp receptor *Bmpr1a* also leads to an expansion of the region in the palate expressing *Barx1* (Liu et al., 2005). *Hoxa2* null embryos have increased *Barx1* expression at the early stages of palate development. An increase in the level of cell proliferation in the posterior region of the palate is also observed in *Hoxa2* null mice (Smith et al., 2009). The alterations in both Fgf and Bmp signaling causing altered *Barx*1 expression support the view that regulation of the regional expression of *Barx1* involves both fami-lies of signaling molecules. Evidence for this comes from *Tp63*$^{-/-}$ mice where expression of *Fgf8* at E11.5 in the anterior region of maxillary processes is down-regulated, which coincides with a reduced anterior expression of its target gene *Barx1* (Thomason et al., 2008). In contrast, the *Tp63*$^{-/-}$ mice (which exhibit cleft lip and palate phenotype) show increased expression of *Bmp4* in the anterior region of the maxillary processes at E10.5 and E11.5. *Barx1* is also regulated by relative levels of *Fgf8* and *Bmp4* in developing chick facial primordia where BMPs reduce *Barx1* expression and antagonize Fgf-8 signaling (Barlow et al., 1999).

AT WHAT STAGE DOES THE ANTERO-POSTERIOR MOLECULAR SIGNALING GET ESTABLISHED?

An intriguing question during palatal development is when does the antero-posterior molecular signaling get established? Although answer to this remains elusive, available data indicates a much earlier time in development and prior to palatal shelf formation. The anterior localization of *Msx1* and posterior local-ization of *Barx1* is set to be determined in the first branchial arch where *Msx1* is localized to distal and *Barx1* to the proximal region (Barlow et al., 1999). In early mice palatal development, *Barx1* expression is visible in the posterior region extending through almost three quarters of the developing palatal shelves, whereas *Msx1* is restricted to a narrow anterior region of the developing palate (Welsh and O'Brien, 2009). Following rostral expansion, the anterior palate extends with the expression of *Msx1* and the first molar tooth bud serves as the posterior boundary of this extended anterior expression (Welsh and O'Brien, 2009). Hence, genes expressed in the presumptive hard and soft palate appear to be set up earlier along an A–P axis in the branchial arches. Consistent with this expression along an A–P axis in the first arch, *Msx1* plays a role in incisor development and *Barx1* in molar tooth development (reviewed in Mitsiadis and Smith, 2006). Interestingly, Bmp-Fgf signaling also governs tooth development in a gradient manner along an A–P axis (Mitsiadis and Smith, 2006). It is likely these genes play a similar role in the orofacial structures. Indeed similar to its role in palate development where *Bmp4* is required to prevent the premature apoptosis of palatal epithelium, *Bmp4* is essential in blocking apoptosis in the dental epithelium in a *Msx1*-dependent manner regulated by *Tgf*-β type I receptor Alk-5 (Zhao et al., 2008).

The transcription factor Tp63 regulates the expression of *Bmp4* in the anterior palate and loss of *Tp63* in the maxillary

processes in the medial region from which the palatal shelves originate, results in improper Bmp signaling and a cleft palate phenotype (Thomason et al., 2008). However, conditional inactivation of *Bmp4* in the early maxillary mesenchyme using *Nestin cre;Bmp4* $^{null/flox}$ *(n/f)* mice did not disrupt secondary palate development but resulted instead in isolated cleft lip (Liu et al., 2005). Loss of *Bmpr1a* in facial primodia of *Nestin cre;Bmpr1a n/f* embryos, which did not impact *Msx1* expression, resulted in reduced mesenchymal cell proliferation in maxillary process prior to the onset of secondary palate outgrowth resulting in smaller palatal shelves and subsequent cleft palate at birth (Liu et al., 2005). In contrast, tissue-specific loss of *Bmpr1a* in palatal mesenchyme in *Osr2-IresCre;Bmpr1a*$^{f/f}$ mutant mice results in reduced expression of *Msx1* and an up-regulation in *Bmp4* lead-ing to submucous cleft of the hard palate (Baek et al., 2011). Thus, the BMP family highlights the complexity of signaling involved in their early tissue specific role in orofacial development. Further early fate determination studies are needed using lineage specific animal models to characterize the complex signaling during early palate development to clearly determine the origins of the A–P molecular signaling.

CROSSTALK BETWEEN NETWORKS/PATHWAYS

Palatal elevation and fusion is governed by transcription fac-tors, various growth factors and their receptors forming inter-connected network of molecular pathways. Relative signals or gradients are strictly required to ensure proper development. The anterior and posterior palatal tissues being the future hard and soft palates differ in function and structure, show differ-ence in the expression patterns along the A–P axis. Numerous pathways/networks in the palate clearly display reciprocal signal-ing between the epithelium and mesenchyme. Genes expressed exclusively in the epithelium have been reported to regulate cel-lular processes and gene expression in the mesenchyme, and vice versa, such that reciprocal signaling occurs between the epithe-lium and mesenchyme (Zhang et al., 2002; Yamamoto et al., 2003; Rice et al., 2004; Nawshad et al., 2007). In recent years it has become increasingly evident that gene expression in the developing palate not only displays epithelial-mesenchymal speci-ficity, but also anterior–posterior (A–P) and oral-nasal specificity (reviewed in Murray and Schutte, 2004; Hilliard et al., 2005; Bush and Jiang, 2012). Interestingly, *Tp63* null mutants have abnormal outgrowth of the palate initially but by E12.5 the A–P specific expression patterns were normal despite abnormal shelf growth confirming the importance of setting up and maintaining the A–P axis (Thomason et al., 2008). In addition to their localized expression, genes have been reported to elicit different responses in different regions of the palate. For example, while exogenous *Fgf10* alters proliferation in the anterior palate, it has no effect on proliferation in the posterior region of the palate (Yu et al., 2005). Such localized expression and function phenomena clearly highlight the importance of regional patterning and differentia-tion within the palate at the molecular level. Overall, the number of genes involved in the development of the palate that dis-play strictly regulated domains of expression is clear evidence of regional differentiation within the palate. *Msx1* and *Bmp4* func-tion in an autoregulatory loop mechanism in the anterior palatal mesenchyme. *Bmp4* induces *Shh* expression in the epithelium which signals backs to mesenchyme to positively regulate Bmp2 to enhance cell proliferation in the mesenchyme (Zhang et al., 2002). Cross talk also exists between *Bmp7* and *Shh*, which plays a role in refining the expression domain of both genes (Han et al., 2009). *Tbx3* and *Bmp4* regulate each other's expression in the palate. *Tbx*3 inhibits the expression of *Bmp4* while *Bmp4* induces *Tbx*3 expression and regulates the levels of cell proliferation in the anterior palatal mesenchyme (Lee et al., 2007). Regulatory feedback loop exists between *Fgfr1b* and *Wnt11*. *Fgfr1b* represses expression of *Wnt11* whereas *Wnt11* signaling molecule nega-tively regulates *Fgfr1b* expression (Lee et al., 2008). Balance is titled toward or away from *Fgfr1b*, to respectively allow cell pro-liferation to proceed (at E13.5) or to recede (at E14) and fusion to occur (Lee et al., 2008). Unlike the anterior palate, molecular mechanisms of palatal outgrowth in the posterior palatal regions are not yet well established. Mn1 directly regulates the expres-sion of *Tbx22* in the palate (Liu et al., 2008) and *Msx1* acts as a repressor of *Tbx22* in the palate (Welsh et al., 2007) which together determines the posterior expression domain of Tbx22 in the palate.

ANTERIOR PALATE-SIGNALING CENTER

Critical events such as elevation, maturation and fusion of sec-ondary palatal shelves follow an anterior to posterior sequence (Taya et al., 1999; Dudas et al., 2004) (**Figure 4**). During mouse palate development, at embryonic day E13.5–E14, the ante-rior palate orients horizontally above the tongue when the pos-terior palate is still lying vertically (Kaufman, 1992) providing a clear indication of the more dynamic growth in the anterior palate compared to the posterior palate. In addition, the initial site of apposition and subsequent fusion of the palatal shelves occur first in the anterior half of the palate and the sequence of palatal closure may be result of signaling activity along the A–P axis.

Although *Shox2* expression remains anterior-specific through-out palatogenesis, it displays a dynamic pattern of expression. At the initial stages of palate growth, *Shox*2 expression is only detected in the most extreme anterior regions of the palate (less than 25% of the length of the palate) (Yu et al., 2005; Li and Ding, 2007). As the palate shelves continue to grow, the expression of *Shox*2 expands until E14.5 when it covers the entire anterior palate and most of the medial palate (60% of the length of the palate shelf). Concurrent with the expansion of *Shox2* expres-sion, the region of the palate expressing the posterior-specific gene *Meox2* shrinks (Li and Ding, 2007). This phenomenon demonstrates normal development of the anterior palate requires recruitment of cells from the posterior, which are converted into *Shox2* anterior-specific cells. This has been suggested to be due to a repression of *Meox2* by *Shox2* or a down-stream target of the *Shox2* pathway (Li and Ding, 2007).

The rugae have been suggested to play an important role in organizing and maintaining the A–P axis (Welsh et al., 2007; Pantalacci et al., 2008; Welsh and O'Brien, 2009). Rugae have been shown to form in the region between the last formed and rugae 8 (the first rugae to form) in a sequential order (Pantalacci et al., 2008; Welsh and O'Brien, 2009). Rugae 8 has been denoted the "boundary rugae" as it appears to act to separate the anterior

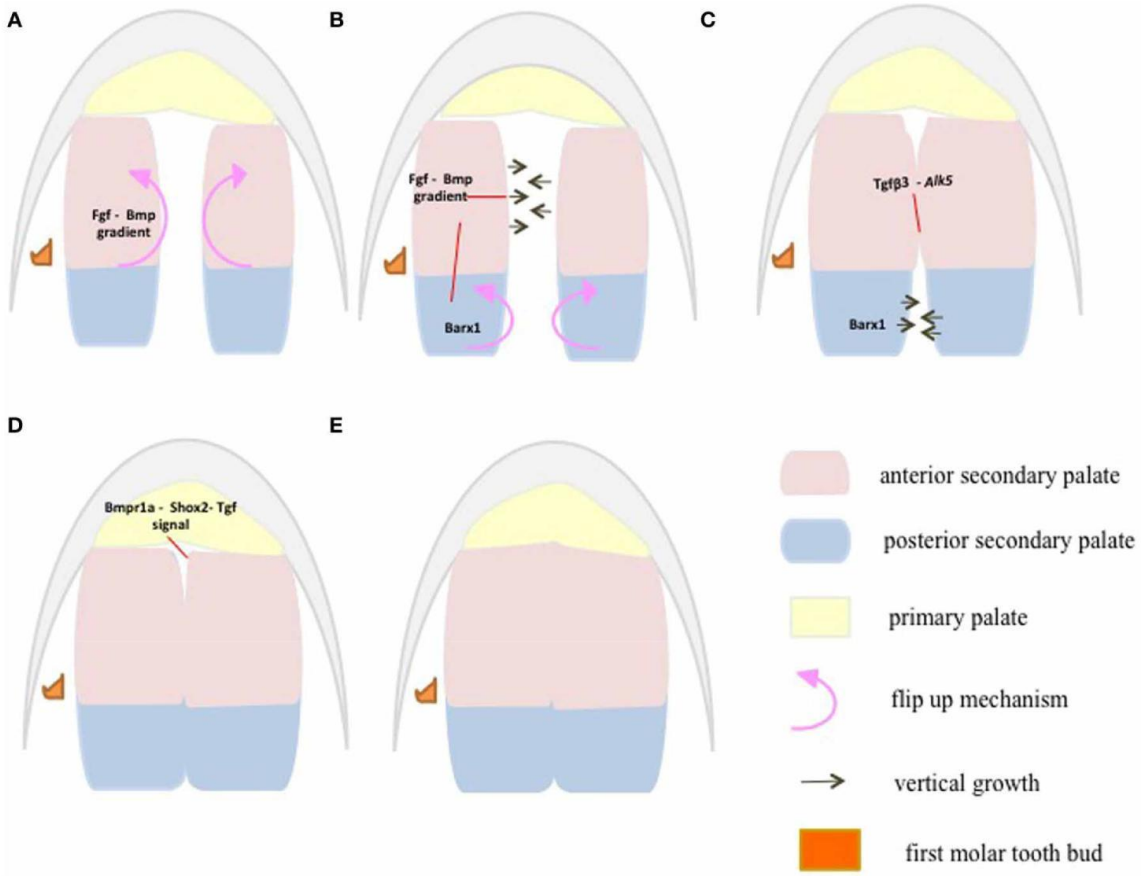

FIGURE 4 | At E13.5, the anterior palatal shelves first flip up to orient vertically when the posterior palatal shelves are still lying horizontal to each other **(A)**. At E14, the posterior palatal shelves follow the anterior palatal shelves in orienting vertically, whereas the anterior palates begin to grow vertically toward each other to make contact **(B)**. At E15, the anterior palatal shelves have made contact and fused, whereas the posterior shelves grow vertically **(C)**. At E15.5, both the anterior and posterior palates have fused **(D)**. At E16, the fusion between the primary and secondary palate occurs at the future secondary choana **(E)**. Palatal shelves are divided into anterior (pink) *Msx1* and posterior (aqua) *Barx1* expression domains **(A–E)** representing future hard and soft palate, respectively. Fgf-Bmp gradients/thresholds maintain proper palatal growth and fusion through proliferation. Anterior *Fgf10* and Bmps control proliferation via *Shh* expression. This directs anterior palate flip up and vertical growth at E13.5–E14 **(A,B)**. Anterior Fgf-Bmp gradients along with posterior *Fgf8* regulate proliferation and growth via *Barx1* in the posterior palate at E14–E15 **(B,C)**. Fusion is initiated at the anterior palate by *Tgf*-β3 through its receptor **(C)**. Then the fusion extends posteriorly through *Tgf*-β-Meox2 **(D)**. The fusion between the primary and secondary palate marks the completion of palatal fusion at E16 **(D,E)**, via *Bmpr1a* mediated *Shox2* and *Tgf* β signaling through its receptors.

and posterior domains of the palate. Throughout palatal development, expression of the anterior specific markers *Shox2* and *Msx1* remain anterior to rugae 8 and *Meox2* and *Tbx22* stay posterior of this boundary (Pantalacci et al., 2008; Welsh and O'Brien, 2009). This rapid expansion of the palate anterior to rugae 8 provides an alternate explanation for the anterior growth of the palate to the one detailed above by Li and Ding (2007). The major difference is that Li and Ding did not detect differences in the proliferation rates of the anterior and posterior palate, while Pantalacci et al. (2008) did detect a higher level in the anterior palate. Which theory is deemed to be correct will require further investigations.

Mice lacking expression of either *Wnt5a* or its noncanoni-cal receptor Ror2 were found to exhibit a cleft palate (Schwabe et al., 2004; He et al., 2008). In addition, both genes were shown to exhibit an expression pattern whereby their expression was higher in the anterior palate than the posterior palate (He et al., 2008), with *Wnt5a* detected exclusively in the mesenchyme (Paiva et al., 2010). The *Wnt5a* signal was consequently shown to act as a chemoattractant causing cells to migrate from the posterior region of the palate toward the anterior region. Evidence sug-gests that Ror2 mediates the role of *Wnt5a* in the palatogenesis (He et al., 2008). As discussed above, *Wnt5a* also regulates the expression of *Bmp4* and *Shh*, both of which play important roles in the development and growth of the anterior palate (He et al., 2008). Hence, simple upregulation of *Shox2* and downregulation of *Meox2* may not result in the conversion of posterior cells to anterior cells if the cells are migrating toward the higher *Wnt5a* signal. As cells enter the anterior region of the palate, *Wnt5a* and potentially other factors may act to alter the expression pro-file of genes in the cells, causing them to transdifferentiate into anterior-specific palate cells.

Collectively, these recent discoveries, suggest that cells may migrate—first from the posterior region of the palate to the ante-rior region of the palate and then to the oral region of the anterior palate—underscore the dynamic processes taking place during palate development. While at any given time cells display a spe-cific set of genes that determine how they react to external stimuli, this set of factors continually changes as development proceeds. In addition, the migration to the anterior region of the palate specifically lends further support to the theory the anterior palate plays a role as a signaling center acting to regulate palatogenesis as a whole. It also demonstrates the importance of maintaining a proper anterior to posterior axis in the palate development.

CONCLUSION

Regulation of palate development appears to be the result of dis-tinct pathways in the anterior and posterior regions of the palate. Development and maintenance of expression of these regional-specific genes is crucial to normal palate development. Anterior-and posterior- specific genes appear to act in a mutually exclusive manner by either directly or indirectly inhibiting reciprocal expression.

Recent findings show posterior palate cells maintain the abil-ity to transform into anterior specific cells upon migration. These data demonstrate the plasticity of these cell populations despite their differential responses to external stimuli.

To date, researchers have often limited their investigations to determining levels of gene expression of putative targets. However, the future of palate research will need to consider the regional specificity of target genes. An important focus of new studies should be to examine the expression domains of potential targets along the A–P axis, as expansion or limitations of these domains can dramatically affect palate development.

ACKNOWLEDGMENTS

Funding for this research was provided by a grant from the Natural Sciences and Engineering Research Council of Canada to Adil J. Nazarali. In the interest of brevity and space limitations we apologize to colleagues whose work may not have been cited.

REFERENCES

Alappat, S., Zhang, Z. Y., and Chen, Y. P. (2003). Msx homeobox gene family and craniofacial development. *Cell Res.* 13, 429–442.

Alappat, S. R., Zhang, Z., Suzuki, K., Zhang, X., Liu, H., Jiang, R., et al. (2005). The cellular and molecular etiology of the cleft secondary palate in *Fgf10* mutant mice. *Dev. Biol.* 277, 102–113.

Alasti, F., Sadeghi, A., Sanati, M. H., Farhadi, M., Stollar, E., Somers, T., et al. (2008). A mutation in HOXA2 is responsible for autosomal-recessive microtia in an Iranian family. *Am. J. Hum. Genet.* 82, 982–991.

Alkuraya, F. S., Saadi, I., Lund, J. J., Turbe-Doan, A., Morton, C. C., and Maas, R. L. (2006). SUMO1 hap-loinsufficiency leads to cleft lip and palate. *Science* 313, 1751.

Almeida de Assis, N., Nowak, S., Ludwig, K. U., Reutter, H., Vollmer, J., Heilmann, S., et al. (2011). SUMO1 as a candidate gene for non-syndromic cleft lip with or without cleft palate: no evidence for the involvement of com-mon or rare variants in Central European patients. *Int. J. Pediatr. Otorhinolaryngol.* 75, 49–52.

Andreou, A. M., Pauws, E., Jones, M. C., Singh, M. K., Bussen, M., Doudney, K., et al. (2007).

TBX22 missense mutations found in patients with X-linked cleft palate affect DNA binding, sumoylation, and transcriptional repression. *Am. J. Hum. Genet.* 81, 700–712.

Baek, J.-A., Lan, Y., Liu, H., Maltby, K. M., Mishina, Y., and Jiang, R. (2011). Bmpr1a signaling plays crit-ical roles in palatal shelf growth and palatal bone formation. *Dev. Biol.* 350, 520–531.

Barlow, A. J., Bogardi, J.-P., Ladher, R., and Francis-West, P. H. (1999). Expression of chick Barx-1 and its differential regulation by FGF-8 and BMP signaling in the maxillary pri-mordia. *Dev. Dyn.* 214, 291–302.

Barrow, J. R., and Capecchi, M. R. (1999). Compensatory defects associated with mutations in Hoxa1 restore normal palatogenesis to Hoxa2 mutants. *Development* 126, 5011–5026.

Bei, M., and Maas, R. (1998). FGFs and *BMP4* induce both Msx1-independent and Msx1-dependent signaling pathways in early tooth development. *Development* 125, 4325–4333.

Berkovitz, B. K. B., Holland, G. R., and Moxham, B. J. (2009). *Oral Anatomy, Histology and Embryology.* 4th Edn. Edinburgh: Elsevier; Mosby.

Bush, J. O., and Jiang, R. (2012).

Palatogenesis: morphogenetic and molecular mechanisms of secondary palate development. *Development* 139, 231–243.

Bush, J. O., and Soriano, P. (2010). Ephrin-B1 forward signaling regu-lates craniofacial morphogenesis by controlling cell proliferation across Eph-ephrin boundaries. *Gen. Dev.* 24, 2068–2080.

Carette, M. J. M., and Ferguson, M. W. J. (1992). The fate of medial edge epithelial cells during palatal fusion *in vitro*: an analysis by DiI labelling and confocal microscopy. *Development* 114, 379–388.

Colvin, J. S., Feldman, B., Nadeau, J. H., Goldfarb, M., and Ornitz, D. M. (1999). Genomic organization and embryonic expression of the mouse fibroblast growth factor 9 gene. *Dev. Dyn.* 216, 72–88.

Colvin, J. S., White, A. C., Pratt, S. J., and Ornitz, D. M. (2001). Lung hypoplasia and neonatal death in Fgf9-null mice identify this gene as an essential regulator of lung mesenchyme. *Development* 128, 2095–2106.

Cui, X.-M., Shiomi, N., Chen, J., Saito, T., Yamamoto, T., Ito, Y., et al. (2005). Overexpression of Smad2 in *Tgf-β3*-null mutant mice res-cues cleft palate. *Dev. Biol.* 278, 193–202.

Davenport, T. G., Jerome-Majewska, L. A., and Papaioannou, V. E. (2003). Mammary gland, limb and yolk sac defects in mice lacking *Tbx3*, the gene mutated in human ulnar mam-mary syndrome. *Development* 130, 2263–2273.

Davy, A., and Soriano, P. (2005). Ephrin signaling *in vivo*: look both ways. *Dev. Dyn.* 232, 1–10.

De Angelis, V., and Nalbandian, J. (1968). Ultrastructure of mouse and rat palatal processes prior to and during secondary palate formation. *Arch. Oral Biol.* 13, 601–608.

Diewert, V. M. (1978). A quantitative coronal plane evaluation of cranio-facial growth and spatial relations during secondary palate develop-ment in the rat. *Arch. Oral Biol.* 23, 607–629.

Diewert, V. M. (1980). Differential changes in cartilage cell prolifera-tion and cell density in the rat cran-iofacial complex during secondary palate development. *Anat. Rec.* 198, 219–228.

Diewert, V. M. (1983). A morphome-tric analysis of craniofacial growth and changes in spatial relations dur-ing secondary palatal development in human embryos and fetuses. *Am. J. Anat.* 167, 495–522.

Dixon, M. J., Marazita, M. L., Beaty, T. H., and Murray, J. C. (2011). Cleft lip and palate: understand-ing genetic and environmental influences. *Nat. Rev. Genet.* 12, 167–178.

Dudas, M., Kim, J., Li, W. Y., Nagy, A., Larsson, J., Karlsson, S., et al. (2006). Epithelial and ectomes-enchymal role of the type I *TGF-*beta receptor ALK5 during facial morphogenesis and palatal fusion. *Dev. Biol.* 296, 298–314.

Dudas, M., Nagy, A., Laping, N. J., Moustakas, A., and Kaartinen,

2 (2004). Tgf-β3-induced palatal fusion is mediated by Alk-5/Smad pathway. *Dev. Biol.* 266, 96–108.

Economou, A. D., Ohazama, A., Porntaveetus, T., Sharpe, P. T., Kondo, S., Basson, M. A., et al. (2012). Periodic stripe formation by a Turing mechanism operating at growth zones in the mammalian palate. *Nat. Genet.* 44, 348–352.

Farbman, A. I. (1968). Electron micro-scope study of palate fusion in mouse embryos. *Dev. Biol.* 18, 93–116.

Ferguson, M. W. J. (1987). Palate development: mechanisms and mal-formations. *Ir. J. Med. Sci.* 156, 309–315.

Ferguson, M. W. J. (1988). Palate devel-opment. *Development* 103(Suppl.), 41–60.

Fitchett, J. E., and Hay, E. D. (1989). Medial edge epithelium transforms to mesenchyme after embryonic palatal shelves fuse. *Dev. Biol.* 131, 455–474.

Fuchs, A., Inthal, A., Herrman, D., Cheng, S., Nakatomi, M., Peters, H., et al. (2010). Regulation of Tbx22 during facial and palatal develop-ment. *Dev. Dyn.* 239, 2860–2874.

Gato, A., Martinez, M. L., Tudela, C., Alonso, I., Moro, J. A., Formoso, M. A., et al. (2002). TGF-β3-induced chondroitin sulphate proteoglycan mediates palatal shelf adhesion. *Dev. Biol.* 250, 393–405.

Gendron-Maguire, M., Mallo, M., Zhang, M., and Gridley, T. (1993). Hoxa-2 mutant mice exhibit homeotic transformation of skeletal elements derived from cranial neural crest. *Cell* 75, 1317–1331.

Gorlin, R. J., Cohen, M. M., and Hennekam, R. C. M. (2001). *Syndromes of the Head and Neck, 4th Edn*. NewYork, NY: Oxford University Press Inc.

Greene, R. M., and Kochhar, D. M. (1974). Surface coat on the epithe-lium of developing palatine shelves in the mouse as revealed by elec-tron microscopy. *J. Embryol. Exp. Morphol.* 31, 683–692.

Greene, R. M., and Pratt, R. M. (1977). Inhibition by diazo-oxo-norleucine (DON) of rat palatal glycoproteins synthesis and epithelial cell adhe-sion *in vitro*. *Exp. Cell Res.* 105, 27–37.

Griffith, C. M., and Hay, E. D. (1992). Epithelial-mesenchymal trans-formation during palatal fusion: carboxyfluorescein traces cells at light and electron microscopic levels. *Development* 116, 1087–1099.

Gupta, V., and Bei, M. (2006). Modification of Msx1 by SUMO-1. *Biochem. Biophys. Res. Commun.* 345, 74–77.

Han, J., Mayo, J., Xu, X., Li, J., Bringas, P., Maas, R. L., et al. (2009). Indirect modulation of Shh signaling by Dlx5 affects the oral-nasal pattern-ing of palate and rescues cleft palate in Msx1-null mice. *Dev. Dis.* 136, 4225–4233.

He, F., Xiong, W., Wang, Y., Li, L., Liu, C., Yamagami, T., et al. (2011). Epithelial Wnt/β-catenin signaling regulates palatal shelf fusion through regulation of Tgfβ3 expression. *Dev. Biol.* 350, 511–519.

He, F., Xiong, W., Wang, Y., Matsui, M., Yu, X., Chai, Y., et al. (2010). Modulation of BMP signaling by Noggin is required for the mainte-nance of palate epithelium integrity during palatogenesis. *Dev. Biol.* 347, 109–121.

He, F., Xiong, W., Yu, X., Espinoza-Lewis, R., Liu, C., Gu, S., et al. (2008). *Wnt5a* regulates directional cell migration and cell proliferation Via Ror2-Mediated noncanonical pathway in mammalian palate development. *Development* 135, 3871–3879.

Herr, A., Meunier, D., Müller, I., Rump, A., Fundele, R., Ropers, H.-H., et al. (2003). Expression of mouse Tbx22 supports its role in palatogenesis and glossogenesis. *Dev. Dyn.* 226, 579–586.

Hilliard, S. A., Yu, L., Gu, S., Zhang, Z., and Chen, Y. P. (2005). Regional reg-ulation of palatal growth and pat-terning along the anterior-posterior axis in mice. *J. Anat.* 207, 655–667.

Hosokawa, R., Deng, X., Takamore, K., Xu, X., Urata, M., Bringas, P. Jr., et al. (2009). Epithelial-specific requirement for *FGFR2* signaling during tooth and palate develop-ment. *J. Exp. Zool.* 312B, 343–350.

Houzelstein, D., Cohen, A., Buckingham, M. E., and Robert, B. (1997). Insertional mutation of the mouse Msx1 homeobox gene by an nlacZ reporter gene. *Mech. Dev.* 65, 123–133.

Huang, X., Goudy, S. L., Ketova, T., Litingtung, Y., and Chiang, C. (2008). Gli3-deficient mice exhibit cleft palate associated with abnor-mal tongue development. *Dev. Dyn.* 237, 3079–3087.

Humphrey, T. (1969). The relation between human fetal mouth open-ing reflexes and closure of the palate. *Am. J. Anat.* 125, 317–344.

Ito, Y., Yeo, J. Y., Chytil, A., Han, J., Bringas, P. Jr., Nakajima, A., et al. (2003). Conditional inactivation of Tgfbr2 in cranial neural crest causes cleft palate and calvaria defects. *Development* 130, 5269–5280.

Iwata, J., Tung, L., Urata, M., Hacia, J. G., Pelikan, R., Suzuki, A., et al. (2012a). Fibroblast growth factor 6 (FGF9)-pituitary homeobox 2 (PITX2) pathway mediates trans-forming growth factor β (TGFβ) signaling to regulate cell proliferation in palatal mesenchyme during mouse palatogenesis. *J. Biol. Chem.* 287, 2353–2363.

Iwata, J., Hacia, J. G., Suzuki, A., Sanchez-Lara, P. A., Urata, M., and Chai, Y. (2012b). Modulation of noncanonical TGF-β signaling pre-vents cleft palate in Tgfbr2 mutant mice. *J. Clin. Invest.* 122, 873–885.

Jin, J. Z., and Ding, J. (2006). Analysis of Meox-2 mutant mice reveals a novel postfusion-based cleft palate. *Dev. Dyn.* 235, 539–546.

Kaartinen, V., Voncken, J. W., Shuler, C. F., Warburton, D., Bu, D.,

Heisterkamp, N., et al. (1995). Abnormal lung development and cleft palate in mice lacking TGF-β3 indicates defects of epithelial-mesenchymal interaction. *Nat. Genet.* 11, 415–421.

Kaufman, M. H. (1992). *The Atlas of Mouse Development.* New York, NY: Academic Press.

Lee, J.-M., Kim, J.-Y., Cho, K.-W., Lee, M.-J., Cho, S.-W., Kwak, S., et al. (2008). Wnt11/Fgfr1b Cross-talk modulates the fate of cells in palate development. *Dev. Biol.* 314, 341–350.

Lee, J.-M., Kim, J.-Y., Cho, K.-W., Lee, M.-J., Cho, S.-W., Zhang, Y., et al. (2007). Modulation of cell proliferation during palatogenesis by the interplay between Tbx3 and Bmp4. *Cell Tissue Res.* 327, 285–292.

Levi, G., Mantero, S., Barbieri, O., Cantatore, D., Paleari, L., Beverdam, A., et al. (2006). Msx1 and Dlx5 act independently in development of craniofacial skeleton, but converge on the regulation of Bmp signaling in palate formation. *Mech. Dev.* 123, 3–16.

Li, L., Lin, M., Wang, Y., Cserjesi, P., Chen, Z., and Chen, Y. (2011). Bmpr1a is required in mesenchymal tissue and has limited redundant function with Bmpr1b in tooth and palate development. *Dev. Biol.* 349, 451–461.

Li, Q., and Ding, J. (2007). Gene expres-sion analysis reveals that formation of the mouse anterior secondary palate involves recruitment of cells from the posterior side. *Int. J. Dev. Biol.* 51, 167–172.

Lidral, A. C., Romitti, P. A., Basart, A. M., Doetschman, T., Leysens, N. J., Daack-Hirsh, S., et al. (1998). Association of MSX1 and TGFβ3 with nonsyndromic clefting in humans. *Am. J. Hum. Genet.* 63, 557–568.

Lin, C., Fisher, A. V., Yin, Y., Maruyama, T., Veith, G. M., Dhandha, M., et al. (2011). The inductive role of Wnt-β-Catenin signaling in the forma-tion of the oral apparatus. *Dev. Biol.* 356, 40–50.

Litingtung, Y., Dahn, R. D., Li, Y., Fallon, J. F., and Chiang, C. (2002). *Shh* and Gli3 are dispensable for limb skeleton formation but reg-ulate digit number and identity. *Nature* 418, 979–983.

Liu, W., Lan, Y., Pauws, E., Meester-Smoor, M. A., Stanier, P., Zwarthoff, E. C., et al. (2008). The Mn1 tran-scription factor acts upstream of Tbx22 and preferentially regulates posterior palate growth in mice. *Development* 135, 3959–3968.

Liu, W., Sun, X., Braut, A., Mishina, Y., Behringer, R. R., Mina, M., et al. (2005). Distinct functions for Bmp signaling in lip and palate fusion in mice. *Development* 132, 1453–1461.

Marçano, A. C. B., Doudney, K., Braybrook, C., Squires, R., Patton, M. A., Lees, M. M., et al. (2004). TBX22 mutations are a frequent cause of cleft palate. *J. Med. Genet.* 41, 68–74.

Martínez-Álvarez, C., Tudela, C., Pérez-Miquelsanz, J., O'Kane, S., Puerta, J., and Ferguson, M. W. J. (2000a). Medial edge epithelial cell fate dur-ing palatal fusion. *Dev. Biol.* 220, 343–357.

Martínez-Álvarez, C., Bonelli, R., Tudela, C., Gato, A., Mena, J., O'Kane, S., et al. (2000b). Bulging medial edge epithelial cells and palatal fusion. *Int. J. Dev. Biol.* 44, 331–335.

Matsumura, K., Taketomi, T., Yoshizaki, K., Arai, S., Sanui, T., Yoshiga, D., et al. (2011). Sprouty2 controls proliferation of palate mesenchyme cells via fibroblast growth factor signaling. *Biochem. Biophys. Res. Commun.* 404, 1076–1082.

Mitsiadis, T. A., and Smith, M. M. (2006). How do genes make teeth to order through development? *J. Exp. Zool. B Mol. Dev. Evol.* 306B, 177–182.

Morgan, P. R., and Pratt, R. M. (1977). Ultrastructure of the expected fusion zone in rat fetuses with diazo-oxo-norleucine (DON) induced cleft palate. *Teratology* 15, 281–289.

Murray, J. C., and Schutte, B. C. (2004). Cleft palate: players, path-ways, and pursuits. *J. Clin. Invest.* 113, 1676–1678.

Nawshad, A. (2008). Palatal seam dis-integration: to die or not to die? that is no longer the question. *Dev. Dyn.* 237, 2643–2656.

Nawshad, A., Medici, D., Liu, C.-C., and Hay, E. D. (2007). TGFβ3 Inhibits E-cadherin gene expres-sion in palate medial-edge epithelial cells through a Smad2-Smad4-LEF1 transcription complex. *J. Cell Sci.* 120, 1646–1653.

Nie, X.-G. (2005). Differential expres-sion of Bmp2, *Bmp4* and Bmp3 in embryonic development of mouse anterior and posterior palate. *Chin. Med. J.* 118, 1710–1716.

Niswander, L. (2003). Pattern forma-tion: old models out on a limb. *Nat. Rev. Genet.* 4, 133–143.

Noden, D. M. (1983). The role of the neural crest in patterning of avian cranial skeletal, connective,

and muscle tissues. *Dev. Biol.* 96, 144–165.

Otero, L., Gutiérrez, S., Cháves, M., Vargas, C., and Bérmudez, L. (2007). Association of MSX1 with nonsyndromic cleft lip and palate in a columbian population. *Cleft Palate Craniofac. J.* 44, 653–656.

Paiva, K. B. S., das Graças Silva-Valenzuela, M., Massironi, S. M. G., Ko, G. M., Siqueira, F. M., and Nunes, F. D. (2010). Differential Shh, Bmp and Wnt gene expressions during craniofacial development in mice. *Acta Histochem.* 112, 508–517.

Pantalacci, S., Prochazka, J., Martin, A., Rothova, M., Lambert, A., Bernard, L., et al. (2008). Patterning of palatal rugae through sequential addition

reveals an anterior/posterior boundary in palatal develop-ment. *BMC Dev. Biol.* 8:116. doi: 10.1186/1471-213X-8-116

Pauws, E., Hoshino, A., Bentley, L., Prajapati, S., Keller, C., Hammond, P., et al. (2009). Tbx22 null mice have a submucous cleft palate due to reduced palatal bone formation and also display ankyloglossia and choanal atresia phenotypes. *Hum. Mol. Genet.* 18, 4171–4179.

Pourtois, M. (1966). Onset of the acquired potentiality for fusion in the palatal shelves of rats. *J. Embryol. Exp. Morphol.* 16, 171–182.

Pratt, R. M., and Hassell, J. R. (1975). Appearance and distribution of carbohydrate-rich macromolecules on the epithelial surface of the developing rat palatal shelf. *Dev. Biol.* 45, 192–198.

Prince, V., and Lumsden, A. (1994). Hoxa-2 expression in normal and transposed rhombomeres: indepen-dent regulation in the neural tube and neural crest. *Development* 120, 911–923.

Proetzel, G., Pawlowski, S. A., Wiles, M. V., Yin, M., Boivin, G. P., Howles, P. N., et al. (1995). Transforming growth factor-β 3 is required for secondary palate fusion. *Nat. Genet.* 11, 409–414.

Rice, R., Connor, E., and Rice, D. P. C. (2006). Expression patterns of hedgehog signalling pathway members during mouse palate development. *Gene Expr. Patterns* 6, 206–212.

Rice, R., Spencer-Dene, B., Connor, E. C., Gritli-Linde, A., McMahon, A. P., Dickson, C., et al. (2004). Disruption of Fgf10/Fgfr2b-coordinated epithelial-mesenchymal interac-tions causes cleft palate. *J. Clin. Invest.* 113, 1692–1700.

Rijli, F. M., Mark, M., Lakkaraju, S., Dierich, A., Dollé, P., and Chambon, P. (1993). A homeotic transformation is generated in the rostral branchial region of the head by disruption of Hoxa-2, which acts as a selector gene. *Cell* 75, 1333–1349.

Riley, B. M., Mansilla, M. A., Ma, J., Daack-Hirsch, S., Maher, B. S., Raffensperger, L. M., et al. (2007). Impaired FGF ignaling contributes to cleft lip and palate. *Proc. Natl. Acad. Sci. U.S.A.* 104, 4512–4517.

Sanford, L. P., Ormsby, I., Gittenberger-de Groot, A. C., Sariola, H., Friedman, R., Bolvin, G. P., et al. (1997). TGFβ 2 knockout mice have multiple developmental defects that are non- overlapping with other TGFβ knockout phenotypes. *Development* 124, 2659–2670.

Santagati, F., Minoux, M., Ren, S.-Y., and Rijli, F. M. (2005). Temporal requirement of Hoxa2 in cranial neural crest skeletal morphogenesis. *Development* 132, 4927–4936.

Satokata, I., and Maas, R. (1994). Msx1 deficient mice exhibit cleft palate and abnormalities of craniofacial and tooth development. *Nat. Genet.* 6, 348–356.

Saunders, J. W. Jr. (1966). Death in embryonic systems. *Science* 154, 604–612.

Schwabe, G. C., Trepczik, B., Suring, K., Brieske, N., Tucker, A. S., Sharpe, P. T., et al. (2004). Ror2 knockout mouse as a model for the developmental pathology of autosomal recessive Robinow syndrome. *Dev. Dyn.* 229, 400–410.

Shim, K., Minowada, G., Coling, D. E., and Martin, G. R. (2005). Sprouty2, a mouse deafness gene, regulates cell fate decisions in the auditory sensory epithelium by antagonizing FGF signaling. *Dev. Cell.* 8, 553–564.

Shuler, C. F. (1995). Programmed cell death and cell transformation in craniofacial development. *Crit. Rev. Oral Biol. Med.* 6, 202–217.

Shuler, C. F., Halpern, D. E., Guo, Y., and Sank, A. C. (1992). Medial edge epithelium fate traced by cell lineage analysis during epithelial-mesenchymal transformation *in vivo*. *Dev. Biol.* 154, 318–330.

Smith, T. M., Wang, X., Zhang, W., Kulyk, W., and Nazarali, A. J. (2009). Hoxa2 plays a direct role in murine palate development. *Dev. Dyn.* 238, 2364–2373.

Song, T., Li, G., Jing, G., Jiao, X., Shi, J., Zhang, B., et al. (2008). SUMO1 polymorphisms are associated with non-syndromic cleft lip with or without cleft palate. *Biochem. Biophys. Res. Commun.* 377, 1265–1268.

Souchon, R. (1975). Surface coat of the palatal shelf epithelium during palatogenesis in mouse embryos. *Anat. Embryol.* 147, 133–142.

Sun, D., Vanderburg, C. R., Odierna, G. S., Hay, E. D. (1998). TGFβ3 promotes transformation of chicken palate medial edge epithelium to mesenchyme *in vitro*. *Development* 125, 95–105.

Suzuki, Y., Jezewski, P. A., Machida, J., Watanabe, Y., Shi, M., Cooper, M. E., et al. (2004). In a Vietnamese population, MSX1 variants con-tribute to cleft lip and palate. *Genet. Med.* 6, 117–125.

Taketomi, T., Yoshiga, D., Taniguchi, K., Kobayashi, T., Nonami, A., Kato, R., et al. (2005). Loss of mammalian Sprouty2 leads to enteric neu-ronal hyperplasia and esophageal achalasia. *Nat. Neurosci.* 8, 855–857.

Taya, Y., O'Kane, S., and Ferguson, M. W. J. (1999). Pathogenesis of cleft palate in TGF-β3 knockout mice. *Development* 126, 3869–3879.

Thomason, H. A., Dixon, M. J., and Dixon, J. (2008). Facial clefting in Tp63 deficient mice results from altered Bmp4, Fgf8 and *Shh* signaling. *Dev. Biol.* 321, 273–282.

Tongkobpetch, S., Siriwan, P., and Shotelersuk, V. (2006). MSX1 mutations contribute to nonsyndromic cleft lip in a Thai population. *J. Hum. Genet.* 51, 671–676.

Tudela, C., Formoso, M. A., Martínez, T., Pérez, R., Aparicio, M., Maestro, C., et al. (2002). TGF-beta3 is required for the adhesion and inter-calation of medial edge epithelial cells during palate fusion. *Int. J. Dev. Biol.* 46, 333–336.

Tümpel, S., Sanz-Ezquerro, J. J., Isaac, A., Eblaghie, M. C., Dobson, J., and Tickle, C. (2002). Regulation of Tbx3 expression by antero-posterior signalling in vertebrate limb development. *Dev. Biol.* 250, 251–262.

Valcourt, U., Thuault, S., Pardali, K., Heldin, C.-H., and Moustakas, A. (2007). Functional role of Meox2 during the epithelial cytostatic response to TGF- β. *Mol. Oncol.* 1, 55–71.

Van den Boogaard, M.-J. H., Dorland, M., Beemer, F. A., van Amstel, H. K. P. (2000). MSX1 mutation is associated with orofacial clefting and tooth agenesis in humans. *Nat. Genet.* 24, 342–343.

Vastardis, H., Karimbux, N., Guthua, S. W., Seidman, J. G., and Seidman, C. E. (1996). A human MSX1 homeodomain missense mutation causes selective tooth agenesis. *Nat. Genet.* 13, 417–421.

Vaziri Sani, F., Hallberg, K., Harfe, B. D., McMahon, A. P., Linde, A., and Gritli-Linde, A. (2005). Fate-mapping of the epithe-lial seam during palatal fusion rules out epithelial-mesenchymal transformation. *Dev. Biol.* 285, 490–495.

Venza, I., Visalli, M., Parrillo, L., De Felice, M., Teti, D., and Venza, M. (2011). MSX1 and TGF-B3 are novel target genes functionally regulated by FOXE1. *Hum. Mol. Genet.* 20, 1016–1025.

Verzi, M. P., Agarwal, P., Brown, C., McCulley, D. J., Schwarz, J. J., and Black, B. L. (2007). The transcrip-tion factor MEF2C is required for craniofacial development. *Dev. Cell* 12, 645–652.

Wang, B., Fallon, J. F., and Beachy, P. A. (2000). Hedgehog-regulated pro-cessing of Gli3 produces an ante-rior/posterior repressor gradient in the developing vertebrate limb. *Cell* 100, 423–434.

Welsh, I. C., Hagge-Greenberg, A., and O'Brien, T. P. (2007). A dosage-dependent role for Spry2 in growth and patterning during palate development. *Mech. Develop.* 124, 746–761.

Welsh, I. C., and O'Brien, T. P. (2009). Signaling intergration in the rugae zone directs sequential SHH signal-ing center formation during rostral outgrowth of the palate. *Dev. Biol.* 336, 53–67.

Xu, X., Han, J., Ito, Y., Bringas, P. Jr., Deng, C., and Chai, Y. (2008). Ectodermal Smad4 and p38 MAPK are functionally redundant in mediating TGF-beta/BMP signaling during tooth and palate development. *Dev. Cell.* 15, 322–329.

Xu, X., Han, J., Ito, Y., Bringas, P. Jr., Urata, M. M., and Chai, Y. (2006). Cell autonomous requirement for Tgfbr2 in the disappearance of medial edge epithelium during palatal fusion. *Dev. Biol.* 297, 238–248.

Yamamoto, T., Cui, X.-M., and Shuler, C. F. (2003). Role of ERK1/2 sig-naling during EGF-induced inhibi-tion of palatal fusion. *Dev. Biol.* 260, 512–521.

Yang, L. T., and Kaartinen, V. (2007). Tgfb1 expressed in the Tgfb3 locus partially rescues the cleft palate phe-notype of Tgfb3 null mutants. *Dev. Biol.* 312, 384–395.

Yu, L., Gu, S., Alappat, S., Song, Y., Yan, M., Zhang, X., et al. (2005). Shox2-deficient mice exhibit a rare type of incomplete clefting of the secondary palate. *Development* 132, 4397–4406.

Zhang, F. P., Mikkonen, L., Toppari, J., Palvimo, J. J., Thesleff, I., and Jänne, O. A. (2008). Sumo-1 func-tion is dispensable in normal mouse development. *Mol. Cell. Biol.* 28, 5381–5390.

Zhang, Z., Song, Y., Zhao, X., Zhang, X., Fermin, C., and Chen, Y. (2002). Rescue of cleft palate in Msx1-deficient mice by trans-genic Bmp4 reveals a network of BMP and Shh signaling in the regulation of mammalian palatogenesis. *Development* 129, 4135–4146.

Zhao, H., Oka, K., Bringas, P., Kaartinen, V., and Chai, Y. (2008). TGF-β type I receptor Alk5 regu-lates tooth initiation and mandible patterning in a type II receptor-independent manner. *Dev. Biol.* 320, 19–29.

Conflict of Interest Statement: The authors declare that the research was conducted in the absence of any commercial or financial relationships that could be construed as a potential conflict of interest.

Received: 16 May 2012; accepted: 14 December 2012; published online: 07 January 2013.

*Citation: Smith TM, Lozanoff S, Iyyanar ‡ and Nazarali AJ (2013) Molecular signaling along the anterior–posterior axis of early palate development. Front. Physio. **3**:488. doi: 10.3389/fphys. 2012.00488*

This article was submitted to Frontiers in Craniofacial Biology, a specialty of Frontiers in Physiology.